NONCOOPERATIVE GAMES FOR CONTROL OF NETWORKED SYSTEMS

BY

TANSU ALPCAN

B.S., Bogazici University, 1998
M.S., University of Illinois at Urbana-Champaign, 2001

DISSERTATION

Submitted in partial fulfillment of the requirements
for the degree of Doctor of Philosophy in Electrical Engineering
in the Graduate College of the
University of Illinois at Urbana-Champaign, 2006

Urbana, Illinois

ABSTRACT

Noncooperative game theory is used as a basis for analyzing, developing, and implementing decision, control, and resource allocation schemes to address various network control problems such as congestion control, code division multiple access (CDMA) power control, and network intrusion detection and response. In the cases of CDMA power control and congestion control, a fairly general, distributed, market-based resource allocation framework is developed and analyzed. The applicability of the underlying noncooperative network game's principles to both network control problems can be considered as an indicator of the generality and usefulness of this approach. Based on this general framework, various algorithms customized according to the specific nature of the network at hand are developed. Making use of a variety of control theoretic tools such as Lyapunov and hybrid system theories, stability and robustness properties of these algorithms are studied rigorously. An analysis of robustness with respect to feedback delays, which is of particular importance, is provided for most of the algorithms considered. In the case of network intrusion detection, dynamic noncooperative games are utilized to model the decision and analysis processes in an IDS. Again, both generic and system-specific schemes and models are considered. In addition to the theoretical analysis of the network control problems addressed, implementation related aspects of the schemes developed are investigated. For each algorithm, theoretical results obtained are supported and demonstrated either via high-level MATLAB simulations or using the NS-2 packet level network simulator. Through extensive simulations, applicability and underlying assumptions of the theoretical models are verified.

To Özlem.

ACKNOWLEDGMENTS

I would like to thank:

Dr. Tamer Başar not only for his guidance and support as my academic adviser but also for providing an ideal research environment and exemplifying how to be a researcher and mentor,

Dr. Sean Meyn, Dr. Rayadurgam Srikant, Dr. Daniel Liberzon, and Dr. Bill Sanders for being helpful members of my committee and all other UIUC faculty who have been my teachers and mentors over the years,

Dr. Tamer Başar, Dr. Rayadurgam Srikant, Dr. Roberto Tempo, Dr. Murat Arcak, Dr. Subhrakanti Dey, Dr. Kurt Rohloff, and Dr. Xingzhe Fan for their collaboration and contributions to this thesis,

Becky Lonberger and Francie Bridges, for being helpful, kind, and patient,

Batu Şat, Serdar Kozat, Nesrin Bakir, Cagri Imer, Jim Melody, Vikrant Sharma, Silvia Mastellone, Kunal Srivastav, Wei Hong, Allen Yang Yang, Serdar Yuksel, Shao Liu, and Hongxia Shen for being friends, office mates, and fellow graduate students along the way,

Nursel, Taner, and Ceyda Alpcan for being there first and being there always no matter where I am,

Özlem Alpcan, for bringing love, friendship, and meaning to my life.

TABLE OF CONTENTS

LIST OF TABLES

LIST OF FIGURES

CHAPTER 1

INTRODUCTION

This dissertation introduces and discusses a line of research where noncooperative game theory is used as a basis for analyzing, developing, and implementing decision, control, and resource allocation schemes. We address the network control problems of congestion control, code division multiple access (CDMA) power control, and network intrusion detection and response within a noncooperative game theoretic framework. In addition, we rigorously analyze stability and robustness properties of the underlying algorithms by making use of classical control theoretic tools such as Lyapunov theory, relatively recently emerging hybrid (switched) system theory, and numerical methods like randomized algorithms. Before discussing these, we first provide below a brief overview of noncooperative game theory, hybrid systems, and randomized algorithms.

Noncooperative game theory involves multiperson decision making, where each person involved pursues his or her own interests which are partly conflicting with others' [1]. Specifically, we focus on *N*-person nonzero sum static and repeated games as a framework to address resource allocation and distributed control problems in networked systems. In most of the cases, we model autonomous parts of the networked systems, which may as well be autonomously functioning computer programs, as players in a network game. These players interact and compete with each other on the same system for limited and shared resources. They are associated with cost functions, which model their cost (utility). Then, each player minimizes its own cost by choosing a strategy from its well defined strategy space. Furthermore, we implicitly make the simplifying assumption of rationality of the players.

For the class of network games considered, Nash equilibrium (NE) [1] provides an appropriate solution concept. At the NE point, an individual player cannot improve its outcome by altering its decision (strategy) unilaterally given that the strategies of other players are fixed. We show that in some special cases NE solution becomes Pareto optimal, where no other joint decision of the players can improve the performance of at least one of them, without degrading the performance of another [1].

Dynamical systems which are described by an interaction between continuous and discrete dynamics are usually called *hybrid systems*. We focus on continuous-time systems with (isolated) discrete switching events, which are also referred to as *switched systems* [2]. Most of the networked

systems considered in this study can be analyzed within a hybrid system framework, where sudden switching events change the nature of the continuous system model. We utilize various switched system models discussed in [2] not only for the stability analysis of algorithms as in the case of multicell power control, but also for control synthesis, as in the adaptive pricing congestion control scheme.

During the investigation of stability and robustness properties of the congestion control and power control schemes, we also make use of numerical methods such as *randomized algorithms*. The study of randomized algorithms for analysis and design of control systems has aroused considerable interest in the systems and control community. Randomized algorithms are efficient and low complexity, and are useful especially when worst case analysis of complex systems is either very difficult or impossible. Unlike more classical methods, these algorithms yield an assessment on the satisfaction of required specifications with a certain probabilistic accuracy. Hence, they constitute a fitting solution for our investigation by providing a trade-off between computational complexity and tightness of the solution.

Randomized algorithms rely heavily on univariate and multivariate methods for sample generations in various sets [3]. Roughly speaking, sample generation techniques can be divided into two main categories: Monte Carlo (MC) (see, e.g., [4]) and quasi-Monte Carlo (QMC) [5]. While the former is classical, statistically based, and assumes an *a priori* knowledge of probability density functions, the latter may be regarded as its deterministic counterpart. The main objective of QMC methods is to reduce the "discrepancy" between the generated samples, and a secondary objective is to avoid the curse of dimensionality that arises in gridding or rejection methods. Therefore, we not only use classical MC methods in sample generation but also QMC methods when they are feasible.

In the remainder of this chapter, we introduce and discuss the topics of congestion CDMA power control, and network intrusion detection. In addition, we summarize contributions of relevant studies in the literature on these subjects. An overview of the congestion control problem in networked systems is given in Section 1.1, which is followed by the discussion of CDMA power control in Section 1.2. Section 1.3 introduces the topic of network intrusion detection and response. We conclude the chapter with a brief outline of this dissertation in Section 1.4.

1.1 Congestion Control in Networked Systems

Packet-based communication networks recently received growing attention in the control literature, as evidenced by the appearance of several special issues devoted to this topic in leading journals in the field, such as [6], [7], and [8] and a recently published book on the topic [9]. Various

approaches and solutions have been developed and studied in this context, including modeling of the Internet traffic, congestion control for available bit rate (ABR) service in asynchronous transmission mode (ATM) networks, packet marking schemes for the Internet, application of low order controllers for active queue management (AQM), as well as related problems.

One of the critical issues that lie at the heart of efficient operation of packet-based networks is *congestion control*. This involves the problem of regulating the source rates in a decentralized and distributed fashion, so that the available bandwidths on different links are used most efficiently while minimizing (or totally eliminating) loss of packets due to queues at buffers exceeding their capacities. This objective has to be accomplished under variations in network conditions such as packet delays (due to propagation as well as queueing) and bottleneck nodes.

The congestion control mechanism of the Internet is based on the Transfer Control Protocol (TCP) [10], which is by far the most widely known and used congestion control scheme. TCP provides an end-to-end congestion control where each user adjusts its flow rate according to the feedback it receives from the network in the form of lost packets. With the evolution of the Internet, we are seeing an effort toward improving and modifying the existing flow and congestion control structure. In recent years, the congestion control problem and modeling of the Internet have caught the attention of the research community. After the introduction of the congestion control algorithm for TCP [10], focus has been on the modeling and analysis of such algorithms. Based on an earlier work by Kelly [11], Kelly et al. [12] have presented the first comprehensive mathematical model and posed the underlying resource allocation in congestion control as an optimization problem. The primal and dual algorithms they have introduced are based on user utility and link pricing (explicit feedback) functions, where the sum of user utilities are maximized within the capacity (bandwidth) constraints of the links. Furthermore, they have established the global stability of these algorithms in the no-delay case as well as under small perturbances. They have also introduced the concept of proportional fairness, which is a relaxed version of min-max fairness [9], as a resource allocation criterion among users.

Subsequent studies [13–17] have investigated variations and generalizations of the distributed congestion control framework of [11, 12]. Low and Lapsley [15] have analyzed the convergence of distributed synchronous and asynchronous discrete algorithms, which solve a similar optimization problem. Mo and Walrand [13] have generalized the proportional fairness, and have proposed a fair end-to-end window-based congestion control scheme, which is similar to primal algorithm. The main difference of this window-based algorithm from the primal algorithm is that it does not need feedback from the routers due to usage of queuing delay as feedback. La and Anantharam [14] have considered a system model similar to that proposed in [13] with a window-based control scheme and static modeling of link buffers. They have investigated convergence properties of the proposed charge-sensitive congestion control scheme, which utilizes a static pricing scheme based on link

queueing delays. In addition, they have established stability of the algorithm at a single bottleneck node. Kunniyur and Srikant [17] have examined the question of how to provide the congestion feedback from the network to the user. They have proposed an explicit congestion notification (ECN) marking scheme combined with dynamic adaptive virtual queues, and have shown using a time-scale decomposition that the system is semiglobally stable in the no-delay case.

In communication networks, delays between users and resources of the network are often not negligible. In the context of the Internet, these delays vary from order of tens to hundreds of milliseconds, and affect the stability of end-to-end congestion control algorithms. The communication delays in the network are in general heterogeneous in the sense that forward delays between the users and the resources are different from the feedback delays. It is possible to consider end-to-end congestion control schemes in this setting as feedback systems with delay where users vary their flow rates in accordance with the delayed feedback they receive from the system resources. Depending on the specific network, this feedback signal may be in the form of packet losses as in TCP, marked packets or variations in round trip time (RTT) the packets experience.

Stability properties of primal, dual, and similar algorithms have recently been investigated in the presence of nonnegligible delays [18–20]. Johari and Tan [20] have analyzed the local stability of a delayed system where the end user implements the primal algorithm. They have considered a single link accessed by a single user, as well as its multiple user extension under the assumption of symmetric delays. In both cases, they have provided sufficient conditions for local stability of the underlying system of equations. Massoulie [19] has extended these local stability results to general network topologies and heterogeneous delays. In another study, Vinnicombe [18] has also provided sufficient conditions for local stability of a user source law which is a generalization of the same algorithm. Elwalid [21] has considered stability of a linear class of algorithms where the source rate varies in proportion to the difference between the buffer content and the target value. Deb and Srikant [16], on the other hand, have focused on the case of single user and a single resource and investigated sufficient conditions for global stability of various nonlinear congestion control schemes under fixed information delays. Liu et al. [22] have extended the framework of [11, 12] by introducing a primal-dual algorithm which has dynamic adaptations at both ends (users and links), and have given a condition for its local stability under delay using the generalized Nyquist criterion. Wen and Arcak [23] have used the passivity framework to unify some of the stability results on primal and dual algorithms without delay, have introduced and analyzed a larger class of such algorithms for stability, and have shown robustness to variations due to delay. In another recent study, Alpcan and Başar [24] have proposed a similar scheme based on game theory, where queueing delays in the network are used as congestion feedback. They have also provided sufficient conditions for global stability at a bottleneck link under nonnegligible communication delays.

Game theory provides a natural framework for developing pricing and congestion control

mechanisms for the Internet. Users on the network can be modeled as players in a congestion control game where they choose their strategies or in this case flow rates. Players are noncooperative in terms of their demands for network resources and have no specific information on other users' strategies. A user's demand or utility for bandwidth is captured in a utility function, and may not be bounded. To compensate for this, one can devise a pricing function, proportional to the bandwidth usage of a user, in order to preserve the network resources and to provide an incentive for the user to implement end-to-end congestion control. End-to-end congestion control schemes, among others, are widely accepted due to their distributed nature, scalability, and ease in implementation [25]. In such a noncooperative congestion control game, NE proves to be a useful and relevant concept. There is a rich literature on game theoretic analysis of flow control problems utilizing both cooperative [26] and noncooperative [27–29] frameworks. In [27] it has been shown that if an appropriate cost function and pricing mechanism are used, one can find an efficient NE for a multiuser network which is further stable under different update algorithms. Orda et. al. [29] have shown the existence and uniqueness of a NE under different classes of cost functions for a simple two-node multiple links system. In [30] a combined routing and flow control problem has been formulated as a Nash game with a large number of players, and nearly-optimal policies have been obtained with non-concave objective functions. Başar and Srikant [31] have incorporated pricing into a flow control game as an active decision variable controlled by the network (service provider), and they study the problem as a hierarchical game in a many-users regime. Game theoretic concepts have also been used in [13, 14, 32].

Although the game theoretic approach provides a suitable framework for formulating and studying congestion and flow control problems in general networks, there are some inherent restrictions on implementable cost functions in the case of Internet-style networks. For example, the current structure of the Internet makes it difficult, if not impossible, for users to obtain detailed real-time information on the state of the network and on other users. Therefore, users are bound to use indirect aggregate metrics that are available to them, such as packet drop rate or variations in the average RTT of packets, in order to infer the current situation in the network. Packet drops, for example, are currently used by most widely deployed versions of the TCP as an indication of congestion. In this part of our study, however, we propose and analyze a pricing and congestion control scheme based on variations in the queueing delay a user experiences. A similar approach has been suggested in a version of TCP, known as TCP Vegas [33]. Although TCP Vegas is more efficient than a widely used version of TCP, TCP Reno [34], the suggested improvements are empirical and based on experimental studies. The studies by Mo and Walrand [13] and by La and Ananatharam [35] also make use of an approach similar to the one we propose; however, they are based on fairness and pricing concepts of Kelly [12]. Furthermore, the former study employs only a narrow set of utility functions in describing user demands, while the latter does not take

into account queue dynamics or the effect of boundaries and propagation delays on stability of the system.

In this dissertation, we propose a fairly general congestion control framework based on noncooperative game theory, which can be utilized in designing algorithms for various types of networks. Making use of pricing and utility concepts, we define a noncooperative network game. Under some mild convexity assumptions the NE solution is identified as the unique operating point of the network. Furthermore, we investigate system dynamics, its stability and robustness properties with respect to communication delays, and variations in network parameters. For Internet-style networks, we propose a specific congestion control algorithm based on variations in queueing delay. Again, we analyze its stability and robustness properties by taking into account queue dynamics, the effect of boundaries, and communication delays. In addition, we utilize randomized algorithms in this context, and present numerical results on stability of the system first for a single bottleneck node and subsequently under general network topologies. The congestion control schemes and the underlying framework are discussed in detail in Chapters 2 and 3, which include our recent research results in these areas. A detailed outline of these chapters is given in Section 1.4, whereas our concluding comments are summarized in Section 8.2.

Our research results on congestion control in networked systems included in this dissertation have been presented in various conferences and appeared in the respective proceedings [24,36–39]. Moreover, parts of this dissertation that are on congestion control have been published in peer-reviewed journals [40–43].

1.2 Multicell CDMA Power Control

The primary objective of power control in a wireless network is to regulate the transmission power level of each mobile in order to obtain and maintain a satisfactory quality of service for as many users as possible. In a CDMA system, where signals of other users can be modeled as interfering noise, the goal of power control is more precisely stated as to achieve a certain signal-to-interference ratio (SIR) regardless of channel conditions while minimizing the interference, and hence improving the overall performance. Although there exists a large body of work for voice traffic where SIR requirements for satisfactory service are fixed and well established, power control for wireless data networks has only recently been a topic of interest [44–50]. Since the SIR requirements for a desired level of service vary from one individual user to another in wireless networks, the power control problem becomes also one of resource allocation. Recent studies [44, 47, 48] make use of concepts and tools from the field of economics, such as pricing and utility functions, to come up with power control schemes that address this question. In [47], a pricing scheme for

the downlink of a wireless network is investigated where users are charged based on their channel quality. The study [48], on the other hand, shows that net utility maximization problem for elastic traffic can be decomposed into simpler problems of obtaining the optimal signal quality and selection of the optimal transmission rate.

In CDMA systems where each mobile interacts with others by affecting the SIR ratio through interference, game theory provides a natural framework for analyzing and developing power control mechanisms. For a mobile in such a network, obtaining individual information on the power level of each of the other users is practically impossible due to the excessive communication and processing overhead required. Therefore, in a distributed power control setting, each user attempts to minimize its own cost (or maximize its utility) in response to the aggregate information on the actions of the other users. This makes the use of noncooperative game theory for uplink power control most appropriate, with the relevant solution concept being the noncooperative Nash equilibrium as in the case of congestion control.

Several studies exist in the literature that use game theoretic schemes to address the power control problem in a single cell [44, 46, 51]. In [44], a framework for power control based on noncooperative game theory and pricing has been presented. The study [51] has shown the existence of a unique NE for a certain type of pricing function and under binary input Gaussian output and binary symmetric channel assumptions. Another study [46] has proposed linear and exponential utility functions based on carrier SIR, and has shown the existence of a NE under some assumptions on the utility functions. In [52], we have made use of the conceptual framework of noncooperative game theory to obtain a distributed and market-based control mechanism. We have proven the existence of a unique NE, and established the stability of two different update algorithms under some specific conditions. Another recent study [49] investigates pricing and power control in a multicell wireless network. Here, existence of a unique NE for a class of quasi-concave utility functions is established without pricing. The effect of linear pricing schemes on the solutions are also analyzed, and it is shown that pricing improves Pareto efficiency of the operating (equilibrium) points.

In wireless communication systems, mobiles frequently update their power levels due to varying channel conditions in order to maintain their SIR (service) level. The power control game leads to distributed power control algorithms as a mean to achieve this goal. An important aspect of a distributed power control scheme is the convergence properties of algorithms, which plays a significant role in performance of the system. The study [53] has presented a standard power control algorithm, and has established its synchronous and asynchronous convergence under some conditions on the interference function. In [54], stochastic power control schemes have been investigated, and the converge of stochastic algorithms in terms of mean-squared error has been proven. Another study [55] has shown the convergence of a coupled power control scheme based on mini-

mum outage probability and multiuser detection by making use of standard interference functions of [53]. In [52], two update algorithms, namely, parallel update and random update have been shown to be globally stable under specific conditions. Finally, in [56] the global convergence of the dynamics of the power control game to a superset of NE has been established for any handoff scheme satisfying a mild condition on average dwell time.

We extend in this dissertation the single cell power control scheme of [52] to multiple cells and to a broader class of cost functions. By making use of hybrid system and noncooperative game theories we model the multicell wireless data network, and develop a market-based distributed power control scheme. The model, the power control game, and the proposed algorithm as well as its stability and robustness properties are discussed in detail in Chapter 4.

We next consider in Chapter 5 a power control game similar to the one in Chapter 4. In this case, however, we capture the preferences of mobiles using a utility function defined as the logarithm of the probability that the frame success rate of the data user is greater than a predefined individual threshold level. We analyze this power control game as well as the global convergence of continuous-time as well as discrete-time synchronous and asynchronous iterative power update algorithms to the unique NE of the game. Furthermore, we show that a stochastic version of the discrete-time update scheme, which models the uncertainty due to quantization and estimation errors, converges almost surely to the unique NE point.

Finally, in Chapter 6, we study an extension to the power control game of Chapters 4 and 5 as well as a formulation of the power control as a team optimization problem. We investigate a hybrid noncooperative game motivated by the practical problem of joint power control and base station (BS) assignment in CDMA wireless data networks, where each mobile's action space not only includes the transmission power level but also the choice of the BS. We analyze the existence and uniqueness of pure NE solutions of the hybrid game, which constitute the operating points for the underlying wireless network, numerically using grid methods and randomized algorithms. In addition, we study power control in multicell CDMA wireless networks as a team optimization problem where each mobile attains at the minimum its individual fixed target signal to interference level and beyond that optimizes its transmission power level according to its individual preferences. Using a Lagrangian relaxation approach similar to [12] we obtain two decentralized dynamic power control algorithms: primal and dual power update, and establish their global stability utilizing both classical Lyapunov theory and the passivity framework [57]. Our results on this subject are outlined in Section 1.4, and our conclusions and comments for future research are included in Section 8.3.

Our research results on CDMA power control in wireless networks included in this dissertation have been presented in various conferences and appeared in the respective proceedings [58–61]. In addition, the sections of this dissertation on power control have been either published in peer-

reviewed journals [52, 56, 62] or accepted for publication [63].

1.3 Intrusion Detection and Response

Today, communication and computer networks are an indispensable part of the modern society, with the prime example being the Internet. Since they bring extensive computing and communication capabilities to individuals, businesses, and organizations over long distances, and often on a global scale, networked systems are being deployed in every level of the society at an exponential rate. Existing information structures and the way information is processed in organizations are increasingly transferred to virtual environments. These revolutionary changes in information systems also pose unique problems. Network security is among the most important of these [64], and hence, it has been extensively investigated in the research community.

The distributed nature of contemporary networks and the complexity of the underlying computing and communication environments prevent administrators and organizations from having absolute control on their networks. Furthermore, network boundaries are often vague, and administrators cannot exercise control outside their local domain [65, 66], which leaves networked systems vulnerable to distant security attacks due to global connectivity. This results in a perpetual struggle between attackers who aim to intrude the deployed systems and security administrators trying to protect them. Emerging security issues such as this cannot be fully addressed by classical approaches like policing. Although technologies like firewalls, encryption, and authentication can harden the network against attacks, they fail to address issues in the case an attack is (partially) successful.

Intrusion detection systems (IDSs) extend the information security paradigm beyond traditional protective and reactive network security. They monitor the events in the networked system and analyze them for signs of security problems [67]. Hence, they increase the controlling ability of the system administrator and help him or her react to security problems. Current IDSs rely mostly on human intervention in the decision and response processes against attacks, that are often automatic and script-based. In other words, the equivalence of a strategic decision making and command-and-control in battleground management is missing [68]. Hence, today's IDSs are inefficient and delayed in responding to security breaches in the network. Furthermore, due to the distributed nature of the networked system a centralized security system poses scalability and efficiency problems [69]. Utilization of autonomous software agents (ASAs) in developing distributed IDSs has recently been proposed to address the issues of automatization and scalability [70–72]. However, a distributed IDS architecture based on ASAs still needs a decision making mechanism which requires as little human intervention as possible.

Given the current overview of the information security and intrusion detection, there is definitely a need for a decision and control framework to address issues like attack modeling, analysis of detected threats, and decision on response actions. A rich set of tools have been developed within game theory to address problems where multiple players with different objectives compete and interact with each other on the same system, and they are successfully used in many disciplines including economics, decision theory, and control. Therefore, game theory is a strong candidate to provide the much-needed mathematical framework for analysis, modeling, decision, and control processes for information security and intrusion detection. Such a mathematical abstraction is useful for generalization of problems, combining the existing ad hoc schemes under a single umbrella, and future research. Furthermore, using game theoretic tools it is also possible to develop practical schemes which can be integrated with existing intrusion detection systems. Because of these reasons, application of game theory to network security area has recently been a topic of interest [73, 74].

In this dissertation we utilize game theory to develop quantitative models for analysis of common trade-offs in information security as well as a formal decision and control framework in network intrusion detection. We propose a generic model for distributed IDSs by defining a network of sensors, and two flexible easy-to-implement schemes. In addition, we study the interaction between the attacker and the IDS as a two-person noncooperative game with dynamic information. Nash equilibrium solutions are derived analytically and analyzed for the finite security game defined in two special cases. Furthermore, the imperfect flow of information from the attacker to the IDS through a virtual sensor network is captured within both finite and continuous-kernel noncooperative network security games.

As an application of the framework proposed, we implement an IDS prototype for access control utilizing usage and misuse anomaly detection sensors based on self-organizing maps, and demonstrate its operation under a simple scenario. A detailed outline of Chapter 7 is presented in the next section. Section 8.4, on the other hand, summarizes our results and describes directions for future research.

Our research results on intrusion detection included in this dissertation have been presented in IEEE conferences on decision and control and appeared in the respective proceedings [75, 76].

1.4 Outline of the Dissertation

We present and discuss in this dissertation the results of our recent research on the three distinct but connected topics introduced above. A brief overview and the outline of it is as follows.

In Chapter 2, we present a fairly general framework for congestion control based on noncoop-

erative game theory. In Section 2.1 the existence and uniqueness of Nash equilibrium in a generic noncooperative game is discussed. In Section 2.1 we introduce a general network model based on fluid approximations and a congestion control game, where the existence and uniqueness of NE is established under reasonable convexity assumptions on the cost function. A simple but efficient gradient descent algorithm is shown to converge to the NE under the same set of assumptions. In Section 2.2.4, we provide sufficient conditions for global stability of this algorithm under heterogeneous delays on a general network topology. A robustness analysis of the congestion control scheme to variations in system parameters such as the number of users, capacity of the links, and routing is given in Section 2.4. Worst-case analysis leads to theoretical bounds only in some special cases. Hence, more general cases are handled numerically in Section 2.5 using randomized algorithms and for a specific cost structure. Finally, Section 2.6 presents the demonstration of the theoretical results obtained through MATLAB simulations.

The congestion control scheme for Internet-style networks introduced in Chapter 3 makes use of a special pricing function, which is proportional to the queueing delay experienced by the user. Through a network model based on fluid approximations and a realistic queueing model, we show in Section 3.1 the existence of a unique equilibrium, which approximates NE under the assumption that the effect of a user's flow on congestion cost is vanishingly small. This assumption holds especially if the number of users is large. In Section 3.2, we establish the global stability of the equilibrium under a general network topology. We also investigate stability of the system in a network with nonnegligible propagation delays, and provide sufficient conditions for stability in the case of a bottleneck node with multiple users in Section 3.3. The effect of boundaries on system stability are rigorously analyzed. In addition, we study in Section 3.4 an adaptive pricing scheme for adjusting the pricing parameter dynamically, and we make use of hybrid (switched) system concepts for its analysis. Based on the theoretical foundations developed, we design a window-based, end-to-end congestion control scheme for Internet-style networks in Section 3.5. It is followed by Section 3.6, where this congestion control scheme is simulated in Network Simulator 2 (NS-2) [77] over Internet Protocol (IP) for various network topologies.

We next analyze in Chapter 3 a discrete-time version of the proposed scheme as any implementation of the continuous time model inevitably involves a discretization synchronized with the RTT of packets. First, an analytical local stability analysis of the single bottleneck node case with symmetric users is given in Section 3.6. Then, we discuss the use of randomized algorithms in the present context. In Section 3.7.1, numerical results are presented for stability of the system first for a single bottleneck node and subsequently under general network topologies.

In Chapter 4, the single cell power control scheme of [52] is extended to multiple cells and to a broader class of cost functions. Specifically, we model the multicell wireless data network as a switched hybrid system where handoffs of mobiles between the individual cells (base stations)

correspond to discrete switching events between different subsystems. Under a set of sufficient conditions, we show in Section 4.1 the existence and global stability of a unique NE for each subsystem. In Section 4.2, we establish the global exponential convergence of the dynamics of the multicell power control game to a minimum convex set of Nash equilibria for any switching (handoff) scheme satisfying a mild condition on average dwell-time. Furthermore, we investigate robustness of these results to various communication constraints such as feedback delays and quantization. In addition, we analyze a quantization scheme to reduce the communication overhead between mobiles and the base stations. Finally, we illustrate the proposed power control scheme through MATLAB simulations in Section 4.3.

In Chapter 5, we consider a power control game similar to the one in Chapter 4, which incorporates a pricing mechanism limiting the overall interference and preserving battery energy of mobiles. We capture the preferences of mobiles using a utility function defined as the logarithm of the probability that the frame success rate of the data user is greater than a predefined individual threshold level. We consider a noncooperative power control game which uses an outage-probability-based (instead of an SIR based) utility function and also incorporates a pricing mechanism. Section 5.1 describes the model adopted and the cost function. In Section 5.2, we show that the noncooperative power control game admits a unique NE under uniformly strictly convex pricing functions and some technical assumptions on the SIR threshold levels. We present in Section 5.3 system dynamics and stability analysis of a continuous-time update scheme. In Section 5.4, convergence properties of both deterministic and stochastic discrete-time update algorithms are investigated. Section 5.5 contains results of MATLAB simulation studies.

In the first half of the Chapter 6, we investigate the hybrid noncooperative game which models the integrated power control and BS assignment problem in such a way that each mobile's action space not only includes the transmission power level but also the choice of the BS. Section 6.3 discusses NE solution of this hybrid game and contains Subsection 6.3.1 which describes randomized algorithms for numerical analysis. We present our simulation results in Section 6.4 where we investigate the existence and uniqueness properties of Nash equilibrium solutions in Subsection 6.4.1, and analyze a power update and BS assignment scheme in Subsection 6.4.2. In the second half of the chapter, we study power control in multicell CDMA wireless networks as a team-optimization problem where each mobile attains at the minimum its individual fixed target signal to interference level and beyond that optimizes its transmission power level according to its individual preferences. We define in Section 6.5 the system problem and its decomposition to user and network problems. In Section 6.6, we investigate a relaxation of the system problem as well as primal and dual algorithms. In addition, system dynamics and a passivity approach for stability and robustness are studied. Section 6.7 discusses some of the basic principles of call admission control from the perspective of the model adopted in this paper. Lastly, we illustrate the power

control schemes introduced through MATLAB simulations in Section 6.8.

We investigate in Chapter 7 the basic decision and analysis processes involved in information security and intrusion detection, as well as possible usage of game theory for developing a formal decision and control framework. We develop a generic model for distributed IDSs by defining a network of sensors, and propose two flexible and easy-to-implement schemes utilizing both cooperative and noncooperative game theoretic concepts [1,78]. In Section 7.1, common trade-offs in information security, attack detection techniques, and application of game theory to intrusion detection are investigated. We introduce a game theoretic framework for distributed IDSs and two schemes making use of game theoretic concepts in Section 7.2. We investigate an application of the game theoretic approach to access control systems in Section 7.4 by demonstrating the concepts introduced in previous sections under various scenarios through simulations in MATLAB. Towards this end, we implement an IDS prototype for access control utilizing "virtual" sensors based on Kohonen self-organizing maps for anomaly detection.

Chapter 8 discusses the results of this dissertation research in general and provides a brief summary of each topic separately, including future research directions and concluding remarks in Sections 8.2, 8.3, and 8.4.

CHAPTER 2

A GAME THEORETIC FRAMEWORK FOR CONGESTION CONTROL

We present in this chapter a fairly general class of noncooperative network games, which can be utilized to design congestion control algorithms for various types of communication networks. The next section discusses existence and uniqueness of NE in a generic noncooperative game. In Section 2.2 we introduce a general network model based on fluid approximations and a congestion control game, where the existence and uniqueness of NE is established under reasonable convexity assumptions on the cost function. Furthermore, a simple but efficient gradient descent algorithm is shown to converge to the NE under the same set of assumptions. We provide in Section 2.2.4 sufficient conditions for global stability of this algorithm under heterogeneous delays on a general network topology. A robustness analysis of the congestion control scheme to variations in system parameters such as the number of users, capacity of the links, and routing is given in Section 2.4. Worst-case analysis leads to theoretical bounds only in some special cases. Therefore, more general cases are handled numerically in Section 2.5 using randomized algorithms and for a specific cost structure. The chapter concludes with Section 2.7, which follows Section 2.6, where we demonstrate the results obtained through MATLAB simulations.

2.1 Nash Equilibrium (NE): Existence and Uniqueness in a Generic Noncooperative Game

We study the existence and uniqueness of NE solution to a generic noncooperative game, and establish the relationship between the NE and optimization (minimization) of a convex multivariable function. Furthermore, we investigate how the variations of the game parameters affect the NE point. Although some of the results we present have been reported earlier in [79], our treatment clarifies the underlying dynamics and brings new insights to the problem.

Consider a noncooperative game Γ with M players, where the i^{th} player is assigned a specific cost function J_i, which it minimizes by adjusting its own strategy (synonymously here, action) x_i. We let J denote the vector composed of the individual cost functions J_i's, i.e., $J = [J_1\ J_2\ \ldots J_M]^T$, where $[.]^T$ denotes the transpose of a vector. The strategy vector $\mathbf{x}$ of players is defined as $\mathbf{x} :=$

$[x_1\, x_2\, \ldots x_M]^T$, and belongs to the strategy space $X \subset \mathbb{R}^M$ of the game. Given the strategy vector of all other users, $\mathbf{x_{-i}}$, the i^{th} player is faced with the following constrained optimization problem:

$$\min_{x_i} J_i(x_i, \mathbf{x_{-i}}), \tag{2.1}$$

where $[x_i\ \mathbf{x_{-i}}]^T \in X$. The NE of the noncooperative game Γ is defined as the strategy vector, $\mathbf{x}^*$ (and corresponding set of costs J^*), with the property that no user can benefit from modifying its strategy while the other players keep theirs fixed. Mathematically speaking, $\mathbf{x}^*$ is in NE, when x_i^* of any i^{th} user is the solution to the optimization problem in (2.1) given all other users have equilibrium strategies, $\mathbf{x}^*_{-i}$.

Let X° be the set of interior points of X [80]. We make the following assumptions on the cost functions of players and on the strategy space of the game.

Assumption 2.1 *The strategy space X of Γ is convex, compact, and has a nonempty interior, $X^\circ \neq \varnothing$.*

Assumption 2.2 *The cost function of the i^{th} player, $J_i(\mathbf{x})$, is twice continuously differentiable in all its arguments and strictly convex in x_i, i.e., $\partial^2 J_i(\mathbf{x})/\partial x_i^2 \geq 0$.*

Let $\overline{\nabla}$ be the pseudo-gradient operator, defined through its application on the cost vector J, as

$$\overline{\nabla} J := [\partial J_1(\mathbf{x})/\partial x_1 \cdots \partial J_M(\mathbf{x})/\partial x_M]^T := g(\mathbf{x}). \tag{2.2}$$

Let $G(\mathbf{x})$ be the Jacobian of $g(\mathbf{x})$ with respect to $\mathbf{x}$:

$$G(\mathbf{x}) := \begin{pmatrix} b_1 & a_{12} & \cdots & a_{1M} \\ \vdots & & \ddots & \vdots \\ a_{M1} & a_{M2} & \cdots & b_M \end{pmatrix}_{M\times M}, \tag{2.3}$$

where b_i and a_{ij} are defined as $b_i := \frac{\partial^2 J_i(\mathbf{x})}{\partial x_i^2}$ and $a_{i,j} := \frac{\partial^2 J_i(\mathbf{x})}{\partial x_i \partial x_j}$, respectively. Based on (2.3), we define the symmetric matrix

$$\mathcal{G}(\mathbf{x}) := G(\mathbf{x}) + G(\mathbf{x})^T. \tag{2.4}$$

In addition, we define a solution $\mathbf{x} \in X$ to be *inner*, if $\mathbf{x} \in X^\circ$ where X° is the set of interior points of X.

The following proposition gives a characterization of an inner NE solution:

Proposition 2.1 *Under Assumptions 2.1 and 2.2, the strategy vector $\mathbf{x}^* \in X^\circ$ is an inner NE solution of the game Γ, if and only if, $g(\mathbf{x}^*) = \overline{\nabla} J(\mathbf{x}^*) = 0$.*

This result follows immediately from the definition of NE, and Assumptions 2.1 and 2.2. We note the similarity between Proposition 2.1, and first- and second-order necessary conditions for local minima of a function, which maps X° to $\mathbb{R}$ [81, p.14]. The next assumption plays a central role in establishing the uniqueness of an inner NE as stated in the proposition following it.

Assumption 2.3 *The symmetric matrix $\mathcal{G}(\mathbf{x})$ defined in (2.4) is positive definite, i.e. $\mathcal{G}(\mathbf{x}) > 0$ for all $\mathbf{x} \in X$.*

Proposition 2.2 *Under Assumptions 2.1, 2.2, and 2.3, there can be at most one inner NE solution, $\mathbf{x}^* \in X^\circ$, in the game Γ.*

Proof. Suppose that there are two inner NEs, represented by two strategy vectors $\mathbf{x}^1 \in X^\circ$ and $\mathbf{x}^0 \in X^\circ$, with elements x_i^0 and x_i^1, respectively. It follows from Proposition 2.1 that $g(\mathbf{x}^0) = 0$ and $g(\mathbf{x}^1) = 0$. Define the strategy vector $\mathbf{x}(\theta)$ as a convex combination of the two equilibrium points $\mathbf{x}^0$, $\mathbf{x}^1$:

$$\mathbf{x}(\theta) = \theta\mathbf{x}^1 + (1-\theta)\mathbf{x}^0,$$

where $0 < \theta < 1$. Take the derivative of $g(\mathbf{x}(\theta))$ with respect to θ,

$$\frac{dg(\mathbf{x}(\theta))}{d\theta} = G(\mathbf{x}(\theta))\frac{dx(\theta)}{d\theta} = G(\mathbf{x}(\theta))(\mathbf{x}^1 - \mathbf{x}^0), \tag{2.5}$$

where $G(\mathbf{x})$ is defined in (2.3). Integrating (2.5) over θ yields

$$0 = g(\mathbf{x}^1) - g(\mathbf{x}^0) = \left[\int_0^1 G(\mathbf{x}(\theta))d\theta\right](\mathbf{x}^1 - \mathbf{x}^0). \tag{2.6}$$

Multiplying (2.6) from left by $(\mathbf{x}^1 - \mathbf{x}^0)^T$, the transpose of (2.6) from right by $(\mathbf{x}^1 - \mathbf{x}^0)$, and adding these two terms, we obtain

$$0 = (\mathbf{x}^1 - \mathbf{x}^0)^T\left[\int_0^1 G(\mathbf{x}(\theta)) + G^T(\mathbf{x}(\theta))d\theta\right](\mathbf{x}^1 - \mathbf{x}^0). \tag{2.7}$$

Since $\mathcal{G}(\mathbf{x}(\theta)) = G(\mathbf{x}(\theta)) + G^T(\mathbf{x}(\theta))$ is positive definite by Assumption 2.3 and the sum of two positive definite matrices is positive definite, the matrix $\int_0^1 G(\mathbf{x}(\theta)) + G^T(\mathbf{x}(\theta))d\theta$ is positive definite. Then, it readily follows from (2.7) that $\mathbf{x}^1 - \mathbf{x}^0 = 0$. Therefore, there cannot be more than one inner NE. □

We now study the existence and uniqueness of NE solutions of the game Γ for the entire strategy space X.

Proposition 2.3 *Under Assumption 2.1, the game Γ admits a Nash equilibrium.*

Proof. The proof follows immediately from a standard theorem of game theory (Theorem 4.4, p.176, in [1]). □

We have already shown that an inner NE point $\mathbf{x}_{in}$ corresponds to a solution to the set of (possibly nonlinear) equations $g(\mathbf{x}_{in}) = 0$. In addition, if Assumptions 2.2 and 2.3 hold, then $g(\mathbf{x}_{in}) = 0$ has a unique solution. In order to establish the uniqueness of the NE including possible boundary solutions, we focus on a class of specifically constructed strategy spaces, X, which are defined through a set constraints.

Assumption 2.4 *The strategy space X of the game Γ is defined as*

$$X := \{\mathbf{x} \in \mathbb{R}^M \,:\, h_j(\mathbf{x}) \leq 0,\ j = 1,\, 2,\, \ldots r\}, \tag{2.8}$$

where $h_j : \mathbb{R}^M \to \mathbb{R}, j = 1,\, 2,\, \ldots r$, $h_j(\mathbf{x})$ is convex in its arguments for all j, and the set X is bounded and has a nonempty interior. In addition, the derivative of at least one of the constraints with respect to x_i, $\{dh_j(\mathbf{x})/dx_i,\ j = 1,\, 2,\, \ldots r\}$, is nonzero for $i = 1,\, 2,\, \ldots M$, $\forall \mathbf{x} \in X$.

Under these conditions, X satisfies Assumption 2.1 [81]. In view of Assumption 2.4, the Lagrangian function for player i in this game is given by

$$L_i(\mathbf{x}, \mu) = J_i(\mathbf{x}) + \sum_{j=1}^{r} \mu_{i,j} h_j(\mathbf{x}), \tag{2.9}$$

where $\mu_{i,j},\ j = 1,\, 2,\, \ldots r$ are the Lagrange multipliers of player i [81, p. 278]. We now provide a proposition for the game Γ with conditions similar to the well known Karush-Kuhn-Tucker necessary conditions (Proposition 3.3.1, p. 310, [81]).

Proposition 2.4 *Let $\mathbf{x}^*$ be a NE point of the game Γ and the strategy space X satisfy Assumption 2.4. There exists a unique set of Lagrange multipliers, $\{\mu^*_{i,j} : \ j = 1,\, 2,\, \ldots r,\ \ i = 1,\, 2,\, \ldots M\}$, such that*

$$\frac{dL(\mathbf{x}^*, \mu^*)}{dx_i} = \frac{dJ_i(\mathbf{x}^*)}{dx_i} + \sum_{j=1}^{r} \mu^*_{i,j} \frac{dh_j(\mathbf{x}^*)}{dx_i} = 0,\ i = 1,\, 2,\, \ldots M,$$

$$\mu^*_{i,j} \geq 0,\ \ \forall i, j\,,$$

$$\mu^*_{i,j} = 0,\ \ \forall j \notin A_i(\mathbf{x}^*), \forall i\,,$$

where $A_i(x^*)$ is the set of active constraints in i^{th} player's minimization problem at NE point $\mathbf{x}^*$.

Proof. The proof essentially follows lines similar to the ones of the Proposition 3.3.1 of [81], where the penalty approach is used to approximate the original constrained problem by an unconstrained problem that involves a violation of the constraints. The main difference we introduce is to repeat this process for each individual x_i at the NE point $\mathbf{x}^*$. □

Let us define for a more compact notation the vector of Lagrangian functions as $L := [L_1, \ldots, L_M]$, and the $M \times M$ diagonal matrix of Lagrange multipliers for the j^{th} constraint as $MU_j = \mathrm{diag}[\mu_{1,\mathrm{j}}, \mu_{2,\mathrm{j}}, \ldots \mu_{\mathrm{M,j}}]$. Finally, we obtain the main existence and uniqueness result:

Theorem 2.1 *There exists a unique NE point in the M-player noncooperative game* Γ *if Assumptions 2.2, 2.3, and 2.4 hold.*

Proof. Existence of the NE follows from Proposition 2.3. By Proposition 2.4 and Assumption 2.4, the NE point $\mathbf{x}^{(1)}$ satisfies

$$\overline{\nabla} L(\mathbf{x}^{(1)}, MU^{(1)}) = g(\mathbf{x}^{(1)}) + \sum_{j=1}^{r} MU_j^{(1)} \overline{\nabla} h_j(\mathbf{x}^{(1)}) = 0, \tag{2.10}$$

where $MU_j^{(1)}$ is unique for each j. Assume there are two different NE points $\mathbf{x}^{(0)}$ and $\mathbf{x}^{(1)}$. Following an argument similar to the one in the proof of Theorem 2 of [79], one can show that this leads to a contradiction. We present a brief outline of a simplified version of that proof for the sake of completeness. It immediately follows from (2.10) that

$$(\mathbf{x}^{(0)} - \mathbf{x}^{(1)})^T \overline{\nabla} L(\mathbf{x}^{(1)}, MU^{(1)}) + (\mathbf{x}^{(1)} - \mathbf{x}^{(0)})^T \overline{\nabla} L(\mathbf{x}^{(0)}, MU^{(0)}) = 0.$$

Rearranging the terms we obtain

$$(\mathbf{x}^{(0)} - \mathbf{x}^{(1)})^T [g(\mathbf{x}^{(1)}) - g(\mathbf{x}^{(0)})] + (\mathbf{x}^{(1)} - \mathbf{x}^{(0)})^T \sum_{j=1}^{r} [MU_j^{(1)} \overline{\nabla} h_j(\mathbf{x}^{(1)}) - MU_j^{(0)} \overline{\nabla} h_j(\mathbf{x}^{(0)})] = 0.$$

It is straightforward to show that the left term of this sum is strictly negative. Making use of convexity of the constraints in their arguments, the right term can be written as

$$\sum_{j=1}^{r} [MU_j^{(1)} - MU_j^{(0)}][h_j(\mathbf{x}^{(1)}) - h_j(\mathbf{x}^{(0)})].$$

Since for each constraint j, $h_j(\mathbf{x}) \leq 0 \ \forall \mathbf{x}$, $MU_j^{(i)} h_j(\mathbf{x}^{(i)}) = 0, \ i = 0, 1$, and MU_j is positive definite, where the latter two follow from Karush-Kuhn-Tucker conditions, this term is also non-

positive. Hence, the left hand side of (2.10) is strictly negative, which results in a contradiction, unless $\mathbf{x}^{(1)} = \mathbf{x}^{(0)}$. Thus, there exists a unique NE point in the game Γ. □

We finally investigate the relationship between the unique inner NE point and the parameters of the game such as the parameters of the cost and the constraint functions.

Proposition 2.5 *Define the vector $\rho = \{\rho_1, \ldots \rho_{max}\}$, which contains the parameters of the cost and constraint functions of the game Γ. Assume 2.2, 2.3, and 2.4 hold, and $\mathbf{x}^* \in X$ to be the unique inner NE point of the game with parameter vector ρ^*. Then, there exist open sets S_ρ and $S_{\mathbf{x}^*}$ containing ρ^* and $\mathbf{x}^*$, respectively, and a continuous function $\Psi : S_\rho \to S_{\mathbf{x}^*}$ such that $\mathbf{x}^* = \Psi(\rho^*)$ and $g(\Psi(\rho), \rho) = 0$ for all $\rho \in S_\rho$.*

The function Ψ is unique in the sense that if $\rho \in S_\rho$, $\mathbf{x} \in S_{\mathbf{x}^*}$, and $g(\mathbf{x}, \rho) = 0$, then $\mathbf{x} = \Psi(\rho)$.

Proof. It follows from Theorem 2.1 that the NE, $\mathbf{x}^*$, of the game Γ is the unique solution to the set of nonlinear equalities

$$\overline{\nabla} J(\mathbf{x}^*) = 0.$$

Since by Theorem 2.1 $J(\mathbf{x})$ is twice continuously differentiable in all its arguments, $g(\mathbf{x})$ is continuously differentiable. In addition, by Theorem 2.3 the matrix $\mathcal{G}(\mathbf{x})$ defined in (2.4) is positive definite. Thus, the result follows immediately from the *Implicit Function Theorem* [81, p. 668]. □

Corollary 2.1 *Let $S_{\mathbf{x}^*}$ be an open set around the unique inner NE point, $\mathbf{x}^*$, of the game Γ with the parameter vector ρ, and assume Theorems 2.2, 2.3, and 2.4 hold. Then small changes in ρ can only result in small variations of the NE point, x^*, as long as the new NE point $\mathbf{x}^{**}$ is in the set $S_{\mathbf{x}^*}$.*

2.2 The Congestion Control Game

2.2.1 The network model and the cost function

We consider a general network model based on fluid approximations. Fluid models are widely used in addressing a variety of network control problems such as congestion control, routing, and pricing. The topology of the network is characterized by a set of nodes $\mathcal{N} = \{1, \ldots, N\}$ and a set of links connecting the nodes, $\mathcal{L} = \{1, \ldots, L\}$, with each link $l \in \mathcal{L}$ having a fixed positive capacity $c_l > 0$, and is associated with a buffer $b_l \geq 0$. Here, we implicitly make the natural

assumption of *connectivity*. There are M users sharing the network, with the set of users being $\mathcal{M} = \{1, \ldots, M\}$. For simplicity, each user is associated with a unique *connection* or path R between a source and destination node. The i^{th} user sends its nonnegative flow $x_i \geq 0$ over its path R_i, which is determined by a routing algorithm, and corresponds to a subset of links $l \in \mathcal{L}$ connecting the source and destination nodes. A routing matrix $\mathbf{A}$ is defined as in [12] that describes the relation between the set of routes $\mathcal{R} = \{1, \ldots, M\}$ associated with the users (connections) and links $l \in \mathcal{L}$,

$$A_{l,i} = \begin{cases} 1, & \text{if source i uses link } l \\ 0, & \text{if source i does not use link } l \end{cases}, \tag{2.11}$$

where $i \in \mathcal{M}$ and $l \in \mathcal{L}$. We assume without loss of any generality that $\mathbf{A}$ has no rows or columns that are identically zero.

Using the routing matrix $\mathbf{A}$, the capacity constraints of the links are given by

$$\mathbf{A}\mathbf{x} \leq \mathbf{c}, \tag{2.12}$$

where $\mathbf{x}$ is the $(M \times 1)$ flow rate vector of users and $\mathbf{c}$ is the $(L \times 1)$ link capacity vector. The flow rate vector $\mathbf{x}$ is said to be feasible if it is nonnegative and satisfies (2.12). Let $\mathbf{x_{-i}}$ be the flow rate vector of all users except the i^{th} one. For a given fixed, feasible $\mathbf{x_{-i}}$, there exists a strict upper-bound $m_i(\mathbf{x_{-i}})$ on flow rate x_i of the i^{th} user based on (2.12): $m_i(\mathbf{x_{-i}}) = \min_{l \in R_i} (c_l - \sum_{j \neq i} A_{l,j}\, x_j) \geq 0$.

For the given general topology network model, we propose a network game with M users. It is assumed that the routing problem has already been solved and individual routes $R \in \mathcal{R}$ do not change during the connection. Our analysis is based on noncooperative game theory. Here, the users (players) are noncooperative in the sense that they have no means of communicating with each other about their preferences, and each user wishes to optimize its usage of the network resources independently. A specific cost function J is assigned to each user, which will be indexed by i for user i. This cost function not only models the user's preferences but also includes a feedback term capturing the current network state. The i^{th} user minimizes this cost function by adjusting its flow rate $0 \leq x_i \leq m_i(\mathbf{x_{-i}})$ given the fixed, feasible flow rates of all other users on its path, $\{x_j : j \in (R_j \cap R_i)\}$.

The cost function of the i^{th} user J_i is the difference between a user-specific pricing function, P_i, and a utility function U_i. The pricing function P_i depends on the current state of the network. This "feedback" term can be interpreted as the price a user pays for using the network resources. There are a variety of approaches in the literature on possible choices for the pricing term, depending on the specific feedback type. For example, studies [12,32] develop an explicit congestion notification

(ECN) mechanism based on packet marking. Another approach [13, 14] makes use of the queuing delays as an indication of congestion level in the network. One advantage of the latter approach is that it is based on measurements of the individual users, and does not require active participation of the network. The prices in this context should be interpreted in terms of network credits, which do not necessarily relate to real money. The pricing structure here, however, does perform one of the main functions of money: measuring and quantifying the resources. This provides a basis for versatile resource allocation schemes.

The utility function of the i^{th} user is defined to be increasing and concave in accordance with elastic traffic as well as with the economic principle, law of diminishing returns. We focus on the bandwidth as the main resource in the system. Therefore, the utility of the i^{th} user depends only on its own flow rate. Thus, the cost function is defined as the difference between the pricing and the utility functions:

$$J_i(\mathbf{x}; \mathbf{c}, \mathbf{A}) = P_i(\mathbf{x}; \mathbf{c}, \mathbf{A}) - U_i(x_i). \tag{2.13}$$

We note that P_i does not necessarily depend on the flow rates of all other users; it can be structured to depend only on the flow rates of the users sharing the same links on the path of user i.

2.2.2 Existence and uniqueness of NE in the network game

In the given context of the network game, the Nash equilibrium is defined as a set of flow rates $\mathbf{x}^*$ (and corresponding costs J^*), with the property that no user can benefit by modifying its flow while the other players keep theirs fixed. Furthermore, if the NE $\mathbf{x}^*$ meets the capacity constraints as well as the positivity constraint with strict inequality, then it is an *inner* solution. Mathematically speaking, $\mathbf{x}^*$ is in NE, when x_i^* of any i^{th} user is the solution to the following optimization problem given that all users on its path have equilibrium flow rates, $\mathbf{x}_{-i}^*$:

$$\min_{0 \le x_i \le m_i(\mathbf{x_{-i}}^*)} J_i(x_i, x_{-i}^*, \mathbf{c}, \mathbf{A}) \ , \tag{2.14}$$

where $\mathbf{x_{-i}}$ denotes the collection $\{x_j : j \in R_j \cap R_i\}_{j=1,\ldots,M}$. To proceed further, we make the following two assumptions.

Assumption 2.5 *$P_i(\mathbf{x})$ is jointly continuous in all its arguments and twice continuously differentiable, non-decreasing and convex in x_i, i.e.*

$$\partial P_i(\mathbf{x})/\partial x_i \ge 0 \ , \ \partial^2 P_i(\mathbf{x})/\partial x_i^2 \ge 0. \tag{2.15}$$

Assumption 2.6 *$U(x_i)$ is jointly continuous in all its arguments and twice continuously differen-*

tiable, nondecreasing and strictly concave in x_i, i.e.

$$\partial U_i(x_i)/\partial x_i \geq 0 \ , \ \partial^2 U_i(x_i)/\partial x_i^2 < 0 \ , \forall x_i$$

Moreover, the optimal solution is an *inner* one, $0 < \sum_j A_{l,j} x_j^* < c_l \ , \forall l$, under the additional assumption:

Assumption 2.7 *The i^{th} user's cost function has the following properties at $x_i = 0$ ($x_i = m_i(\mathbf{x_{-i}})$) : $\partial J_i(\mathbf{x} : x_i = 0)/\partial x_i < 0 \ \forall \mathbf{x}$ ($\partial J_i(\mathbf{x} : x_i = m_i(\mathbf{x_{-i}}))/\partial x_i > 0 \ \forall \mathbf{x}$), respectively.*

Theorem 2.2 below establishes that the congestion control game admits a unique NE under the following further assumption:

Assumption 2.8 *The price function $P_i(\mathbf{x})$ of the i^{th} user is defined as the sum of link price functions on its path,*

$$P_i = \sum_{l \in R_i} P_l(\sum_{j : l \in R_j} x_j),$$

where P_l is defined as a function of the aggregate flow on link l, and satisfies (2.15) with i replaced by l.

Theorem 2.2 *Under Assumptions 2.5-2.8, the network game admits a unique inner Nash equilibrium.*

Proof. The proof of this theorem is a slightly modified version of the one of Theorem 2.1, and is given here for completeness. Let $X := \{\mathbf{x} \in \mathbb{R}^M : \mathbf{A}\mathbf{x} \leq \mathbf{c} \ , \mathbf{x} \geq 0\}$ be the set of feasible flow rate vectors (or strategy space) of the users. The flow rate of a generic i^{th} user is nonnegative and bounded above by the minimum link capacity on its route, $0 \leq x_i < \min_{l \in R_i} c_l$. The set X is clearly closed and bounded, hence, compact. Next, we show that X has a nonempty interior and is convex. Define the following flow rate vector: $\mathbf{x}^{max} := \min_l c_l/M$. Clearly, $\mathbf{x}^{max} \in X$ is feasible and positive as $c_l > 0 \, \forall l$. Hence, there exists at least one positive and feasible flow rate vector in the set X, which is an interior point. Thus, the set X has a nonempty interior. Let $\mathbf{x}^1 \, , \mathbf{x}^2 \in X$ be two feasible flow rate vectors, and $0 < \lambda < 1$ be a real number. We have, for any $\mathbf{x}^\lambda := \lambda \mathbf{x}^1 + (1 - \lambda)\mathbf{x}^2$,

$$\mathbf{A}\mathbf{x}^\lambda = \mathbf{A}(\lambda \mathbf{x}^1 + (1 - \lambda)\mathbf{x}^2) \leq \mathbf{c}$$

Furthermore, $\mathbf{x}^\lambda \geq 0$ by definition. Hence, $\mathbf{x}^\lambda$ is feasible and is in X for any $0 < \lambda < 1$. Thus, the set X is convex. By a standard theorem of game theory (Theorem 4.4, p.176, in [1]), the network game admits a NE.

We now prove uniqueness. Differentiating (2.13) with respect to x_i, and using Assumptions 2.5 and 2.6, we have

$$f_i(\mathbf{x}) := \frac{\partial J_i(\mathbf{x})}{\partial x_i} = \frac{\partial P_i(\mathbf{x})}{\partial x_i} - \frac{\partial U_i(x_i)}{\partial x_i} \ . \tag{2.16}$$

As a simplification of notation, $\mathbf{c}$ and $\mathbf{A}$ are suppressed as arguments of the functions for the rest of this proof.

Differentiating $J_i(\mathbf{x})$ twice with respect to x_i yields

$$\frac{\partial f_i(\mathbf{x})}{\partial x_i} = \frac{\partial^2 J_i(\mathbf{x})}{\partial x_i^2} = \frac{\partial^2 P_i(\mathbf{x})}{\partial x_i^2} - \frac{\partial^2 U_i(x_i)}{\partial x_i^2} > 0$$

Hence, J_i is unimodal and has a unique minimum. Based on Assumption 2.7, $f_i(\mathbf{x})$ attains the zero value at $m_i(\mathbf{x_{-i}}) > x_i > 0$ given a fixed feasible $\mathbf{x_{-i}}$. Thus, the optimization problem (2.14) admits a unique positive solution.

To preserve notation, let $\frac{\partial^2 J(\mathbf{x})}{\partial x_i^2}$ be denoted by B_i. Further introduce, for $i, j \in \mathcal{M}$, $j \neq i$,

$$\frac{\partial^2 J_i(\mathbf{x})}{\partial x_i \partial x_j} = \frac{\partial^2 P_i(\mathbf{x})}{\partial x_i \partial x_j} =: A_{i,j} \ ,$$

with both B_i and $A_{i,j}$ defined on the space where $\mathbf{x}$ is nonnegative, and bounded by the link capacities. Suppose that there are two NEs, represented by two flow vectors $\mathbf{x}^1$ and $\mathbf{x}^0$, with elements x_i^0 and x_i^1, respectively.

As the NE is necessarily an inner solution, it follows from first-order optimality condition that $g(\mathbf{x}^0) = 0$ and $g(\mathbf{x}^1) = 0$, where $g(\mathbf{x})$ was defined in (2.2). Define the flow vector $\mathbf{x}(\theta)$ as a convex combination of the two equilibrium points $\mathbf{x}^0$, $\mathbf{x}^1$:

$$\mathbf{x}(\theta) = \theta \mathbf{x}^0 + (1 - \theta)\mathbf{x}^1$$

where $0 < \theta < 1$. By differentiating $\mathbf{x}(\theta)$ with respect to θ,

$$\frac{dg(\mathbf{x}(\theta))}{d\theta} = G(\mathbf{x}(\theta))\frac{dx(\theta)}{d\theta} = G(\mathbf{x}(\theta))(\mathbf{x}^1 - \mathbf{x}^0) \ , \tag{2.17}$$

where $G(\mathbf{x})$ is the Jacobian of $g(\mathbf{x})$ with respect to $\mathbf{x}$:

$$G(\mathbf{x}) := \begin{pmatrix} B_1 & A_{12} & \cdots & A_{1M} \\ \vdots & & \ddots & \vdots \\ A_{M1} & A_{M2} & \cdots & B_M \end{pmatrix}_{M \times M} \ . \tag{2.18}$$

We also note that, by Assumption 2.8:

$$\sum_{l\in(R_i\cap R_j)} \frac{\partial^2 J_l(\mathbf{x})}{\partial x_i \partial x_j} = \sum_{l\in(R_i\cap R_j)} \frac{\partial^2 J_l(\mathbf{x})}{\partial x_i \partial x_j}$$

$$\Rightarrow A(i,j) = A(j,i) \;\; i,j \in \mathcal{M} \; .$$

Hence, $G(\mathbf{x})$ is symmetric. Integrating (2.17) over θ,

$$0 = g(\mathbf{x}^1) - g(\mathbf{x}^0) = \left[\int_0^1 G(\mathbf{x}(\theta))d\theta\right](\mathbf{x}^1 - \mathbf{x}^0) \; , \tag{2.19}$$

where $(\mathbf{x}^1 - \mathbf{x}^0)$ is a constant flow vector. Let $\overline{B_i(\mathbf{x})} = \int_0^1 B_i(\mathbf{x}(\theta))d\theta$ and $\overline{A_{ij}(\mathbf{x})} = \int_0^1 A_{ij}(\mathbf{x}(\theta))d\theta$. In view of Assumptions 2.6 and 2.8, $B_i(\mathbf{x}) > A_{ij}(\mathbf{x}) > 0 \; , \; \forall i,j$. Thus, $\overline{B_i(\mathbf{x})} > \overline{A_{ij}(\mathbf{x})} > 0$, for any $\mathbf{x}(\theta)$. In order to simplify the notation, define the matrix $\mathcal{G}(\mathbf{x}^1, \mathbf{x}^0) := \int_0^1 G(\mathbf{x}(\theta))d\theta$, which can be shown to be full rank for any fixed $\mathbf{x}$. Rewriting (2.19) as, $0 = \mathcal{G} \cdot [\mathbf{x}^1 - \mathbf{x}^0]$, since $\mathcal{G}$ is full rank, it readily follows that $\mathbf{x}^1 - \mathbf{x}^0 = 0$. Therefore, the NE is unique.

Under Assumption 2.7, the NE has to be an inner solution, as the following argument shows. First, $\mathbf{x} \geq 0$, with $x_i = 0$ for at least one i, cannot be an equilibrium point since user i can decrease its cost by increasing its flow rate. Similarly, the boundary points $\{\mathbf{x} \in \mathbb{R}^M : \mathbf{Ax} \leq \mathbf{c} \; , \; \mathbf{x} \geq 0, \text{with } (Ax)_l = c_l \text{ for at least one link } l\}$ cannot constitute NE, as users whose flows pass through the link can decrease their flow rates under Assumption 2.7. Thus, under Assumptions 2.5-2.8 the network game admits a unique inner NE. □

2.2.3 Global stability

We consider a simple dynamic model of the network game where each user changes its flow rate in proportion with the gradient of its cost function with respect to its flow rate. Note that this corresponds to the well-known steepest descent algorithm in nonlinear programming [81]. Hence, the user update algorithm is

$$\begin{aligned} \dot{x}_i(t) &= \frac{dx_i(t)}{dt} = -\frac{\partial J_i(\mathbf{x}(t))}{\partial x_i} \\ &= \frac{dU_i(x_i)}{dx_i} - \textstyle\sum_{l\in R_i} f_l\Big(\sum_{j\in\mathcal{M}_l} x_j\Big) := \Theta_i(\mathbf{x}), \end{aligned} \tag{2.20}$$

for all $i = 1, \ldots, M$, where $\mathcal{M}_l(M_l)$ is the set (number) of users whose flows pass through the link, $l \in R_i$; t is the time variable, which we drop in the second line for a more compact notation;

and f_l is defined as $f_l(\cdot) := \partial P_l(\cdot)/\partial x_i$.

By Assumption 2.7, the partial derivative of f_l with respect to x_i, $\partial f_l(\cdot)/\partial x_i$, is nonnegative. Furthermore, since $P_l(\mathbf{x})$ is convex and jointly continuous in x_i for all i whose flows pass through the link l, on the compact set of feasible flow rate vectors, $X := \{\mathbf{x} \in \mathbb{R}^M : \mathbf{A}\mathbf{x} \leq \mathbf{c}\ ,\ \mathbf{x} \geq 0\}$, the derivative $\partial f_l(.)/\partial x_i$ can be bounded above by a constant $\alpha_l > 0$. Hence,

$$0 \leq \frac{\partial f_l(\bar{x}_l)}{\partial x_i} \leq \alpha_l, \tag{2.21}$$

where $\bar{x}_l = \sum_{i \in \mathcal{M}_l} x_i$.

Next, we establish the result that the system defined by (2.20) is asymptotically stable on the set X, which is invariant by Assumption 2.8 under the gradient update algorithm (2.20). In order to see the invariance of X , we investigate each boundary of X separately. When $x_i = 0$ for some $i \in \mathcal{M}$, we have $\dot{x}_i > 0$ from (2.20) under Assumption 2.8 due to the gradient descent algorithm of user i. Hence, the system trajectory moves toward inside of X. Likewise, in the case of $\bar{x}_l = c_l$ for some $l \in \mathcal{L}$, it follows from (2.20) and Assumption 2.8 that $\dot{x}_i < 0\ \forall i \in \mathcal{M}_l$, and hence, the trajectory remains inside the set X.

The equilibrium state of the system (2.20) in X is of course the unique NE $\mathbf{x}^*$ referred to in Theorem 2.2. Let us define a candidate Lyapunov function $V : \mathbb{R}^M \to \mathbb{R}^+$ as

$$V(\mathbf{x}) := \frac{1}{2}\sum_{i=1}^{M} \Theta_i^2(\mathbf{x}),$$

which is in fact restricted to the domain X. Further let $\mathbf{\Theta} := [\Theta_1, \ldots, \Theta_M]$. Taking the derivative of V with respect to t on the trajectories generated by (2.20), we obtain

$$\dot{V}(\mathbf{x}) = \sum_{i=1}^{M} \frac{d^2 U_i(x_i)}{dx_i^2}\Theta_i^2(\mathbf{x}) - \mathbf{\Theta}^T(\mathbf{x})A^T K A \mathbf{\Theta}(\mathbf{x}),$$

where A is the routing matrix, and K is a diagonal matrix defined as

$$K := \mathrm{diag}\big[\frac{\partial \mathrm{f}_1(\bar{\mathrm{x}})}{\partial \bar{\mathrm{x}}}, \frac{\partial \mathrm{f}_2(\bar{\mathrm{x}})}{\partial \bar{\mathrm{x}}}, \ldots, \frac{\partial \mathrm{f}_\mathrm{M}(\bar{\mathrm{x}})}{\partial \bar{\mathrm{x}}}\big].$$

Since $A^T K A$ is nonnegative definite and d^2U_i/dx_i^2 is uniformly negative definite, $V(\mathbf{x})$ is strictly decreasing, $\dot{V}(\mathbf{x}) < 0$, on the trajectory of (2.20). Thus, the system is asymptotically stable on the invariant set X by Lyapunov's stability theorem (see Theorem 3.1 in [82]).

Theorem 2.3 *Assume that Assumptions 2.5-2.8 hold. Then, the unique Nash equilibrium of the network game is globally stable on the compact set of feasible flow rate vectors,* $X := \{\mathbf{x} \in \mathbb{R}^M :$

$\mathbf{Ax} \leq \mathbf{c}$, $\mathbf{x} \geq 0\}$ *under the gradient algorithm given by*

$$\dot{x_i} = -\frac{\partial J_i(\mathbf{x})}{\partial x_i} \, , i = 1, \ldots, M.$$

We note that under *A2* one can bound $\dot{V}$ above by

$$\dot{V}(\phi(\mathbf{x}(t))) \leq -\varepsilon V(\phi(\mathbf{x}(t))),$$

where

$$\varepsilon := \min_i \min_{x_i \in X} \frac{d^2 U_i(x_i)}{dx_i^2}. \tag{2.22}$$

Remark 2.1 *If $\varepsilon > 0$, then the unique Nash equilibrium of the network game is exponentially stable.*

2.2.4 System problem and optimality of NE

We investigate the optimality of NE with respect to the "system problem" for the network game studied above, and discuss its relationship with the models of Kelly et al. [12] and subsequent studies [13, 14, 32], where the system problem is defined as the constrained optimization problem

$$\begin{array}{c} \max_{\mathbf{x} \geq 0} \ \sum_{i \in \mathcal{M}} U_i(x_i) \\ \text{subject to } \ \mathbf{Ax} \leq [c_1 \ldots c_L]^T, \end{array} \tag{2.23}$$

or a relaxed version of it. This system goal is motivated by the fact that the sum of the utilities of users is maximized, whereas aggregate cost at the links is minimized. The cost function at a link may be chosen as the average delay a packet experiences or the percentage of dropped packets with respect to the total flow at the link.

The centralized problem (2.23) is solved by introducing a user problem and a network problem [12] which leads to distributed algorithms. The user problem can be seen as a "trivial game," and is defined for the i^{th} user as

$$\min_{x_i \geq 0} \{\lambda_i x_i - U_i(x_i)\} \, , \tag{2.24}$$

where λ_i represents the price per unit flow rate, and is assumed not to be a function of x_i. The network problem, on the other hand, yields these λ_i's. In order to solve the network problem, however, a centralized knowledge of the user preferences is necessary. This difficulty is circumvented by introducing a system of coupled differential equations for x_i and λ_i. The solutions to these differential equations converge to the optimal solutions of the user and network problems, and hence to the solution of the system problem (2.23).

In this study, we consider a system problem of the form

$$\min_{\mathbf{x}} \sum_{l\in\mathcal{L}} P_l(\sum_{i:l\in R_i} x_i) - \sum_{i\in\mathcal{M}} U_i(x_i). \tag{2.25}$$

In our formulation, unlike previous ones, the user problem is not decoupled, and is a genuine game as defined by (2.14). Furthermore, we show below that the NE of this game (whose existence and uniqueness have already been established) solves the system problem (2.25), where users take the effect of their strategies into account when optimizing their costs. Thus, the Nash solution of the network game is efficient regardless of the number of users in the network.

Theorem 2.4 *The unique NE of the game (2.14) solves the following system problem:*

$$\min_{\mathbf{x}} Sys(\mathbf{x}) = \min_{\mathbf{x}} \left[\sum_{l\in\mathcal{L}} P_l(\sum_{i:l\in R_i} x_i) - \sum_{i\in\mathcal{M}} U_i(x_i)\right], \tag{2.26}$$

where P_l and U_i satisfy assumptions A1-A3 for all $i \in \mathcal{M}$ and $l \in \mathcal{L}$.

Proof. To solve the unconstrained optimization problem (2.26), we take the gradient of $Sys(\mathbf{x})$ with respect to user flow rates $\mathbf{x}$ and obtain the first-order necessary condition for optimality: $\nabla Sys(\mathbf{x}) = 0$. Notice that the partial derivatives of the link costs at the links not on the path of the i^{th} user with respect to x_i yield zero. Likewise, the utility function of each user depends only on that user's flow rate. Hence, the first-order necessary condition of this problem coincides with $g(\mathbf{x}^*) = \overline{\nabla} J(\mathbf{x}^*) = 0$, which was introduced in (2.2). Furthermore, the solution to (2.26) is unique as $\nabla^2 Sys(\mathbf{x})$ is equal to $G(\mathbf{x})$ in (2.18), and thus is positive definite. Therefore, the NE, $\mathbf{x}^*$, solves the system problem (2.26). □

2.3 Global Stability under Bounded and Heterogeneous Communication Delays

We now investigate global stability of the gradient algorithm (2.20) under bounded and heterogeneous communication delays. The pricing function of the i^{th} user is defined in accordance with assumption *A4* as

$$P_i = \sum_{l\in R_i} P_l(\sum_{j\in\mathcal{M}_l} x_j),$$

where R_i is the path (route) of user i, and P_l is the pricing function at link $l \in \mathcal{L}$. The update algorithm with communication delays is then given by

$$\dot{x_i}(t) = \frac{dU_i(x_i(t))}{dx_i} - \sum_{l \in R_i} f_l\Big(\sum_{j \in \mathcal{M}_l} x_j(t - r_{li} - r_{lj})\Big) \tag{2.27}$$

where r_{li} and r_{lj} are fixed communication delays between the l^{th} link and the i^{th} and j^{th} users respectively. [1] To simplify the notation we define

$$\bar{x}_l^i(t-r) := \sum_{j \in \mathcal{M}_l} x_j(t - r_{li} - r_{lj}).$$

In addition, let q be an upper-bound on the maximum round-trip time (RTT) in the system:

$$q := 2 \max_i \sum_{l \in R_i} r_{li} - r_{(l-1)i},$$

where $r_{0i} = 0 \ \forall i$. Finally, define $\mathbf{x}_t := \{\mathbf{x}(t+s),\ -q \leq s \leq 0\}$, and by a slight abuse of notation let $\Theta_i(\mathbf{x}_t)$ denote the right hand side of (2.27).

We next make use of the stability theory for autonomous systems of [83], and generalize the scalar analysis of [84] and also of Chapter 5.4 of [83] to the multidimensional (multiuser) case. Let $\phi_i \in \mathcal{C}\big([-r_i, 0], \mathbb{R}\big)$ be a feasible flow rate function (initial condition) for the i^{th} user's dynamics (2.27) at time $t = 0$, where $\mathcal{C}$ is the set of continuous functions. In addition, let $\mathbf{x}(\phi)(t)$ be the solution of (2.27) through ϕ for $t \geq 0$, and $\dot{\mathbf{x}}(\phi_i)(t)$ be its derivative. In order to simplify the notation, we will use $\mathbf{x}(\phi)$ and $\mathbf{x}$, as well as $\Theta(\phi)$ and Θ and their respective derivatives, interchangeably for the remainder of the paper.

A continuously differentiable and positive function $V : \mathcal{C}^M \to \mathbb{R}^+$ is defined as

$$V(\mathbf{x}_t(\phi)) := \frac{1}{2}\sum_{i=1}^{M} \Theta_i^2(\mathbf{x}_t(\phi)) = \frac{1}{2}\mathbf{\Theta}^T(\mathbf{x}_t(\phi))\mathbf{\Theta}(\mathbf{x}_t(\phi)).$$

We introduce the candidate Lyapunov function $\overline{V} : \mathbb{R}^+ \times \mathcal{C}^M \to \mathbb{R}^+$,

$$\overline{V}(t;\phi) := \sup_{t-2q \leq s \leq t} V(\mathbf{x}_s(\phi)).\ ^{[2]}$$

Let $\dot{\overline{V}}(t;\phi)$ and $\dot{V}(t;\phi)$ be defined as the upper right-hand derivatives of $\overline{V}(t;\phi)$ and $V(t;\phi)$,

[1] Here we implicitly make the assumption that queueing delays are negligible compared to the fixed propagation delays in the system.

[2] Without any loss of generality, we define $V(\mathbf{x}_s) = 0,\ s \in [-2q, -q]$.

respectively along $\mathbf{x}_t(\phi)$. In order for $\overline{V}(t;\phi)$ to be nonincreasing, $\dot{\overline{V}}(t;\phi) \leq 0$, the set

$$\Phi = \{\phi \in \mathcal{C} : \overline{V}(t;\phi) = V(\mathbf{x}_t(\phi)); \dot{V}(\mathbf{x}_t(\phi)) > 0 \; \forall t \geq 0\} \tag{2.28}$$

has to be empty. To see this consider the case when the set Φ is not empty. Then, by definition, there exists a time t and an $h > 0$ such that $\dot{\overline{V}}(\mathbf{x}_{t+h}(\phi)) > \dot{\overline{V}}(\mathbf{x}_t(\phi))$, and hence, $\dot{V}(\mathbf{x}_t(\phi))$ cannot be nonincreasing. We now show that the set Φ is indeed empty.

Assume otherwise. Then, for any given t, there exists an $\epsilon > 0$ such that

$$\overline{V}(t;\phi) = V(\mathbf{x}_t(\phi)) = \sum_{i=1}^{M} \Theta_i^2(\mathbf{x}_t(\phi)) = \epsilon \tag{2.29}$$

and

$$V(\mathbf{x}_s(\phi)) = \sum_{i=1}^{M} \Theta_i^2(\mathbf{x}_s) \leq \epsilon \; , \; s \in [t-2q \, , \, t].$$

Thus, the following bound on Θ_i, and thus on $\dot{x}_i$, follows immediately:

$$|\Theta_i(\mathbf{x}_s)| = |\dot{x}_i(s)| \leq \sqrt{\epsilon} \; , \; s \in [t-2q \, , \, t]. \tag{2.30}$$

Taking the derivative of $\dot{x}_i(t)$ with respect to t, we obtain

$$\ddot{x}_i(t) = \frac{\partial \dot{x}_i(t)}{\partial t} = \dot{\Theta}_i(\mathbf{x}_t) = \frac{d^2 U_i(x_i)}{dx_i^2}\dot{x}_i(t) - \sum_{l \in R_i} \frac{\partial f_l(\bar{x}_l^i(t-r))}{\partial \bar{x}_l^i} \sum_{j \in \mathcal{M}_l} \dot{x}_j(t - r_i - r_j). \tag{2.31}$$

Let $\delta_i := -\min_{x_i \in X} \dfrac{d^2 U_i(x_i)}{dx_i^2} > 0$. Using (2.30) and (2.31), it is possible to bound $\dot{\Theta}_i(\mathbf{x}_s)$ and $\ddot{x}_i(s)$ on $s \in [t-q, t]$ with

$$|\dot{\Theta}_i(\mathbf{x}_s)| = |\ddot{x}_i(s)| \leq \delta_i |\dot{x}_i(s)| + \sum_{l \in R_i} \frac{\partial f_l(\bar{x}_l^i(s-r))}{\partial \bar{x}_l^i} |\bar{x}_l^i(s-r)| \leq (\delta_i + \sum_{l \in R_i} M_l \alpha_l)\sqrt{\epsilon}. \tag{2.32}$$

To simplify the notation, define

$$y_i := \delta_i + \sum_{l \in R_i} M_l \alpha_l.$$

Hence, we have the following bound on $\Theta_i(\mathbf{x}_s), \; s \in [t-q, t]$:

$$\Theta_i(\mathbf{x}_t) - q y_i \sqrt{\epsilon} \leq \Theta_i(\mathbf{x}_s) \leq \Theta_i(\mathbf{x}_t) + q y_i \sqrt{\epsilon}. \tag{2.33}$$

We next show that $V(\mathbf{x}_t(\phi))$ is nonincreasing, and obtain a contradiction to the initial hypothesis that the set Φ is not empty. Assume that $\partial f_l(\bar{x}_l^i(t-r))/\partial \bar{x}_l^i = \partial f_l(\bar{x}_l^j(t-r))/\partial \bar{x}_l^j$, $\forall i,j \in \mathcal{M}_l,\ \forall t$ for each link l. This assumption holds for example when f_l is linear in its argument. Let B be defined in such a way that $B^TB := A^TKA$, where the positive diagonal matrix K is defined in Section 2.2.3. Also define the positive diagonal matrix

$$D(\mathbf{x}) := \mathrm{diag}\left[|\mathrm{D}_1(\mathrm{x}_1)|, |\mathrm{D}_2(\mathrm{x}_2)|, \ldots, |\mathrm{D}_\mathrm{M}(\mathrm{x}_\mathrm{M})|\right],$$

where $D_i(\mathbf{x}) := d^2U_i(x_i)/dx_i^2$. Then, using (2.33), we obtain

$$\begin{aligned}\dot{V}(\mathbf{x}_t) = & -\sum_{i=1}^{M} D_i(x_i)\Theta_i^2(\mathbf{x}_t) - \sum_{i=1}^{M}\Theta_i(\mathbf{x}_t)\cdot\sum_{l\in R_i}\frac{\partial f_l(\bar{x}_l^i(t-r))}{\partial \bar{x}_l^i}\sum_{j\in\mathcal{M}_l}\Theta_j(\mathbf{x}_{t-r_{li}-r_{lj}}) \\ \leq & -\mathbf{\Theta}^TD\mathbf{\Theta} - \mathbf{\Theta}^TB^TB\mathbf{\Theta} + q\sqrt{\epsilon}|\mathbf{\Theta}^TB^TB\mathbf{y}|,\end{aligned} \tag{2.34}$$

where everything is evaluated at t. Now, for any fixed trajectory generated by (2.27), and for a frozen time t, a sufficient condition for $\dot{V}(\mathbf{x}_t) \leq 0$ is

$$q\sqrt{\epsilon} \leq \frac{||B\mathbf{\Theta}||^2 + ||\sqrt{D}\mathbf{\Theta}||^2}{||B\mathbf{\Theta}||\ ||B\mathbf{y}||},$$

where $||\cdot||$ is the Euclidean norm.

Let $k := \frac{||B\mathbf{\Theta}||}{||B\mathbf{y}||} > 0$. Rewriting the sufficient condition we obtain

$$q\sqrt{\epsilon} \leq k + \frac{1}{k}\mu,$$

where $\mu := \frac{||\sqrt{D}\mathbf{\Theta}||^2}{||B\mathbf{y}||^2} > 0$. The following worst-case bound on q can be derived by a simple minimization:

$$q\sqrt{\epsilon} \leq 2\sqrt{\mu}. \tag{2.35}$$

We next find a lower bound on μ. From (2.29) it follows that $||\sqrt{D}\mathbf{\Theta}(\mathbf{x}_t)||^2 \geq \bar{d}\epsilon$, where $\bar{d} := \min_i \min_{x_i\in X}\left|\frac{d^2U_i(x_i)}{dx_i^2}\right|$, and $\sqrt{D}$ is the unique positive definite matrix whose square is D. Furthermore,

$$||B\mathbf{y}||^2 \leq \sum_{i=1}^{M} y_i \sum_{l\in R_i}\alpha_l \sum_{j\in\mathcal{M}_l} y_j.$$

Define also the following upper-bound on y_i:

$$b := \max_i \left(\delta_i + \sum_{l \in R_i} M_l \alpha_l \right).$$

Since $\delta_i > 0$, one obtains $||B\mathbf{y}||^2 \leq Mb^3$, and hence,

$$\mu \geq \frac{\bar{d}\epsilon}{Mb^3}.$$

Thus, from (2.35) a sufficient condition for $V(\mathbf{x}_t)$ to be nonincreasing is

$$q \leq \frac{2\sqrt{\bar{d}}}{\sqrt{M}b^{3/2}}, \tag{2.36}$$

which now holds for all $t \geq 0$.

Finally, we make use of Definition 3.1 and Theorem 3.1 of [83] to establish global asymptotic stability of the system (2.27). Let $S := \{\phi \in \mathcal{C} : \overline{\dot{V}}(t;\phi) = \dot{V}(\mathbf{x}_t(\phi)) = 0\}$. From (2.27) and (2.34) it follows that

$$S' = \{\phi \in \mathcal{C} : \phi(\tau) = \mathbf{x}^*,\ -q \leq \tau \leq 0\} \subset S, \text{ as}$$
$$\mathbf{\Theta}(\mathbf{x}_\tau) = \dot{\mathbf{x}}(\tau) = 0 \Leftrightarrow \mathbf{x}_\tau = \mathbf{x}^* \Rightarrow \dot{V}(\mathbf{x}_\tau) = 0.$$

Hence, S' is the largest invariant set in S, and for any trajectory of the system that belongs identically to S, we have $\mathbf{x}_\tau = \mathbf{x}^*$. In other words, the only solution that can stay identically in S is the unique equilibrium of the system. This then leads to the following theorem:

Theorem 2.5 *Assume that*

$$\partial f_l(\bar{x}_l^i(s-r))/\partial \bar{x}_l^i = \partial f_l(\bar{x}_l^j(s-r))/\partial \bar{x}_l^j,\ \forall i,j \in \mathcal{M}_l\ \forall t.$$

Then, the unique Nash equilibrium of the network game is globally asymptotically stable on the compact set of feasible flow rate vectors, $X := \{\mathbf{x} \in \mathbb{R}^M : \mathbf{A}\mathbf{x} \leq \mathbf{c}\ ,\ \mathbf{x} \geq 0\}$ *under the gradient algorithm*

$$\dot{x}_i(t) = \frac{dU_i(x_i(t))}{dx_i} - \sum_{l \in R_i} f_l\Big(\sum_{j \in \mathcal{M}_l} x_j(t - r_{li} - r_{lj}) \Big),$$

in the presence of fixed heterogeneous delays, $r_{li} \geq 0$*, for all users* $i = 1, \ldots, M$*, and links* $l \in \mathcal{L}$*, if the following condition is satisfied*

$$q \leq \frac{2\sqrt{\bar{d}}}{\sqrt{M}b^{3/2}},$$

where

$$b := \max_i \left(- \min_{x_i \in X} \frac{d^2 U_i(x_i)}{dx_i^2} + \sum_{l \in R_i} M_l \alpha_l \right),$$

and

$$\bar{d} := \min_i \min_{x_i \in X} \left| \frac{d^2 U_i(x_i)}{dx_i^2} \right|.$$

Remark 2.2 *If the user reaction function is scaled by a user-independent gain constant λ then the i^{th} user's response is given by*

$$\dot{x}_i = -\lambda \frac{\partial J_i(\mathbf{x}(t))}{\partial x_i},$$

and the sufficient condition for global stability turns out to be

$$q \leq \frac{2\sqrt{\bar{d}}}{\sqrt{M}\lambda^{3/2} b^{3/2}}.$$

Notice that, for any $\lambda < 1$, the upper-bound on maximum RTT, q, is relaxed proportionally with $\lambda^{3/2}$.

2.4 Robustness Analysis

We have established in Section 2.2.3 the global stability of the unique NE $\mathbf{x}^*$ under the gradient algorithm (2.20). Furthermore, we have presented in Section 2.2.4 a sufficient condition for stability under bounded and heterogeneous communication delays. We next study robustness of the system dynamics to disturbances like variations in number of users, link capacities, and routes.

The set of parameters of the network game, $\{M,\ \mathbf{A},\ \mathbf{c}\}$, were implicitly assumed to be constant throughout the stability analyses in Sections 2.2.3 and 2.2.4. For the robustness analysis, the changes in these parameters caused by the disturbances can be modeled as sudden jumps when compared with the continuous dynamics of the network game (2.20). Therefore, *hybrid system theory* [2] provides a natural framework to study this continuous time system with *discrete events*.

Consider each network game with a specific set of parameters $\{M,\ \mathbf{A},\ \mathbf{c}\}$ as a *subsystem* q of a hybrid system, and let the set of all subsystems be Q. Then, each disturbance varying the fundamental parameters of the network game corresponds to switching from one subsystem to another, and is called a *switching event*. We note that by Theorem 2.2 there exists a unique NE in each network game (subsystem) q. In the analysis of the switching events' effects on overall system stability we make use of the concept of *dwell-time* τ which quantifies the minimum amount of time between two switches, and *average dwell-time*, which is much less restrictive than the dwell-time. Let us denote the number of discontinuities of a switching signal σ on an interval

(t, T) by $N_\sigma(t, T)$. Using the definition in [2], σ has average dwell time τ_a if there exists a positive integer N_0 such that

$$N_\sigma(t, T) \leq N_0 + \frac{T - t}{\tau_a}, \ \forall T \geq t \geq 0.$$

The next theorem is a modified version of Theorem III.4 of [58], and extends the results of Theorem 3.2 of [2] to multiple equilibrium points.

Theorem 2.6 *Consider a family of systems Q defined by $\dot{\mathbf{x}} = F^{(q)}(\mathbf{x}), \forall q \in Q \ \forall \mathbf{x} \in X^{(q)}$ with $\mathbf{x}^{*(q)} \in X^{(q)}$ being the unique NE and $X^{(q)}$ being the strategy space of the q^{th} system. Suppose that there exist $\mathcal{C}^1$ functions $V^{(q)} : X^{(q)} \to \mathbb{R}$, $q \in Q$, class $\mathcal{K}_\infty$ functions $\chi_1^{(q)}$ and $\chi_2^{(q)}$, and a positive number ε such that we have*

$$\chi_1^{(q)}(||\mathbf{x} - \mathbf{x}^{*(q)}||) \leq V^{(q)}(\mathbf{x}) \leq \chi_2^{(q)}(||\mathbf{x} - \mathbf{x}_q^{*(q)}||), \ \forall q \in Q, \tag{2.37}$$

and

$$\dot{V}^{(q)}(\mathbf{x}) \leq -\varepsilon V^{(q)}(\mathbf{x}), \ \forall \mathbf{x} \in X^{(q)}. \tag{2.38}$$

Let $\overline{\mathcal{N}}$ be the union of the smallest level sets of $V^{(q)}, \ \forall q \in Q$ that contain the superset of equilibria $\mathcal{N}(\kappa) := \{\mathbf{x} : ||\mathbf{x} - \mathbf{x}^{*(q)}|| < \kappa, \forall q \in Q\}$, where $\kappa > 0$ is a small positive constant. Suppose also that there exists a finite $\mu(\kappa) > 1$ [3] such that [4]

$$\frac{V^{(q)}(\mathbf{x})}{V^{(r)}(\mathbf{x})} \leq \mu, \quad q, r \in Q, \ \forall \mathbf{x} \in (X^{(q)} \cap X^{(r)}) - \overline{\mathcal{N}}. \tag{2.39}$$

Then, the switched system globally asymptotically converges to the set $\overline{\mathcal{N}}$ for every switching signal σ with average dwell-time

$$\tau_a > \frac{\log \mu}{\varepsilon}. \tag{2.40}$$

Furthermore, $\overline{\mathcal{N}}$ is invariant under the same set of conditions if the dwell-time τ satisfies

$$\tau > \frac{\log \mu}{\varepsilon}, \ \forall t. \tag{2.41}$$

Proof. Let us consider the time interval $(0, T)$ with switching times $t_1, \ldots, t_S$ where we define $T > 0$, $t_0 := 0$, and $S := T/\tau_a$ without loss of generality. Given the switching signal σ, define the

[3] We are naturally interested in switching events, where $\mu > 1$, in order to obtain an upper-bound. Therefore, q and r are labeled accordingly.

[4] We drop the constant κ from the argument of μ to simplify the notation in the remainder of the analysis.

piecewise differentiable function $W(t)$ as

$$W(t) := e^{\varepsilon t} V^{(\sigma)}.$$

On each interval $[t_i, t_{i+1})$ (between switching times), we have from (2.38),

$$\dot{W}(t) \leq \varepsilon W(t) - e^{\varepsilon t} V^{(\sigma)} \leq 0.$$

By (2.39), this implies that

$$W(t_{i+1}) \leq \mu e^{\varepsilon t_i} V^{(\sigma)}(x(t_i)) \leq \mu W(t_i).$$

Notice that the system trajectory may make a jump at time t_{i+1} if $\mathbf{x}(t_{i+1}^-)$ is not feasible anymore after the switch. For the sake of argument, denote the system before the switch as q and the one afterwards as r. If $\mathbf{x}(t_{i+1}^-) \notin X^{(r)}$, then the trajectory jumps at time t_{i+1} to a feasible point $\mathbf{x}(t_{i+1}^+) \in X^{(r)}$ from the point $\mathbf{x}(t_{i+1}^-) \in X^{(q)}$.

Repeating this for all $i = 0, \ldots, S-1$, and using the definition of $W(t)$ we obtain

$$V^{(\sigma)}(x(T^-)) \leq e^{-\varepsilon T} \mu^S V^{(\sigma)}(\mathbf{x}(0)).$$

Then, from (2.40) and definition of S we have

$$V^{(\sigma)}(\mathbf{x}(T^-)) \leq e^{(\frac{\log \mu}{\tau_a} - \varepsilon)T} V^{(\sigma)}(\mathbf{x}(0)). \tag{2.42}$$

It directly follows that $V^{(q)}$ decreases and $\mathbf{x}$ converges to $\mathbf{x}^{*(q)}$ at time T^- for some system $q \in Q$ as T increases. Thus, by the definition of $\overline{\mathcal{N}}$ there exists a $t_0 \in (0, T^-]$ for all $\epsilon > 0$ as T increases, such that for $t \geq t_0$, $||\mathbf{x} - \overline{\mathcal{N}}|| < \epsilon$. In other words, the system trajectory converges globally asymptotically to $\overline{\mathcal{N}}$. More precisely, the trajectory $\mathbf{x}(t)$ converges to $\overline{\mathcal{N}} \cap X^{(\sigma(t))}$ at time t, where $\sigma(t) \in Q$. Notice that, since at the time of switching the system equilibrium shifts from one point to another, no point in the system can be asymptotically stable. The set $\overline{\mathcal{N}}$ of a system with four NE points is illustrated in Figure 2.1.

We now show the invariance of $\overline{\mathcal{N}}$ under (2.41). Suppose that $\overline{\mathcal{N}}$ is not invariant. Then, there exists a trajectory that starts at a point $\mathbf{x} \in \overline{\mathcal{N}}$ and leaves this set. This, however, would correspond to an increase in $V^{(q)}$ for some $q \in Q$, which leads to a contradiction by (2.41) and (2.42). Hence, $\overline{\mathcal{N}}$ is invariant under the set of conditions of the theorem. □

Remark 2.3 *Due to the properties of V and by definition in (2.39), $\mu(\kappa)$ is nonincreasing in κ.*

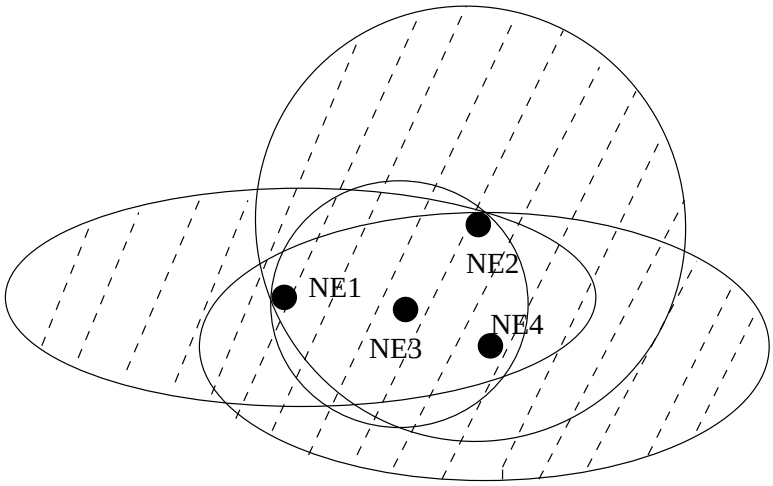

Figure 2.1: The set $\overline{\mathcal{N}}$ of a system with four NE points.

Using the results of Theorem 2.6, we investigate the effect of three specific types of disturbances on system stability: variations in number of users, changes in link capacities, and routing changes. A lower bound on the (average) dwell-time is obtained such that global asymptotic stability of the defined hybrid system is preserved under these disturbances. To simplify the analysis, one can study this hybrid system in fast and slow time scales. Although in the long run parameters of the network game such as number of users, routes of the connections, etc. may change significantly, the variations of these parameters are limited in the fast time scale. Thus, we focus on variations within a relatively short time span, where the parameters of the network game take their values in their respective compact sets.

Let us redefine the number of users M as a variable taking integer values in the interval $[M_{min}\,,\, M_{max}] := Q^{(1)}$. Each value of M corresponds to a different subsystem, say q, in the family of subsystems $Q^{(1)}$, with its own NE point, $\mathbf{x}^{*(q)}$, and feasible flow (strategy) space $X^{(q)}$. Likewise, the routing matrix, A, of the network game with M players takes values in the finite set $\mathcal{A}_M = \{A_1,\, A_2,\, A_{max,M}\} := Q^{(2)}$, which represent all possible routing changes in the short run. Note that, these two disturbances can be modeled using a finite number of subsystems (network games).

Another important parameter of the congestion control game considered is the link capacity vector, $\mathbf{c}$. In wireless networks, link capacity may vary over time due to channel noise and interference [85]. In the Internet-style networks, on the other hand, effective bandwidth may be up to 20% below the maximum capacity due to unresponsive flows on the network [86]. Hence, capacity of each link, $c_l \in \mathbf{c}$ takes values in $[c_{l,min},\, c_{l,max}] := Q_l^{(3)}$. Note that in this case the set of subsystems, $Q^{(3)} = Q_1^{(3)} \times Q_2^{(3)} \times \cdots \times Q_L^{(3)}$, is continuous with infinite number of elements. By Corollary 2.1, small changes in $\mathbf{c}$ results in small shifts of the NE, and hence, does not have a

significant effect on the stability of the system. Therefore, we focus on sudden jumps in link capacities $\mathbf{c}$ and assume that the capacity remains constant for the purposes of this analysis between jumps. Thus, the set of subsystems can again be modeled with a finite number of elements as in the case of other disturbances.

In Theorem 2.6, a lower bound on the average dwell time is given as $\tau_a > \frac{\log \mu}{\varepsilon}$, where μ is defined in (2.39), and the variable ε is given by (2.22) for the network game. Suppose that there exist $\mu_i,\ i = 1, 2, 3$, for variations in the number of users M, in the link capacities $\mathbf{c}$, and in the routing matrix A, respectively, such that $V^{(q^{(i)})}/V^{(r^{(i)})} \leq \mu_i,\ i = 1, 2, 3$. Using the definition of $V(\mathbf{x}(t))$ we can describe the effect of a single disturbance as

$$\frac{V^{(q)}}{V^{(r)}} = \frac{\sum_{j\in\mathcal{M}_u} \phi_j^2(\mathbf{x}(t)) + \sum_{j\in\mathcal{M}_a} \bar{\phi}_j^2(\mathbf{x}(t))}{\sum_{j=1}^{M} \phi_j^2(\mathbf{x}(t))},$$

where $\mathcal{M}_u$ is the set of users not affected, and $\mathcal{M}_a$ is the set of users affected by the disturbance, respectively. The function $\bar{\phi}_j(\mathbf{x}(t)) \neq \phi_j(\mathbf{x}(t))$ of the j^{th} user has at least one parameter as an argument, which is varied by the disturbance.

In order to derive a lower bound on τ_a under the combined effect of all these three disturbances, we calculate μ as:

$$\frac{V^{(q)}}{V^{(r)}} \leq \frac{V^{(q^1)}}{V^{(r^1)}} \frac{V^{(q^2)}}{V^{(r^2)}} \frac{V^{(q^3)}}{V^{(r^3)}} \leq \mu_1\mu_2\mu_3 := \mu,$$

It immediately follows that

$$\tau_a = \tau_1 + \tau_2 + \tau_3 > \frac{\log \mu_1 + \log \mu_2 + \log \mu_3}{\varepsilon}.$$

Then, we have the following result as a special case of Theorem 2.6:

Theorem 2.7 *Let Assumptions 2.5-2.8 hold and ε defined in (2.22) be strictly positive for the network game. Suppose that there exist $\mu_i,\ i = 1, 2, 3$, for variations in the number of users M, in the link capacities $\mathbf{c}$, and in the routing matrix A, respectively, such that*

$$\frac{V^{(q^{(i)})}}{V^{(r^{(i)})}} \leq \mu_i,\ i = 1, 2, 3,\ \ q, r \in Q^{(i)},\ \forall \mathbf{x} \in (X_q^{(i)} \cap X_r^{(i)}) - \overline{\mathcal{N}},$$

where the set of subsystems, $Q^{(i)}\ i = 1, 2, 3$, are associated with the respective disturbance. Furthermore, the set of all subsystems is given by $Q = Q^{(1)} \times Q^{(2)} \times Q^{(3)}$, and $\overline{\mathcal{N}}$ is the union of the smallest level sets of $V^{(q)},\ \forall q \in Q$ that contain the set of equilibria $\mathcal{N} := \{\mathbf{x}^{*(q)}, \forall q \in Q\}$.

The dynamics of the congestion control game globally asymptotically converges to the set $\overline{\mathcal{N}}$

for every switching signal σ with average dwell-time

$$\tau_a > \sum_{i=1}^{3} \frac{\log \mu_i}{\varepsilon}.$$

Furthermore, $\overline{\mathcal{N}}$ is invariant under the same set of conditions if the dwell-time τ satisfies

$$\tau > \sum_{i=1}^{3} \frac{\log \mu_i}{\varepsilon}, \ \forall t.$$

2.4.1 Worst-case bounds

It is difficult –if not impossible– to derive an analytical expression for the lower bound on the average dwell-time τ_a in Theorem 2.7 under general network topologies and cost structures. Therefore, we study a single bottleneck case with a specific cost function, which is symmetric for all users, and obtain analytical worst-case lower bounds on τ_a for each disturbance, separately. First, we investigate the effect of link capacity variations, and then the effect of changes in the number of users in the network on the average dwell-time.

Let the user utility function for the i^{th} user be given by

$$U(x_i) = u \log(\mathbf{x}_i + 1),$$

and the link pricing function be chosen as

$$P(\mathbf{x}) = \frac{\alpha}{2C} \bar{x}^2,$$

where $\bar{x}$ is the sum of flows on the link, and C the capacity of the link.

We consider a dynamic model of the network game similar to the one in (2.20), where each user changes its flow rate proportional to the gradient of its cost function with respect to its flow rate. Hence, the system given by

$$\dot{x}_i = \frac{u}{x_i + 1} - \alpha \frac{\bar{x}}{C}, \quad i = 1, \ldots, M \tag{2.43}$$

has a unique positive NE point, which is symmetric for all users:

$$x_i^* = x_j^* = \sqrt{\frac{1}{4} + \frac{u\,C}{\alpha\,M}} - \frac{1}{2} \ \forall\, i, j \in \mathcal{M}. \tag{2.44}$$

A Lyapunov function $V : \mathbb{R}^M \to \mathbb{R}$ for the network game is defined as

$$V(\mathbf{x}) = \sum_{j=1}^{M} \left(\frac{u}{x_i + 1} - \alpha \frac{\bar{x}}{C} \right)^2 .$$

Variations in link capacity

Let the interval $[C_{min},\, C_{max}]$ be the set where the link capacity C takes its values. To simplify the notation, we define $\Omega(q, r) := (X^{(q)} \cap X^{(r)}) - \overline{\mathcal{N}}$. Then, one can bound μ above by

$$\mu = \max_{\mathbf{x} \in \Omega(q,r)} \frac{\sum_{j=1}^{M} \left(\frac{u}{x_j + 1} - \alpha \frac{\bar{x}}{C_1} \right)^2}{\sum_{j=1}^{M} \left(\frac{u}{x_j + 1} - \alpha \frac{\bar{x}}{C_2} \right)^2} \leq \frac{\max_{\mathbf{x} \in \Omega(q,r)} V^{(q)}(\mathbf{x})}{\min_{\mathbf{x} \in \Omega(q,r)} V^{(r)}(\mathbf{x})}, \tag{2.45}$$

where $C_1,\, C_2 \in [C_{min},\, C_{max}]$ are parameters of the subsystems q and r, respectively.

We first establish a lower bound on $\min_{\mathbf{x} \in \Omega(q,r)} V^{(r)}$ in (2.45). From the strict convexity of V and definition of $\overline{\mathcal{N}}$ it follows that

$$\min_{\mathbf{x} \in \Omega(q,r)} V^{(r)} = \min\{V^{(q)}(\mathbf{x}^{*(r)}), V^{(r)}(\mathbf{x}^{*(q)})\}.$$

Definitions of the Lyapunov function and the NE point in (2.44) then yield

$$V^{(q)}(\mathbf{x}^{*(r)}) = M \left(\frac{u}{\theta(C_2, M) + 0.5} - \frac{\alpha M \left[\theta(C_2, M) - 0.5\right]}{C_1} \right)^2 ,$$

and

$$V^{(r)}(\mathbf{x}^{*(q)}) = M \left(\frac{u}{\theta(C_1, M) + 0.5} - \frac{\alpha M \left[\theta(C_1, M) - 0.5\right]}{C_2} \right)^2 ,$$

where

$$\theta(C, M) := \sqrt{\frac{1}{4} + \frac{uC}{\alpha M}}.$$

Let without loss of generality $C_1 = k\, C_2$, where $k > 1$. Furthermore, define $\beta(C, M)$ as $\theta(C, M) + 0.5$ and $\gamma(k)$ as $\frac{k}{(k-1)}$. We thus obtain through simple algebraic manipulations

$$\min_{\mathbf{x} \in \Omega(q,r)} V^{(r)} = \frac{M u^2}{\beta^2(C_1, M)\gamma^2(k)}.$$

Note that in the worst possible case, where the value of k is maximum, $C_1 = C_{max}$ and $C_2 = C_{min}$.

We next make the assumptions $u \geq 1$ and $uC \geq \alpha M$, and establish an upper bound on

$\max_{\mathbf{x}\in\Omega(q,r)} V^{(q)}(\mathbf{x})$ in (2.45) given by

$$\max_{\mathbf{x}\in\Omega(q,r)} V^{(q)}(\mathbf{x}) \leq Mu^2.$$

Finally, again under the assumptions $u \geq 1$ and $uC \geq \alpha M$, we obtain an upper-bound on μ:

$$\mu \leq \beta^2(C_1, M)\gamma^2(k),$$

where β and γ are defined above, and $k = C_{max}/C_{min}$. Thus,

$$\tau_a \geq \frac{2\log(\beta(C_1, M)\gamma(k))}{\varepsilon}.$$

For example, in the case $M = 10$, $C_1 = 10^6$, $\alpha = 0.2$, and $k = 4$ a worst-case lower bound on the value of τ_a is approximately $6.25/\varepsilon$.

Variations in the number of users

We repeat the analysis in the previous section to investigate the effect of variations in the number of users at a bottleneck link with fixed capacity C. Therefore, we give only an outline of the derivation of the lower bound on average dwell-time. Let the number of users sharing the bottleneck link vary between M_{min} and M_{max}.

By strict convexity of V and by definition of $\overline{\mathcal{N}}$ we again have

$$\min_{\mathbf{x}\in\Omega(q,r)} V^{(r)} = \min\{V^{(q)}(\mathbf{x}^{*(r)}), V^{(r)}(\mathbf{x}^{*(q)})\},$$

where

$$V^{(q)}(\mathbf{x}^{*(r)}) = M_1\left(\frac{u}{\theta(C, M_2) + 0.5} - \frac{\alpha M_1\left[\theta(C, M_2) - 0.5\right]}{C}\right)^2,$$

$$V^{(r)}(\mathbf{x}^{*(q)}) = M_2\left(\frac{u}{\theta(C, M_1) + 0.5} - \frac{\alpha M_2\left[\theta(C, M_1) - 0.5\right]}{C}\right)^2,$$

and $M_1,\ M_2 \in \{M_{min},\ M_{min}+1, \ldots, M_{max}\}$ are the parameters of the subsystems q and r, respectively.

Let, without loss of generality, $M_1 = kM_2$, where $k > 1$. Then, repeating the steps of previous analysis yields

$$\min_{\mathbf{x}\in\Omega(q,r)}\{V^{(q)}, V^{(r)}\} \geq \frac{M_2u^2k^2}{\beta^2(C, M_1)\gamma^2(k)},$$

Likewise,

$$\max_{\mathbf{x}\in\Omega(q,r)} V^{(q)}(\mathbf{x}) \leq M_1 u^2 k^2.$$

Finally, we establish the upper-bound on μ as

$$\mu \leq 4k\beta^2(C, M_1),$$

where $k = \frac{M_{max}}{M_{min}}$ in the worst-case. This leads to

$$\tau_a \geq \frac{2\log(2\sqrt{k}\beta(C, M_1))}{\varepsilon}.$$

For example, in the case $M_2 = 10$, $C = 10^6$, $\alpha = 0.2$, and $k = 4$ a worst-case lower bound on the value of τ_a is approximately $5.95/\varepsilon$.

2.5 Randomized Algorithms for Robustness Analysis

The worst-case bounds on (average) dwell time, which we have derived in Section 2.4.1 are obviously very conservative. Moreover, counterparts of these analytical worst-case bounds cannot be obtained for arbitrary cost functions, for user specific parameters or in the case of general network topologies. Therefore, we resort to *randomized algorithms* for a probabilistic robustness analysis.

Randomized algorithms have been used by the systems and control community for analysis and design of control systems due to their efficiency and low complexity. They are useful, especially when worst-case analysis of complex systems is either very difficult or impossible, as they provide an alternative solution with a trade-off between computational complexity and tightness of the solution [38, 40].

We use randomized algorithms to study robustness properties of the system defined in 2.4.1. Specifically, we investigate the upper-bound on μ as well as its average value. Hence, we gain further insight to the lower bound on dwell-time by comparing the results obtained using randomized algorithms with the worst-case results. Samples are generated by employing Monte Carlo (MC) methods, which are classical and statistically based. Since we do not have an *a priori* probability density function on the parameter variations in the state space, we assume a uniform distribution of samples.

The feasible state space of the network game at a single link shared by M users, and with capacity C is defined as $\mathcal{S} := \{\mathbf{x} \in \mathbb{R}^M : \sum_{i=1}^{M} x_i \leq C,\ \mathbf{x} > 0\}$. Our objective, from definition of μ in (2.45), is to generate sample points uniformly distributed on the set $\Omega(q, r)$ for subsystems q and r. Notice that the dimension of this set is proportional to the number of users M and, hence,

can be very large. Sample generation in such high dimensional sets is feasible only in very special systems, which are affected by real parametric uncertainty bounded in rectangles or spheres [3]. We therefore use the well known *rejection method* (see, e.g., [87]), where we perform rejection from an overbounding set. In this case, we overbound the set $\Omega(q,r)$ by $\mathcal{S}$, which corresponds to the positive quadrant of the real ball

$$B(C) = \{\mathbf{x} \in \mathbb{R}^M : ||\mathbf{x}||_1 \leq C\},$$

where $||\cdot||_1$ is the standard $\mathcal{L}_1$ norm. Thus, we make use of a modified version of the algorithm given in [88] for real uniform sample generation on $\Omega(q,r)$, and obtain an efficient rejection method.

1. Generate M independent identically distributed (i.i.d.) scalar random variables y_i $(i \in \mathcal{M})$ with Laplacian distribution $f_{\mathbf{x}_i}(x_i) = \frac{1}{2}e^{-|x_i|}$.
2. Construct the positive vector $\mathbf{y} > 0$.
3. Generate $z = w^{1/M}$, where w is a random variable uniformly distributed in the interval $[0,1]$.
4. Obtain $\mathbf{x} = Cz\frac{\mathbf{y}}{||\mathbf{y}||_1}$.
5. If $\mathbf{x} \in \Omega(q,r)$, then return $\mathbf{x}$.

In the last step, we determine whether $\mathbf{x}$ is in $\overline{\mathcal{N}}$ or not by comparing $V^{(q)}(\mathbf{x})$ and $V^{(r)}(\mathbf{x})$ with $V^{(q)}(\mathbf{x}^{*(r)})$ and $V^{(r)}(\mathbf{x}^{*(q)})$, respectively. If the former is greater than the latter in both cases, then the sample is accepted as valid by also taking the boundaries of $X^{(q)}$ and $X^{(r)}$ into account. As a result, we obtain an efficient algorithm for generating the flow rate samples, $\mathbf{x}$, uniformly distributed on the target set.

Let us assume that there are N sample points. At each sample point $\mathbf{x}_{(i)} \in \Omega(q,r)$, $i = 1,\ldots,N$, the value of $\mu(\mathbf{x}_{(i)})$ is calculated by

$$\mu(\mathbf{x}_{(i)}) = \frac{V^{(q)}(\mathbf{x}_{(i)})}{V^{(r)}(\mathbf{x}_{(i)})}. \tag{2.46}$$

Then, the maximum value of μ is

$$\mu_{max} := \max_{\mathbf{x}_{(i)},\, i \in N} \mu(\mathbf{x}_{(i)}),$$

and its average value is

$$\bar{\mu} := \frac{1}{N}\sum_{i=1}^{N} \mu(\mathbf{x}_{(i)}).$$

We note that, for a finite sample size, it is important to know how many samples N are needed to obtain "reliable" probabilistic estimates μ_{max} and $\bar{\mu}$. To this end, classical results, such as the Chernoff bound can be used. However, the number of required vector samples is independent of the problem dimension [40]. In this study, the number of samples generated is simply determined by the available computational power.

2.5.1 Numerical evaluation

We investigate numerically the effect of variations in the number of users M and capacity C on the average dwell-time in a single bottleneck link. We also analyze the effect of routing changes on a simple network consisting of two parallel links. The values of μ_{max} and $\bar{\mu}$ are calculated in each case to obtain further insight to the average dwell time. The pricing parameter of the network game defined in Section 2.4.1 is chosen as $\alpha = 0.01$.

Variations in the number of users

Two different methods are employed in order to calculate μ_{max} and $\bar{\mu}$ under the effect of user number variations. First, we randomly choose the number of users $M^{(q)}$ and $M^{(r)}$ of the subsystems q and r, respectively, according to a uniform distribution on the set $[M_{min}, M_{max}] \times [M_{min}, M_{max}]$. Then, for each pair $(M^{(q)}, M^{(r)})$ a specific number of uniformly distributed points $\mathbf{x}$ are generated on the set $\Omega(q, r)$ using the algorithm described in Section 2.5. In the second method, a worst-case simulation is considered, where the number of users jumps directly from M_{min} to M_{max}. Again, μ is calculated using the sample points $\mathbf{x}$ generated.

The parameters are chosen as $M_{min} = 10$ and $M_{max} = 15$ unless otherwise stated. For the first method, 100 random user number pairs and 1000 samples for each pair are generated. A set of randomly generated user number pairs are illustrated in Figure 2.2 as an example. For the worst-case method N is chosen as $10\,000$. The results for various values of link capacity, C, are shown in Table 2.1. In the last row of this table, M_{min} and M_{max} are chosen as 6 and 9, respectively. We note that samples generating μ_{max} values correspond to rare extreme cases. This is further illustrated in Figure 2.3. From Table 2.1, we observe that μ_{max} is increasing in C and decreasing in M under the worst-case simulations, which is in accordance with the results in Section 2.4.1. On the other hand, the value of $\bar{\mu}$ is larger for smaller M under the same capacity C, whereas changing C has only a small effect on $\bar{\mu}$. Finally, an important observation is that the values of $\bar{\mu}$ and μ_{max} are much smaller than the ones in the analytical worst-case bound.

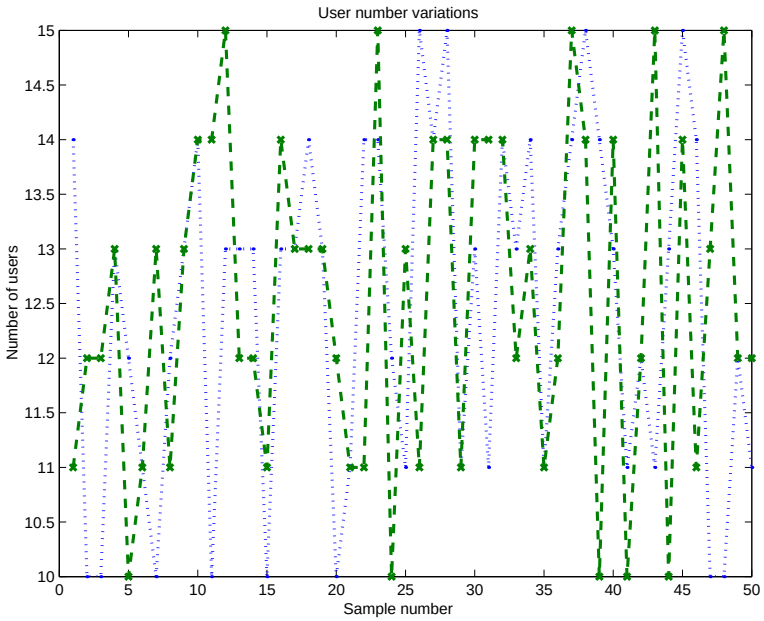

Figure 2.2: A subset of the randomly generated variations in number of users, which are uniformly distributed between 10 and 15.

Table 2.1: Values of μ_{max} and $\bar{\mu}$ for various link capacities.

Capacity		Uniform	Worst-case
$C = 10^3$	$\bar{\mu}$	2.1509	7.0882
	μ_{max}	73.0298	189.2202
$C = 10^4$	$\bar{\mu}$	1.8978	8.9312
	μ_{max}	38.1840	166.2722
$C = 10^6$	$\bar{\mu}$	2.1468	8.5310
	μ_{max}	16.6524	60.2700
$C = 10^6$	$\bar{\mu}$	2.4507	9.4710
	μ_{max}	180.2856	292.2815

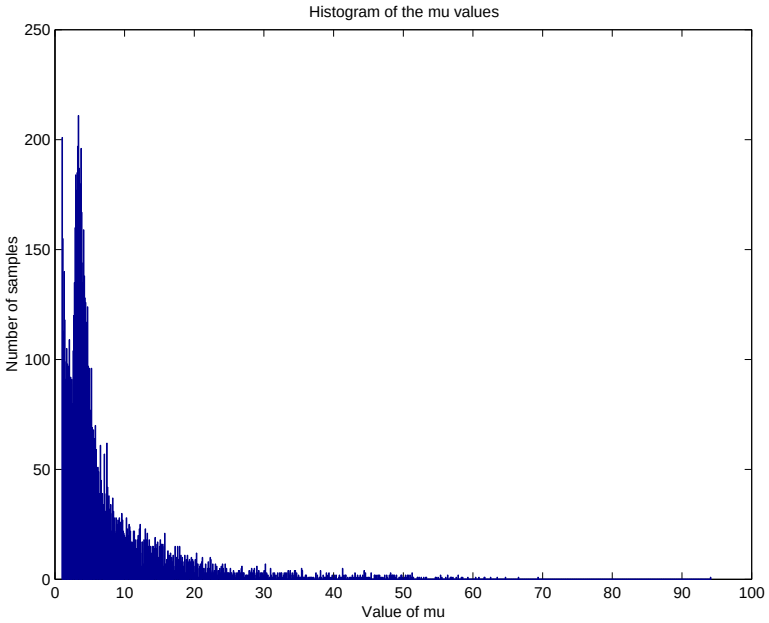

Figure 2.3: An example histogram of μ.

Variations in link capacity

We repeat the analysis of Section 2.5.1. The parameters in this case are chosen as $C_{min} = 0.5 \cdot 10^6$ and $C_{max} = 10^6$. For the first method, generated capacity pairs, $(C^{(q)}, C^{(r)})$, are uniformly distributed on the continuous set $[C_{min}, C_{max}] \times [C_{min}, C_{max}]$. Figure 2.4 exemplifies 30 of such pairs. For the worst-case simulation, the capacity is decreased from maximum to minimum. The number of samples for both methods are the same as the ones in Section 2.5.1. The results are given by the last row, $C_{min} = 0.5 \cdot 10^3$ and $M = 10^3$.

From Table 2.2, we make observations similar to the ones in Section 2.5.1. On the other hand, the values of $\bar{\mu}$ and μ_{max} due to variations in link capacity are smaller than the ones due to variations in number of users. This may be explained by considering the closeness of the equilibrium points, and hence, of the Lyapunov function values of subsystems distinguished only by capacity.

Variations in routing

We consider a simple network consisting of two parallel links with the same capacity, and study the effect of variations in flow routes. We randomly generate 100 pairs of routing matrices, and 1000 samples of flow rates $\mathbf{x}$ uniformly distributed on $\Omega(q, r)$. The results obtained for various number of users and capacities are shown in Table 2.3. We note that the value of μ_{max} is increasing in C. On the other hand, when the value of $\bar{\mu}$ due to routing variations is compared with the ones due to variations in capacity or number of users, we observe that it is close to the sum of the others for the

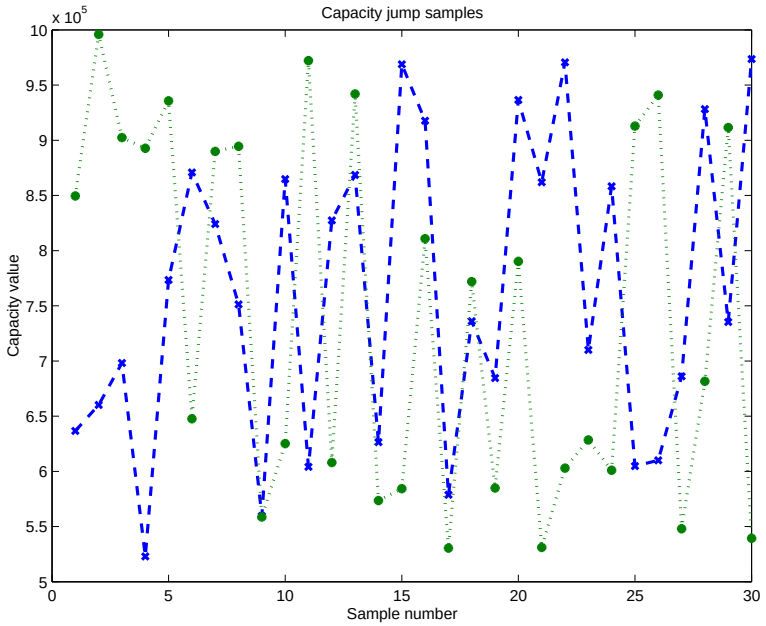

Figure 2.4: A set of randomly generated capacity pairs, $(C^{(q)}, C^{(r)})$, which are uniformly distributed between $0.5 \cdot 10^6$ and 10^6.

Table 2.2: Values of μ_{max} and $\bar{\mu}$ for various number of users.

Number of users		Uniform	Worst-case
$M = 5$	$\bar{\mu}$	1.3006	4.0112
	μ_{max}	3.5442	4.5114
$M = 10$	$\bar{\mu}$	1.2553	4.0079
	μ_{max}	3.3602	4.2463
$M = 15$	$\bar{\mu}$	1.2844	4.0088
	μ_{max}	3.3037	4.1524
$M = 10$	$\bar{\mu}$	1.2509	2.1835
	μ_{max}	12.8131	11.7366

same number of users and capacities. Considering the fact that routing changes cause variations both in link capacities and in the number of users, this observation is not surprising.

Table 2.3: Values of μ_{max} and $\bar{\mu}$ for various number of users and link capacities.

Number of users	Capacity		Values
$M = 10$	$C = 10^3$	$\bar{\mu}$	1.0883
		μ_{max}	3.0617
$M = 10$	$C = 10^4$	$\bar{\mu}$	3.3252
		μ_{max}	3896
$M = 15$	$C = 10^3$	$\bar{\mu}$	1.0815
		μ_{max}	4.0513

2.6 Simulation Studies

2.6.1 Communication delays

The results presented in Section 2.2.4 for the congestion control game defined are evaluated numerically using MATLAB. The delay differential equations are solved using the delay differential solver, *dde23* [89]. The utility function for the i^{th} user is chosen as

$$U_i = u_i \log(x_i + 1),$$

where u_i is a user-specific positive preference parameter. The pricing function at the link l is defined as

$$P_l = \frac{\alpha}{2}(\sum_{j:l\in R_j} x_j)^2,$$

where α is the pricing constant. We choose here the cost function, cost parameters, and link capacities in accordance with Assumptions 2.5-2.8. [5] In the case of a single link shared by M users, the user update algorithm follows directly from (2.27), and is given by

$$\dot{x_i}(t) = \frac{u_i}{x_i(t)+1} - \alpha \sum_{j:l\in R_j} x_j(t - r_j - r_i), \quad \forall i = 1, \ldots, M.$$

We first investigate single-user on a single-link case for illustrative purposes. The parameters in user's cost function are chosen as $u = 1$ and $\alpha = 1$. We simulate the system under communication

[5] We note, however, that in a network implementation cost parameters α and u can be adjusted "online" through an adaptive algorithm, which takes capacity constraints on the network into account, in order to satisfy *A3* and make the NE an inner solution.

delays of $r = 0.5,\ 1$, and 2 as observed in Figure 2.5. From Theorem 2.5, the condition for stability is calculated as $r < 0.42$. Since this condition is only sufficient the system could remain stable for $r > 0.42$, which is indeed what happens. However, the rate of convergence decreases significantly for increasing r, and for delays $r > 2$ the system becomes unstable.

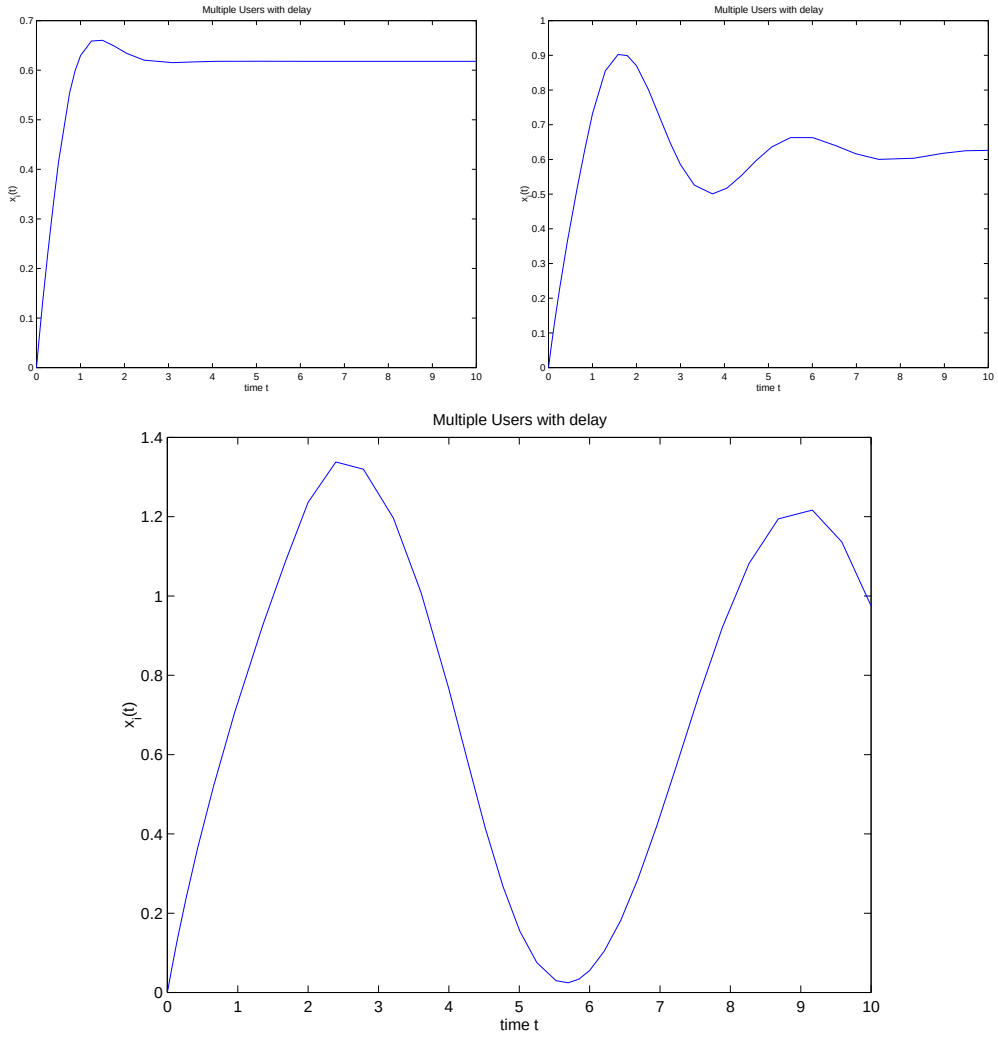

Figure 2.5: Flow rate versus time of a single-user on a single-link with utility and pricing functions $U = \log(x + 1)$, $P = \frac{1}{2}x^2(t - 2r)$, and communication delays (from top to bottom) $r = 0.5$, 1, 2.

The effect of the number of users on system stability is demonstrated in the next simulation. The delay in the system is symmetric and chosen as $r_i = 0.5,\ \forall i$. Figure 2.6 shows that increasing the number of users has a similar effect as increasing the delay as captured in Theorem 2.5.

In the next set of simulations, the number of users sharing a single link is $M = 10$. The user utility parameters, u_i and delay r_i are randomly chosen with uniform distribution in the ranges $u_i \in [10,\ 20]$ and $r_i \in [0.1,\ 0.5]$, respectively. Figure 2.7(a) shows flow rates of individual users for

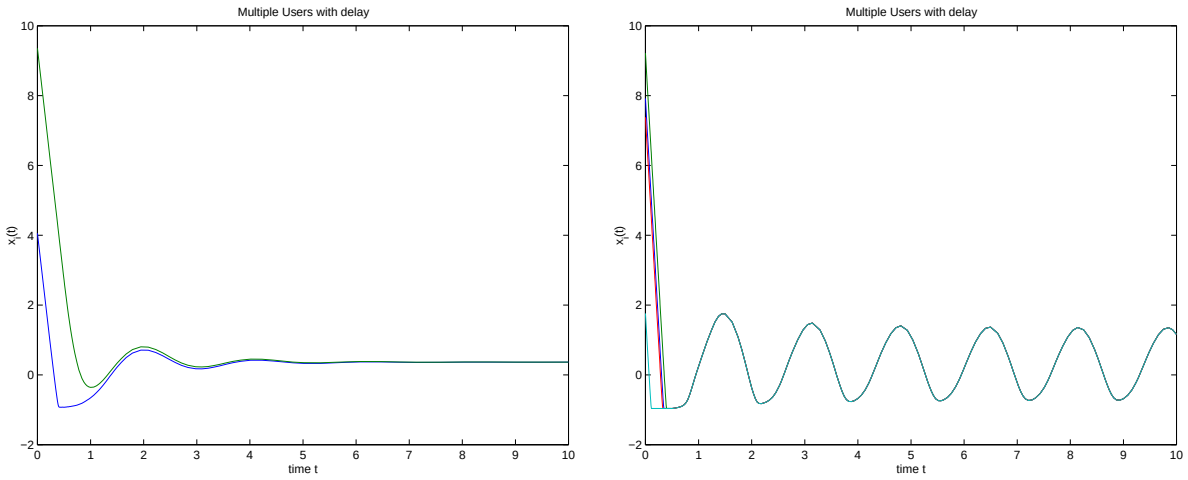

(a) (b)

Figure 2.6: Flow rates of two and four users versus time under the delay $r_i = 0.5,\ \forall i$ shown in (a) and (b), respectively.

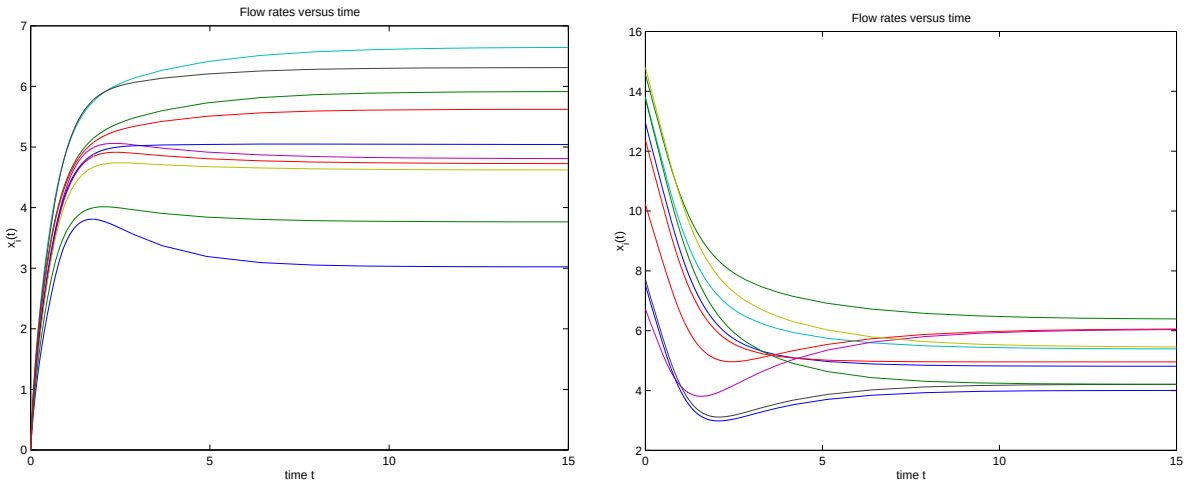

(a) (b)

Figure 2.7: Flow rates of 10 users versus time with origin as the starting point (a), and random initial conditions (b).

the initial condition being the origin for all users and Figure 2.7(b) shows the same for a randomly picked initial condition. Although the delays are larger than the theoretical bound $r_{max} < 0.05$, the system can be seen to be stable.

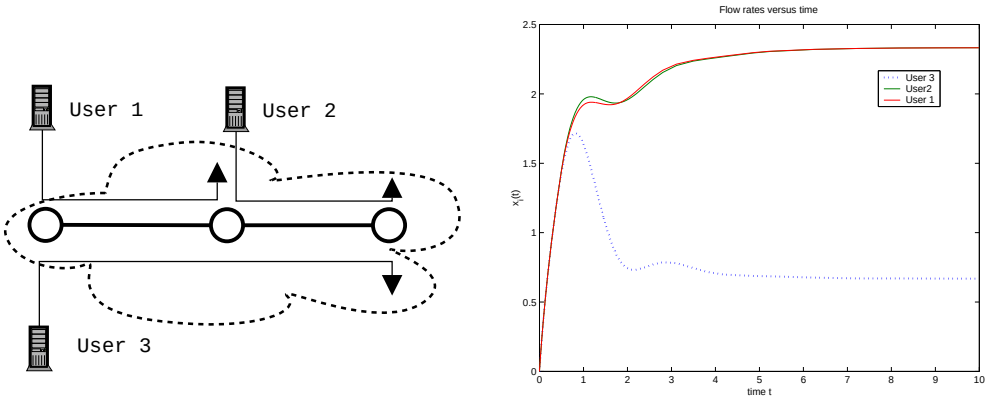

Figure 2.8: Flow rates of three users versus time on the basic topology shown.

We next explore extensions to general topologies. Due to computational limitations of the *dde23* solver, we choose a simple network topology with two links as shown in Figure 2.8. The propagation delay between the two links is 0.2 and users' delays to their corresponding links are chosen randomly with a uniform distribution in the range $[0.1,\, 0.3]$. Cost parameters are $u = 5$ and $\alpha = 0.5$ and are symmetric for all three users. The results observed in Figure 2.8 are also in accordance with the results of Theorem 2.5.

2.6.2 Variations in the network parameters

The robustness properties of the network game are studied numerically using MATLAB. We simulate a discrete counterpart of the system (2.43) first on a single link shared by M users, and then on a linear network topology of two links. The set of user update algorithms are

$$x_i(t+1) = x_i(t) + \kappa \left[\frac{u_i}{x_i(t)+1} - \alpha \frac{\bar{x}(t)}{C} \right], \; i = 1, \ldots, M, \tag{2.47}$$

where u_i is the utility parameter of user i and κ is the stepsize.

We first investigate the effect of variations in the number of users sharing a link with capacity $C = 10^6$. At each time step, probability of a new user to arrive (start a connection) and an old user to depart (terminate its connection) are chosen equally as 0.5%. Hence, the number of users sharing the link are varied randomly within the upper and lower bounds of $1 \leq M \leq 40$. The parameters of the cost function are fixed during the simulation, and are chosen as follows: u_i are uniformly randomly distributed on $[9.5\,10^5,\, 10.5\,10^5]$, $\kappa = 10$, and $\alpha = 100$. Figure 2.9 shows

both the number of the users sharing the link at a given time and flow rates of the users. We observe that the flow rates converge to the new equilibrium levels within a short period of time in accordance with the analysis in Section 2.5.

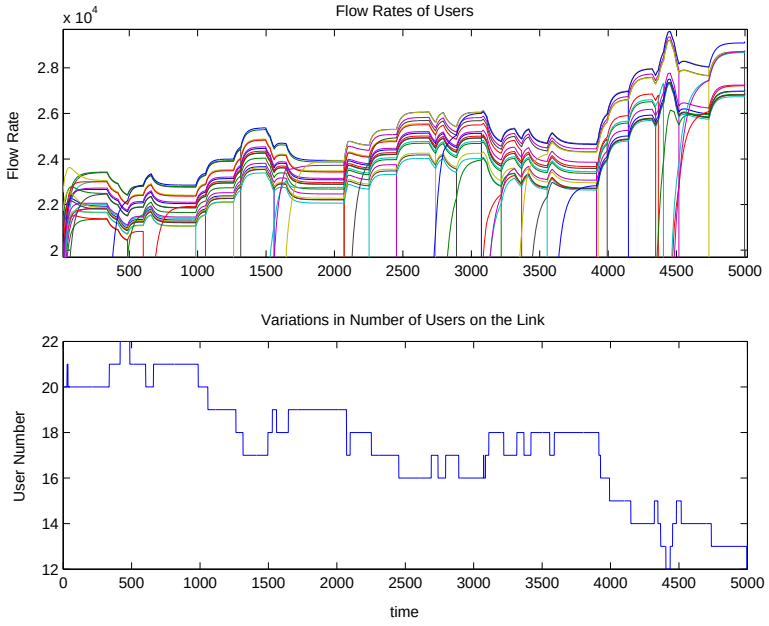

Figure 2.9: Flow rates and number of users sharing a link with capacity $C = 10^6$.

We next fix the number of users at $M = 20$, and vary the capacity of the link, C, at each time step by adding an amount uniformly randomly distributed on $[-10^4, 10^4]$. The capacity of the link is bounded above by 10^6. We observe from Figure 2.10 that the results justify the model in Section 2.4, and are again in accordance with the analysis in Section 2.5.

Finally, we simulate a simple linear network of two links each of capacity 10^6. There are $M = 10$ users, whose routes (connections) vary with probability 0.1% at each time step. The initial routing matrix is given by

$$A_{init} = \begin{pmatrix} 1 & 1 & 1 & 1 & 1 & 1 & 1 & 1 & 0 & 0 \\ 0 & 0 & 0 & 1 & 1 & 1 & 1 & 1 & 1 & 1 \end{pmatrix}.$$

Figure 2.11 shows the results of the simulation. We observe that in the event of a route change converge rate of the system is slower as it causes variations in both available link capacities to other users and in the number of users sharing each link as argued in Section 2.5.

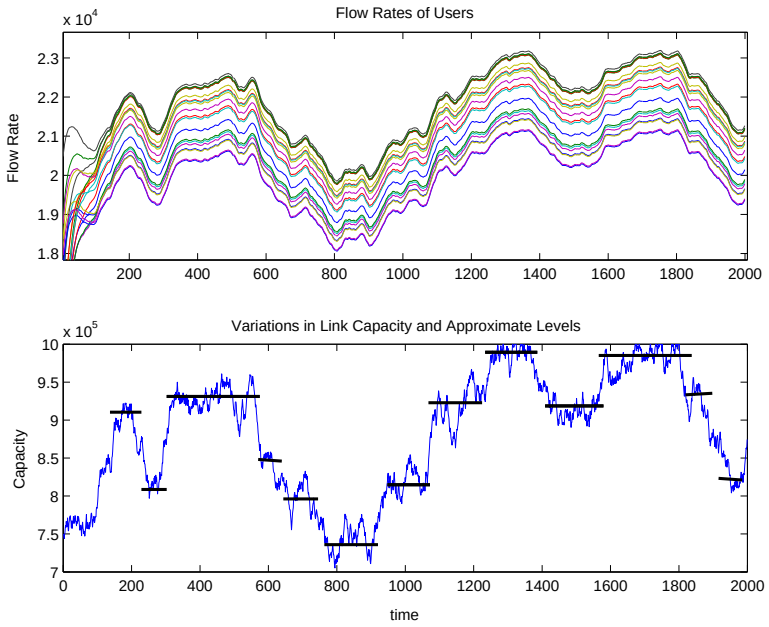

Figure 2.10: Flow rates of the users and variations in the capacity of the link shared by the users.

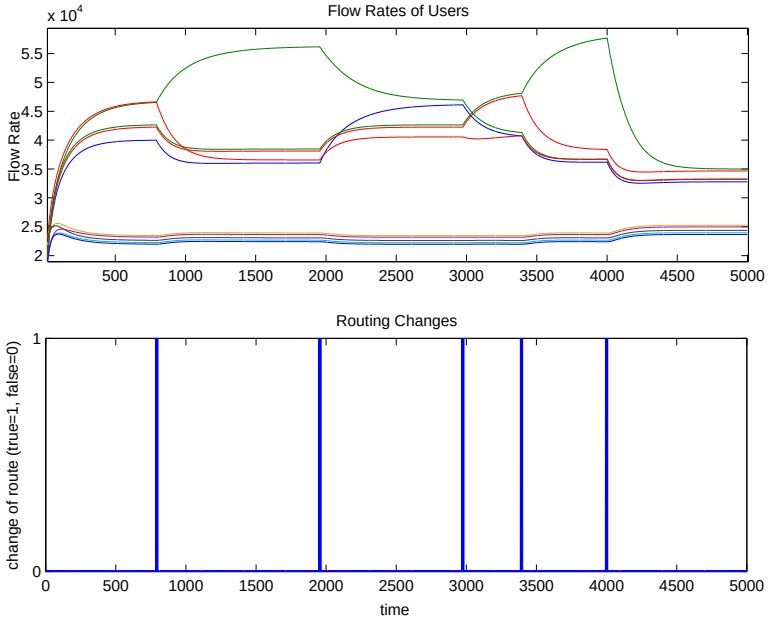

Figure 2.11: Flow rates of the users and instances of routing changes.

2.7 Conclusions

In this chapter we have introduced a fairly general congestion control framework for general network topologies based on a noncooperative congestion control game. Existence and uniqueness of a NE as the operating point of the game has been established under reasonable convexity assumptions on the cost function, and a simple but efficient gradient descent algorithm has been shown to converge to the NE under the same set of assumptions. In addition, stability and robustness properties of the proposed congestion control scheme have been investigated. Specifically, we have analyzed robustness of the algorithm to both heterogeneous communication delays on a general network topology and variations in system parameters such as the number of users, capacity of the links, and routing. In the robustness study, we have utilized both hybrid system theory and randomized algorithms, and have demonstrated the results obtained through MATLAB simulations.

In the next chapter, we focus on Internet-style networks by extending the network model of Section 2.2.1, and present a specific congestion control scheme for such networks.

CHAPTER 3

A CONGESTION CONTROL SCHEME FOR INTERNET-STYLE NETWORKS

We introduce in this chapter a congestion control scheme for Internet-style networks based on a special pricing function, which is proportional to the queueing delay experienced by the user. This pricing structure is motivated by the communication constraints of this type of networks. Through a network model based on fluid approximations and a realistic queueing model, we show in Section 3.1 the existence of a unique equilibrium, which approximates Nash Equilibrium (NE) under the assumption that the effect of a user's flow on congestion cost is vanishingly small. In Section 3.2, we establish the global stability of the equilibrium under a general network topology. We also investigate stability of the system in a network with nonnegligible propagation delays, and provide sufficient conditions for stability in the case of a bottleneck node with multiple users in Section 3.3. The effect of boundaries on system stability are analyzed rigorously. In addition, we study in Section 3.4 an adaptive pricing scheme for adjusting the pricing parameter dynamically, and make use of hybrid (switched) system concepts for its analysis. Based on the theoretical foundations developed, we design a window-based, end-to-end congestion control scheme for Internet-style networks in Section 3.5. It is followed by Section 3.6, where this congestion control scheme is simulated in Network Simulator 2 (NS-2) over Internet protocol for various network topologies. We next analyze a discrete-time version of the proposed scheme as any implementation of the continuous time model will inevitably involve a discretization synchronized with the rount-trip-time (RTT) of packets. First, an analytical local stability analysis of the single bottleneck node case with symmetric users is given in Section 3.6. Then, we discuss the use of randomized algorithms in the present context. In Section 3.7.1, numerical results are presented for stability of the system first for a single bottleneck node and subsequently under general network topologies. The chapter concludes with remarks in Section 3.9.

3.1 The Model

3.1.1 The network model

We extend the network model of Section 2.2.1 by taking buffer dynamics and packet losses into account. The i^{th} user's flow rate satisfies the bounds $0 \leq x_i \leq x_{i,max}$, where the upper bound $x_{i,max}$ may be a user specific physical limitation. If the aggregate sending rate of users whose flows pass through link l exceeds the capacity C_l of that link then the arriving packets are queued (generally on a first-come first-serve basis) in the buffer b_l of the link with $b_{l,max}$ being the maximum buffer size. Furthermore, if the buffer of the link is full, incoming packets have to be dropped.[1] Let the total flow on link l be given by $\bar{x}_l := \sum_{i:l \in R_i} x_i$. Thus, the buffer level at link l evolves in accordance with

$$\dot{b}_l(t) = \begin{cases} [\bar{x}_l - C_l]^-, & \text{if } b_l(t) = b_{l,max} \\ \bar{x}_l - C_l, & \text{if } 0 < b_l(t) < b_{l,max} \\ [\bar{x}_l - C_l]^+, & \text{if } b_l(t) = 0 \end{cases} \tag{3.1}$$

where $\dot{b}_l(t)$ denotes $(\partial b_l(t)/\partial t)$, $[.]^+$ represents the function $\max(.\,, 0)$, and $[.]^-$ represents the function $\min(.\,, 0)$. In addition, let $\dot{\mathbf{b}} := [\dot{b}_1, \ldots, \dot{b}_L]$ be the $(L \times 1)$ link buffer rate vector, and $\mathbf{O} := [O_1, \ldots, O_L]$ be defined as the $(L \times 1)$ flow loss rate vector at the links, where

$$O_l := \begin{cases} [\bar{x}_l - C_l]^+, & \text{if } b_l = b_{l,max} \\ 0, & \text{otherwise} \end{cases}$$

Taking the buffer dynamics and packet losses into account, we redefine the capacity constraints at the links as

$$\mathbf{A}\mathbf{x}(t) - \dot{\mathbf{b}}(t) - \mathbf{O}(t) \leq \mathbf{c}. \tag{3.2}$$

3.1.2 The cost (objective) function

An important indication of congestion for Internet-style networks is the variation in queueing delay d, which is defined as the difference between the actual delay experienced by a packet d^a and the fixed propagation delay of the connection d^p. If the incoming flow rate to a router exceeds its capacity, packets are queued (generally on a first-come first-serve basis) in the existing buffer of the router, leading to an increase in the RTT of packets. Hence, RTT on a congested path is larger than the base RTT, which is defined as the sum of propagation and processing delays on the path of a packet. The queueing delay at the l^{th} link, d_l, is a nonlinear function of the excess flow on that

[1] We assume a drop-tail queueing scheme for the rest of the analysis.

link, given by

$$\dot{d}_l(\mathbf{x},t) = \begin{cases} \left[\dfrac{1}{C_l}(\bar{x}_l - C_l)\right]^-, & \text{if } d_l(t) = d_{l,max} \\ \dfrac{1}{C_l}(\bar{x}_l - C_l), & \text{if } 0 < d_l(t) < d_{l,max} \\ \left[\dfrac{1}{C_l}(\bar{x}_l - C_l)\right]^+, & \text{if } d_l(t) = 0 \end{cases} \tag{3.3}$$

in accordance with the buffer model described in (3.1), with $d_{l,max} := b_{l,max}/C_l$ being the maximum possible queueing delay. Thus, the total queueing delay, D_i, a user experiences is the sum of queueing delays on its path, namely $D_i(\mathbf{x},t) = \sum_{l \in R_i} d_l(\mathbf{x},t),\ i \in \mathcal{M}$, which we henceforth write as $D_i(t),\ i \in \mathcal{M}$.

Let us define a cost function for each user as the difference between pricing and utility functions. The pricing function of the i^{th} user is linear in x_i for each fixed total queueing delay D_i of the user, and is linear in D_i with x_i fixed (hence it is a bilinear function of x_i and D_i). The utility function $U_i(x_i)$ is assumed to be strictly increasing, differentiable, and strictly concave; it basically describes the user's demand for bandwidth. Accordingly, we make use of variations in RTT to devise a congestion control and pricing scheme. The cost (objective) function for the i^{th} user at time t is thus given by

$$J_i(\mathbf{x},t) = \alpha_i D_i(t)\, x_i\ - U_i(x_i)\ , \tag{3.4}$$

which he or she wishes to minimize. In accordance with this objective, we consider a simple dynamic model of the network game where each user changes her or his flow rate in proportion with the gradient of her/his cost function with respect to her/his flow rate, $\dot{x}_i = -\partial J_i(\mathbf{x})/\partial x_i$. Taking into consideration also the boundary effects, the update algorithm for the i^{th} user thus is:

$$\dot{x}_i = \begin{cases} \left[\dfrac{dU_i(x_i)}{dx_i} - \alpha_i\, D_i(t)\right]^-, & \text{if } x_i = x_{i,max} \\ \dfrac{dU_i(x_i)}{dx_i} - \alpha_i\, D_i(t), & \text{if } 0 < x_i < x_{i,max} \\ \left[\dfrac{dU_i(x_i)}{dx_i} - \alpha_i\, D_i(t)\right]^+, & \text{if } x_i = 0 \end{cases} \tag{3.5}$$

where the effect of the i^{th} user on the delay $D_i(t)$ she or he experiences is ignored. This assumption can be justified for networks with a large number of users, where the effect of each user is vanishingly small. Furthermore, from a practical point of view, it is extremely difficult if not impossible for a user to estimate her or his own effect on queueing delay.

3.1.3 Model assumptions

We provide in this subsection a summary of the main assumptions which will be utilized in Sections 3.2, 3.3, and 3.4. These simplifying assumptions are necessary to arrive a mathematically tractable model, and most of them are shared by the majority of the literature on the subject, including the works we have cited in Chapter 1. We note that the analytical results obtained based on these assumptions are demonstrated via realistic packet level simulations in Section 3.6.

- The network model considered is based on fluid approximations, where individual packets are replaced with flows.
- For simplicity, each user is associated with a unique connection and a corresponding fixed route (path). The routing matrix $\mathbf{A}$ is assumed to be of full row rank as nonbottleneck links have no effect on the equilibrium point due to zero queuing delay on those links.
- The effect of individual packet losses on the flow rates are ignored. This approximation is reasonable as one of the main goals of our congestion control scheme is to minimize or totally eliminate packet losses.
- Information delays in Section 3.3 are assumed to be fixed for tractability of analysis.
- We assume first-in first-out (FIFO) finite queues (buffers) with droptail packet dropping policies.
- The effect of a user on his/her own queueing delay is ignored, which is justified for networks with a large number of users.
- The utility function $U_i(x_i)$ of the i^{th} user is assumed to be strictly increasing and concave in x_i.

3.2 Stability Analysis

In this section, we analyze the stability of the system described by (3.3) and (3.5). First, we investigate the simple case of a single link with a single user in order to gain further insight into the system.[2] We then generalize the analysis to the case of multiple users with again a single link. Finally, we establish stability for a general network topology with multiple links and users.

[2] Admittedly, in this case the assumption of an individual user not affecting the delay on a link is violated, but still this exercise is useful for the subsequent analysis dealing with the multiple users case.

3.2.1 Stability for a single link with a single user

For a single user on a single link, the equations describing the dynamics of the system consist of the user algorithm, which is a simplified version of (3.5), and queueing delay equation for a single user derived from (3.3). For the time being, we ignore the effects of boundaries on the system, and write the dynamics as

$$\begin{aligned} \dot{x}(t) &= \frac{dU(x)}{dx} - \alpha d(t) \\ \dot{d}(t) &= \frac{x}{C} - 1 \end{aligned} \tag{3.6}$$

where d is the queueing delay, x is the user flow rate, and C is the link capacity.

The system (3.6) has a unique equilibrium point (x^*, d^*) given by $x^* = C$ and $d^* = (1/\alpha)\, dU(x^*)/dx$. Defining the queueing delay and flow rate around the equilibrium point as $\tilde{d} := d - d^*$ and $\tilde{x} := x - x^*$, we obtain the following equivalent system around the equilibrium:

$$\begin{aligned} \dot{\tilde{x}}(t) &= g(\tilde{x}) - \alpha \tilde{d}(t), \\ \dot{\tilde{d}}(t) &= \frac{1}{C}\tilde{x}, \end{aligned} \tag{3.7}$$

where the function $g(\tilde{x})$ is defined as

$$g(\tilde{x}) := \frac{dU(x)}{dx} - \frac{dU(x^*)}{dx}.$$

Note that

$$g(\tilde{x}) \begin{cases} > 0 & , \text{ if } \tilde{x} < 0 \\ < 0 & , \text{ if } \tilde{x} > 0 \\ = 0 & , \text{ if } \tilde{x} = 0, \end{cases} \tag{3.8}$$

because $U(x)$ is strictly concave in x, and hence, $(dU(x)/dx)$ is strictly decreasing.

The system (3.7) can be viewed as a generalized pendulum equation with $g(\tilde{x})$ as the friction term [82]. Let us introduce an energylike Lyapunov function:

$$V(\tilde{x}, \tilde{d}) = \frac{1}{\alpha}(\tilde{x})^2 + C(\tilde{d})^2 \ , \tag{3.9}$$

which is positive definite. The derivative of V along the system trajectories is given by

$$\dot{V}(\tilde{x}, \tilde{d}) = \frac{2}{\alpha} g(\tilde{x})\, \tilde{x} \leq 0 \ \ ,$$

where the inequality follows from (3.8). Thus, $\dot{V}(\tilde{x}, \tilde{d})$ is negative semidefinite. Let $S := \{(\tilde{x}, \tilde{d}) \in \mathbb{R}^2 : \dot{V}(\tilde{x}, \tilde{d}) = 0\}$. It follows from (3.8) that $S = \{(\tilde{x}, \tilde{d}) \in \mathbb{R}^2 : \tilde{x} = 0\}$. Hence, for any trajectory

of the system that belongs to S, we have $\tilde{x} \equiv 0$. It follows then directly from (3.7) and the fact that $g(0) = 0$ that

$$\tilde{x} \equiv 0 \Rightarrow \dot{\tilde{x}} = 0 \Rightarrow \tilde{d} = 0 \ .$$

Therefore, the only solution that can stay identically in S is the zero solution, which corresponds to the unique equilibrium of the original system (3.6). Furthermore, it is globally asymptotically stable by LaSalle's invariance theorem [82]. This completes the proof of stability without the boundary effects.

To account for boundary effects, let us introduce the feasible set Ω for the system defined by (3.3) and (3.5), as

$$\Omega = \{(x, d) \in \mathbb{R}^2 : 0 \leq x \leq x_{max} \text{and } 0 \leq d \leq d_{max}\}, \tag{3.10}$$

where d_{max} and x_{max} are the finite upper bounds on d and x, respectively. Assume that $x_{max} > C$. First, we investigate the existence and uniqueness of an inner equilibrium point, $0 < d^* < d_{max}$ and $0 < x^* = C < x_{max}$, on the set Ω. From (3.3), (3.5), and the definition of Ω, the only possible equilibrium points on the boundaries (of Ω) are $(C, 0)$ and (C, d_{max}). Clearly, the former cannot be an equilibrium as $\dot{x} > 0$ when $d = 0$. For the latter not to be an equilibrium point we choose α in such a way that it satisfies

$$\alpha > \frac{1}{d_{max}} \frac{dU(x)}{dx}\bigg|_{x=C} . \tag{3.11}$$

Thus, under (3.11) the equilibrium queueing delay satisfies $0 < d^* < d_{max}$, and the single-user single-link system admits a unique inner solution, (x^*, d^*), on Ω.

We next analyze the effect of the boundaries on system stability to gain further insight into the problem. A rigorous comprehensive study on the effect of boundaries will actually be undertaken in Section 3.2.3 for a general network topology with multiple users. For this reason, we will simply outline the procedure here, without details.

We argue that each time the trajectory of the system hits a boundary, it has to leave the boundary in finite time. Consider the boundary of Ω where $d = 0$. From (3.5), $\dot{x}$ is positive, and by (3.3) the trajectory leaves this boundary as soon as $x > C$. Likewise, when $x = 0$ we have $\dot{d} < 0$, and hence, the flow rate becomes positive in finite time.

We proceed with the other two boundaries in a similar fashion. In the case $x = x_{max} > C$, $\dot{d}$ is positive due to (3.3). Since $(dU(x)/dx)$ is strictly decreasing in its argument and α satisfies the condition in (3.11), there exists a $d^0 < d_{max}$ such that $\dot{x}(x_{max}, d^0) < 0$. Finally, on the boundary where $d = d_{max}$, if $x < C$ then the trajectory immediately leaves it. Otherwise, from condition (3.11) $\dot{x} < 0$, and hence, the trajectory cannot stay on the boundary indefinitely. It was already established that $\dot{V} \leq 0$ inside the set Ω. Furthermore, chattering of the trajectory is

not possible since $\dot{V} \leq 0$ along the boundaries as we will show in Section 3.2.3. We conclude, therefore, that the unique inner equilibrium point of the system given by (3.3) and (3.5) is globally asymptotically stable on the set Ω by LaSalle's invariance theorem.

3.2.2 Stability for a single link with multiple users

The analysis for a single link with multiple users is a fairly straightforward generalization of the single-link single-user case discussed above. The generalized system is given by

$$\begin{aligned} \dot{x}_i(t) &= \frac{dU_i(x_i)}{dx_i} - \alpha_i d(t),\ i = 1, \ldots, M, \\ \dot{d}(t) &= \frac{\sum_{i=1}^{M} x_i}{C} - 1, \end{aligned} \tag{3.12}$$

where $U_1(x_1), \ldots, U_M(x_M)$ are strictly concave user utility functions, and the boundary point behavior is described by (3.3) and (3.5). Let us define the corresponding constraint set Ω as

$$\Omega = \{(\mathbf{x}, d) \in \mathbb{R}^{M+1} : 0 \leq x_i \leq x_{i,max},\ \forall i \in \mathcal{M} \text{and } 0 \leq d \leq d_{max}\}, \tag{3.13}$$

where d_{max} and $x_{i,max}$ are upper bounds on d and x_i respectively.

We investigate the existence of a unique inner equilibrium point under the assumption $x_{i,max} > C, \forall i \in \mathcal{M}$. To simplify the notation, let $p_i(x_i) := dU_i(x_i)/dx_i$, where p_i is strictly decreasing in x_i due to strict concavity of U_i. Further define $P(\alpha, d) := \sum_{i=1}^{M} p_i^{-1}(\alpha_i d)$ where p_i^{-1} is the inverse of the function p_i. We note that $p_i^{-1}(\alpha_i d)$ is strictly decreasing in both α_i and d, and therefore $P(\alpha, d)$ is also decreasing in the pair (α, d). Ignoring the boundary effects, the equilibrium point of (3.12) is given by

$$x_i^* = p_i^{-1}(\alpha_i d^*),\ \forall i \in \mathcal{M}, \tag{3.14}$$

where d^* is solved from

$$P(\alpha, d^*) := \sum_{i=1}^{M} p_i^{-1}(\alpha_i d^*) = C. \tag{3.15}$$

We now show that $(\mathbf{x}^*, d^*)$ is indeed an inner equilibrium solution to (3.12) on the set Ω for some range of α values. Let the vector α belong to the compact set $\{\alpha \in \mathbb{R}^M : 0 \leq \alpha_{i,min} \leq \alpha_i \leq \alpha_{i,max},\ \forall i \in \mathcal{M}\}$. Define $\epsilon > 0$ to be arbitrarily small. It follows from the definition of $P(\alpha, d)$ that $P(\alpha_{max}, \epsilon) > C$ for arbitrarily large values of $\alpha_{i,max}\ \forall i \in \mathcal{M}$. Furthermore, given d_{max} one can find a vector α_{min} such that

$$P(\alpha_{min}, d_{max}) < C, \tag{3.16}$$

Using the intermediate value theorem, we conclude that there exists a unique $d^* \in (d_{min}, d_{max})$

such that $P(\alpha, d^*) = C$. In addition, (3.14) yields a unique $\mathbf{x}^*$ corresponding to d^*. We finally note that there cannot be an equilibrium point on the boundary of the set Ω since the system trajectory cannot stay on the boundary indefinitely as we will show in Section 3.2.3.

Proposition 3.1 *Let $0 \leq \alpha_{i,min} \leq \alpha_i \leq \alpha_{i,max},\ \forall i \in \mathcal{M}$, where the elements of the vector α_{max} are arbitrarily large. If α_{min} and d_{max} satisfy the condition (3.16), then there exists a unique equilibrium solution, (x^*, d^*), to the system (3.12) on the set Ω, which is further an inner point of Ω.*

Remark 3.1 *In the special case of logarithmic utility functions, $U_i(x_i) = u_i \log(x_i + 1)$, condition (3.16) can be explicitly given as*

$$0 < \frac{1}{C + M} \sum_{i=1}^{M} \frac{u_i}{\alpha_i} < d_{max}.$$

In addition, as $d_{max} \to \infty$ the system admits a unique inner equilibrium solution for any finite value of α.

We now define the system around the unique inner equilibrium point as in (3.7):

$$\begin{aligned} \dot{\tilde{x}}_i(t) &= g_i(\tilde{x}_i) - \alpha_i \tilde{d}(t)\ ,\ i = 1, \ldots, M, \\ \dot{\tilde{d}}(t) &= \frac{1}{C} \sum_{i=1}^{M} \tilde{x}_i, \end{aligned} \tag{3.17}$$

where the functions $g_i(x_i)$ are defined similarly as in the case of (3.8). Define next a Lyapunov function similar to the one of (3.9):

$$V(\tilde{\mathbf{x}}, \tilde{d}) = \sum_{i=1}^{M} \frac{1}{\alpha_i} (\tilde{x}_i)^2 + C(\tilde{d})^2\ , \tag{3.18}$$

which is positive definite.

The derivative of V along the system trajectories is given by $\dot{V} = \sum_{i=1}^{M} (2/\alpha_i) g_i(\tilde{x}_i) \tilde{x}_i \leq 0$, and is equal to zero only if $\tilde{x}_i = 0 \, \forall i \Rightarrow \tilde{d} = 0$. Let $S := \{(\tilde{\mathbf{x}}, \tilde{d}) \in \mathbb{R}^{M+1} : \dot{V}(\tilde{\mathbf{x}}, \tilde{d}) = 0\}$. It follows from (3.8) that $S = \{(\tilde{\mathbf{x}}, \tilde{d}) \in \mathbb{R}^{M+1} : \tilde{\mathbf{x}} = 0\}$. Hence, for any trajectory of the system that belongs to S, we have $\tilde{\mathbf{x}} \equiv 0$. It follows then directly from (3.17) and the fact that $g_i(0) = 0\ \forall i$ that $\tilde{\mathbf{x}} \equiv 0 \Rightarrow \dot{\tilde{x}}_i = 0\ \forall i \Rightarrow \tilde{d} = 0$. Therefore, the only solution that can stay identically in S is the zero solution, which corresponds to the unique equilibrium of the original system (3.12). Furthermore, it is globally asymptotically stable by LaSalle's invariance theorem [82]. This completes the proof of stability without the boundary effects. Since global stability under the boundary effects for a

more general case will be provided in Theorem 3.1. We postpone the treatment of boundaries until then.

3.2.3 Stability for a general network topology with multiple users

We now establish the stability of the system under a general network topology with multiple links, and with a general routing matrix $\mathbf{A}$ as defined in (2.11). The generalized system is described by

$$\begin{aligned} \dot{x}_i(t) &= \frac{dU_i(x_i)}{dx_i} - \alpha_i D_i(t) \ , \ i = 1, \ldots, M \ , \\ \dot{d}_l(t) &= \frac{\bar{x}_l}{C_l} - 1 \ , \ l = 1, \ldots, L \ , \end{aligned} \tag{3.19}$$

with the boundary behavior given by (3.3) and (3.5). Define the feasible set Ω (as before) as

$$\begin{aligned} \Omega = \{(\mathbf{x}, \mathbf{d}) \in \mathbb{R}^{M+L} : 0 \leq x_i \leq x_{i,max} \\ \text{and } 0 \leq d_l \leq d_{l,max} \ , \ \forall i \ , l\}, \end{aligned}$$

where $d_{l,max}$ and $x_{i,max}$ are upper bounds on d_l and x_i, respectively. Define

$$\mathbf{d}_{max} := [d_{1,max}, \ldots, d_{L,max}].$$

We first investigate existence and uniqueness of an inner equilibrium on the set Ω under the assumption of $x_{i,max} > C_l, \forall l$. Toward this end, we assume that $\mathbf{A}$ is a full row rank matrix with $M \geq L$, which is in fact no loss of generality as nonbottleneck links on the network have no effect on the equilibrium point, and can safely be left out.

The study of existence follows lines similar to the ones in the case of a single link. Supposing that (3.19) admits an inner equilibrium and by setting $\dot{x}_i(t)$ and $\dot{d}_l(t)$ equal to zero for all l and i one obtains

$$\mathbf{A}\,\mathbf{x} = \mathbf{c} \tag{3.20}$$

$$\mathbf{f}(\alpha, \mathbf{x}) = \mathbf{A}^T \mathbf{d} \ , \tag{3.21}$$

where $\mathbf{d} := [d_1, \ldots, d_L]^T$ is the delay vector at the links, $\mathbf{c}$ is the capacity vector introduced earlier, and the nonlinear vector function $\mathbf{f}$ is defined as

$$\mathbf{f}(\alpha, \mathbf{x}) := \left[\frac{1}{\alpha_1} \frac{dU_1}{dx_1}, \ldots, \frac{1}{\alpha_M} \frac{dU_M}{dx_M} \right]^T . \tag{3.22}$$

Define $X := \{\mathbf{x} \in \mathbb{R}^M : \mathbf{A}\mathbf{x} = \mathbf{c}\}$ as the set of flows, $\mathbf{x}$, which satisfy (3.20).

Multiplying (3.21) from left by $\mathbf{A}$ yields

$$\mathbf{A}\,\mathbf{f}(\alpha, \mathbf{x}^*) = \mathbf{A}\mathbf{A}^T\mathbf{d}.$$

Since $\mathbf{A}$ is of full row rank, the square matrix $\mathbf{A}\mathbf{A}^T$ is full rank and, hence, invertible. Thus, for a given flow vector $\mathbf{x}$ and pricing vector α,

$$\mathbf{d}(\alpha, \mathbf{x}) = (\mathbf{A}\mathbf{A}^T)^{-1}\mathbf{A}\mathbf{f}(\alpha, \mathbf{x}), \tag{3.23}$$

is unique. From the definition of $\mathbf{f}$, $\mathbf{d}(\alpha, \mathbf{x})$ is a linear combination of $p_i(x_i)/\alpha_i$, and hence, strictly decreasing in α. Since the set X is compact, the continuous function $\mathbf{d}(\alpha, \mathbf{x})$ admits a maximum value on the set X for a given α. Therefore, for each $\epsilon > 0$ one can choose the elements of α_{max} sufficiently large such that

$$0 < \max_{\mathbf{x}\in X} \mathbf{d}(\alpha_{max}, \mathbf{x}) < \epsilon.$$

In addition, given X and $\mathbf{d}_{max}$, one can find α_{min} such that

$$0 < \max_{\mathbf{x}\in X} \mathbf{d}(\alpha_{min}, \mathbf{x}) < \mathbf{d}_{max}, \tag{3.24}$$

Hence, we conclude that there is at least one inner equilibrium solution, $(\mathbf{x}^*, \mathbf{d}^*)$, on the set Ω, which satisfies (3.20) and (3.21).

We next establish the uniqueness of the equilibrium. Suppose that there are two different equilibrium points, $(\mathbf{x}_1^*, \mathbf{d}_1^*)$ and $(\mathbf{x}_2^*, \mathbf{d}_2^*)$. Then, from (3.20) it follows that

$$\mathbf{A}\,(\mathbf{x}_1^* - \mathbf{x}_2^*) = 0 \;\Leftrightarrow\; (\mathbf{x}_1^* - \mathbf{x}_2^*)^T\mathbf{A}^T = 0.$$

Similarly, from (3.21) we have

$$\mathbf{f}(\alpha, \mathbf{x}_1^*) - \mathbf{f}(\alpha, \mathbf{x}_2^*) = \mathbf{A}^T(\mathbf{d}_1^* - \mathbf{d}_2^*)\ .$$

Multiplying this with $(\mathbf{x}_1^* - \mathbf{x}_2^*)^T$ from left we obtain

$$(\mathbf{x}_1^* - \mathbf{x}_2^*)^T\left[\mathbf{f}(\alpha, \mathbf{x}_1^*) - \mathbf{f}(\alpha, \mathbf{x}_2^*)\right] = 0.$$

We rewrite this as

$$\sum_{i=1}^{M}(\mathbf{x}_{1i}^* - \mathbf{x}_{2i}^*)\frac{1}{\alpha_i}\left[\frac{dU_i(x_{1i}^*)}{dx_i} - \frac{dU_i(x_{2i}^*)}{dx_i}\right] = 0.$$

Since U_i's are strictly concave, each term (say the i^{th} one) in the summation is negative when-

ever $x^*_{1\,i} \neq x^*_{2\,i}$ with equality holding only if $x^*_{1i} = x^*_{2i}$. Hence, we conclude that x^* has to be unique, that is

$$\mathbf{x}^* = \mathbf{x}^*_1 = \mathbf{x}^*_2 \ .$$

From this, and (3.19), it immediately follows that $D_i, i = 1, \ldots, M$ are unique. This does not however immediately imply that $d_l, l = 1, \ldots, L$ are also unique, which in fact may not be the case if $\mathbf{A}$ is not full row rank. The uniqueness of d_l's, however, follow from (3.23), where we obtain a unique $\mathbf{d}^*$ for a given equilibrium flow vector $\mathbf{x}^*$:

$$\mathbf{d}^* = (\mathbf{A}\mathbf{A}^T)^{-1}\mathbf{A}\mathbf{f}(\alpha, \mathbf{x}^*).$$

As a result, $(\mathbf{x}^*, \mathbf{d}^*)$, obtained from (3.20) and (3.21) constitutes a unique inner equilibrium point on the set Ω.

Proposition 3.2 *Let $0 \leq \alpha_{i,min} \leq \alpha_i \leq \alpha_{i,max},\ \forall i \in \mathcal{M}$ where the elements of the vector α_{max} are arbitrarily large, and $\mathbf{A}$ be of full row rank. Given X, if α_{min} and $\mathbf{d}_{max}$ satisfy*

$$0 < \max_{\mathbf{x} \in X} \mathbf{d}(\alpha_{min}, \mathbf{x}) < \mathbf{d}_{max},$$

where $\mathbf{d}(\alpha, \mathbf{x})$ is defined in (3.23), then the system (3.19) has a unique equilibrium point, $(\mathbf{x}^*, \mathbf{d}^*)$, which is in the interior of the set Ω.

Defining the delays at links d_l and user flow rates x_i around the equilibrium as $\tilde{d}_l := d_l - d^*_l$ and $\tilde{x}_i := x_i - x^*_i$, respectively, for all l and i, we obtain the following system inside the set Ω and around the equilibrium:

$$\begin{aligned} \dot{\tilde{x}}_i(t) &= g_i(\tilde{x}_i) - \alpha_i \tilde{D}_i(t) \ , \ i = 1, \ldots, M \ , \\ \dot{\tilde{d}}_l(t) &= \frac{1}{C_l} \sum_{i: l \in R_i} \tilde{x}_i \ , \ l = 1, \ldots, L \ , \end{aligned} \tag{3.25}$$

where $\tilde{D}_i = \sum_{l \in R_i} \tilde{d}_l$, and $g_i(.)$ is defined as in (3.8).

We define a positive definite Lyapunov function as a generalized version of (3.18):

$$V(\tilde{\mathbf{x}}, \tilde{\mathbf{d}}) = \sum_{i=1}^{M} \frac{1}{\alpha_i} (\tilde{x}_i)^2 + \sum_{l=1}^{L} C_l (\tilde{d}_l)^2. \tag{3.26}$$

The time derivative of $V(\tilde{x}, \tilde{d})$ along the system trajectories is given by

$$\dot{V}(\tilde{\mathbf{x}}, \tilde{\mathbf{d}}) = \sum_{i=1}^{M} \frac{2}{\alpha_i} g_i(\tilde{x}_i)\, \tilde{x}_i \leq 0,$$

where the inequality follows because $g_i(\tilde{x}_i)\,\tilde{x}_i \leq 0\,\forall i$. Thus, $\dot{V}(\tilde{\mathbf{x}}, \tilde{\mathbf{d}})$ is negative semidefinite. Let $S := \{(\tilde{\mathbf{x}}, \tilde{\mathbf{d}}) \in \mathbb{R}^{M+L} : \dot{V}(\tilde{\mathbf{x}}, \tilde{\mathbf{d}}) = 0\}$. It follows as before that $S = \{(\tilde{\mathbf{x}}, \tilde{\mathbf{d}}) \in \mathbb{R}^{M+L} : \tilde{\mathbf{x}} = 0\}$. Hence, for any trajectory of the system that belongs identically to the set S, we have $\tilde{\mathbf{x}} = 0$. It follows directly from (3.25) and the fact that $g_i(0) = 0\ \forall i$ that

$$\tilde{\mathbf{x}} = 0 \Rightarrow \dot{\tilde{\mathbf{x}}} = 0 \Rightarrow \tilde{D}_i = 0\ \forall i \Rightarrow \tilde{d}_l = 0\ \forall l,$$

where the last implication is due to the fact that $\tilde{D} = \mathbf{A}^T\,\tilde{\mathbf{d}}^*$ and the matrix $\mathbf{A}$ is of full row rank. Therefore, the only solution that can stay identically in S is the zero solution, which corresponds to the unique inner equilibrium of the original system.

Let us redefine the feasible set in terms of the tilde'd quantities, $\tilde{\mathbf{x}}$ and $\tilde{\mathbf{d}}$, as follows:

$$\begin{aligned}\tilde{\Omega} := \{(\tilde{\mathbf{x}}, \tilde{\mathbf{d}}) \in \mathbb{R}^{M+L} : & -x_i^* \leq \tilde{x}_i \leq x_{i,max} - x_i^* \\ & \text{and } -d_l^* \leq \tilde{d}_l \leq d_{l,max} - d_l^*\ ,\ \forall i\ , l\}.\end{aligned}$$

We note that the set $\tilde{\Omega}$ can also be defined through a set of (linear) inequalities $h_j(\tilde{\mathbf{x}}, \tilde{\mathbf{d}}) \leq 0,\ j \in \mathcal{H} := \{1, \ldots, H\}$. Given X, let $\mathbf{d}_{max}$ and α_{min} be chosen such that (3.24) holds. Then, by Proposition 3.2 the unique equilibrium point, $(0, 0)$, is an inner solution on $\tilde{\Omega}$, where $h_j(0, 0) < 0\ \forall j \in \mathcal{H}$.

We now investigate the effect of the boundaries given in $\tilde{\Omega}$ and described by (3.3) and (3.5). The system (3.25) can also be written compactly as

$$\dot{\mathbf{z}} := \begin{pmatrix} \dot{\tilde{\mathbf{x}}} \\ \dot{\tilde{\mathbf{d}}} \end{pmatrix} = \mathbf{F} \begin{pmatrix} \tilde{\mathbf{x}} \\ \tilde{\mathbf{d}} \end{pmatrix} := \mathbf{F}(\mathbf{z}), \tag{3.27}$$

with the definition of $\mathbf{F}$ being obvious from (3.25). We have shown earlier that $\dot{V} \leq 0$ when the system trajectory is strictly inside the set $\tilde{\Omega}$. On the other hand, if the trajectory hits the boundary, then it stays on the boundary as long as the system gradient $\mathbf{F}(\mathbf{z})$ in (3.27) points toward the boundary. This is known as *sliding mode* behavior, which we define in this context as follows:

Definition 3.1 *Let the gradient vector and the corresponding unit vector of the boundary surface* $\{\mathbf{z} : h(\mathbf{z}) = 0\}$ *be given by* $\mathbf{n}(\mathbf{z}) := \nabla h(\mathbf{z})$ *and* $\mathbf{n}_u(\mathbf{z}) := \mathbf{n}(\mathbf{z})/||\mathbf{n}(\mathbf{z})||$*, respectively. Suppose that the trajectory of the system* $\dot{\mathbf{z}} = \mathbf{F}(\mathbf{z})$ *is inside the surface,* $h(\mathbf{z}) \leq 0\ \forall \mathbf{z}$*. Then, the system exhibits sliding mode behavior on the boundary surface* $\{\mathbf{z} : h(\mathbf{z}) = 0\}$*, if and only if,*

$$\mathbf{n}(\mathbf{z}) \cdot \mathbf{F}(\mathbf{z}) \geq 0,$$

where $\mathbf{n} \cdot \mathbf{F}$ *denotes the dot product of the vectors* $\mathbf{n}$ *and* $\mathbf{F}$*. Furthermore, the gradient of the system*

trajectory during sliding mode is given by

$$\mathbf{F}_s := \mathbf{F} - (\mathbf{F} \cdot \mathbf{n}_u)\mathbf{n}_u \,.$$

We next establish the relationship between the Lyapunov function $V(\mathbf{z})$ in (3.26) and the sliding mode behavior of the trajectory along the boundaries.

Proposition 3.3 *Assume that the system (3.27) has a unique inner equilibrium point, $\mathbf{z}^*$, in the compact and convex feasible set $\tilde{\Omega}$, and*

$$\dot{V}(\mathbf{z})|_{trajectory} := \nabla_{\mathbf{z}} V(\mathbf{z}) \cdot \mathbf{F}(\mathbf{z}) \leq 0,$$

for all $\mathbf{z}$ such that $h_j(\mathbf{z}) < 0 \, \forall j \in \mathcal{H}$, where the Lyapunov function $V(\mathbf{z})$ is given by (3.26). The system trajectory exhibits sliding mode behavior along the j^{th} boundary $\{\mathbf{z} : h_j(\mathbf{z}) = 0\}$ $j \in \mathcal{H}$, if and only if,

$$\dot{V}(\mathbf{z})|_{sliding} \leq \dot{V}(\mathbf{z})|_{trajectory} \leq 0, \tag{3.28}$$

where $\dot{V}(\mathbf{z})|_{sliding} := \nabla_{\mathbf{z}} V(\mathbf{z}) \cdot \mathbf{F}_s(\mathbf{z}), \ \forall \mathbf{z} \in \{\mathbf{z} : h_j(\mathbf{z}) = 0\}$.

Proof. It follows from the definition of $\mathbf{F}_s$ that

$$\dot{V}|_{sliding} = \nabla_{\mathbf{z}} V(\mathbf{z}) \cdot [\mathbf{F} - (\mathbf{F} \cdot \mathbf{n}_u)\mathbf{n}_u] \,, \tag{3.29}$$

where we drop the arguments $\mathbf{z}$ and j to simplify the notation. From (3.26), $\nabla_{\mathbf{z}} V(\mathbf{z})$ is given by

$$\nabla_{\mathbf{z}} V(\mathbf{z}) = \left[\frac{2\tilde{x}_1}{\alpha_1}, \ldots, \frac{2\tilde{x}_M}{\alpha_M}, 2C_1 d_1, \ldots, 2C_L d_L \right].$$

On the other hand, by the definition of $\tilde{\Omega}$, the vector $\mathbf{n}$, of length $M + L$, has all zero entries except the kth one, which is

$$n_k = \begin{cases} \text{sign}(\tilde{\text{x}}_\text{k}), & \text{if } 1 \leq k \leq M \\ \text{sign}(\tilde{\text{d}}_\text{k}), & \text{if } M+1 \leq k \leq M+L, \end{cases}$$

where $sign(\cdot)$ is the sign function. Note that, $\mathbf{n}_u = \mathbf{n}$ by definition. Thus, on the boundary $\{\mathbf{z} : h(\mathbf{z}) = 0\}$ the term $\nabla_{\mathbf{z}} V(\mathbf{z}) \cdot \mathbf{n}_u$ yields either $|\tilde{x}_k|$ or $\left|\tilde{d}_k\right|$, and we obtain

$$\nabla_{\mathbf{z}} V(\mathbf{z}) \cdot \mathbf{n}_u \geq 0.$$

We now show the necessity: if the trajectory exhibits sliding mode behavior along the bound-

ary, then we have $\mathbf{n}(\mathbf{z}) \cdot \mathbf{F}(\mathbf{z}) \geq 0$ and $\nabla_{\mathbf{z}} V(\mathbf{z}) \cdot \mathbf{n}_u \geq 0$. Hence, the result in (3.28) follows immediately from (3.29). Next, in order to show the sufficiency we note that (3.28) yields

$$\nabla_{\mathbf{z}} V(\mathbf{z}) \cdot (\mathbf{F} \cdot \mathbf{n}_u)\mathbf{n}_u \geq 0.$$

Since $\nabla_{\mathbf{z}} V(\mathbf{z}) \cdot \mathbf{n}_u \geq 0$ is already established on the boundary, we immediately obtain $\mathbf{n} \cdot \mathbf{F} \geq 0$, which corresponds to sliding mode behavior of the trajectory. □

Now, as a corollary to this proposition, we have the following result.

Corollary 3.1 *Consider the system (3.27) on the feasible set $\tilde{\Omega}$ with the unique inner equilibrium point $\mathbf{z}^*$. Furthermore, let the time derivative of the Lyapunov function V of (3.26) be nonincreasing along the system trajectory without boundary effect. Then, the system trajectory exhibits sliding mode behavior, if and only if, the rate of decrease in V at the boundary point is less than or equal to the one without the boundary effect.*

From Proposition 3.3, we have $\dot{V} \leq 0$ for all $(\tilde{\mathbf{x}}, \tilde{\mathbf{d}}) \in \tilde{\Omega}$. It was already shown that the unique inner equilibrium solution, $(\mathbf{x}^*, \mathbf{d}^*)$, is the only invariant solution in $S \cap \tilde{\Omega}$. Thus, the asymptotic stability of the system follows from LaSalle's invariance theorem. This is captured in the following theorem.

Theorem 3.1 *Let $0 \leq \alpha_{min} \leq \alpha \leq \alpha_{max}$, where α_{max} is arbitrarily large, and $\mathbf{A}$ be of full row rank. Given X, suppose that α_{min} and $\mathbf{d}_{max}$ are chosen such that*

$$0 < \max_{\mathbf{x} \in X} \mathbf{d}(\alpha_{min}, \mathbf{x}) < \mathbf{d}_{max},$$

holds, and hence, the system

$$\begin{aligned} \dot{x}_i(t) &= \frac{dU_i(x_i)}{dx_i} - \alpha_i D_i(t) \ , \ i = 1, \ldots, M \ , \\ \dot{d}_l(t) &= \frac{\bar{x}_l}{C_l} - 1 \ , \ l = 1, \ldots, L \ , \end{aligned}$$

admits the unique inner equilibrium point $(\mathbf{x}^*, \mathbf{d}^*)$. Then, this system with its boundary point behavior described by (3.3) and (3.5) is globally asymptotically stable on the set

$$\begin{aligned} \Omega := \{(x, \mathbf{d}) \in \mathbb{R}^{M+L} : 0 \leq x_i \leq x_{i,max} \\ \textit{and } 0 \leq d_l \leq d_{l,max}, \ \forall i \ , l\}. \end{aligned} \tag{3.30}$$

We note that the unique equilibrium point of the system is only an approximation to the Nash equilibrium since the effect of the i^{th} user on the delay, $D_i(\mathbf{x}, t)$, he or she experiences has been

ignored. This approximation becomes more accurate as the number of users in the network increases.

Remark 3.2 *The unique equilibrium solution* (x^*, d^*) *of the system (3.19) solves the following resource allocation problem*

$$\max_{(\mathbf{x},\mathbf{d})} \sum_{i=1}^{M} \frac{1}{\alpha_i} U_i(x_i) - \sum_{l=1}^{L} \int_0^{\bar{x}_l} d_l(\tau) d\tau,$$

which is a relaxed and scaled version of the original optimization problem $\max_{\mathbf{x}} \sum_{i=1}^{M} U_i(x_i)$ *of [11] under link capacity and positivity of flow rate conditions. This is due to the fact that the partial derivatives of the costs at the links, and not on the path of the* i^{th} *user, with respect to* x_i *yield zero. Likewise, the utility function of each user depends only on that user's flow rate. In addition, we have* $\mathbf{Ax} = \mathbf{C}$ *at the equilibrium point,* $(\mathbf{x}^*, \mathbf{d}^*)$*, i.e., full capacity usage. Furthermore, for* $U_i = w_i \log(x_i)$*, where* w_i *is a user-specific preference parameter, the unique system equilibrium* $(\mathbf{x}^*, \mathbf{d}^*)$ *approximates a proportionally fair allocation [9,12].*

3.3 Stability under Information Delay

We have shown in Section 3.2 that the system described by (3.3) and (3.5) is globally asymptotically stable under a general network topology. We now investigate the global stability of the system under arbitrary propagation delays, which we are also going to refer to as *information delay*, and denote by r. First, we analyze the simple case of a single link with a single user to gain insight into the problem. Next, we generalize the analysis to a general network with a single bottleneck node and multiple users. We do not consider the case of multiple users on a general network topology with multiple links, since the problem in that case is quite intractable under arbitrary information delays.

3.3.1 Stability for a single link with a single user under information delay

For the case of a single user on a single link, we modify equation (3.6) describing the system around the equilibrium by introducing a maximum propagation (information) delay r between the user and the link, which we assume to be a constant :

$$\begin{aligned} \dot{x}(t) &= \frac{dU(x(t))}{dx} - \alpha d(t-r) \\ \dot{d}(t) &= \frac{x(t-r)}{C} - 1 \end{aligned} . \tag{3.31}$$

We again assume that $\alpha > \frac{1}{d_{max}} \frac{dU(C)}{dx}$, and $x_{max} > C$, so that $x^* = C,\ d^* = \frac{1}{\alpha} \frac{dU(C)}{dx}$ is the unique equilibrium of (3.31), which is in the interior of the feasible set.

Defining the queueing delay and flow rate around the unique inner equilibrium point as in the no delay case, we obtain the following equivalent system:

$$\begin{aligned} \dot{\tilde{x}}(t) &= g(\tilde{x}(t)) - \alpha \tilde{d}(t-r) \\ \dot{\tilde{d}}(t) &= \frac{1}{C} \tilde{x}(t-r) \end{aligned} \quad . \tag{3.32}$$

Notice that (3.32) is a set of delay differential equations. Such systems have been studied extensively in the literature; see, e.g. [83, 90]. Here we will make particular use of the methods presented in Chapter 4.2 of [90]. From (3.32), we immediately have

$$\dot{\tilde{x}}(t) = g(\tilde{x}(t)) - \alpha \tilde{d}(t+r) + \alpha[\tilde{d}(t+r) - \tilde{d}(t-r)],$$

and

$$\dot{\tilde{x}}(t-r) = g(\tilde{x}(t-r)) - \alpha \tilde{d}(t) + \frac{\alpha}{C} \int_{-2r}^{0} \tilde{x}(t+s) ds \, .$$

We define a Lyapunov function

$$V(\tilde{x}, \tilde{d}) = \frac{1}{\alpha} (\tilde{x}(t-r))^2 + C(\tilde{d}(t))^2 + \frac{1}{C} \int_{-2r}^{0} \int_{t+s}^{t} \tilde{x}^2(u-r) du \, ds, \tag{3.33}$$

which is positive definite. Taking the time-derivative of V along the system trajectories, we obtain

$$\begin{aligned} \dot{V}(\tilde{x}, \tilde{d}) = \ & \frac{2}{\alpha} g(\tilde{x}(t-r)) \tilde{x}(t-r) \\ & + \frac{2}{C} \int_{-2r}^{0} \tilde{x}(t-r) \tilde{x}(t+s-r) ds \\ & + \frac{1}{C} \int_{-2r}^{0} [\tilde{x}^2(t-r) - \tilde{x}^2(t+s-r)] ds. \end{aligned}$$

Using the simple algebraic inequality

$$2\tilde{x}(t-r)\tilde{x}(t+s-r) \leq \tilde{x}^2(t-r) + \tilde{x}^2(t+s-r),$$

one can bound $\dot{V}$ above by

$$\dot{V}(\tilde{x}, \tilde{d}) \leq \frac{2}{\alpha} g(\tilde{x}(t-r)) \tilde{x}(t-r) + \frac{4r}{C} \tilde{x}^2(t-r).$$

Thus, $\dot{V}(\tilde{x}, \tilde{d})$ can be made negative semidefinite by imposing a condition on the maximum

delay r. In this case, let $S := \{(\tilde{x}, \tilde{d}) \in \tilde{\Omega} : \dot{V}(\tilde{x}, \tilde{d}) = 0\}$. It follows immediately that $S = \{(\tilde{x}, \tilde{d}) \in \tilde{\Omega} : \tilde{x} = 0\}$. Hence, for any trajectory of the system that belongs to S, we have $\tilde{x} \equiv 0$. It also follows directly from (3.32), since $g(0) = 0$, that

$$\tilde{x} \equiv 0 \Rightarrow \dot{\tilde{x}} = 0 \Rightarrow \tilde{d} = 0 \, .$$

Therefore, the only solution that can stay identically in S is the zero solution, which corresponds to the unique equilibrium of the original system (3.6).

We thus conclude that the system (3.32) is asymptotically stable by LaSalle's invariance theorem if the maximum delay r satisfies the condition

$$r < \frac{C}{2\alpha} k \, , \tag{3.34}$$

where k is defined as

$$k := \inf_{-C \leq \tilde{x} \leq x_{max} - C} \left| \frac{g(\tilde{x})}{\tilde{x}} \right| .$$

In order to gain further insight into this condition, we compute the parameter k for the specific case when the utility function is taken as the logarithmic one; that is, $U(x) = u \log(x + 1)$. In this case we obtain

$$g(\tilde{x}) = \frac{u}{x+1} - \frac{u}{C+1} = \frac{-u\tilde{x}}{(x+1)(C+1)}$$

and hence

$$k = \min_{0 \leq x \leq x_{max}} \frac{u}{(x+1)(C+1)} = \frac{u}{(x_{max}+1)(C+1)}.$$

Hence, a safe bound on r is

$$r < \frac{uC}{2\alpha(x_{max}+1)(C+1)}.$$

Of course a better bound can be obtained if we know that the trajectory remains in a small neighborhood of the equilibrium, C. This would very much be dependent on the application at hand.

The analysis of the effect of boundaries on system stability is almost identical to the one of the case without delay, and we again make use of Proposition 3.3. This now brings us to the following theorem, where again LaSalle's invariance theorem is invoked:

Theorem 3.2 *Let* $\alpha > \dfrac{1}{d_{max}} \dfrac{dU(C)}{dx}$*, and* $x_{max} > C$*. Then, the system*

$$\begin{aligned} \dot{x}(t) &= \frac{dU(x(t))}{dx} - \alpha d(t - r) \\ \dot{d}(t) &= \frac{1}{C} x(t - r) - 1, \end{aligned}$$

with the unique inner equilibrium point $(x^* = C, d^* = \frac{1}{\alpha}\frac{dU(C)}{dx})$ *and boundary point behavior described by the delayed versions of (3.3) and (3.5) is globally asymptotically stable on the set* Ω *if the maximum delay,* r*, in the system satisfies the condition*

$$r < \frac{kC}{2\alpha},$$

where $k := \inf_{-x^* \leq \tilde{x} \leq x_{max} - x^*} |g(\tilde{x})/\tilde{x}|$*, and* $x^* = C$*.*

3.3.2 Stability for a single (bottleneck) link with multiple users under information delay

We now generalize the preceding analysis of a single link with a single user to multiple users by introducing user-specific maximum propagation delays $r = [r_1, \ldots, r_M]$ between the link and the users. We invoke the assumptions of Section 3.2 so that the system has a unique inner equilibrium point $(\mathbf{x}^*, d^*)$ as characterized in Section 3.2. Modifying the system equations (3.17) around this equilibrium point by introducing the associated maximum propagation delays, we obtain

$$\begin{aligned} \dot{\tilde{x}}_i(t) &= g_i(\tilde{x}_i(t)) - \alpha_i \tilde{d}(t - r_i)\ ,\ i = 1, \ldots, M \\ \dot{\tilde{d}}(t) &= \frac{1}{C}\sum_{i=1}^{M} \tilde{x}_i(t - r_i). \end{aligned} \tag{3.35}$$

Following an approach similar to the one in the single user case with delay, one gets for the i^{th} user

$$\dot{\tilde{x}}_i(t - r_i) = g_i(\tilde{x}_i(t - r_i)) - \alpha_i \tilde{d}(t) + \frac{\alpha_i}{C}\int_{-2r_i}^{0} \sum_{j=1}^{M} \tilde{x}_j(t + s - r_j) ds.$$

We again define a positive definite Lyapunov function:

$$\begin{aligned} V(\tilde{\mathbf{x}}, \tilde{d}) = \ & \textstyle\sum_{i=1}^{M} \frac{1}{\alpha_i}(\tilde{x}_i(t - r_i))^2 + C(\tilde{d}(t))^2 \\ & + \frac{M}{C}\textstyle\sum_{i=1}^{M} \int_{-2r_i}^{0} \int_{t+s}^{t} \tilde{x}_i^2(u - r_i) du\ ds. \end{aligned} \tag{3.36}$$

Taking the derivative of V along the system trajectories, we obtain

$$\begin{aligned}
&\dot{V}(\tilde{\mathbf{x}}, \tilde{d}) = \textstyle\sum_{i=1}^{M} \dfrac{2}{\alpha_i} g_i(\tilde{x}_i(t-r_i))\tilde{x}(t-r_i) \\
&+\frac{1}{C}\textstyle\int_{-2r_i}^{0} \sum_{i=1}^{M}\sum_{j=1}^{M} 2\tilde{x}_i(t-r_i)\tilde{x}_j(t+s-r_j)ds \\
&+\frac{M}{C}\textstyle\sum_{i=1}^{M}\int_{-2r_i}^{0}[\tilde{x}_i^2(t-r) - \tilde{x}_i^2(t+s-r)]ds.
\end{aligned}$$

We bound the derivative $\dot{V}$ from above by

$$\begin{aligned}
\dot{V}(\tilde{\mathbf{x}}, \tilde{d}) \leq \quad & \sum_{i=1}^{M} \frac{2}{\alpha_i} g_i(\tilde{x}_i(t-r_i))\tilde{x}_i(t-r_i) \\
& +\frac{4Mr_i}{C}\tilde{x}_i^2(t-r_i)
\end{aligned}$$

This can be made negative semidefinite by imposing a condition on the maximum delay in the system, $r_{max} := \max_i r_i$. Let $S := \{(\tilde{\mathbf{x}}, \tilde{d}) \in \tilde{\Omega} : \dot{V}(\tilde{\mathbf{x}}, \tilde{d}) = 0\}$. It follows as before that $S = \{(\tilde{\mathbf{x}}, \tilde{d}) \in \tilde{\Omega} : \tilde{\mathbf{x}} = 0\}$. Hence, for any trajectory of the system that belongs identically to the set S, we have $\tilde{\mathbf{x}} = 0$. It also follows directly from (3.35), and the fact that $g_i(0) = 0\ \forall i$, that

$$\tilde{\mathbf{x}} = 0 \Rightarrow \dot{\tilde{\mathbf{x}}} = 0 \Rightarrow \tilde{d} = 0,$$

where we have made use of the fact that the matrix $\mathbf{A}$ is of full row rank. Therefore, the only solution that can stay identically in S is the zero solution, which corresponds to the unique equilibrium of the original system. As a result, the system (3.35) is asymptotically stable by LaSalle's invariance theorem if the maximum delay in the system r_{max} satisfies the condition

$$r_{max} < \frac{k_{min}}{2\alpha_{max}} \frac{C}{M}\,, \tag{3.37}$$

where α_{max} and k_{min} are defined as

$$\begin{aligned}
&\alpha_{max} := \max_i \alpha_i \\
&k_{min} := \min_i \inf_{-x_i^* \leq \tilde{x}_i \leq x_{i,max} - x_i^*} \left| \frac{g(\tilde{x}_i)}{\tilde{x}_i} \right|.
\end{aligned} \tag{3.38}$$

Notice that the bound on the maximum delay required for the stability of the system is affected by, among other things, the maximum pricing parameter and the capacity per user C/M. Since the link capacity C will be provisioned in the network design stage according to the expected maximum number of users the proposed algorithm is in practice scalable for the given capacity per user.

The analysis of the boundary effects is identical to earlier ones, and therefore will be omitted. The following theorem now extends the results of Theorem 3.2 to the multiuser case.

Theorem 3.3 *Let the conditions in Theorem 3.1 hold such that the system*

$$\dot{x}_i(t) = \frac{dU_i(x_i(t))}{dx_i} - \alpha_i d(\mathbf{x}, t-r) \ , \ i = 1, \ldots, M \ ,$$
$$\dot{d}(t) = \frac{1}{C}\sum_{i=1}^{M} x_i(t-r_i) - 1,$$

with the boundary point behavior described by (3.3) and (3.5) admits a unique inner equilibrium point $(\mathbf{x}^*, d^*)$*. This system is globally asymptotically stable on the corresponding set* Ω *defined by (3.30), if the maximum delay,* r_{max}*, in the system satisfies the condition*

$$r_{max} < \frac{k_{min}}{2\alpha_{max}} \frac{C}{M} \ ,$$

where α_{max} *and* k_{min} *are defined in (3.38).*

3.4 An Adaptive Pricing Scheme

In Sections 3.2 and 3.3, we have shown that the pricing parameter α can be chosen such that the equilibrium point is feasible, $\mathbf{d}^* < \mathbf{d}_{max}$, if $\mathbf{x}^* < \mathbf{x}_{max}$. In other words, we have assumed either that the equilibrium queue sizes (delays) are less than the maximum queue size (delay) or that there are infinite buffers at all nodes. In fact, the buffer sizes on a real network are limited, and choosing the parameter α appropriately in a dynamic networking environment with varying numbers of users and changing preferences is not a trivial task. If α is chosen to be "too high", then the proposed congestion control scheme becomes less robust. On the other hand, a "too small" α may lead to large queueing delays as well as packet losses. Furthermore, it is not possible to choose α in a centralized manner due to communication constraints.

Given the capacity vector $\mathbf{c}$, it is possible to derive $\mathbf{d}_{max}$ directly from maximum queue sizes at the network nodes. Consequently, the vector $\mathbf{d}_{max}$ denotes a strict physical bound on the maximum queueing delays. The nonlinear vector function $\mathbf{f}$ is strictly decreasing in α by (3.22). Hence, from (3.23) the unique equilibrium $\mathbf{d}^*$ is strictly decreasing in α. Then, a natural strategy for making the equilibrium queue size at node l, d_l^*, feasible is to increase α_i for all users whose flows pass through link l. At the same time, those users will experience packet losses at node l if $d_l^* > d_{l,max}$ (i.e., equilibrium queue size (delay) is larger than the maximum one). By making use of the packet losses experienced by the users as a signal to increase prices it is possible to minimize packet losses. On the other hand, α should not be "too high" for the congestion control scheme to

be robust. Thus, we slowly decrease α until a networkwide lower bound is reached unless there is a packet loss. As a result, we obtain a distributed, dynamic, and adaptive pricing scheme, which improves robustness of the congestion control scheme to variations in network parameters, such as the number of users, user preferences, link capacities, etc. We also note that if a virtual queueing scheme [17] is implemented at the buffers and marked packets are used as the signal, then one can prevent packet losses altogether, and set an upper-bound on the maximum delay in the system.

3.4.1 Hybrid modeling of the adaptive pricing scheme

We model the proposed adaptive pricing scheme as a *switched (hybrid) system*, and analyze its stability. In this context, a switched hybrid system can be defined as a continuous-time system with isolated discrete switching events [2]. Let us first consider for illustrative purposes the case of a single user on a single link with capacity C. If the equilibrium queueing delay is larger than the maximum delay, $d^* > d_{max}$, then the system trajectory will hit the boundary $\mathcal{B} := \{(x,d) \in \mathbb{R}^2 : 0 \leq x \leq x_{max}, \text{ and } d = d_{max}\}$ at a point where $x > C$. We again implicitly assume that $x_{max} > C$. Since the vector field points toward $\mathcal{B}$, $\dot{d} > 0$, the trajectory cannot leave the boundary, resulting in a *sliding mode* behavior on the set $\{(x,d) \in \mathbb{R}^2 : C \leq x \leq x_{max}, \text{ and } d = d_{max}\}$. Then, the resulting vector field is a projection of the original system dynamics onto the boundary $\mathcal{B}$. A simplified sketch of the sliding mode behavior is shown in Figure 3.1.

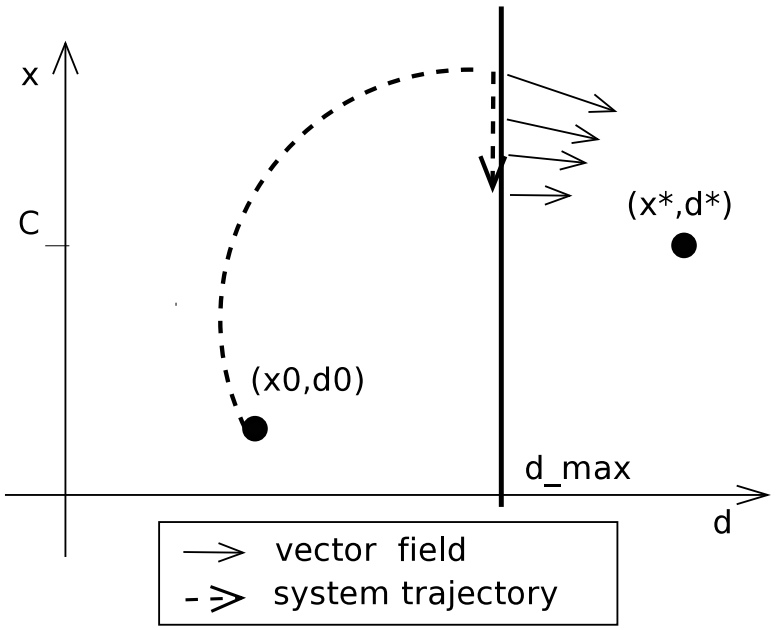

Figure 3.1: Sliding mode behavior of a single user on a single link with capacity C.

For a general network topology, let the boundary $\mathcal{B}_g$ be defined as

$$\mathcal{B}_g := \{(\mathbf{x}, \mathbf{d}) \in \mathbb{R}^{M+L} \, : \, 0 \leq x_i \leq x_{i,max}, \text{and } d_l = d_{l,max}, \; \forall i, \; l\}$$

In the case the system trajectory hits $\mathcal{B}_g$, the set of users whose flows pass through the links l, where $d_l = d_{l,max}$, will experience packet losses. Let us define this set as

$$\mathcal{M}_{loss}(t) := \{i \in \mathcal{M} : \exists l \in R_i, \text{where } d_l(t) = d_{l,max}, \; l \in \mathcal{L}\}. \tag{3.39}$$

Then, in the case of a packet loss, each user $i \in \mathcal{M}_{loss}$ dynamically increases $\alpha_i(t)$ multiplicatively, with a proportionality constant $\lambda > 0$. Otherwise, $\alpha_i(t)$ is decreased with a rate $1/\alpha_i(t)$ until the networkwide lower bound α_{min} is reached. Thus, the adaptive pricing scheme is defined by, $\forall i \in \mathcal{M}$,

$$\dot{\alpha}_i(t) = \begin{cases} \lambda \, \alpha_i(t) \; , \text{ if } (\mathbf{x}, \mathbf{d}) \in \mathcal{B}_g \text{ and } i \in \mathcal{M}_{loss}(t) \\ -\dfrac{1}{\alpha_i(t)}, \text{ if } \alpha_i > \alpha_{min}, (\mathbf{x}, \mathbf{d}) \notin \mathcal{B}_g, \text{ and } \; i \notin \mathcal{M}_{loss}(t) \\ 0, \text{ if } \alpha_i = \alpha_{min}, \; (\mathbf{x}, \mathbf{d}) \notin \mathcal{B}_g, \text{ and } i \notin \mathcal{M}_{loss}(t) \end{cases} \tag{3.40}$$

with system dynamics given in (3.19), and α_{min} being the networkwide lower bound on α. Global asymptotic stability of the system (3.19) was shown in Theorem 3.1 for an inner equilibrium point. We now argue that the system is globally asymptotically stable under the adaptive pricing scheme (3.40). Consider the case when the system trajectory hits the boundary $\mathcal{B}_g$ and exhibits sliding mode behavior. Then, $\alpha(t)$ increases exponentially by (3.40) until the trajectory leaves the boundary, $\dot{\mathbf{d}} < 0$. Hence, we have a sequence of equilibria $(\mathbf{x}^*(\alpha), \mathbf{d}^*(\alpha))$ for each value of α. This has to happen in finite time, say t_0, since by (3.19) there exists an α' such that $\mathbf{x}'_l < C_l$ for all links l. Furthermore, at time t_0, the unique equilibrium of the system $(\mathbf{x}^*(\alpha'), \mathbf{d}^*(\alpha'))$ becomes feasible by (3.23), as otherwise the trajectory cannot leave the boundary. For any feasible equilibrium point, we can define a sufficiently small level set S_l for the Lyapunov function V given by (3.26), which does not intersect with $\mathcal{B}_g$. Each hit of the system trajectory to $\mathcal{B}_g$ further shifts the equilibrium point by (3.23) and increases the size of the set S_l. Then, by global asymptotic stability of the system (see Theorem 3.1) the trajectory has to enter this invariant level set in finite time $t_1 \geq t_0$, and converge asymptotically to the unique equilibrium point. Thus, we have the following theorem summarizing this result:

Theorem 3.4 *Let* $\mathbf{A}$ *be full row rank, and let the boundary* $\mathcal{B}_g$ *be given by* $\mathcal{B}_g := \{(\mathbf{x}, \mathbf{d}) \in \mathbb{R}^{M+L} : 0 \leq x_i \leq x_{i,max}$, *and* $d_l = d_{l,max}, \; \forall i, \; l\}$ *due to the limited buffer sizes at the nodes of the network. Let the set of users experiencing packet losses be given by (3.39). Define the adaptive*

pricing scheme as

$$\dot{\alpha}_i(t) = \begin{cases} \lambda\, \alpha_i(t)\ ,\ \textit{if}\ (\mathbf{x}, \mathbf{d}) \in \mathcal{B}_g\ \textit{and}\ i \in \mathcal{M}_{loss}(t) \\ -\dfrac{1}{\alpha_i(t)},\ \textit{if}\ \alpha_i > \alpha_{min}, (\mathbf{x}, \mathbf{d}) \notin \mathcal{B}_g,\ \textit{and}\ \ i \notin \mathcal{M}_{loss}(t) \\ 0,\ \textit{if}\ \alpha_i = \alpha_{min},\ (\mathbf{x}, \mathbf{d}) \notin \mathcal{B}_g,\ \textit{and}\ i \notin \mathcal{M}_{loss}(t) \end{cases}$$

for all $i \in \mathcal{M}$. If $(\mathbf{x}^*(\alpha), \mathbf{d}^*(\alpha)) \in \mathcal{B}_g$ then there exists a finite time t_0 such that the sequence of unique equilibria $(\mathbf{x}^*(\alpha), \mathbf{d}^*(\alpha))$ of the system (3.19), indexed by α, converges to a feasible inner solution $(\mathbf{x}^*_{inner}, \mathbf{d}^*_{inner}) \in \Omega$, where Ω is as defined in (3.30). Furthermore, the sequence of equilibria $(\mathbf{x}^*(\alpha), \mathbf{d}^*(\alpha))$ cannot leave the feasible set Ω except for a finite time.

We note that the Theorem 3.4 can be straightforwardly extended to capture the single bottleneck system with propagation delays described in (3.35).

Remark 3.3 *The convergence of the system to a feasible equilibrium point with adaptive pricing scheme occurs in two different time scales. In the fast time scale, the vector $\alpha(t)$ converges through the dynamics given by (3.40) to a specific value which is associated with an inner equilibrium point of Ω. With the value of α very slowly changing as described, the system (3.19) then asymptotically converges in the slower time scale to this unique inner equilibrium point.*

Remark 3.4 *Since the implementation of the adaptation algorithm and the system will be in discrete-time, relocation of the equilibrium and increase in the pricing parameter α will occur in discrete jumps separated by RTT instead of a continuous shift.*

Remark 3.5 *Under the adaptive pricing scheme introduced, individual users are charged according to the congestion levels on their current path. If some of the links on the path of the user are very congested, then this leads to packet losses and higher prices (3.40). This is similar to existing pricing mechanisms such as peak hours versus night and weekends in current telecommunication (voice) networks. We also note that due to the bursty nature of packet losses on the links, approximately all of the users using that link experience the packet loss event that leads to a fair price adjustment. This conjecture is supported by the simulation results observed in Section 3.6 (see Figure 3.10). In addition, the dynamic nature of (3.40) enables the prices adapt to variations in congestion levels, resulting in a more efficient and fair bandwidth allocation.*

3.5 An Implementation of the Congestion Control Scheme

The user responses in Section 3.1 are based on a continuous time formulation. In reality, however, users update their flow rates only at discrete time instances corresponding to multiples of

RTT. Hence, for implementation purposes, we discretize the reaction function of the i^{th} user, and normalize it with respect to the RTT of the user. In addition, we need a specific utility function in order to quantify the user response in (3.5). Logarithmic utility functions are widely used in the literature not only because they have nice properties like strict concavity but also because they adequately capture several important concepts from economics, such as the law of diminishing returns. We choose the following utility function for i^{th} user:

$$U_i(x_i) = u_i \log(x_i + 1),$$

where u_i is a user-specific utility parameter. The optimal user response is, therefore, a discretized version of (3.5), and is given by

$$x_i(t+1) = \left[x_i(t) + \kappa_i \Big[\frac{u_i}{x_i(t)+1} - \alpha_i \sum_{l \in R_i} d_l(t) \Big] \right]^+, \tag{3.41}$$

where κ_i is a (user-specific) step-size constant. The adaptive pricing scheme (described in Section 3.4) for the i^{th} user is given by (again in the discrete-time domain)

$$\alpha_i(t+1) = \begin{cases} \lambda\, \alpha_i(t), \text{ if a packet loss occurs} \\ -\dfrac{base\_RTT}{\alpha_i(t)}, \text{ if } \alpha_i > \alpha_{min} \text{ and no packet loss} \\ \alpha_i(t), \quad \text{if } \alpha_i = \alpha_{min} \text{ and no packet loss} \end{cases} \tag{3.42}$$

where λ is chosen as 1.20, and $base\_RTT$ is the minimum RTT experienced by the user.

Remark 3.6 *In the actual implementation, the proposed decentralized pricing mechanism, including the update of α_i and calculation of d_i, for the i^{th} user has to be performed by a closed (software) module at the user node, which cannot be manipulated by the user. Then, prices in terms of network credits can be related to real world prices. Alternatively, it is possible to implement the whole cost structure on a voluntary basis by the users as in the case of TCP.*

The congestion control scheme characterized by the user response (3.41) is implemented in a Game (theory) Based Congestion Control (GBCC) protocol using the Network Simulator 2 (NS-2) [77]. The NS-2 is chosen because it provides both a realistic environment for testing the proposed congestion control scheme and a level of abstraction for easy implementation. GBCC is a simple window-based protocol for best-effort data traffic. It is devised as an end-to-end sliding window protocol [91], where the sender side adjusts its window size according to the reaction function (3.41). For simplicity, receiver window size is chosen as one. We also implement a version with a simple slow start mechanism where the window size is increased by one per RTT until

a packet loss is observed. The GBCC scheme is then extended to Adaptive GBCC (AGBCC) using the adaptive pricing (3.42). We next provide an overview on the GBCC and AGBCC schemes by summarizing the sender and receiver side functionalities.

3.5.1 GBCC protocol

Because one of the goals of GBCC protocol is compatibility with existing protocols, most of the functionality is on the sender side. Specifically, the sender side has the following functions:

- The sender puts sequence number and time stamp into the packet header. It estimates RTT and base RTT, where the latter is calculated as the minimum of the RTTs up to that point, by using the received acknowledgment (ack) packets. The estimation method for RTT is the same as the one in [92].

- If a double ack is received (i.e., the same packet is acknowledged twice by the receiver), then it retransmits the packages beginning from the last acknowledged packet number. We note that this *go back n* scheme [91] is implemented for its simplicity. In fact, better mechanisms with receiver window size being larger than 1 do exist.

- The sender updates the window size according to (3.41) using the current value of queueing delay, which is taken as the difference between the current RTT and the base RTT. The window size, W, is strictly positive.

- If no ack packet is received within, say $2\,RTT$, then sender retransmits previous packets beginning from the last acknowledged one, and reduces the window size.

The receiver side, on the other hand, has the function of acknowledging received packets. If no packet is received for a specific time, say $4\,RTT$, the last received packet is acknowledged again.

3.5.2 AGBCC protocol

In the AGBCC protocol, sender and receiver have the same functionality as in GBCC. However, in addition to standard functions, each sender also adjusts its own pricing parameter α at each packet loss in accordance with the adaptive pricing scheme (3.42). The change of α is proportional to base RTT if there are no packet losses and $\alpha > \alpha_{min}$ in order to equalize the rate of change among users with different delays.

3.6 Simulations

We simulate the proposed congestion control schemes, GBCC and AGBCC, on NS-2. The underlying protocol used for routing is the standard IP. Links and queues are chosen to be duplex and drop-tail, respectively. For simplicity, we fix the packet sizes to $1000\ bytes$. In most of the cases, queueing delays on the links are much smaller than the propagation delays that we choose. Hence, RTTs are approximately equal to twice the propagation delays.

First, we simulate GBCC without a slow start mechanism in the simple single-user single-link case. The parameters in (3.41) are chosen as $\alpha = 30$ and $u = 10\,000$. The buffer size is 50 kB and propagation delay on the link is varied from 5 ms to 25 ms, and to 100 ms. We observe in Figure 3.2 that as RTT gets too large, the system becomes unstable in accordance with the analysis in Section 3.3 Notice that it takes up to 7 s for the flow to reach its capacity in this simulation. Therefore, we use the slow start version of GBCC for the rest of the study.

We next explore the interaction between GBCC and TCP on a single bottleneck link with 10 ms propagation delay. GBCC is TCP-friendly [25] since its long-term rate does not exceed the one of the TCP flow as observed in Figure 3.3. The fluctuation in the first 2 s is due to the slow start mechanism which requires a packet loss for termination. In the final simulation on a single bottleneck link, there are 20 identical users with parameters $\alpha = 50$, $u = 400\,000$, and propagation delays are randomly chosen between 2 ms and 50 ms according to a uniform distribution. We observe flows of 3 specific users with respective propagation delays of 2 ms, 15 ms, and 50 ms in Figure 3.4. The system again converges to the equilibrium, however similar to TCP, GBCC favors flows with smaller RTT as it is a window-based scheme.

We then carry out a simulation with three users on a simple three node network topology with two 5 Mb/s links of 20 ms propagation delay as shown in Figure 3.5. While flows of users 1 and 2 pass through links 1 and 2 respectively, the flow of user 3 passes through both links. Cost parameters are chosen as $\alpha = 30$ and $u = 400\,000$. User 3 is "charged" more than others through summation of queueing delays as she or he uses resources on both links. Thus, having the same utility parameter as others, she or he obtains a smaller fraction of the bandwidth. Figure 3.6 depicts the flow rates of users 2 and 3, as observed in node 2.

We next simulate 10 users with various routes and experiencing various information delays on a seven node arbitrary topology network (Figure 3.7) with all links except the one between nodes 5 and 6 having capacity of 5 Mb/s each. The link between nodes 5 and 6, on the other hand, has a capacity of 10 Mb/s. The links have equal propagation delays of 5 ms each, except the links to nodes 7, 8, and 9, which have delays of 5 ms, 10 ms, and 25 ms, respectively. The users at nodes 7, 8, and 9 all have connections to node 6 and each experiences a different propagation delay. Figure 3.8 shows only the flows of these three users as measured at node 6. We note that although

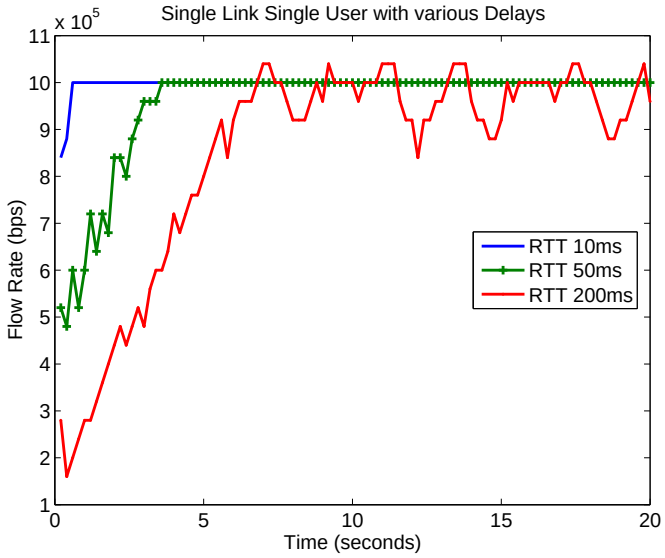

Figure 3.2: A single user on a single link with $RTT = 10, 50,$ and 200 ms. This version of GBCC has no slow start mechanism.

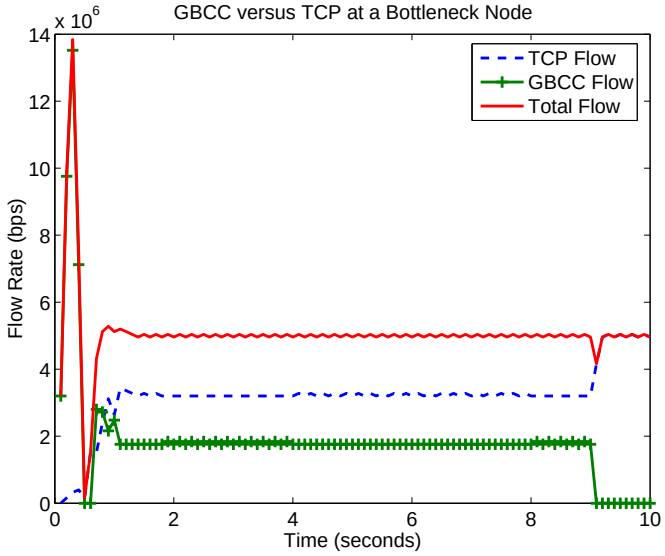

Figure 3.3: GBCC flow versus TCP flow on a bottleneck link with 10 ms propagation delay.

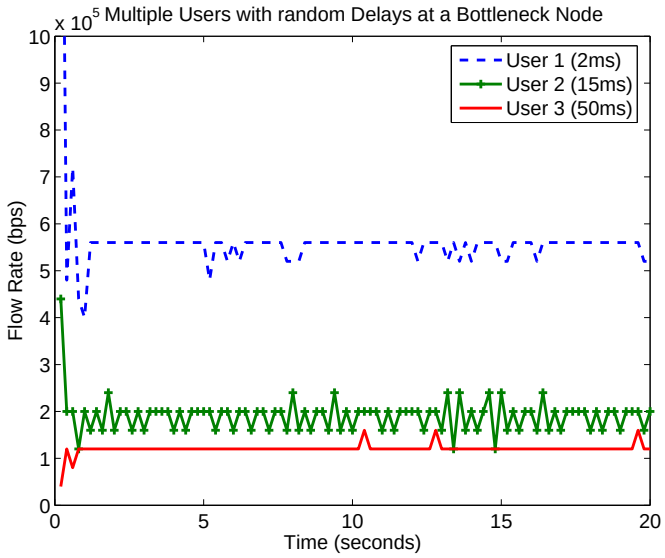

Figure 3.4: Three out of 20 flows with various propagation delays (2 ms, 15 ms, and 50 ms) sharing a 5 Mb/s bottleneck link.

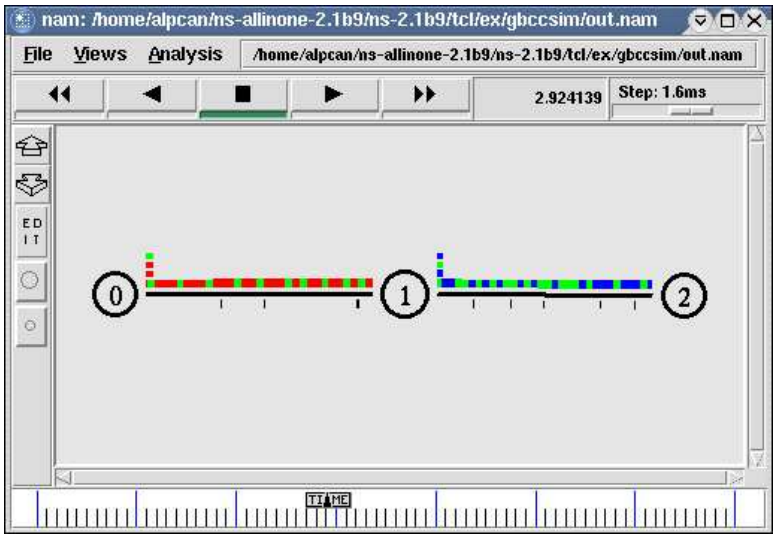

Figure 3.5: A *Nam* screenshot of the simple network. Links are symmetric, and have a capacity of 5 Mb/s with 20 ms propagation delay.

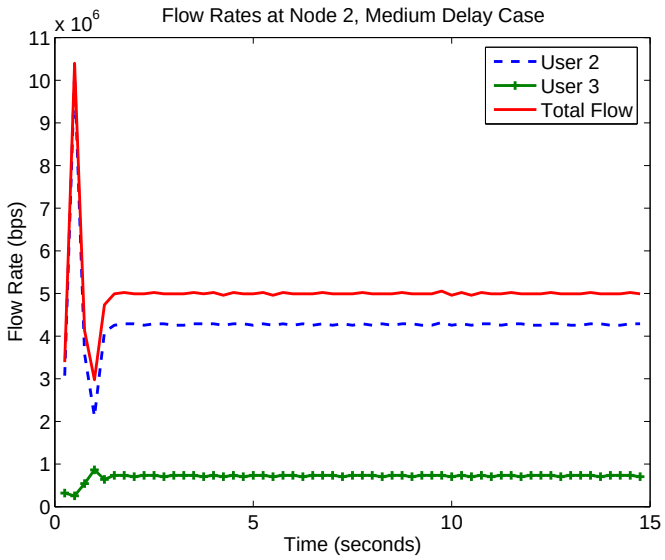

Figure 3.6: Flows of users 2, 3, and total flow at node 2 are observed for 15 s.

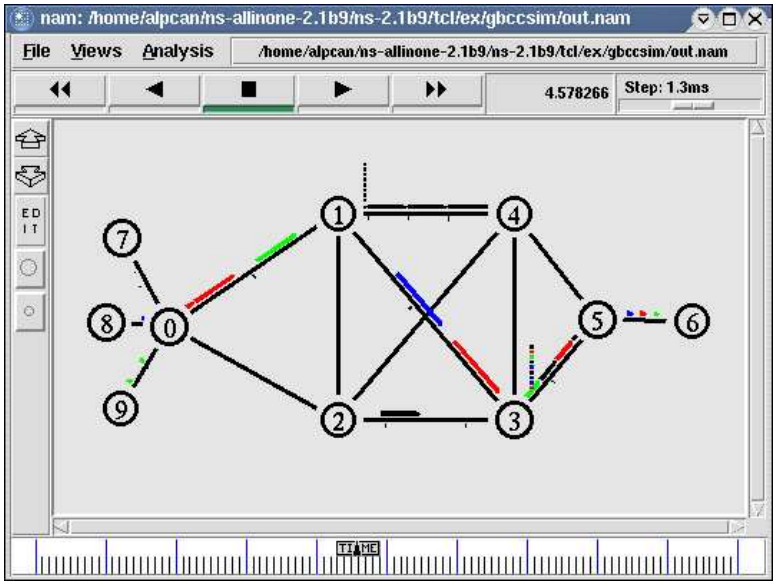

Figure 3.7: A *Nam* screenshot of the general (arbitrary) topology network.

the number of links in this simulation is equal to the number of users, the number of bottleneck links that affect the equilibrium flows is actually smaller. Hence, the routing matrix $\mathbf{A}$ is of full row rank.

The adaptive pricing scheme studied in Section 3.4 is simulated with a single AGBCC user on a single-link with a capacity of 1 Mb/s and 5 ms propagation delay. The parameters in (3.41) are chosen as $\alpha = 30$, $u = 100\,000$, and a maximum buffer size of 5 packets in order to enforce packet losses. Figure 3.9 shows the actual number of packets in the queue as well as the number of lost packets at the link. Due to the packet losses in the beginning of the simulation pricing parameter is increased, and hence the operating point of the system is shifted such that no additional losses occur for the rest of the simulation. Note that thanks to the adaptive pricing scheme, one can set an upper bound on the maximum delay in the system by choosing specific maximum queue lengths. We finally simulate 20 AGBCC users, which are divided into two groups on a single bottleneck link of 5 Mb/s capacity. The first group of users starts transmitting immediately, whereas the second group starts transmission at $t = 12$ s. The flow rates of three selected users two of which belonging to the first group are shown in Figure 3.10. We also observe in Figure 3.11 the number of packets in the queue and the number of lost packets at the bottleneck link. Again, the results show that the adaptive pricing scheme functions in accordance with Theorem 3.4.

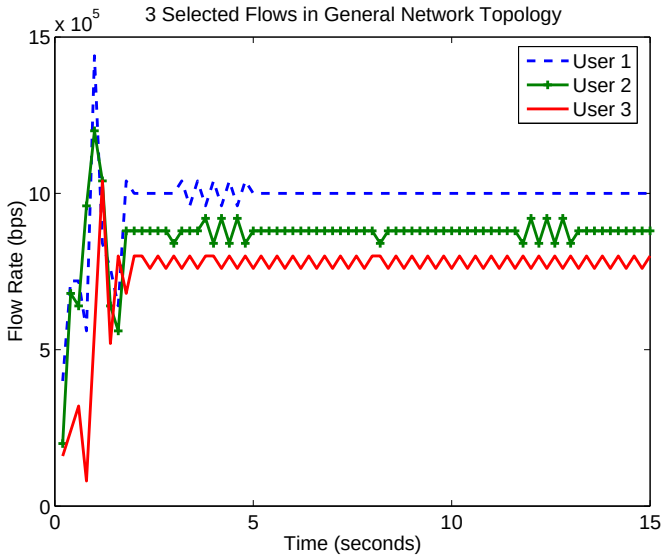

Figure 3.8: Three flows from nodes 7, 8, and 9 to node 6 are shown where these users are symmetric and have the following cost parameters: $\alpha = 30$ and $u = 200\,000$.

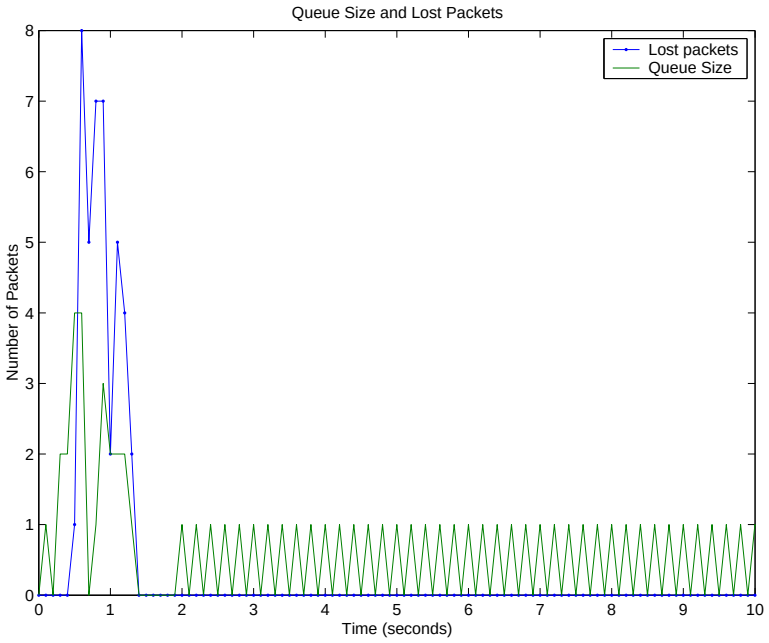

Figure 3.9: The packet losses of a single AGBCC user on a single-link and the queue size.

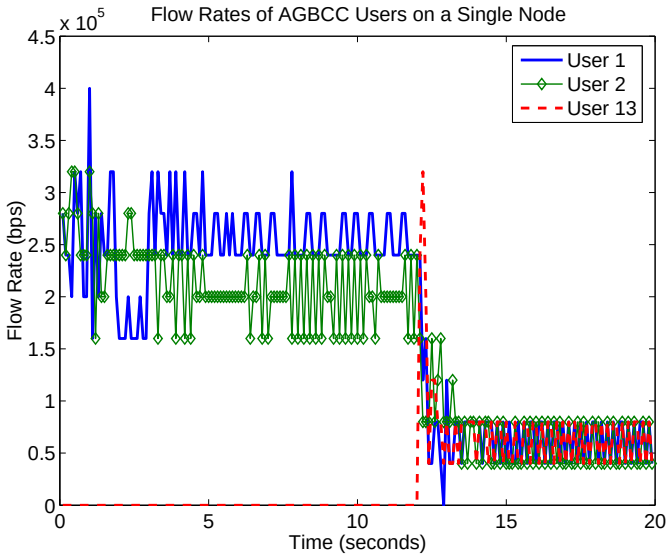

Figure 3.10: The flow rates of three selected AGBCC users out of 20 on a single bottleneck link.

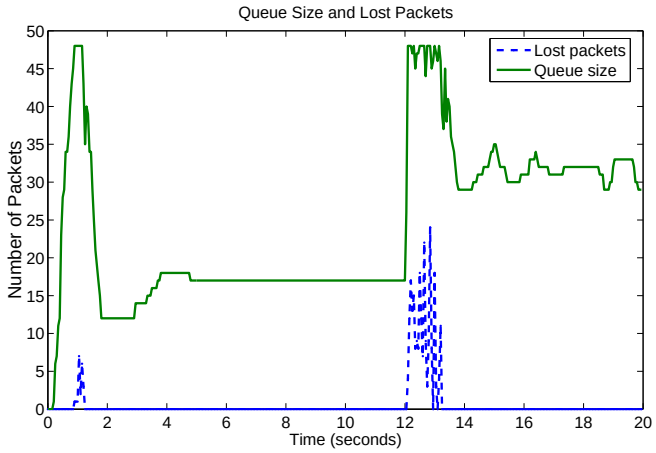

Figure 3.11: Queue size and the number of packets lost at the bottleneck link shared by 20 AGBCC users.

3.7 An Analysis of the Congestion Control Scheme in Discrete Time

In a realistic implementation of the update algorithm of Section 3.1, the users would update their flow rates only at discrete time instances corresponding to multiples of RTT. Hence, we discretize the reaction function of the i^{th} user, and normalize it with respect to the RTT of the user. In addition, we consider a somewhat simplified version of the general network model introduced in Section 3.1 by ignoring boundary effects. The optimal user response is, therefore, a discrete-time version of (3.5), and is given by,[3]

$$x_i(t+1) = x_i(t) + \kappa_i \left[\frac{u_i}{x_i(t)+1} - \alpha_i \sum_{l \in R_i} d_l(t) \right], \quad t = 0, 1, \ldots, \quad i \in \mathcal{M}, \tag{3.43}$$

where κ_i is a (user-specific) step-size constant which will be taken to be 1 for the rest of the paper, which is no loss of generality since it can be absorbed into the other parameters u_i and α_i; furthermore, we take $x_i(0) = 0, \ i \in \mathcal{M}$, without any loss of generality. The queue model is discretized in a similar manner, with the queueing delay at link l being (as a discretized version of (3.3)):

$$d_l(t+1) = d_l(t) + \frac{1}{C_l} \sum_{i: l \in R_i} x_i(t) - 1, \quad t = 0, 1, \ldots, \tag{3.44}$$

with $d_l(0) = 0, \quad l \in \mathcal{L}$.

[3]We have abused the notation here, as t here does not correspond to the t in the CT description. Since the CT description will not be used in the rest of the Chapter, this should not create any ambiguity or confusion.

3.7.1 Stability of the symmetric single bottleneck case

Let us consider the case of a single bottleneck node, with M users having connections passing through that node. Hence, we have essentially a single link of interest, for which we denote the associated delay by d (that is without the subscript "l"), and likewise the associated capacity by C. Then, the equilibrium state of the system described by (3.43) and (3.44) follows readily as

$$\begin{aligned} x_i^* &= \frac{u_i}{\alpha_i d^*} - 1\,, \quad i \in \mathcal{M} \\ d^* &= \frac{1}{C+M} \sum_{i=1}^{M} \frac{u_i}{\alpha_i}\,, \end{aligned} \tag{3.45}$$

which is unique.

Let $\tilde{x}_i(t) := x_i(t) - x_i^*\,,\ i \in \mathcal{M}$ and $\tilde{d}(t) := d(t) - d^*$. The system (3.43)-(3.44) with a single bottleneck link and with $\kappa_i = 1$ can now be rewritten around the equilibrium state as

$$\begin{aligned} \tilde{x}_i(t+1) &= \tilde{x}_i(t) + \frac{u_i}{\tilde{x}_i(t) + x_i^* + 1} - \alpha_i(\tilde{d}(t) + d^*)\,, \quad i \in \mathcal{M} \\ \tilde{d}(t+1) &= \tilde{d}(t) + \frac{1}{C} \sum_{i=1}^{M} \tilde{x}_i(t). \end{aligned} \tag{3.46}$$

Let $\widetilde{\mathbf{x}}$ denote the M-dimensional column vector whose entries are the $\tilde{x}_i$'s; likewise let the M-dimensional column vector whose entries are the $\tilde{x}_i^*$'s be denoted by $\widetilde{\mathbf{x}}^*$. Linearizing (3.46) around $(\widetilde{\mathbf{x}}^*, \tilde{d}^*) = (0, 0)$, we obtain

$$\begin{aligned} \tilde{x}_i(t+1) &= \left[1 - \frac{u_i}{(x_i^*+1)^2}\right] \tilde{x}_i(t) - \alpha_i \tilde{d}(t)\,, \quad i \in \mathcal{M} \\ \tilde{d}(t+1) &= \tilde{d}(t) + \frac{1}{C} \sum_{i=1}^{M} \tilde{x}_i(t)\,. \end{aligned} \tag{3.47}$$

Let

$$\alpha := [\alpha_1, \alpha_2, \ldots, \alpha_M] \ \text{ and } \ \beta := [\beta_1, \beta_2, \ldots, \beta_M]\,,$$

where

$$\beta_i := u_i/(x_i^* + 1)^2\,, \quad i \in \mathcal{M}\,. \tag{3.48}$$

The system equations (3.47) can then be expressed in matrix form:

$$\begin{pmatrix} \widetilde{\mathbf{x}}(t+1) \\ \tilde{d}(t+1) \end{pmatrix} = \mathbf{L}(\alpha, \beta, C) \begin{pmatrix} \widetilde{\mathbf{x}}(t) \\ \tilde{d}(t) \end{pmatrix} \tag{3.49}$$

where

$$\mathbf{L}(\alpha,\beta,C)=\begin{pmatrix}1-\beta_1 & 0 & \cdots & -\alpha_1\\ 0 & 1-\beta_2 & & -\alpha_2\\ \vdots & & \ddots & \vdots\\ \frac{1}{C} & \frac{1}{C} & \cdots & 1\end{pmatrix}. \tag{3.50}$$

Hence the system (3.46) is locally asymptotically stable if and only if $\mathbf{L}=\mathbf{L}(\alpha,\beta,C)$ is *Schur*, that is all its eigenvalues, $\lambda(\alpha,\beta,C)$, are in the open unit circle. The goal now is to find the region in the parameter space (with the parameters being α, β, and C), such that $|\lambda(\alpha,\beta,C)|<1$. We consider first the special case of symmetric users having the same pricing and utility preference parameters, that is $u_i=u$ and $\alpha_i=\alpha$ for all $i\in\mathcal{M}$, which also implies that $\beta_i=\beta$ for all $i\in\mathcal{M}$. When the number of users is two ($M=2$), one can explicitly determine the eigenvalues of the matrix $\mathbf{L}$. They are given by

$$\begin{aligned}\lambda_1&=1-\beta\\ \lambda_{2,3}&=1-\frac{\beta}{2}\pm\sqrt{\frac{\beta^2}{4}-2\frac{\alpha}{C}}\end{aligned} \tag{3.51}$$

which are in the open unit circle if and only if

$$\frac{2\alpha}{C}<\beta<2\,.$$

The lemma below and the proposition that follows generalizes this result to M users.

Lemma 3.1 *If the user preference parameters and prices are symmetric across all M users, that is $u_i=u$ and $\alpha_i=\alpha$ (which further implies that $\beta_i=\beta$), then the characteristic equation of the matrix $\mathbf{L}$ is given by*

$$\det|\lambda\mathrm{I}-\mathbf{L}|=(\lambda-(1-\beta))^{\mathrm{M}-1}\left[\lambda^2-(2-\beta)\lambda+1-\beta+\frac{\mathrm{M}\alpha}{\mathrm{C}}\right]. \tag{3.52}$$

Thus, $\mathbf{L}$ has $M-1$ real eigenvalues at $1-\beta$ and two possibly complex eigenvalues at

$$1-\beta/2\pm\sqrt{\beta^2/4-M\alpha/C}\,.$$

Proof. The lemma is proven by induction. It is already shown in (3.51) that the statement holds when $M=2$. Next, we assume that the statement holds for a given M, say $M=m$, and prove

that it also holds for $m+1$. Now note that

$$\begin{aligned}\det|\lambda I_{m+2} - \mathbf{L}_{m+1}| = \; & (\lambda-(1-\beta))\big[(\lambda-(1-\beta))^{m-1}\big(\lambda^2-(2-\beta)\lambda+1-\beta+\frac{m\alpha}{C}\big)\big] \\ & +\frac{\alpha}{C}(\lambda-(1-\beta))^m \\ = \; & (\lambda-(1-\beta))^m\left[\lambda^2-(2-\beta)\lambda+1-\beta+(m+1)\frac{\alpha}{C}\right].\end{aligned}$$

Thus, the given expression for the characteristic equation holds for $M = m+1$, and hence for all $M \geq 2$. □

We now determine the region in the parameter space where $\mathbf{L}$ is Schur matrix. It readily follows from the lemma that the condition $0 < \beta < 2$ is both necessary and sufficient for $M-1$ real roots $(1-\beta)$ to be in the open unit circle. On the other hand, the remaining two possibly complex roots of (3.52) have their absolute values strictly less than one, $|\lambda| < 1$, if and only if the following holds:

$$\beta \in \Big(\min\left\{\frac{M\alpha}{C}, 2\sqrt{\frac{M\alpha}{C}}\right\}, 2+\frac{M\alpha}{2C}\Big).$$

Combining this with the earlier condition $0 < \beta < 2$, we arrive at the following necessary and sufficient condition for local stability of the equilibrium state of system (3.46) in the symmetric user case:

$$\beta \in \Big(\min\left\{\frac{M\alpha}{C}, 2\sqrt{\frac{M\alpha}{C}}\right\}, 2\Big)$$

This, in turn, is equivalent to the condition

$$\frac{M\alpha}{C} < \beta < 2\,. \tag{3.53}$$

We summarize this result in the following proposition.

Proposition 3.4 *If the user preference parameters and prices are symmetric across all M users (that is, $u_i = u$ and $\alpha_i = \alpha$, which further implies that $\beta_i = \beta$), the single bottleneck system given by (3.46) is locally stable around its equilibrium state (3.45) if and only if the parameters α, β, and C lie in the region*

$$\frac{M\alpha}{C} < \beta < 2\,.$$

Remark 3.7 *If the capacity of the link is linearly proportional to M (that is, $C = \mu M$, for some positive constant μ), then the necessary and sufficient condition becomes*

$$\frac{\alpha}{\mu} < \beta < 2\,.$$

The condition in Proposition 3.4 can also be expressed in terms of the user preference parameter u, together with the pricing parameter α and capacity C. First note the relationship

$$\beta = \left(\frac{M}{C+M}\right)^2 u\,,$$

which readily follows from (3.45) and (3.48) by taking u_i, α_i and β_i independent of the user index i. In view of this relationship between β and u, we immediately have the following corollary to Proposition 3.4.

Corollary 3.2 *For the symmetric parameter case, the single bottleneck system given by (3.46) is locally stable around its equilibrium state (3.45) if and only if the parameters α, u, and C lie in the region*

$$\left(1+\frac{M}{C}\right)\left(1+\frac{C}{M}\right)\alpha < u < 2\left(1+\frac{C}{M}\right)^2 .$$

Finally, we generalize Proposition 3.4 by removing the symmetry in the pricing parameter α, while retaining the symmetry in β.

Proposition 3.5 *Let the parameter β be symmetric across all M users, $\beta_i = \beta$, while the pricing vector $\alpha = [a_1, \ldots, a_M]$ to be general. Then, the characteristic equation of the matrix $\mathbf{L}$ is given by*

$$\det|\lambda \mathrm{I} - \mathbf{L}| = (\lambda - (1-\beta))^{\mathrm{M}-1}\left[\lambda^2 - (2-\beta)\lambda + 1 - \beta + \sum_{\mathrm{i}=1}^{\mathrm{M}} \frac{\alpha_{\mathrm{i}}}{\mathrm{C}}\right]. \tag{3.54}$$

The matrix $\mathbf{L}$ has $M-1$ real eigenvalues at $1-\beta$ and two possibly complex eigenvalues at

$$1 - \frac{\beta}{2} \pm \sqrt{\frac{\beta^2}{4} - \sum_{i=1}^{M} \frac{\alpha_i}{C}}\ .$$

Furthermore, the single bottleneck link system given by (3.46) is locally stable around its equilibrium state (3.45) if and only if the parameters $\{\alpha_i\,,\ i \in \mathcal{M}\}$, β, and C lie in the region

$$\frac{1}{C}\sum_{i=1}^{M} \alpha_i < \beta < 2\,.$$

Proof. The proof follows from the those of Lemma 3.1 and Proposition 3.4, by simply replacing $M\alpha$ with $\displaystyle\sum_{i=1}^{M} \alpha_i$. □

3.8 Randomized Algorithms and Stability Analysis for the Nonsymmetric Case

We have seen in the previous section that local stability and robustness can be studied analytically (because the eigenvalues of $\mathbf{L}$ can be computed explicitly) when the user utility preference parameters, u_i's, are the same for all users (or equivalently when the β_i's are the same). If this is not the case, however, then the eigenvalues of $\mathbf{L}$ cannot be expressed in closed form, making it very challenging (if not impossible) to deduce any reasonable stability and robustness results using analytical techniques. Then, one has to resort to numerically based or simulation-based methods, and as mentioned earlier *randomized algorithms* stand out as the most promising. However, before trying out randomized algorithms on the problem at hand, we first provide, in this section, a general introduction to the topic for the uninitiated reader. This section also serves to introduce the conceptual framework and the terminology, which will be utilized in the next section.

3.8.1 Monte Carlo methods

In Monte Carlo methods, the first step is to take the parameter vectors α and β to be random with given probability density functions f_α and f_β, having support sets $\mathcal{B}_\alpha$ and $\mathcal{B}_\beta$, respectively. We can take, for example, $\mathcal{B}_\alpha$ and $\mathcal{B}_\beta$ to be the hyperrectangular sets

$$\begin{aligned} \mathcal{B}_\alpha &= \{\alpha : \alpha_i \in [\alpha_i^-, \alpha_i^+]\,,\ i = 1, 2, \ldots, M\}\,, \\ \mathcal{B}_\beta &= \{\beta : \beta_i \in [\beta_i^-, \beta_i^+]\,,\ i = 1, 2, \ldots, M\}\,, \end{aligned}$$

and the density functions f_α and f_β to be uniform on these sets. That is, for $i = 1, 2, \ldots, M$,

$$f_{\alpha_i} = \begin{cases} \dfrac{1}{\alpha_i^+ - \alpha_i^-} & \text{if } \alpha_i \in [\alpha_i^-, \alpha_i^+] \\ 0 & \text{otherwise} \end{cases} \tag{3.55}$$

and

$$f_{\beta_i} = \begin{cases} \dfrac{1}{\beta_i^+ - \beta_i^-} & \text{if } \beta_i \in [\beta_i^-, \beta_i^+] \\ 0 & \text{otherwise} \end{cases}\,. \tag{3.56}$$

Then, we generate N independent identically distributed (i.i.d.) vector samples from the set $\mathcal{B}_\alpha$ ($\mathcal{B}_\beta$) according to the density function f_α: $\alpha^1, \alpha^2, \ldots, \alpha^N$ (f_β: $\beta^1, \beta^2, \ldots, \beta^N$), respectively. Subsequently, using (3.50) we compute $\mathbf{L}(\alpha^i, \beta^i)$ for $i = 1, 2, \ldots, N$, where we have suppressed the dependence on C.

The next step is to construct the indicator function

$$\mathcal{I}(\alpha^i, \beta^i) := \begin{cases} 1 & \text{if } \mathbf{L}(\alpha^i, \beta^i) \text{ is Schur} \\ 0 & \text{otherwise.} \end{cases}$$

The estimated *probability of stability* is readily given by

$$\widehat{p}_N = \frac{1}{N} \sum_{i=1}^{N} \mathcal{I}(\alpha^i, \beta^i), \tag{3.57}$$

which is equivalent to

$$\widehat{p}_N = \frac{N_{good}}{N},$$

where N_{good} is the number of vector samples such that $\mathbf{L}(\alpha^i, \beta^i)$ is a Schur matrix. The estimate $\widehat{p}_N$ is usually referred to as *empirical probability*.

Clearly, for a finite sample size, it is important to know how many samples N are needed to obtain a "reliable" probabilistic estimate $\widehat{p}_N$. To this end, classical results, such as the Chernoff bound can be used. The Chernoff bound [93] states that for any $\epsilon \in (0,\, 1)$ and $\delta \in (0,\, 1)$ if

$$N \geq \frac{1}{2\epsilon^2} \ln \left(\frac{2}{\delta} \right), \tag{3.58}$$

then, with probability greater than $1 - \delta$, we have $|\widehat{p}_N - p_{true}| < \epsilon$, where p_{true} denotes the real probability of stability. It is important to remark, however, that the number of required vector samples is independent of the problem dimension, e.g. of the size of the matrix $\mathbf{L}(\alpha, \beta)$ and of the number of users M. Hence, this problem independent explicit bound can be computed *a priori*. We refer to [94] and [95] for further details.

As pointed out in Section 1, an important issue in Monte Carlo methods is the development of efficient algorithms for sample generation in various sets according to different distributions. In particular, the problem is how to efficiently generate N vector samples (α^i, β^i) according to the given densities f_α and f_β, and support sets $\mathcal{B}_\alpha$ and $\mathcal{B}_\beta$.

For univariate density functions, this specific problem is equivalent to the one of generating uniform random numbers in the interval $[0, 1]$. Good random number generators are required to provide uniform and independent samples and they should be also reproducible and fast. It is well-known that computer methods for random generation produce only *pseudo-random* sequences, which may show cyclicities and correlations. The problem of univariate random number generation constitutes a whole field of study in its own. As a starting point for the reader interested in further details, we refer to [96], as well as to the more recent paper [93]. We note that, even

though this is a well-established topic, current research is performed with the objective to produce extremely fast and reliable algorithms for various applications including, in particular, cryptography.

The case of multivariate distributions is definitely more difficult. For general distributions and support sets, rejection methods can be used (see e.g., [87]). There are two kinds of rejection methods: The first one is based on the concept of rejection from a "dominating density." The second class of methods may be used for uniform densities and it performs rejection from an over bounding set. These two methods are obviously related and a critical issue in both is their efficiency since the rejection rate may be exponential. Alternatively, adaptive Monte Carlo methods based on Markov chains or Metropolis-like algorithms may be utilized but the critical issue is the rate of convergence, which may be slow.

3.8.2 Quasi-Monte Carlo methods

In the case of Quasi-Monte Carlo methods, the empirical probability can still be computed using the indicator function and (3.57) but the sample generation is obtained in a completely different way. That is, no probability density functions f_α and f_β are specified or used and the samples are generated according to a purely deterministic mechanism. Therefore, the sequences $\alpha^1, \alpha^2, \ldots, \alpha^N$ and $\beta^1, \beta^2, \ldots, \beta^N$ are now quasi-random and are chosen in order to minimize the so-called discrepancy, which is a measure of how "uniform" a sample set is distributed within a given set.

Formally, the discrepancy $D(S, \mathcal{B})$ of a sample set $S \in \mathcal{B}$ of cardinality N

$$S := s^1, s^2, \ldots, s^N$$

is defined as [5]

$$D(S, \mathcal{B}) = \sup_{B \in \mathcal{B}} \left| \frac{|S \cap B|}{N} - \text{Vol}(B) \right| \tag{3.59}$$

where B is any subset of $\mathcal{B}$, $\text{Vol}(B)$ is the volume of B and $|\cdot|$ denotes the cardinality of a set.

The idea is to "cover" the set $\mathcal{B}$ as uniformly as possible for a given sample size. One can ask, on the other hand, why a simple uniform grid providing low discrepancy is not preferred. Even though the apparent randomness of quasi-random sequences may be attractive for various reasons, the main benefit is to avoid the curse of dimensionality which is inherent to gridding techniques. That is, as the dimension of the parameter space increases, the number of samples required to cover the set $\mathcal{B}$ with a uniform grid grows exponentially. On the other hand, the advantage is that the number of samples in the Quasi-Monte Carlo method is independent of the problem dimension, exactly as in the Monte Carlo method. Various classical low discrepancy sequences are available

in the literature, including Halton, Sobol, Niederreiter and others. Some plots showing specific generations are shown in Figure 3.12. Finally, we would like to mention that discrepancy is not the only criterion used. For example, the so-called *dispersion*, which is a normalized lower bound on the discrepancy, is also studied. We do not further dwell on this issue, but we refer to [5] and [97] for additional details.

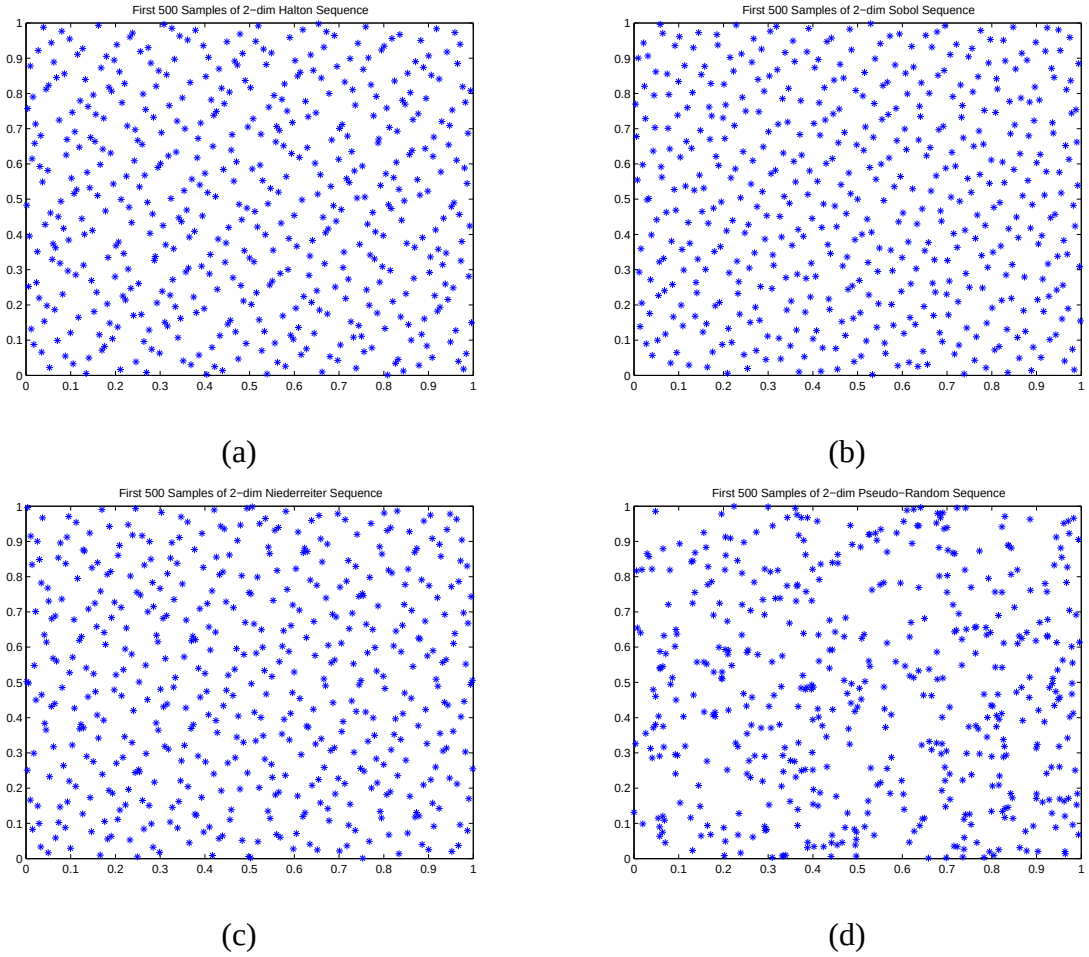

Figure 3.12: First 500 samples of various 2-dim quasi-random sequences: (a) Halton, (b) Sobol, (c) Niederreiter, and (d) uniformly distributed pseudo-random sequence.

3.8.3 Numerical evaluation

In Section 3.7.1 we have investigated the range of values for the parameters (α, β, C) for which the system is locally stable in the special symmetric parameter case. This analytical approach, however, cannot be further generalized, as it becomes extremely difficult to find a closed form expression for the eigenvalues of the matrix $\mathbf{L}$.

The uncertainty in the general case consists of nonlinearly coupled parameters even in the single bottleneck link case as shown in (3.50). Therefore, the use of randomized algorithms instead of classical worst-case analysis is a natural choice for investigating the robustness of the system at hand. For the remainder of the paper, the term *stability* will be used in the probabilistic sense, referring to probability of stability, or its deterministic counterpart, see e.g. [94], if Quasi-Monte Carlo is used.

In order to gain further insight into the properties of $\mathbf{L}$, the eigenvalues of a single 20-dimensional randomly generated sample $\mathbf{L}$ matrix are calculated and shown in Figure 3.13. We note that $\mathbf{L}$ is ill-conditioned with a condition number in the order of 10^5.

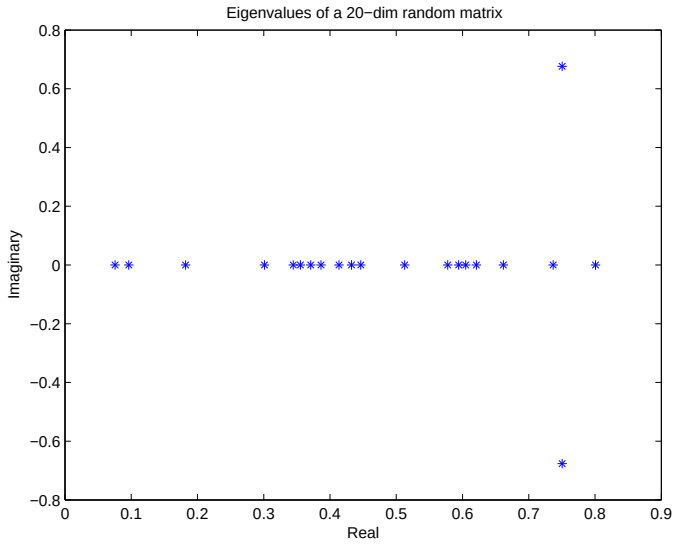

Figure 3.13: Eigenvalues of a single 20-dimensional randomly generated sample $\mathbf{L}$ matrix on complex plane.

We next investigate stability properties of the linearized single bottleneck link system (3.47) through simulations, and then generalize the simulations to cover multiple bottleneck systems. Our main goal is to investigate the effect of pricing and user parameters on local stability of the system.

Single bottleneck link with multiple users

We have seen earlier in Section 3.6 that it is possible to study local stability and robustness in two different parameter spaces, namely (α, u, C) and (α, β, C), where the former admits an interpretation in terms of the original model, whereas the latter is just a transformation which was introduced for convenience. In any analytical study, such as the one in Section 3, it does not make any difference whether one works with the former or the latter, since there is a one-to-one transformation between the two parameter spaces. In the case of randomized algorithms, however, it does make a

difference, since the distribution one uses for one space does not necessarily correspond to the one used for the other. For this reason we carry out the analysis with randomized algorithms in both parameter spaces.

For the case of a single bottleneck link network, we first study local stability and robustness in the $u - \alpha$ parameter space:

$$p = [\alpha_1, \ldots, \alpha_M, u_1, \ldots, u_M, C].$$

The matrix in question is (3.50), which is expressed in terms of β_i's, which however can be expressed in terms of u_i's through (3.48).

Subsequently, we carry out the study in the $\alpha - \beta$ parameter space, where the p vector is now

$$p = [\alpha_1, \ldots, \alpha_M, \beta_1, \ldots, \beta_M, C]\,.$$

In both cases, we use not only MC methods as the probabilistic model for the system, but also QMC sequences like, Halton, Sobol, and Niederreiter in order to–presumably–obtain a better coverage of the $2M + 1$-dimensional parameter space.

The $u - \alpha$ parameter space We first simulate the effect of bottleneck link capacity C on the local stability of the system for various values of u and α. In this simulation we use MC, QMC, and grid methods together, which enables us to compare the performance of these methods. Note that the grid method is the most reliable one as it covers the parameter space deterministically. However, it is prohibitive due to its computational complexity in higher dimensional systems. Due to this limitation, we simulate a system with 4 users only.

For all methods, the parameter ranges $0 < \alpha_i < 0.2$ and $0 < u_i < 20\,000,\ i = 1, \ldots, 4$, are chosen with 100% tolerance around their nominal values. For the probabilistic model for parameters, we use a uniform distribution. We choose a level of confidence $\delta = 0.001$ and accuracy $\varepsilon = 0.008$. Using the Chernoff bound given in (3.58) we determine the minimum sample size: $N \geq 59\,383$.To simplify the grid construction we choose $N = 65\,536$, which guarantees for the Monte Carlo simulation with probability greater than 0.999 that $|\widehat{p}_N - p_{true}| < 0.008$. Then, on the unit interval $[0, 1]$, the grid is constructed through points spaced as $[0.125\ 0.375\ 0.625\ 0.875]$ in each dimension. Results of this simulation are shown in Figure 3.14. We observe that the system is locally stable only for a certain range of capacity C. Considering the analysis for the symmetric case given in Corollary 3.2, this result aligns with the theoretical predictions.

We have observed after a series of simulations is that all of the implementations of QMC algorithms that we use have limitations as dimension of the system increases. The implementations

of QMC algorithms that we use, for dimensions higher than 16, output sequences with a very specific pattern, which produces unreliable results. Hence, for a large number of users, we limit our analysis to MC methods only.

Finally, we investigate the robustness of the system with respect to various user and pricing parameters given a fixed capacity at the bottleneck link. For each case, the user and pricing parameters are uniformly distributed with up to 100% tolerance around their nominal values . The capacity of the system is chosen as $C = 2\,000\,000$, and number of users $M = 20$. We choose the number of samples as $N = 100\,000$, which easily guarantees a level of confidence $\delta = 0.001$ and accuracy $\varepsilon = 0.007$. We observe in Figure 3.15 that local stability decreases as nominal values of u and α increase. As before, this observation is in line with the analytical results given in Corollary 3.2.

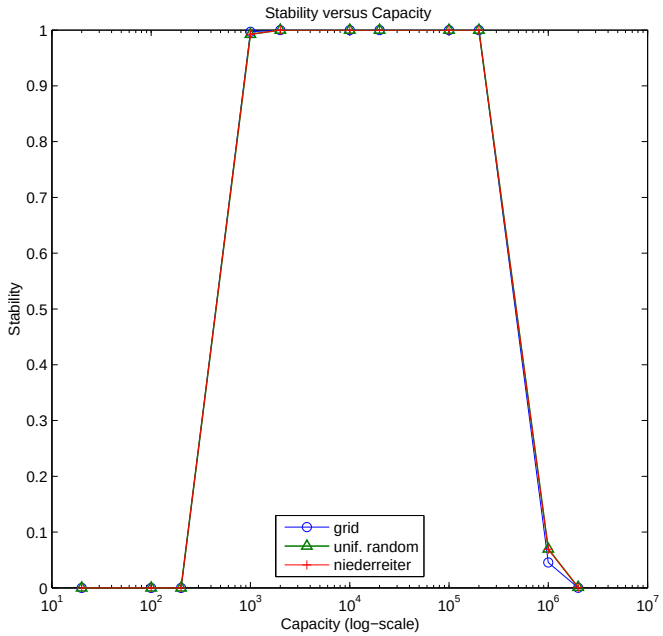

Figure 3.14: Stability versus capacity (logarithmic scale) for $M = 4$ users using Monte Carlo, Quasi-Monte Carlo, and grid methods. Parameters have 100% tolerance around nominal values.

$\alpha - \beta$ parameter space We now carry out the preceding analysis in the $\alpha - \beta$ parameter space. As noted earlier, the $\alpha - \beta$ space is a nonlinear transformation of the $u - \alpha$ space, and hence any sample distribution in the former corresponds to some other sample distribution in the latter.

We first look at the effect of capacity. We simulate a system with again 4 users. For all the methods, the parameter ranges are taken to be $0 < \beta_i < 1$ and $0 < \alpha_i < 1000,\ i = 1, \ldots, 4$. As the probabilistic model for parameters, we use a uniform distribution. The grid is constructed

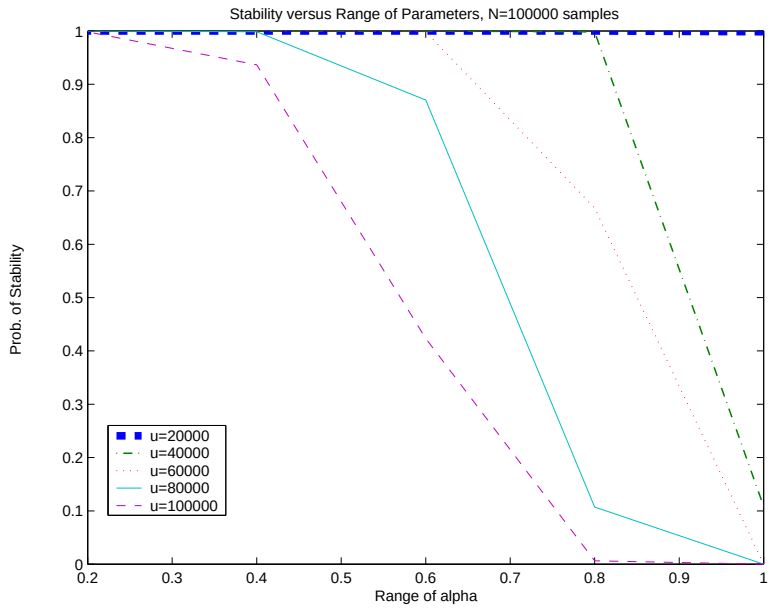

Figure 3.15: Stability versus parameter ranges for $M = 20$ users. Parameters have 100% tolerance around nominal values.

through points spaced as $[0.1\ 0.3\ 0.5\ 0.7\ 0.9] \times R_{max}$ in each dimension, where R_{max} is 1 for ε and 1000 for α. The number of samples is then $N = 390\,625$, which guarantees a level of confidence $\delta = 0.001$ and accuracy $\varepsilon = 0.004$ for the Monte Carlo simulation. Results of this simulation are shown in Figure 3.16 and a close-up version in Figure 3.17. We observe that the stability of the system improves as capacity C increases as indicated by the condition (3.53) and analytical results in Propositions 3.4 and 3.5.

In the next simulation we investigate robustness of the system with respect to a range of parameters $(\alpha - \beta)$ using uniform random distribution within the ranges $[0, 1]$ for β and $[0, 1000]$ for α. The capacity of the system is chosen as $C = 25,000$, and number of users $M = 20$. The number of samples is $N = 100,000$ ensuring a level of confidence $\delta = 0.001$ and accuracy $\varepsilon = 0.007$. We observe in Figure 3.18 that local stability degrades as the ranges of ε_i's and α_i's increase confirming analytical results in Propositions 3.4 and 3.5.

General network topology

We now turn our attention to local stability and robustness of a general topology network with multiple bottleneck links, and routing matrix $\mathbf{A}$ as described in (2.11). The system equations are given in (3.43) and (3.44).

Let $\tilde{x}_i(t) = x_i(t) - x_i^*$ for the i^{th} user and $\tilde{d}_l(t) = d_l(t) - d_l^*$ for the l^{th} link, given the existence of a unique equilibrium point, $(\mathbf{x}^*, \mathbf{d}^*)$, by Proposition 3.1. The system (3.43)-(3.44), with $\kappa = 1$,

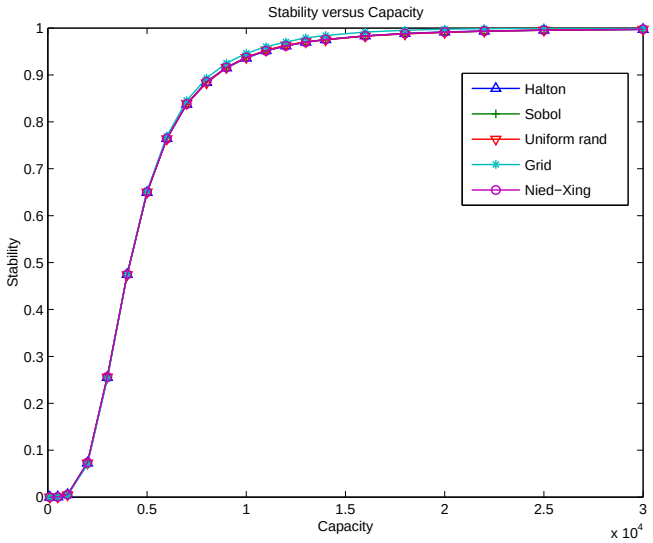

Figure 3.16: Stability versus capacity for $M = 4$ users using Monte Carlo, Quasi-Monte Carlo, and grid methods. Parameter ranges are $0 < \beta_i < 1$ and $0 < \alpha_i < 1000\ ,\ i = 1, \ldots, 4$.

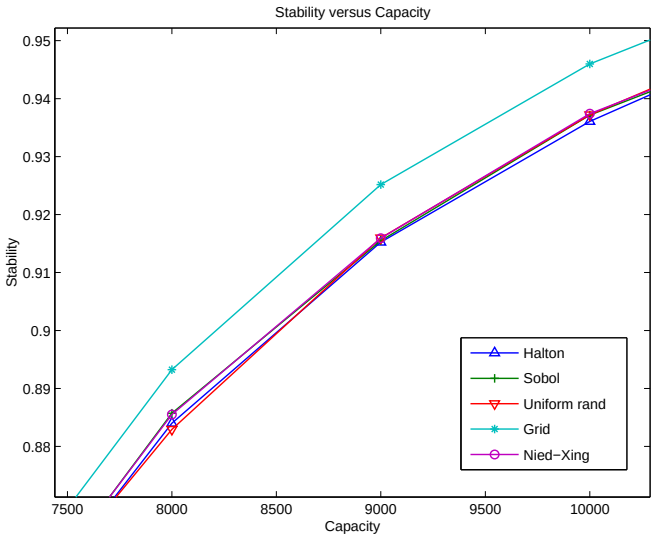

Figure 3.17: A closer look at Figure 3.16

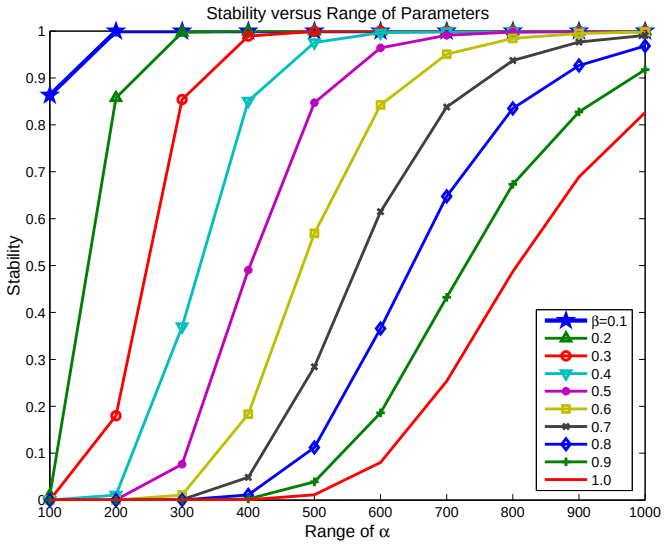

Figure 3.18: Stability versus parameter ranges for $M = 20$ users using a uniform random distribution within the range.

can be rewritten around the equilibrium state as

$$\begin{aligned}\tilde{x}_i(t+1) &= \tilde{x}_i(t) + \frac{u_i}{\tilde{x}_i(t) + x_i^* + 1} - \alpha_i \sum_{l \in R_i} (\tilde{d}_l(t) + d_l^*)\,,\ t = 0, 1, \ldots; \quad i \in \mathcal{M} \\ \tilde{d}_l(t+1) &= \tilde{d}_l(t) + \frac{1}{C_l} \sum_{j : l \in R_j} \tilde{x}_j(t)\,,\ t = 0, 1, \ldots; \quad l \in \mathcal{L}\,.\end{aligned} \tag{3.60}$$

Linearizing the system (3.60) around the equilibrium point $(\tilde{\mathbf{x}}^*, \tilde{d}^*) = (0, 0)$, we obtain

$$\begin{aligned}\tilde{x}_i(t+1) &= \left[1 - \frac{u_i}{(x_i^* + 1)^2}\right] \tilde{x}_i(t) - \alpha_i \sum_{l \in R_i} \tilde{d}_l(t)\,,\ t = 0, 1, \ldots; \quad i \in \mathcal{M} \\ \tilde{d}_l(t+1) &= \tilde{d}_l(t) + \frac{1}{C_l} \sum_{j : l \in R_j} \tilde{x}_j(t)\,,\ t = 0, 1, \ldots; \quad l \in \mathcal{L}\,,\end{aligned} \tag{3.61}$$

which can be described in matrix form as

$$\begin{pmatrix} \tilde{\mathbf{x}}(t+1) \\ \tilde{d}(t+1) \end{pmatrix} = \mathbf{G} \begin{pmatrix} \tilde{\mathbf{x}}(t) \\ \tilde{d}(t) \end{pmatrix}.$$

For the system (3.60) to be locally stable around the equilibrium, the eigenvalues λ of the matrix $\mathbf{G}$ have to be in the open unit circle, or $|\lambda| < 1$. We next study this condition only in the

$\alpha - \beta$ parameter space. The reason why we do not consider the $u - \alpha$ space is because the entries of the matrix in that case depend also on the equilibrium state, which however cannot be expressed in closed form in terms of the system parameters, since it is the solution of a set of nonlinear equations.

$\alpha - \beta$ parameter space We analyze the local stability and robustness of the linearized system (3.61) in $\alpha - \beta$ space, defined by the vector

$$p = [\alpha_1, \ldots, \alpha_M, \beta_1, \ldots, \beta_M, c_1, \ldots, c_L].$$

In addition, connections between users as described by the routing matrix $\mathbf{A}$ can also be taken as a variable, extending the parameter space to that described by the extended vector

$$p = [\alpha_1, \ldots, \alpha_M, \beta_1, \ldots, \beta_M, c_1, \ldots, c_L, \{A_{l,i}, l \in \mathcal{L}, i \in \mathcal{M}\}].$$

In this extended space, we study the stability of the network under all possible routing configurations for a given number of users and nodes.

Illustrative example

We first study at the effect of capacity on stability of the linearized system (3.8.3) using an illustrative example with three users and two links. The number of users and links is chosen small in order to be able to visualize the results. The routing matrix is fixed in this example, and is given by

$$\mathbf{A} \equiv \begin{pmatrix} 1 & 1 & 0 \\ 1 & 0 & 1 \end{pmatrix}.$$

The corresponding network configuration is shown in Figure 3.19. The matrix $\mathbf{G}$ for this example can now be written out explicitly as

$$\begin{pmatrix} 1-\beta_1 & 0 & 0 & -\alpha_1 & -\alpha_1 \\ 0 & 1-\beta_2 & 0 & -\alpha_2 & 0 \\ 0 & 0 & 1-\beta_3 & 0 & -\alpha_3 \\ \frac{1}{C_1} & \frac{1}{C_1} & 0 & 1 & 0 \\ \frac{1}{C_2} & 0 & \frac{1}{C_2} & 0 & 1 \end{pmatrix}.$$

As in previous simulations, the parameter ranges are chosen as $0 < \beta_i < 1$ and $0 < \alpha_i < 1000$, and a uniform distribution within the given range is used as the probabilistic model for the parame-

ters. Capacities of the links are varied exponentially from 10^2 to 10^6. Results of the simulation are shown in Figure 3.20. We observe that probability of stability increases with increasing capacity of the links, which is consistent with earlier results on the single bottleneck link case.

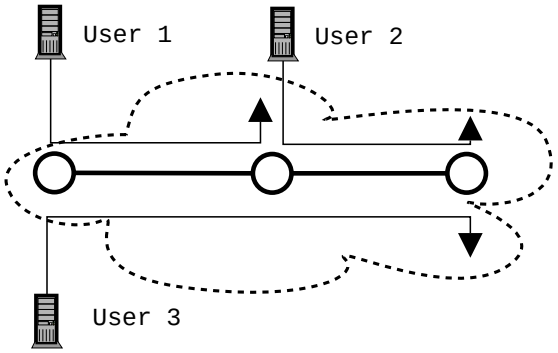

Figure 3.19: Network diagram for the illustrative example in Section 3.8.3.

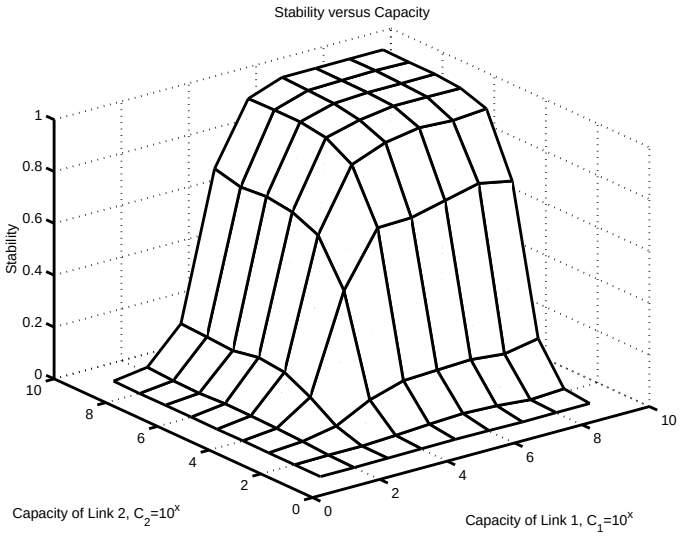

Figure 3.20: Probability of stability for various capacities of network links in the illustrative example of Section 3.8.3.

Simulations under general network topologies

We next simulate the system under an arbitrary network topology described by the routing matrix $\mathbf{A}$ given below with 5 links and 12 users:

$$\mathbf{A} = \begin{pmatrix} 1 & 1 & 1 & 0 & 0 & 0 & 0 & 1 & 0 & 0 & 0 & 0 \\ 1 & 1 & 0 & 1 & 1 & 1 & 1 & 0 & 1 & 0 & 0 & 0 \\ 0 & 0 & 1 & 1 & 1 & 1 & 0 & 0 & 0 & 1 & 0 & 0 \\ 1 & 0 & 0 & 0 & 1 & 0 & 1 & 0 & 0 & 0 & 1 & 0 \\ 0 & 1 & 0 & 1 & 0 & 0 & 1 & 0 & 0 & 0 & 0 & 1 \end{pmatrix}$$

It is in fact possible to repeat this simulation for arbitrarily large networks. The network structure adopted for this particular simulation is shown in Figure 3.21. We investigate the local stability of the system for different parameter ranges varying from 0.1 to 1 for β and from 100 to 1000 for α. A uniform distribution is used as probabilistic model within each given range of parameters. Capacities of the links $C_1, \ldots, C_5$ are arbitrarily fixed to values $[35\ 50\ 30\ 15\ 20]\ 10^3$. As a result of computational constraints, the number of samples is chosen to be $N = 10\,000$, which guarantees a level of confidence $\delta = 0.001$ and accuracy $\varepsilon = 0.02$. As we observe from Figure 3.22, results are comparable to the ones obtained for the single bottleneck link case.

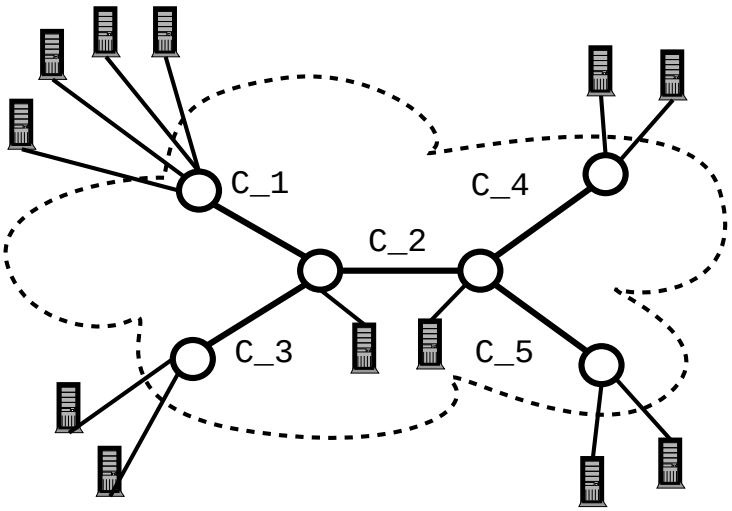

Figure 3.21: The network topology of 5 links with capacities $[35\,50\,30\,15\,20]\,10^3$ shared by 12 users.

Finally, we investigate robustness of the linearized system to different routes. The number of users and links are the same as in the previous simulation. However, the routing matrix, and hence, the topology and routes in the network, are generated randomly in addition to the parameters which

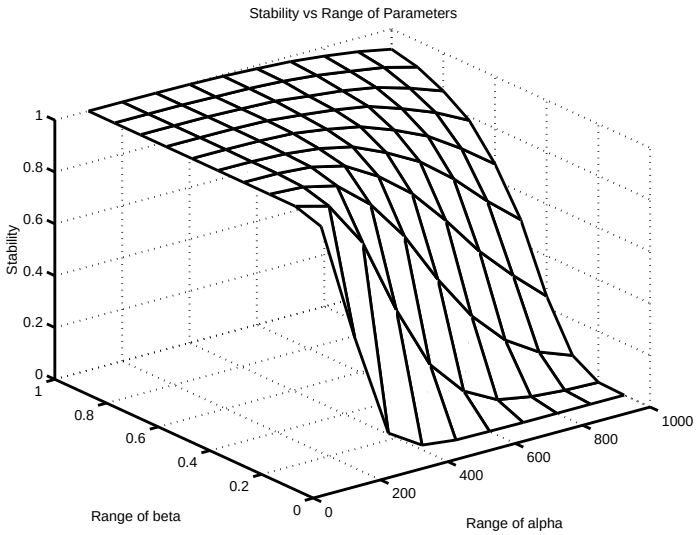

Figure 3.22: Network stability for various ranges of parameters under the arbitrary network topology given by Figure 3.21.

are generated using a uniform distribution within the ranges $0 < \beta_i < 1$ and $0 < \alpha_i < 1000\,,\ i = 1, \ldots, 4$. The number of different topologies randomly generated is 50, and number of samples per topology is chosen as 5000, ensuring a level of confidence $\delta = 0.001$ and accuracy $\varepsilon = 0.03$. We observe that the system is stable with a probability of 0.70. If we increase the capacities of the links tenfold to $[35\ 50\ 30\ 15\ 20]\,10^4$, however, the probability of stability increases to 0.99. These observations are consistent with earlier simulation and analytical results obtained.

As noted earlier, any simulation in the $u - \alpha$ space is not feasible under general network topologies with multiple bottleneck links, as the explicit calculation of the unique equilibrium state requires the solution of a set of nonlinear equations.

3.8.4 Packet level simulations

We investigate and demonstrate the results observed in numerical simulations through realistic packet level simulations using the NS-2 network simulator [77].

We first simulate the case of a single bottleneck link of capacity $C = 10^6$ shared by 20 identical users with parameters $\alpha = 0.5$ and $u = 20\,000$, which are consistent with earlier parameter choices. We observe in Figure 3.23(a) that the system is stable under 1 ms delay consistent with earlier simulation results. While the system is unstable under 10 ms delay as shown in Figure 3.23(b) the variations in flow rates are small enough for practical purposes. Next, we simulate the linear network (Figure 3.19) with 3 users analyzed in the illustrative example 3.8.3. The parameters are chosen as $\alpha = 500$ and $u = 10\,000$ similar to the ones in the example. Both of the

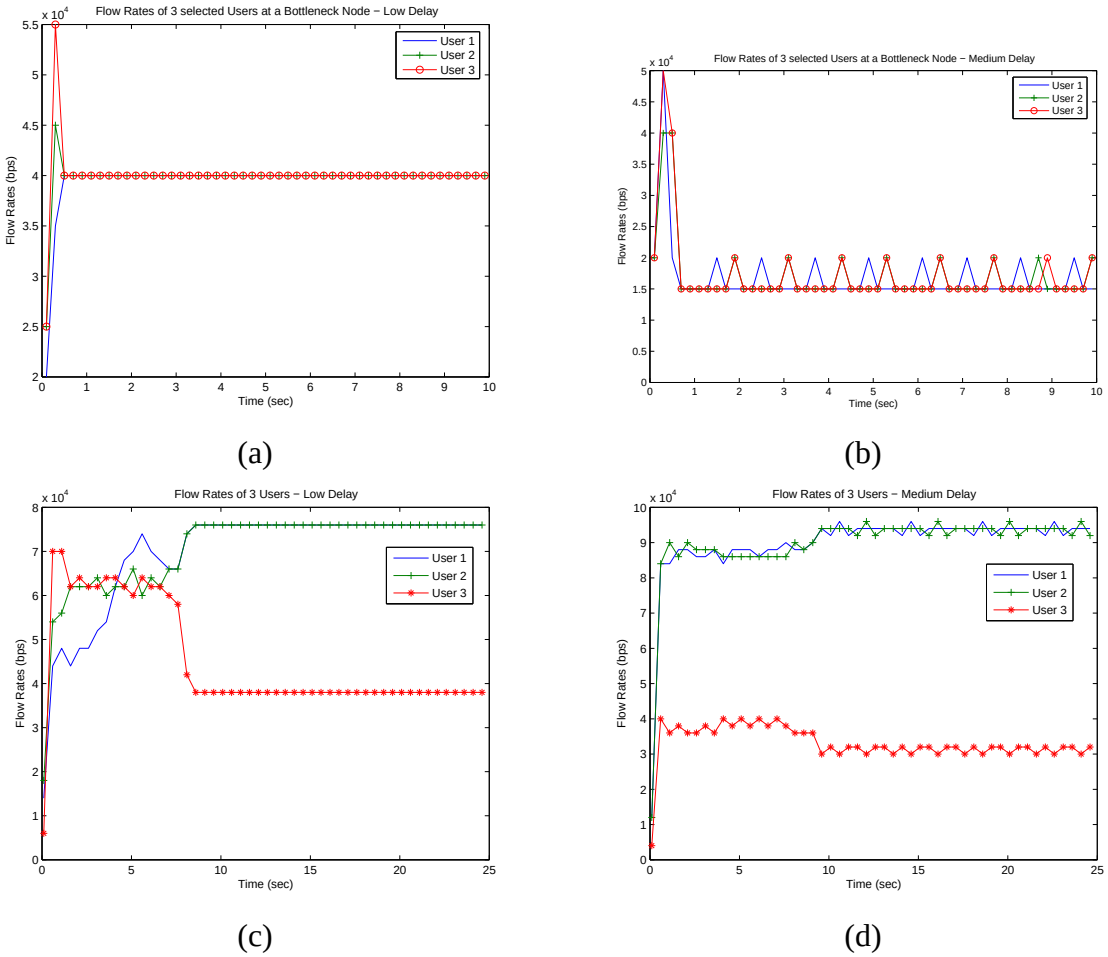

Figure 3.23: NS-2 simulations depicting flow rates of selected users sharing a bottleneck link under low (a) and medium (b) delays. Flow rates of three users on the linear network of Figure 3.19 under low (c) and medium (d) delays.

link capacities are $C_1 = C_2 = 10^5$. The flow rates of users are depicted in Figure 3.23(c) for low (1 ms) link delays and Figure 3.23(d) for medium (10 ms) link delays, respectively. Again the results are consistent with the ones in the illustrative example 3.8.3 although some limited fluctuations are observed under medium delay. Thus, these packet level NS-2 simulations demonstrate and are consistent with the previous analytical and numerical results based on fluid approximations.

3.9 Conclusions

We have presented a congestion control scheme for Internet-style networks by modifying the framework of Chapter 2, and including a realistic model of queue dynamics. Existence of a unique equilibrium point, which approximates NE, has been shown. Stability properties of the proposed

scheme are rigorously investigated by taking boundary effects into account. Furthermore, stability of the algorithm in a network with nonnegligible propagation delays has been established under some sufficient conditions in the case of a bottleneck node with multiple users. In addition, we have presented an adaptive pricing scheme for adjusting the pricing parameter dynamically, and have made use of hybrid (switched) system concepts for its analysis. Based on the congestion control scheme developed, we have designed a window-based, end-to-end congestion control scheme for Internet-style networks, and have simulated it in NS-2 over Internet protocol for various network topologies. We have also analyzed a discrete-time version of the proposed scheme, and its robustness properties using randomized algorithms.

CHAPTER 4

A HYBRID SYSTEM MODEL FOR POWER CONTROL IN MULTICELL WIRELESS DATA NETWORKS

In this chapter, we extend the single cell power control scheme of [52] to multiple cells and to a broader class of cost functions. Specifically, we model the multicell wireless data network as a switched hybrid system where handoffs of mobiles between the individual cells (base stations) correspond to discrete switching events between different subsystems. Under a set of sufficient conditions, we show in Section 4.1 the existence and global stability of a unique NE for each subsystem. In Section 4.2, we establish the global exponential convergence of the dynamics of the multicell power control game to a minimum convex set of Nash equilibria for any switching (handoff) scheme satisfying a mild condition on average dwell-time. Furthermore, we investigate robustness of these results to various communication constraints such as feedback delays and quantization. In addition, we analyze a quantization scheme to reduce the communication overhead between mobiles and the base stations. Finally, we illustrate the proposed power control scheme through MATLAB simulations in Section 4.3, which is followed by the concluding remarks of Section 4.4.

4.1 The Model, Cost Function, and NE

We consider a multicell CDMA wireless network model similar to the ones described in [49, 52]. The system consists of a set $\mathcal{L} := \{1, \ldots, \bar{L}\}$ of cells, with M_l users in cell l, $l \in \mathcal{L}$. The number of users in each cell is limited through an admission control scheme. We let $\mathcal{M}_l := \{1, \ldots, M_l\},\ l \in \mathcal{L}$ and $\mathcal{M} := \cup_l \mathcal{M}_l$. We associate a single base station (BS) with each cell in the system, and define $0 < h_{ij} < 1$ as the channel gain between the i^{th} mobile and the j^{th} BS. In each cell l, we consider a background noise of a cell specific variance σ_l^2. Furthermore, we assume that each mobile is connected to a single BS at any given time. Figure 4.1 shows a simple depiction of the wireless network model considered.

The i^{th} mobile transmits with an uplink power level of $p_i \leq p_{i,max}$, where $p_{i,max}$ is an upper-bound imposed by physical limitations of the mobile. Thus, the SIR obtained by mobile i at the

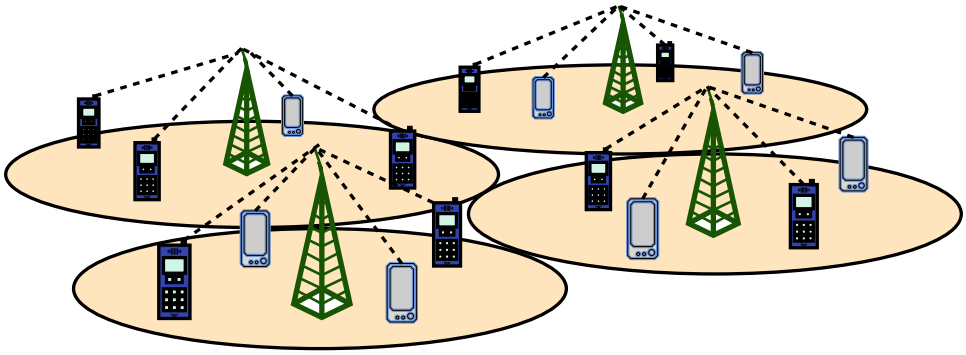

Figure 4.1: A simple multicell wireless network.

base station j is given by

$$\gamma_{ij} := \frac{Lh_{ij}p_i}{\sum_{k\in\mathcal{M},\, k\neq i} h_{kj}p_k + \sigma_j^2}. \tag{4.1}$$

Here, $L := W/R > 1$ is the spreading gain of the CDMA system, where W is the chip rate and R is the data rate of the user. Thus, by taking the intra-cell effects into account we consider a more complex and realistic interference model than the one in [58].

Define the power level of mobile i received at the j^{th} BS as $x_{ij} := h_{ij}p_i$, and let

$$\mathbf{x} := [x_{11}, \ldots, x_{M_1 1}, \ldots, x_{1L}, \ldots, x_{M_L L}].$$

Also let $\mathbf{x}_{-i} := \sum_{k\in\mathcal{M},\, k\neq i} h_{kj}p_k$ be the sum of the received power levels of all mobiles, except the i^{th} one, at the j^{th} BS. In order to simplify the notation we will drop the index of the BS (e.g. $x_i := x_{ij}$) in cases when it is obvious from the context that mobile i is connected to the j^{th} BS.

The i^{th} user's cost function is defined as the difference between the utility function of the user and its pricing function, $J_i = P_i - U_i$, similar to the one in [52]. The utility function, $U_i(\gamma_i)$, is a function of the SIR, γ_i, of the i^{th} user, and quantifies approximately the demand or *willingness to pay* of the user for bandwidth. The pricing function, $P_i(p_i)$, on the other hand, is imposed by the system to limit the interference created by the mobile, and hence to improve the system performance [49]. At the same time, it can also be interpreted as a cost on the battery usage of the user. As a result, the cost function of the i^{th} user connected to a specific BS is given by

$$J_i(x_i, \mathbf{x}_{-i}, h_i) = P_i(x_i) - U_i(\gamma_i(\mathbf{x}))\,, \tag{4.2}$$

where we have used x_i, instead of p_i, as the argument of P_i, by a possible redefinition of the latter. We now make the following assumptions on the cost functions:

Assumption 4.1 *$P_i(x_i)$ is twice continuously differentiable, nondecreasing and strictly convex in*

x_i, *i.e.,*

$$\partial P_i(x_i)/\partial x_i \geq 0, \partial^2 P_i(x_i)/\partial x_i^2 > 0, \forall x_i.$$

Assumption 4.2 *$U_i(\gamma_i(\mathbf{x}))$ is jointly continuous in all its arguments and twice continuously differentiable, nondecreasing and strictly concave in x_i, i.e., $\partial U_i(\mathbf{x})/\partial x_i \geq 0$, $\partial^2 U_i(\mathbf{x})/\partial x_i^2 < 0$, $\forall x_i$.*

Assumption 4.3 *$U_i(\gamma_i)$ satisfies the inequality*

$$\left|\frac{d^2U_i}{d\gamma_i^2}\right| \gamma_i < \frac{dU_i}{d\gamma_i} < (L+\gamma_i)\left|\frac{d^2U_i}{d\gamma_i^2}\right|,$$

where $|.|$ denotes the absolute value function.

Assumption 4.4 *The i^{th} user's cost function has the following properties: At $x_i = 0$, $J_i(\mathbf{x} : x_i = 0) > J_i(\mathbf{x})$, $\forall \mathbf{x}$ $x_i \neq 0$, and at $x_{i,max} = x_{i,max}$, $J_i(\mathbf{x} : x_i = x_{i,max}) > J_i(\mathbf{x})$, $\forall \mathbf{x}$ $x_i < x_{i,max}$, respectively.*

Thanks to Assumptions 4.1 and 4.2 the cost function J_i is strictly convex, and belongs to a fairly large subclass of convex functions. Hence, there exists a unique solution to the i^{th} user's minimization problem, which is that of minimization of J_i, given the system parameters and the power levels of all other users. The Nash equilibrium (NE) is defined as a set of power levels ϕ^* (and corresponding set of costs J^*) with the property that no user can benefit by modifying its power level while the other players keep theirs fixed. Furthermore, Assumption 4.4 ensures that any equilibrium solution is an *inner* one; i.e., boundary solutions $x_i^* = 0$ $(x_i^* = x_{i,max})$ $\forall i$ cannot be equilibrium points. Mathematically speaking, $\mathbf{x}^*$ is in NE, when x_i^* of any i^{th} user is the solution to the following optimization problem given the equilibrium power levels of other mobiles, $\mathbf{x}_{-i}^*$:

$$\min_{0 \leq x_i \leq x_{i,max}} J_i(x_i, \mathbf{x}_{-i}^*, h_i). \tag{4.3}$$

Theorem 4.1 *Under Assumptions 4.1-4.4, the multicell power control game admits a unique inner Nash equilibrium solution.*

Proof. The proof of this theorem is similar to the one of Theorem 2.2. It is briefly outlined here for completeness. Let $X := \{\mathbf{x} \in \mathbb{R}^M : 0 \leq \mathbf{x} \leq \mathbf{x}_{max}\}$ be a set of feasible received power levels at the base stations in the system. Clearly, X is closed and bounded, and hence compact. Furthermore, it is also convex, and has a nonempty interior. By a standard theorem of game theory

(Theorem 4.4, p.176, in [1]) the power control game admits a Nash equilibrium. In addition, by Assumption 4.4 this solution has to be inner. It follows from Assumption 4.3 that

$$\frac{\partial^2 J_i}{\partial x_i^2} > \frac{\partial^2 J_i}{\partial x_i \partial x_j} > 0.$$

Finally, using an argument similar to the one in the proof of Theorem 2.2 one can show that the inner NE solution is unique. Thus, there exists a unique inner NE in the multicell power control game. □

4.2 Hybrid Modeling and Stability

We consider a dynamic model of the power control game where each mobile uses a gradient algorithm to solve its own optimization problem (4.3). The update scheme of the i^{th} mobile is given by

$$\dot{p}_i = \frac{dp_i}{dt} = -\lambda_i \frac{\partial J_i}{\partial p_i},$$

where $\lambda_i > 0$ is a user-dependent stepsize. This can also be described in terms of the received power level x_i at the BS l to which mobile i is connected:

$$\dot{x}_i = \frac{dU_i}{d\gamma_i} \frac{L\lambda_i h_i^2}{\sum_{j\neq i}(h_{jl}/h_j)x_j + \sigma_l^2} - \lambda_i h_i \frac{dP_i}{dp_i} := \phi_i(\mathbf{x}), \tag{4.4}$$

where h_j denotes the channel gain of mobile j to its own BS. Thus, we obtain a distributed power control algorithm that brings minimum overhead to the network for the only information the mobile needs in order to update its power level, other than its own most recent power level and the system parameters, is the level of total received power at the BS.

4.2.1 Stability in the static case

We first establish the stability of the update scheme (4.4) under some sufficiency conditions in the *static case*, where each mobile is connected to a specific base station (belongs to a cell) for all times. By taking the second derivative of x_i (connected to cell l) with respect to time we obtain

$$\ddot{x}_i = \left(-a_i - \frac{d^2 P_i}{dp_i^2}\right)\dot{x}_i + \sum_{j\in\mathcal{M}_l,\, j\neq i} b_i \dot{x}_j + \sum_{k\notin\mathcal{M}_l} b_i \frac{h_{kl}}{h_k}\dot{x}_k := \dot{\phi}_i(\mathbf{x}), \tag{4.5}$$

where a_i and b_i are defined as

$$a_i := \left|\frac{d^2U_i}{d\gamma_i^2}\right| \frac{L^2\lambda_i h_i^2}{(\sum_{j\neq i}(h_{jl}/h_j)x_j + \sigma_l^2)^2},$$

and

$$b_i := \frac{a_i}{L}\gamma_i - \frac{dU_i}{d\gamma_i}\frac{L\lambda_i h_i^2}{(\sum_{j\neq i}(h_{jl}/h_j)x_j + \sigma_l^2)^2}.$$

Notice that, a_i is positive, and under Assumption 4.3, b_i is negative.

Let us introduce the candidate quadratic Lyapunov function

$$V := \sum_{i\in\mathcal{M}} \phi_i^2(\mathbf{x}) \ . \tag{4.6}$$

First note that because of the uniqueness of the NE, $\mathbf{x}^*$, $\phi_i(\mathbf{x}) = 0\ \forall i$ if and only if $\mathbf{x} = \mathbf{x}^*$. Hence, V is positive for all $\mathbf{x}$ except for $\mathbf{x} = \mathbf{x}^*$. Furthermore, as $||\mathbf{x}|| \to \infty$,

$$\frac{\frac{dU_i}{d\gamma_i}(L\lambda_i h_i^2)}{\sum_{j\neq i}\frac{h_{jl}}{h_j}(x_j + \sigma_l^2)}$$

is bounded by Assumption 4.2 and $|\lambda_i h_i dP_i/dp_i| \to \infty$ by Assumption 4.1. Hence, V is radially unbounded, $V \to \infty \Leftrightarrow ||\mathbf{x}|| \to \infty$, where $||.||$ denotes the norm operator.

Taking the derivative of V with respect to t we have

$$\dot{V} \leq \sum_{i\in\mathcal{M}} -2a_i\phi_i^2 + \sum_{i\in\mathcal{M}} |b_i| \sum_{j\neq i} 2\frac{h_{ji}}{h_j}|\phi_i\phi_j|,$$

where h_{ji} denotes the channel gain of mobile j to the BS to which mobile i is connected. We note that $\frac{h_{ji}}{h_j} < 1$ for all $i, j \in \mathcal{M}$, and $\frac{h_{ji}}{h_j} \ll 1$ if there is a large geographic distance between the mobiles i and j.

It follows from a simple algebraic manipulation that

$$\sum_{i\in\mathcal{M}} |b_i| \sum_{j\neq i} 2\frac{h_{ji}}{h_j}|\phi_i\phi_j| \leq 2(M_{eff} - 1)\max_i |b_i| \sum_{i\in\mathcal{M}} \phi_i^2,$$

where M_{eff} is defined as the largest cluster of users who have a nonnegligible effect on each other's SIR levels through in-cell and intracell interference. It immediately follows that, $\max_l M_l <$

$M_{eff} \leq M$. In practice, a possible definition of M_{eff} would be

$$M_{eff} := \max_l M_l + \sum_{k \in Neighbor(l)} M_k,$$

where $Neighbor(l)$ is defined as the set of first-tier neighbors of the cell l, due to negligible effect of mobiles in other cells, which are farther away.

Using this to bound $\dot{V}$ yields

$$\dot{V} \leq (-\min_i 2a_i + 2(M_{eff} - 1) \max_i |b_i|) \sum_{i \in \mathcal{M}} \phi_i^2.$$

Next, we refine Assumption 4.3 as follows:

Assumption 4.5 *$U_i(\gamma_i)$ satisfies the inequality*

$$\left| \frac{d^2 U_i}{d\gamma_i^2} \right| \gamma_i < \frac{dU_i}{d\gamma_i} < (1 + \gamma_i) \left| \frac{d^2 U_i}{d\gamma_i^2} \right|.$$

Remark 4.1 *A large class of logarithmic utility functions, $U_i = u_i log(k\gamma_i + 1)$, where $k > 1$ and $u_i > 0$ are scalar parameters, satisfy Assumptions 4.2 and 4.5.*

Under Assumption 4.5, we have $0 \leq |b_i| \leq a_i/L$. Hence, a sufficient condition for $\dot{V} < 0$, uniformly in the x_i's, is

$$L > m(M_{eff} - 1), \tag{4.7}$$

where m is defined as

$$m := \max_{\mathbf{x} \in X} \frac{\max_{i \in \mathcal{M}} a_i}{\min_{i \in \mathcal{M}} a_i}. \tag{4.8}$$

Thus, V is indeed a Lyapunov function, and being also radially unbounded in x_i's, it readily follows that $\phi_i(\mathbf{x}(t)) = \dot{x}_i(t) \to 0, \ \forall\, i$. This in turn implies that $x_i(t)$'s converge to the unique Nash equilibrium. Hence, the unique NE point (Theorem 4.1) is globally asymptotically stable with respect to the update scheme (4.4) under the sufficient condition (4.7). This result is stated in the following theorem:

Theorem 4.2 *Let $\mathbf{x}^{NE} := [\mathbf{x}_1^*, \mathbf{x}_2^*, \ldots, \mathbf{x}_L^*]$ be the unique NE of a static multicell CDMA wireless network, where $\mathbf{x}_i^* := [x_{1i}^*, x_{2i}^*, \ldots, x_{M_l i}^*]$, and each mobile $i \in \mathcal{M}_l$ in cell $l \in \mathcal{L}$ stays connected to the respective BS for all times. Then, the system dynamics are globally asymptotically stable if*

$$L > m(M_{eff} - 1),$$

where M_{eff} is defined as the largest cluster of users who have a nonnegligible effect on each other's SIR levels and m is given by (4.8).

4.2.2 The dynamic case and hybrid modeling

In the static case there are no handoffs (switches) in the network. Consider now the *dynamic case*, where mobiles connect to base stations dynamically using criteria like SIR or channel gain as they move along the cells. Then, it is possible to consider each *static case* with a fixed distribution of users among cells as a separate subsystem q belonging to a family (set) of systems denoted by Q. This leads to a hybrid system where each handoff corresponds to switching from one system to another. In the study of this hybrid system we make use of the concept of *dwell-time* τ, which quantifies the minimum amount of time between two switches. However, in a wireless network handoffs are random in nature, and they may occur in short bursts. Therefore, we also make use of the concept of *average dwell-time*, which is much less restrictive than the dwell-time [98]. Let us denote the number of discontinuities of a switching signal σ on an interval (t, T) by $N_\sigma(t, T)$. Using the definition in [2], σ has average dwell-time $\tau_a >$ if there exists a positive integer N_0 such that

$$N_\sigma(t, T) \leq N_0 + \frac{T - t}{\tau_a},\ \forall T \geq t \geq 0.$$

Based on our previous analysis for the static case, we define a quadratic Lyapunov function $V^{(q)}$ as in (4.6) for the subsystem $q \in Q$. Modifying condition (4.7) as

$$L > m(M_{eff} - 1) + \epsilon \tag{4.9}$$

where $\epsilon > 0$ is a positive constant yields

$$\dot{V}^{(q)} \leq -\epsilon V^{(q)}.$$

The unique NE, $\mathbf{x}_q^{NE}$, of the q^{th} subsystem is then globally exponentially stable by Theorem 4.2.

To simplify the rest of the analysis, we will make the following assumption without any loss of generality:

Assumption 4.6 *In the multicell wireless network, no two handoffs can occur at the same time.*

Since, under Assumption 4.6, the times of occurrence of multiple handoffs may still be arbitrarily close to each other, this technical assumption is not restrictive in practice. As a result of Assumption 4.6, switching can happen only between "neighbor" subsystems, due to the handoff of a single mobile between two neighboring cells in the network. Hence, there exists a finite $\mu(\kappa) > 1$

such that

$$\frac{V^{(q)}}{V^{(r)}} \leq \mu(\kappa),\ \forall \mathbf{x} \in (X^{(q)} \cap X^{(r)}) - \{\mathbf{x} : ||\mathbf{x} - \mathbf{x}_i^{NE}|| < \kappa,\ i = q, r\}$$

where $q,\ r \in Q$ are any two "neighbor" subsystems and $\kappa > 0$ is a small positive constant. Let us also define the set of NE for all subsystems as

$$\mathcal{N} := \{\mathbf{x}_q^{NE}, \forall q \in Q\}.$$

At a given time instance the system has only one NE which is an element of the set $\mathcal{N}$. However, this unique NE also switches from one equilibrium to the next in the set $\mathcal{N}$ with each handoff in the system.

Based on Theorem 2.6 we next give the following result on the multicell wireless network:

Theorem 4.3 *Assume that the following condition holds for all the cells in the wireless network, for some $\epsilon > 0$:*

$$L > m\left(M_{eff} - 1\right) + \epsilon\ , \forall l \in \mathcal{L},$$

where

$$m := \max_{\mathbf{x} \in X} \frac{\max_{i \in \mathcal{M}} a_i}{\min_{i \in \mathcal{M}} a_i}.$$

Let $\overline{\mathcal{N}}$ be the union of the smallest level sets of $V^{(q)}(x)$ that contain a superset of the set of Nash equilibria, $\mathcal{N}$, defined as $\{\mathbf{x} : ||\mathbf{x} - \mathbf{x}_q^{NE}|| < \kappa\}$, which are "neighbor" to $q,\ \forall q \in Q$. Then, under the set of Assumptions 4.1-4.6, the dynamics of the multicell power control game globally exponentially converge to $\overline{\mathcal{N}}$ for every switching signal σ with average dwell-time

$$\tau_a > \frac{\log \mu(\kappa)}{\epsilon}.$$

Furthermore, $\overline{\mathcal{N}}$ is invariant under the same set of conditions if the dwell-time τ satisfies

$$\tau > \frac{\log \mu(\kappa)}{\epsilon},\ \forall t.$$

Proof. The conditions (2.37) and (2.38) in Theorem 2.6 follow directly from (4.9) and from the properties of V under the Assumptions 4.1-4.6. We note that, due to the Assumption 4.6, $\overline{\mathcal{N}}$ is a smaller set in this special case than the most general one. The rest of the proof follows the same lines as the ones in Theorem 2.6. □

Remark 4.2 *By Assumption 4.6, the equilibrium point of the system jumps from NE of a subsystem*

to the NE of a "neighbor" subsystem which is close in "distance" to it, where the distance is defined by a chosen norm. Hence, in a wireless network where distribution of mobiles changes slowly over time, the operating point of the system may stay in a subset of $\mathcal{N}$ over a time interval much longer than the update interval. In this case, the practical "size" of the set $\overline{\mathcal{N}}$ is much smaller than the one in Theorem 4.3.

Proposition 4.1 *Consider a wireless network with M mobiles and $\bar{L}$ nonempty cells. If $M \to \infty$ then $\mu \to 1$, and hence, $\tau \to 0$.*

Proof. Without loss of generality, assume that the k^{th} mobile switches from a cell $m \in \mathcal{L}$ to cell $n \in \mathcal{L}$. Then, by definition of μ, and showing explicitly its dependence on M,

$$\mu^{(M)} = \frac{\Xi_{m,n} + \sum_{i \in \mathcal{M}_m} \phi_i^2 + \sum_{i \in \mathcal{M}_n} \phi_i^2}{\Xi_{m,n} + \sum_{i \in \mathcal{M}_m, i \neq k} \bar{\phi}_i^2 + \sum_{i \in \mathcal{M}_n} \bar{\phi}_i^2 + \phi_k^2},$$

where $\Xi_{m,n} = \sum_{l \in \mathcal{L}, l \neq m,n} \sum_{i \in \mathcal{M}_l} \phi_i^2$. As $M \to \infty$,

$$\Xi_{m,n} \gg \sum_{i \in \mathcal{M}_m} \phi_i^2 + \sum_{i \in \mathcal{M}_n} \phi_i^2 \text{ and } \bar{\phi}_i^2 \to \phi_i^2, \forall i \in \mathcal{M}_n, \mathcal{M}_m.$$

Hence, $\mu^{(M)}$ converges asymptotically to 1. Therefore, by Theorem 4.3 average dwell-time, τ, diminishes to zero. □

4.2.3 Stability under feedback delays

Even if we assume that mobiles have perfect information on their channel gain, cost, and system parameters, they still need the total received power level to be provided by the base station in order to implement the dynamic update algorithm (4.4). The BS determines the total received power level through measurements, and sends it to the mobile. Measuring, processing (both at BS and mobile), and signaling of this information takes time, which results in non-negligible delays in the network, which can go up to 0.5 s in GSM systems (see [50], p. 28). Here we model such delays as a single fixed feedback delay. Since propagation delays are negligible for cellular wireless networks, all mobiles in a cell experience almost the same amount of feedback delay. In other words, delays are symmetric within a cell. Hence, the power update function of the i^{th} mobile in

terms of x_i becomes

$$\dot{x}_i(t) = \frac{dU_i}{d\gamma_i} \frac{L\lambda_i h_i^2}{\sum_{j\neq i,\, j\in\mathcal{M}_l} x_j(t-r) + \sigma_l^2} - \lambda_i h_i \frac{dP_i}{dp_i}(t) := \phi_i(\mathbf{x}(t)), \tag{4.10}$$

where $r > 0$ denotes the feedback delay in the network.[1]

We now investigate stability of a single cell l by introducing the radially unbounded, quadratic Lyapunov function

$$V_l(\mathbf{x}(t)) := \sum_{i\in\mathcal{M}_l} \phi_i^2(\mathbf{x}(t)) + (\max_{\mathbf{x}\in X_l} \max_i |b_i|)(M_l - 1) \sum_{i\in\mathcal{M}_l} \int_{t-r}^{t} \phi_i^2(\mathbf{x}(s))ds.$$

Assuming Assumptions 4.1, 4.2, 4.4, and 4.5 to hold, we essentially repeat the Lyapunov analysis of Section 4.2.1. Taking the derivative of $V_l(\mathbf{x}(t))$ with respect to t, we have

$$\begin{aligned}\dot{V}_l(\mathbf{x}(t)) \quad &\leq \textstyle\sum_{i\in\mathcal{M}_l} -2a_i\phi_i^2(\mathbf{x}(t)) + (\max_{\mathbf{x}\in X_l} \max_i |b_i|) \\ &\quad \cdot \Bigg[\textstyle\sum_{i\in\mathcal{M}_l} \sum_{j\in\mathcal{M}_l\,,\, j\neq i} 2|\phi_i(\mathbf{x}(t))\phi_j(\mathbf{x}(t-r))| \\ &\qquad +(M_l - 1)\Big(\phi_i(\mathbf{x}(t))^2 - \phi_i(\mathbf{x}(t-r))^2\Big)\Bigg].\end{aligned}$$

It again follows from a simple algebraic manipulation that

$$\sum_{i\in\mathcal{M}_l} \sum_{j\in\mathcal{M}_l\,,\, j\neq i} 2|\phi_i(\mathbf{x}(t))\phi_j(\mathbf{x}(t-r))| \leq (M_l - 1) \sum_{i\in\mathcal{M}_l} \phi_i^2(\mathbf{x}(t)) + \phi_i^2(\mathbf{x}(t-r)).$$

Using this to bound V_l further above yields

$$\dot{V}_l(\mathbf{x}(t)) \leq (-\min_i 2a_i + 2(M_l - 1)) \max_{\mathbf{x}\in X_l} \max_i |b_i| \sum_{i\in\mathcal{M}_l} \phi_i^2(t)$$

Hence, a sufficient condition for $\dot{V}_l(\mathbf{x}(t)) < 0$, uniformly in the x_i's, is

$$L > m_l(M_l - 1), \tag{4.11}$$

where m_l is defined as

$$m_l := \frac{\max_{\mathbf{x}\in X_l} \max_{i\in\mathcal{M}_l} a_i}{\min_{\mathbf{x}\in X_l} \min_{i\in\mathcal{M}_l} a_i}.$$

Thus, the unique NE point (Theorem 4.1) of cell l is globally asymptotically stable with respect

[1]Here, to avoid cumbersome notational complexity we ignore the interference from neighboring cells; for extensions to multicell environments, see Remark 4.3.

to the update scheme (4.10) under the sufficient condition (4.11) for any feedback delay r. Note that the condition in (4.11) is more restrictive than the one in (4.7). Moreover, although the value of r does not affect stability, large delays may result in slower convergence rates, and they may decrease the robustness of the system.

Remark 4.3 *The analysis above can be extended in a natural way to the static and dynamic multiple cell cases to obtain counterparts of Theorems 4.2 and 4.3 for the delayed information case; we have not carried out this extension here in order to keep the basic message clear.*

4.2.4 Communication constraints

Total received power level $\sum_{i\in\mathcal{M}} h_{il}p_i + \sigma_l^2$ at the BS of the cell l constitutes the main information flow in the distributed power update scheme (4.4). BS has to send mobiles this quantity (state information) as frequently as possible in order for the update algorithm to converge. This, however, may bring a significant overhead to the system, if not implemented efficiently. We investigate here a simple practical scheme which lessens the communication overhead, and hence, increases the efficiency through quantization (see Figure 4.2).

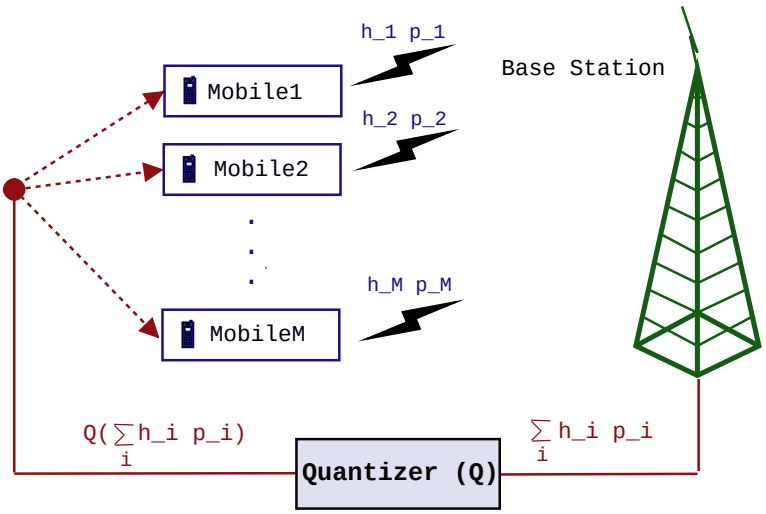

Figure 4.2: A simple quantization scheme for reducing overhead in the system.

Although total received power level can be measured to a great accuracy at the BS, it is not necessary to send this information to the mobile in its most accurate form as this would waste valuable bandwidth. Instead, this value can be quantized without destroying system stability. We consider, for its simplicity and ease of implementation, a uniform quantization scheme. Assume that there exists a fixed practical upper bound on $\sum_{i\in\mathcal{M}} h_{il}p_i + \sigma_l^2$, defined as F for any cell l.

Then, a K level quantization of aggregate received power level is

$$0 \leq \theta_K(\sum_{i \in \mathcal{M}} h_{il} p_i + \sigma_l^2) \leq F, \, \forall l \in L$$

where θ_K is a K level uniform quantizer. As long as $\sum_{i \in \mathcal{M}} h_{il} p_i + \sigma_l^2 \in [0, F]$ holds for all cells, the maximum quantization error $\mathbf{x_{-i}}$ is defined as $\mathbf{x_{-i}} := F/2K$.

A derivation similar to the one in Section 4.2.1 results in the following modified version of the sufficient condition in (4.11) for stability of the system in the presence of the quantization error $\mathbf{x_{-i}}$,

$$L > \overline{m}(M_{eff} - 1),$$

where $\overline{m}$ is defined as

$$\overline{m} := \frac{\max_i \left| \frac{d^2 U_i}{d\gamma_i^2} \right| \frac{L^2 \lambda_i h_i^2}{(\sum_{j \neq i} (h_{ji}/h_j) x_j + \sigma_l^2)^2 + \mathbf{x_{-i}}}}{\min_i \left| \frac{d^2 U_i}{d\gamma_i^2} \right| \frac{L^2 \lambda_i h_i^2}{(\sum_{j \neq i} (h_{ji}/h_j) x_j + \sigma_l^2)^2 - \mathbf{x_{-i}}}}.$$

Hence, given a sufficiently large L, there exists an upper-bound on $\mathbf{x_{-i}}$ which preserves stability. Using this value of $\mathbf{x_{-i}}$ we obtain the minimum number of bits to represent the feedback information,

$$bit_{min} = \lceil \log_2 F/(2\mathbf{x_{-i}}) \rceil,$$

where $\lceil . \rceil$ denotes ceiling function (rounding up to the next integer). Assume that the mobile update frequency is $f_{update} Hertz$. Then, the system overhead in the downlink for a mobile is given by

$$bitrate = f_{update} \lceil \log_2 F/(2\mathbf{x_{-i}}) \rceil \text{ b/s (bits-per-second)}.$$

The rate of change in the total received power level in a cell can be bounded above by F_{var},

$$\frac{\partial(\sum_{i \in \mathcal{M}} h_{il} p_i + \sigma_l^2)}{\partial t} \leq F_{var}.$$

Therefore, sending the mobiles the incremental changes in the total received power level instead of sending the whole information each time results in bandwidth savings. In this case, in order to maintain the given maximum quantization error $\mathbf{x_{-i}}$, the minimum number of bits to use is

$$\overline{bit}_{min} = \lceil \log_2 \frac{F_{var}}{2\mathbf{x_{-i}} f_{update}} \rceil,$$

and the bit rate is given by

$$\overline{bitrate} = f_{update}\lceil \log_2 \frac{F_{var}}{2\mathbf{x}_{-\mathbf{i}} f_{update}} \rceil \text{ b/s}.$$

We note that this incremental delivery of feedback information results in significant savings of overhead bandwidth.

4.3 Simulations

We simulated the power control scheme developed in MATLAB. The cost function for the i^{th} user (mobile) was chosen as

$$J_i(x_i, \mathbf{x}_{-i}, h_i) = \frac{1}{2}\alpha_i x_i^2 - u_i \log(\gamma_i + 1), \tag{4.12}$$

where $\alpha_i > 0$ and $u_i > 0$ are user specific pricing and utility parameters respectively. Notice that the quadratic pricing and logarithmic utility functions in (4.12) satisfy Assumptions 4.1, 4.2, 4.4, and 4.5 with an appropriate choice of parameter values. Therefore, results of Theorem 4.3 apply to the following power update algorithm of the i^{th} mobile, which is connected to BS l,

$$\dot{p}_i = \lambda_i \frac{u_i}{p_i + \frac{1}{Lh_i}(\sum_{j\neq i} h_{jl} p_j + \sigma_l^2)} - \lambda_i \alpha_i h_i p_i,$$

if Assumption 4.6 and condition on average dwell-time are satisfied. In the simulations, a discretized version of this update scheme was implemented:

$$p_i^{(n+1)} = p_i^{(n)} + \frac{u_i}{p_i^{(n)} + \frac{1}{Lh_i}(\sum_{j\neq i} h_{jl} p_j^{(n)} + \sigma_l^2)} - \alpha_i h_i p_i^{(n)}.$$

The scenario we adopted is the following. We have a simple multicell wireless network consisting of six rectangular shaped cells with 40 users. Base stations are located near the center of each cell. The system parameters are chosen as $L = 128$ and $\sigma_l^2 = 1\ \forall l$. Cost parameters are the same for all users, $u_i = 100,\ \alpha_i = 1,\ \lambda_i = 1\ \forall i$, and they are fixed for the duration of the simulation. Mobiles are initially located randomly in the system, and their movement is modeled as a random walk with a speed of 0.0001 units per update, where we set the update frequency to 100 Hz. Hence, if we assume a system with unit size of 1000 m, then mobiles move with a speed of 10 m/s.

The channel gain of the i^{th} mobile is determined by a simple large-scale path loss formula

$h_i = (0.1/d_i)^2$ where d_i denotes the distance to the BS, and the path loss exponent is chosen as 2 corresponding to open air path loss. The channel gain h_i is chosen as one if $d_i < 0.1$. However, fast and random movement of mobiles result in higher variations in the channel gains, and hence, compensate for this simplification. We use the channel gain as the handoff criterion. Each mobile connects to the base station with highest channel gain, which in turn corresponds to the nearest one. In Figure 4.3, locations of base stations and the paths of all mobiles in the network are shown. A sample path of a single mobile is shown in Figure 4.4.

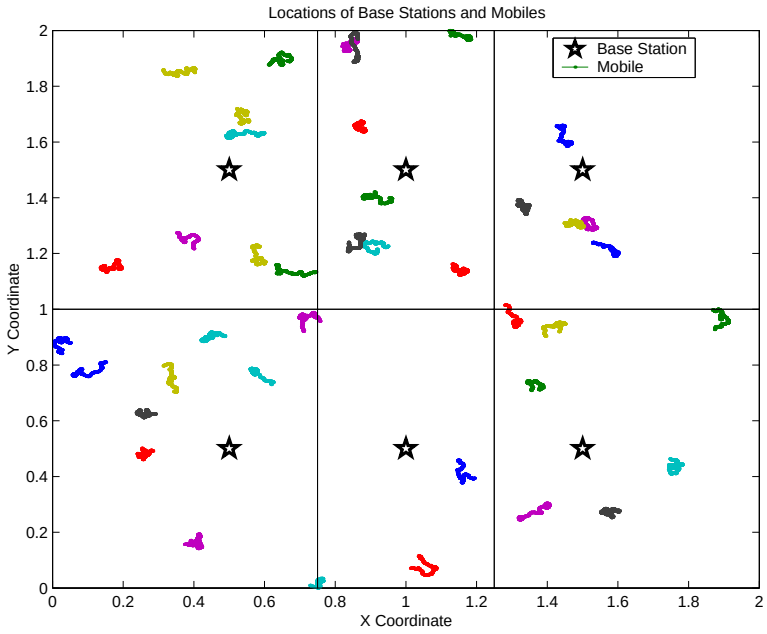

Figure 4.3: Locations of base stations and the paths of mobiles.

Figures 4.5 and 4.6 depict the power levels and SIR values of mobiles for the duration of the simulation. Notice that the power levels converge to the equilibrium points, which shift due to handoffs in the system. Jumps in SIR values can be observed in Figure 4.6 when a mobile moves from a less congested cell with a smaller number of mobiles to a more congested one or vice versa. Variations in congestion levels in the cells and in channel gains are also the reasons why not all mobiles have the same SIR levels despite having the same cost parameters. The simulation was repeated with the same setup but with a 50 steps (0.5 s) communication delay between the base station and mobiles. In accordance with the results in Section 4.2.3, convergence characteristics of the system are not significantly affected by the presence of feedback delay except for the convergence rate, as it can be seen in Figure 4.7. Figure 4.8 shows the aggregate received power levels at the base stations. The "relative" smoothness of these values indicate significant savings in system overhead when the feedback quantization scheme analyzed in Section 4.2.4 is implemented.

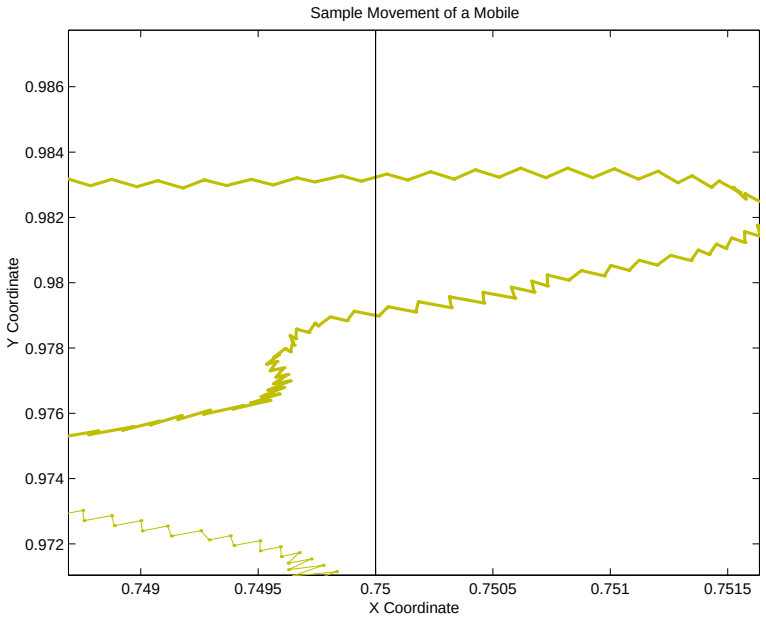

Figure 4.4: A sample path of a mobile.

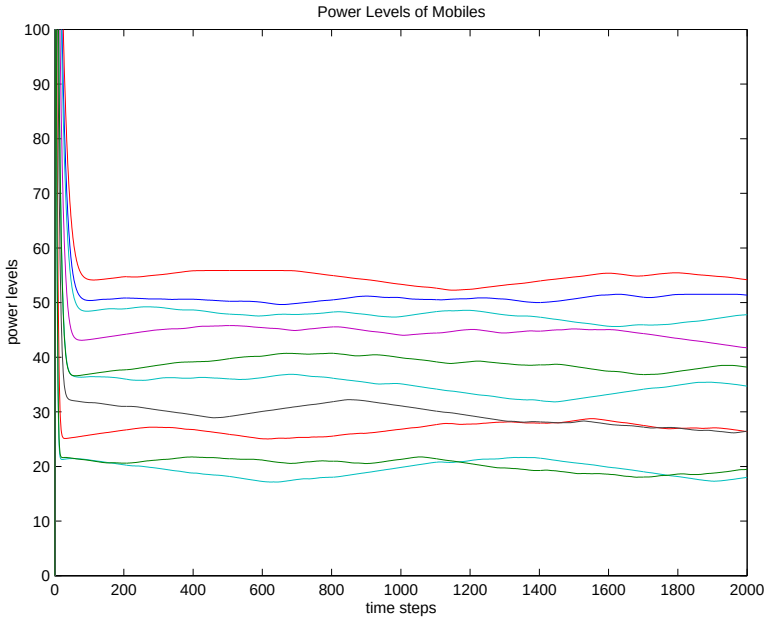

Figure 4.5: Power levels of 10 selected mobiles with respect to time.

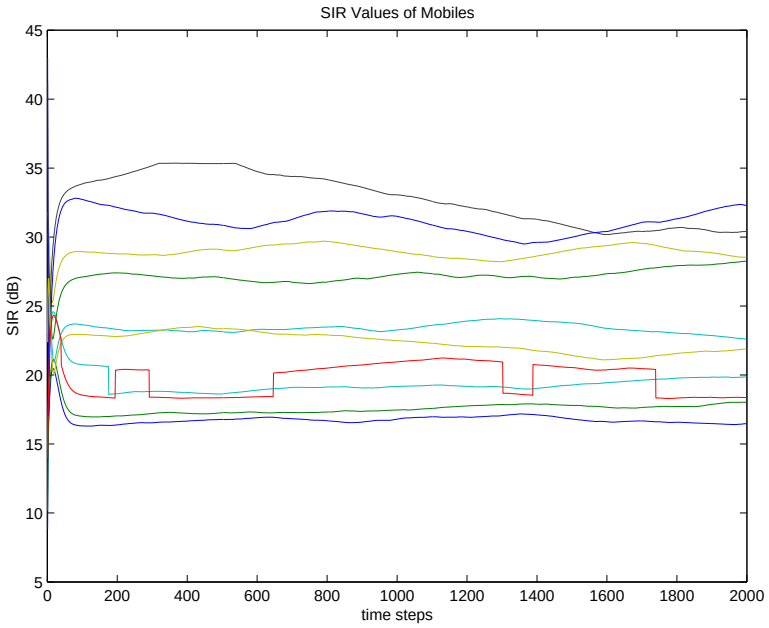

Figure 4.6: SIR values of 10 selected mobiles (in dB) with respect to time.

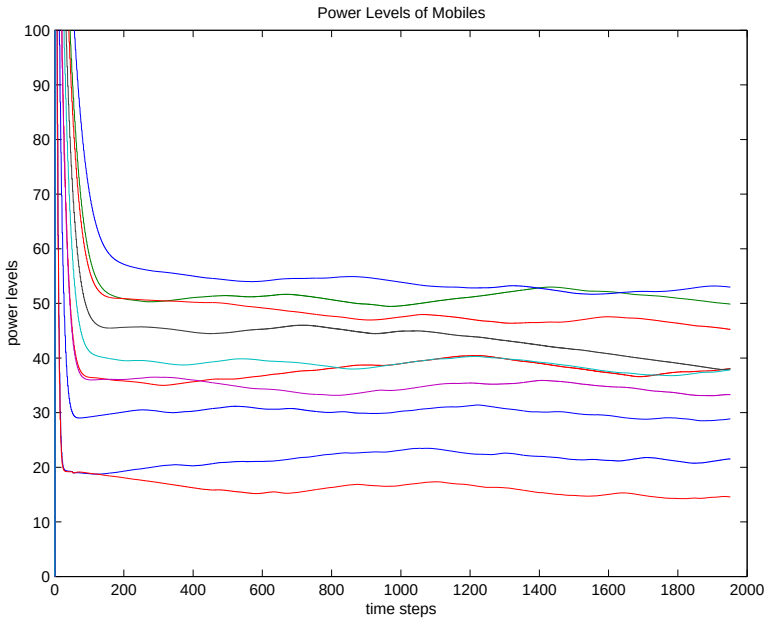

Figure 4.7: Power levels of 10 selected mobiles with respect to time under a communication delay of 50 steps.

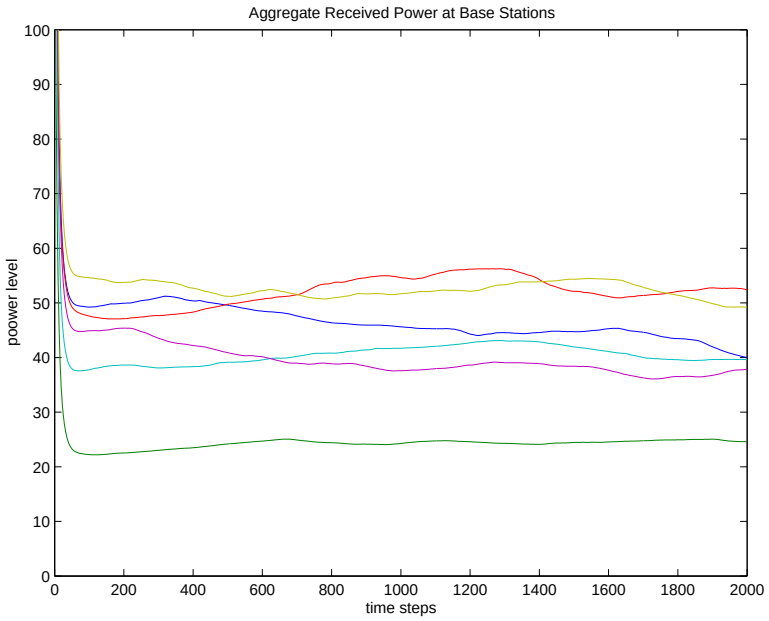

Figure 4.8: Aggregate received power levels at the base stations.

4.4 Conclusions

In this chapter, we have formulated a noncooperative power control game in a multicell CDMA wireless network, which is modeled as a switched hybrid system where handoffs of mobiles between different cells correspond to discrete switching events between different subsystems. Under a set of sufficient conditions, we have shown the existence and global exponential stability of a unique NE for each subsystem under a gradient algorithm. We have also established the global convergence of the dynamics of the multicell power control game to a convex superset of Nash equilibria for any switching (handoff) scheme satisfying a mild condition on average dwell-time. We have investigated the robustness of these results to communication constraints, such as feedback delays and quantization, and have presented a scheme to reduce the communication overhead between mobiles and the base stations. We have also illustrated the proposed power control scheme through MATLAB simulations.

The mathematical model developed captures a fairly broad class of convex cost functions, and addresses the multicell resource allocation problem in CDMA wireless networks. The gradient update algorithm used is market-based, distributed in nature, robust with respect to feedback delays, and requires little overhead in terms of system resources. These theoretical results are also supported through realistic simulations.

CHAPTER 5

A POWER CONTROL GAME BASED ON OUTAGE PROBABILITIES

In this chapter, we consider a power control game similar to the one in [56] and Chapter 4, which incorporates a pricing mechanism limiting the overall interference and preserving battery energy of mobiles. We capture the preferences of mobiles using a utility function, which is defined as the logarithm of the probability that the frame success rate of the data user is greater than a predefined individual threshold level. This utility function can also be described in terms of frame outage probabilities [99]. In the context of a two-time scale channel gain model, we consider a noncooperative power control game which uses an outage-probability-based (instead of a signal-to-interference ratio (SIR) based) utility function and also incorporates a pricing mechanism. The Section 5.1 describes the model adopted and the cost function. In Section 5.2, we show that the noncooperative power control game admits a unique Nash equilibrium (NE) under uniformly strictly convex pricing functions and some technical assumptions on the SIR threshold levels. We present in Section 5.3 system dynamics and stability analysis of a continuous-time update scheme. In Section 5.4, convergence properties of both deterministic and stochastic discrete-time update algorithms are investigated. Section 5.5 contains results on MATLAB simulation studies demonstrating the convergence and robustness properties of these schemes. The Chapter concludes with a recap of the results and elucidation of directions for future research in Section 5.6.

5.1 The Model and the Cost Function

We consider the multicell CDMA wireless network model described in Chapter 4 with a more realistic interference model. Specifically, we define $h_{il}f_{il}p_i$ as the instantaneous received power level from user i at the l^{th} BS. The quantities h_{il} $(0 < h_{il} < 1)$ and f_{il} $(f_{il} > 0)$ represent the *slow-varying* channel gain (excluding any fading) and fast time-scale Rayleigh fading between the i^{th} mobile and the l^{th} BS, respectively [85]. We assume that the factors affecting h_{il} do not change significantly over the time scale of this analysis, and the terms f_{il} (static over individual data frames but varying from one frame to another) are unit mean independent exponentially distributed random variables (Rayleigh fading). As in Chapter 4, let $\mathcal{M}_{l,eff}$ denote the set of users in the neighborhood of cell l who have a nonnegligible effect on each other's SIR levels through in-cell

and intracell interference. It immediately follows that $\mathcal{M}_l \subset M_{l,eff} \subset \mathcal{M}$. Without loss of any generality, we define the set $\mathcal{M}_{l,eff}$ here as

$$\mathcal{M}_{l,eff} := \mathcal{M}_l \cup \left(\cup_{k \in Neighbor(l)} \mathcal{M}_k\right),$$

where $Neighbor(l)$ is defined as the set of first-tier neighbors of cell l. Thus, in accordance with the interference model considered, the SIR obtained by mobile i at the base station l is given by (static over one data frame)

$$\gamma_{il} := \frac{L h_{il} f_{il} p_i}{\sum_{j \in \mathcal{M}_{l,eff},\, j \neq i} h_{jl} f_{jl} p_j + \sigma_l^2}.$$

The outage probability of user i, denoted O_{il}, is defined as the proportion of time that some SIR threshold, $\bar{\gamma}_{il}$, is not met for sufficient reception at the l^{th} BS receiver [55]. By a careful choice of $\bar{\gamma}_{il}$, a quality of service level can be established for each user (see [99] for details on how a minimum frame success rate can be converted to an appropriate SIR threshold for a specific modulation and coding scheme). The outage probability, $O_{il} = Pr(\gamma_i \leq \bar{\gamma}_{il})$, of the i^{th} mobile at the l^{th} BS is defined as

$$O_{il} = Pr\left(h_{il} f_{il} p_i \leq \bar{\gamma}_{il} \left[\sum_{j \in \mathcal{M}_{l,eff},\, j \neq i} h_{jl} f_{jl} p_j + \sigma_l^2\right]\right), \tag{5.1}$$

where $Pr(\gamma_i \leq \bar{\gamma}_{il})$ denotes the probability of the event corresponding to $\gamma_i \leq \bar{\gamma}_{il}$.

For analysis purposes, the mean power level of mobile i received at the l^{th} BS can be defined without any loss of generality, as $x_{il} := h_{il} p_i$, since the mean value of the Rayleigh fading channel can be incorporated into the value h_{il}. Let the received power level vector of cell l be $\mathbf{x}_l := [(x_{jl})], j \in \mathcal{M}_{l,eff}$. Then, the systemwide vector $\mathbf{x} := [\mathbf{x}_1, \ldots, \mathbf{x}_{\bar{L}}]$ has the cardinality $Mx := \sum_{l \in \mathcal{L}} M_{l,eff}$, where $M_{l,eff}$ is the number of elements of the set $\mathcal{M}_{l,eff}$. In order to simplify the notation, we will drop the index identifying the BS (e.g. $x_i := x_{il}$) in cases where it is obvious from the context that mobile i is connected to the l^{th} BS. As a further simplification, we let the threshold SIR for the i^{th} mobile be defined as $\bar{\gamma}_i := \bar{\gamma}_{il} = \bar{\gamma}_{ik}\ \forall l,\ k \in \mathcal{L}$. We note that the outage probability in (5.1) can be expressed in analytical form which we reproduce here without derivation. Its derivation can be found in [100], and in [101] for a simplified version of the expression. The outage probability of the i^{th} mobile connected to the l^{th} BS is thus given by

$$O_{il}(\mathbf{x}, \bar{\gamma}_i) = 1 - \exp\left(\frac{-\sigma^2 \bar{\gamma}_i}{x_{il}}\right) \prod_{j \in \mathcal{M}_{l,eff},\, j \neq i} \frac{1}{1 + \dfrac{\bar{\gamma}_i x_{jl}}{x_{il}}}, \tag{5.2}$$

Henceforth we drop the index "l" from x_{il} and O_{il}, and adopt the convention that $j \neq i$ stands for $j \in \mathcal{M}_{l,eff}$, $j \neq i$, where l is the BS to which mobile i is connected.

The i^{th} user's cost function is defined as the difference between the utility function of the user and its pricing function, $J_i = P_i - U_i$, similar to the one in Chapter 4. The utility function, $U_i(Pr_i(\gamma_i \geq \bar{\gamma}_i)$, is a logarithmic function of the probability that the SIR of the i^{th} user is larger than the predefined threshold $\bar{\gamma}_i$ and quantifies approximately the demand or *willingness to pay* of the user for a certain level of service. Notice that, $Pr_i(\gamma_i \geq \bar{\gamma}_i)$ is equal to $1 - O_i$, where O_i is the outage probability in (5.2). Hence, the utility function for user i is defined by

$$U_i(\mathbf{x}) := u_i \log(Pr_i(\gamma_i(\mathbf{x}) \geq \bar{\gamma}_i) = u_i \log(1 - O_i(\mathbf{x}, \bar{\gamma}_i)), \tag{5.3}$$

where u_i is a user-specific utility parameter.

The pricing function, $P_i(p_i)$, on the other hand, is imposed by the system to limit the interference created by the mobile, and hence to improve the system performance [49]. At the same time, it can also be interpreted as a cost on the battery usage of the user. As a result, the cost function of the i^{th} user connected to a specific BS is given by

$$J_i(\mathbf{x}) = P_i(x_i) - u_i \log(Pr_i(\gamma_i(\mathbf{x}) \geq \bar{\gamma}_i)), \tag{5.4}$$

where we have used x_i, instead of p_i, as the argument of P_i, by a possible redefinition of the latter.

5.2 Existence and Uniqueness of Nash Equilibrium

It follows from (5.3) immediately that the utility function $U_i(\mathbf{x})$ is continuously differentiable in its arguments. In order to calculate the derivatives of the utility function with respect to x, we first evaluate $\partial Pr_i(\gamma_i(\mathbf{x}) \geq \bar{\gamma}_i)/\partial x_i$ using (5.1) and (5.2):

$$\frac{\partial Pr_i(\gamma_i(\mathbf{x}) \geq \bar{\gamma}_i)}{\partial x_i} = Pr_i(\gamma_i(\mathbf{x}) \geq \bar{\gamma}_i) \cdot \left(\frac{\sigma_l^2 \bar{\gamma}_i}{x_i^2} + \sum_{j \neq i} \frac{1}{x_i + \frac{x_i^2}{\bar{\gamma}_i x_{jl}}} \right). \tag{5.5}$$

Thus, the first and second order derivatives of mobile i's utility function, $U_i(\mathbf{x})$, with respect to x_i are given by

$$\frac{\partial U_i(\mathbf{x})}{\partial x_i} = \frac{u_i \sigma_l^2 \bar{\gamma}_i}{x_i^2} + \sum_{j \neq i} \frac{u_i}{x_i + \frac{x_i^2}{\bar{\gamma}_i x_{jl}}} > 0,$$

and

$$\frac{\partial^2 U_i(\mathbf{x})}{\partial x_i^2} = \frac{-2u_i\sigma_l^2\bar{\gamma}_i}{x_i^3} - u_i \sum_{j\neq i} \frac{1+\frac{2x_i}{\bar{\gamma}_i x_{jl}}}{\left(x_i + \frac{x_i^2}{\bar{\gamma}_i x_{jl}}\right)^2} < 0,$$

respectively. Furthermore, for $j \neq i$,

$$\frac{\partial^2 U_i(\mathbf{x})}{\partial x_i\, \partial x_{jl}} = \frac{u_i\bar{\gamma}_i}{(x_i + \bar{\gamma}_i x_{jl})^2} > 0.$$

Let us define x_{min} and x_{max} as lower and upper bounds on x_{il} $\forall i,\, l$, i.e., $x_{min} < x_{il} < x_{max}\, \forall i,\, l$. If the mean received power level of a mobile at the BS is less than x_{min}, then its effect is negligible and it is modeled as part of the background noise. The upper-bound x_{max} is further bounded above by p_{max} with a possible equality in the case of no channel attenuation. We also define $\bar{\gamma}_{min}$ (u_{min}) and $\bar{\gamma}_{max}$ (u_{max}) in such a way that $\bar{\gamma}_{min} < \bar{\gamma}_i < \bar{\gamma}_{max}$ $(u_{min} < u_i < u_{max})\ \forall i$. We now make the following three assumptions on the price function P_i, for all mobiles i.

Assumption 5.1 *The pricing function $P_i(x_i)$ is twice continuously differentiable, nondecreasing and uniformly strictly convex in x_i, i.e.,*

$$dP_i(x_i)/dx_i \geq 0,\ d^2P_i(x_i)/dx_i^2 \geq v > 0,\ \forall x_i,$$

for some $v > 0$.

Assumption 5.2 *Given the set of parameters $\{M_{l,eff},\ \bar{\gamma}_{min},\ \bar{\gamma}_{max},\ x_{min},\ x_{max}\}$, v in A1 above satisfies the following inequality:*

$$v(\bar{\gamma}_{min}+1)\frac{x_{min}^2}{u_{max}} + (M_{l,eff}-1)\bar{\gamma}_{min}\frac{u_{min}}{u_{max}}\frac{x_{min}^3}{x_{max}^3} > 1$$

Assumption 5.3 *The pricing function P_i and the parameter of the utility function are further picked in such a way that the i^{th} user's cost function, J_i, has the following properties at $x_i = x_{min}$ $(x_i = x_{max})$: $\partial J_i(\mathbf{x} : x_i = x_{min})/\partial x_i < 0\ \forall \mathbf{x}$ $(\partial J_i(\mathbf{x} : x_i = x_{max})/\partial x_i > 0\ \forall \mathbf{x})$, respectively.*

The NE in a cell is defined as a set of power levels, p^* (and corresponding set of costs J^*), with the property that no user in the cell can benefit by modifying its power level while the other players keep theirs fixed. Mathematically speaking, $\mathbf{x}^*$ is in NE when x_i^* of any i^{th} user is the solution to the following optimization problem given the equilibrium power levels of other mobiles (in the set $\mathcal{M}_{l,eff}$), $\mathbf{x}_{-i}^*$:

$$\min_{x_{min}\leq x_i \leq x_{max}} J_i(x_i, \mathbf{x}_{-i}^*). \tag{5.6}$$

Note that given the channel gains, the NE point $\mathbf{x}^*$ is equivalent to p^*.

Thanks to Assumption 5.1, the cost function J_i is strictly convex and belongs to a fairly large subclass of convex functions. Hence, there exists a unique solution to the i^{th} user's minimization problem, which is that of minimization of J_i, given the system parameters and the power levels of all other users. We will next make use of the technical Assumption 5.2 in the proof of existence of a unique NE. Notice that, $\mathbf{x}_{min}$ is bounded below by definition. Hence, Assumption 5.2 is easily satisfied for a large number of users M or high SIR thresholds $\bar{\gamma}_{min}$ even if v is small. Assumption 5.3, on the other hand, ensures that any equilibrium solution is an *inner* one, i.e., boundary solutions $x_i^* = x_{min}$ $(x_i^* = x_{max})$ $\forall i$ cannot be equilibrium points.

Theorem 5.1 *Under Assumptions 5.1-5.3, the multicell power control game defined admits a unique inner Nash equilibrium solution.*

Proof. The proof of this theorem is similar to the one of Theorem 2.1. It is briefly outlined here for completeness. Let $X := \{\mathbf{x} \in \mathbb{R}^{Mx} : x_{min} \leq x_{il} \leq x_{max}\ \forall i,\ l\}$ be a set of feasible received power levels at the base stations under the interference model considered. Clearly, X is closed and bounded, and hence compact. Furthermore, it is also convex, and has a nonempty interior. By a standard theorem of game theory (Theorem 4.4, p.176, in [1]) the power control game admits a Nash equilibrium. In addition, by Assumption 5.3 this solution has to be inner.

Let $A_{i,j} := \frac{\partial^2 J_i}{\partial x_i \partial x_{jl}}$ and $B_i := \frac{\partial^2 J_i}{\partial x_i^2}$, where mobile i is connected to the BS l. Define $M \times M$ matrix $G(\mathbf{x})$ with diagonal entries B_i and nonzero entries $A_{i,j}$, if $j \in \mathcal{M}_{l,eff}$. It follows from Assumptin 5.2 that $B_i > |A_{i,j}|\ \ \forall i, j$. Hence, the symmetric matrix $G(\mathbf{x}) + G(\mathbf{x})^T$ is positive definite. Then, using an argument similar to the one in the proof of Theorem 3.1 in [36] one can show that the inner NE solution is unique. Thus, there exists a unique inner NE in the multicell power control game. □

5.3 System Dynamics and Stability Analysis

We consider a dynamic model of the power control game similar to the one of [56] where each mobile uses a gradient algorithm to solve its own optimization problem (5.6). Accordingly, the power update algorithm of the i^{th} mobile is

$$\dot{p}_i = \frac{dp_i}{dt} = -\frac{\partial J_i}{\partial p_i},$$

for all $i \in \mathcal{M}$. This can also be described in terms of the received power level, x_i, at the l^{th} BS

$$\dot{x}_i = h_i^2 \left(\frac{\partial U_i(\mathbf{x})}{\partial x_i} - \frac{dP_i(x_i)}{dx_i} \right) := \phi_i(\mathbf{x}), \ \forall i. \tag{5.7}$$

By taking the second derivative of x_i with respect to time, we obtain

$$\ddot{x}_i = h_i^2 \left(-a_i - \frac{d^2 P_i(x_i)}{dx_i^2} \right) \dot{x}_i + h_i^2 \sum_{j \neq i} b_{i,j} \dot{x}_{jl} := \dot{\phi}_i(\mathbf{x}),$$

where a_i and $b_{i,j}$ are defined as

$$a_i := -\frac{\partial^2 U_i(\mathbf{x})}{\partial x_i^2} = u_i \frac{2\sigma_l^2 + \bar{\gamma}_i}{x_i^3} + u_i \sum_{j \neq i} \frac{1 + \dfrac{2x_i}{\bar{\gamma}_i x_{jl}}}{\left(x_i + \dfrac{x_i^2}{\bar{\gamma}_i x_{jl}} \right)^2},$$

and

$$b_{i,j} := \frac{\partial^2 U_i(\mathbf{x})}{\partial x_i \, \partial x_{jl}} = u_i \frac{\bar{\gamma}_i}{(x_i + \bar{\gamma}_i x_{jl})^2}.$$

Notice that both a_i and $b_{i,j}$ are positive.

We establish the stability of the power update scheme (5.7) under some sufficient conditions. The set of feasible received power levels is invariant by Assumption 5.3, which immediately follows from a boundary analysis. When $x_i = x_{min}$ for some $i \in \mathcal{M}$, we have $\dot{x}_i > 0$ under Assumption 5.3. Hence, the system trajectory moves toward inside of X. Likewise, in the case of $x_i = x_{max}$ for some $i \in \mathcal{M}$, $\dot{x}_i < 0$, and hence, the trajectory remains inside the set X. Let us introduce a candidate Lyapunov function $V : \mathbb{R}^{Mx} \to \mathbb{R}$ as

$$V(\mathbf{x}) := \sum_{i \in \mathcal{M}} \frac{1}{h_i^2} \phi_i^2(\mathbf{x}) \ ,$$

which is in fact restricted to the domain X. Note that because of the uniqueness of the NE, $\mathbf{x}^*$, $\phi_i(\mathbf{x}) = 0 \ \forall i$ if and only if $\mathbf{x} = \mathbf{x}^*$. Hence, V is positive for all $\mathbf{x}$ except for $\mathbf{x} = \mathbf{x}^*$.

Taking the derivative of V with respect to t on the trajectories generated by (5.7), we obtain

$$\dot{V}(\mathbf{x}) \leq \sum_{i \in \mathcal{M}} -(2v + 2a_i)\phi_i^2 + \sum_{i \in \mathcal{M}} \max_j b_{i,j} \sum_{j \neq i} 2|\phi_i \phi_j|.$$

It follows from a simple algebraic manipulation that

$$\sum_{i\in\mathcal{M}} \max_j b_{i,j} \sum_{j\neq i} 2|\phi_i\phi_j| \leq 2(M_{eff}-1)\max_{i,j} b_{i,j} \sum_{i\in\mathcal{M}} \phi_i^2,$$

where $M_{eff} := \max_l M_{l,eff}$.

Using this to bound $\dot{V}$ further yields

$$\dot{V}(\mathbf{x}) \leq (-(2v + \min_i 2a_i) + 2(M_{eff}-1)\max_{i,j} b_{i,j}) \sum_{i\in\mathcal{M}} \phi_i^2.$$

Next, we modify Assumption 5.2 as follows:

Assumption 5.4 *Assume that the following inequality holds:*

$$v(\bar{\gamma}_{min}+1)\frac{x_{min}^2}{u_{max}} + (M_{l,eff}-1)\bar{\gamma}_{min}\frac{u_{min}}{u_{max}}\frac{x_{min}^3}{x_{max}^3} > M_{eff}-1 \ \ \forall l.$$

Remark 5.1 *Assumption 5.4 holds when $\bar{\gamma}_{min}$ and/or v are sufficiently large.*

Under Assumption 5.4, we have $\dot{V}(\mathbf{x}) < 0$, uniformly in the x_i's on the trajectory of (5.7). Thus, V is indeed a Lyapunov function, and it readily follows that $\phi_i(\mathbf{x}(t)) = \dot{x}_i(t) \to 0, \ \forall\, i$. This in turn implies that $x_i(t)$'s converge to the unique NE. Hence, the unique NE point (Theorem 5.1) is globally asymptotically stable on the invariant set X with respect to the update scheme (5.7) under Assumptions 5.1, 5.3 and 5.4 by Lyapunov's stability theorem (see Theorem 3.1 in [82]).

5.4 Iterative Power Control Algorithms

We investigate in this section stability properties of synchronous and asynchronous iterative power control schemes as they are of practical importance. We first analyze gradient based synchronous and asynchronous update algorithms of the power control game in Section 5.2. Consequently, we study convergence of stochastic iterations to the unique NE solution by taking communication constraints and estimation errors into account.

5.4.1 Synchronous and asynchronous update schemes

Consider a discrete-time counterpart of the update scheme in (5.7) in a system with M mobiles where each mobile uses a gradient algorithm to solve its optimization problem (5.6):

$$p_i(n+1) = p_i(n) - \lambda_i \frac{\partial J_i}{\partial p_i} \ \ \forall i \in \mathcal{M}\ ,$$

where $n = 1, 2, \ldots$, denotes the update instances and λ_i is the user-specific step size defined by $\lambda_i := \lambda/h_i$. Here, λ denotes the system wide step size constant. For notational convenience this can also be defined as a mapping from the received power levels at the BS to the updated power levels, $\mathbf{x}(n+1) = T(\mathbf{x}(n))$, i.e.,

$$x_i(n+1) = T_i(\mathbf{x}(n)) := x_i(n) - \lambda \frac{\partial J_i}{\partial x_i} \;\; \forall i \in \mathcal{M} \; . \tag{5.8}$$

In the case of synchronous update algorithm, each mobile updates its power level at the same time instance. We study here sufficient conditions for convergence of the system to the unique NE, $\mathbf{x}^*$, under the synchronous update. This analysis follows lines similar to those in the proof of Proposition 1.10 of [102, p. 193]. Let $\mathbf{x} \in X = \{\mathbf{x} \in \mathbb{R}^{Mx} : x_{min} \leq x_{il} \leq x_{max} \; \forall i, \, l\}$ and define a function $g_i(\tau) : \; [0,1] \rightarrow \mathbb{R}$ for the i^{th} mobile by

$$g_i(\tau) = \tau x_i + (1-\tau) x_i^* + \lambda \phi_i(\tau \mathbf{x} + (1-\tau)\mathbf{x}^*),$$

where ϕ_i is defined in (5.7). We then have

$$|T_i(\mathbf{x}) - T_i(\mathbf{x}^*)| = |g_i(1) - g_i(0)| = \left| \int_0^1 \frac{dg_i(\tau)}{d\tau} d\tau \right| \leq \int_0^1 \left| \frac{dg_i(\tau)}{d\tau} \right| d\tau \leq \max_{\tau \in [0,1]} \left| \frac{dg_i(\tau)}{d\tau} \right|,$$

where $\mathbf{x}^*$, the NE, is the fixed point of the mapping T. We bound $\left| \frac{dg_i(\tau)}{d\tau} \right|$ above by

$$\left| \frac{dg_i(\tau)}{d\tau} \right| \leq \left| x_i - x_i^* - \lambda \sum_{j \in \mathcal{M}_{l,eff}} \frac{\partial \phi_i}{\partial x_j} \cdot (x_j - x_j^*) \right| \leq \left| 1 - \lambda \frac{\partial \phi_i}{\partial x_i} \right| |x_i - x_i^*| + \sum_{j \neq i} \lambda \frac{\partial \phi_i}{\partial x_{jl}} \left| x_{jl} - x_{jl}^* \right| .$$

Imposing the condition $\lambda \partial \phi_i / \partial x_i < 1$, we have

$$\left| \frac{dg_i(\tau)}{d\tau} \right| \leq \left(1 - \lambda \left[\frac{\partial \phi_i}{\partial x_i} - \sum_{j \neq i} \frac{\partial \phi_i}{\partial x_{jl}} \right] \right) \|\mathbf{x} - \mathbf{x}^*\| ,$$

where $\|\mathbf{x}\| := \max_i |x_i|$ is the maximum norm. Define

$$K_i := \max_{\mathbf{x} \in X} \frac{\partial \phi_i(\mathbf{x})}{\partial x_i} \text{ and } \rho_i := 1 - \lambda \left(\frac{\partial \phi_i}{\partial x_i} - \sum_{j \neq i} \frac{\partial \phi_i}{\partial x_{jl}} \right),$$

which leads to $|T_i(\mathbf{x}) - x_i^*| \leq \rho_i \|\mathbf{x} - \mathbf{x}^*\|$ for each i. Let $\rho := \max_i \rho_i$ and $K := \max_i K_i$. We obtain then $\|T(\mathbf{x}) - \mathbf{x}^*\| \leq \rho \|\mathbf{x} - \mathbf{x}^*\|$, if $\lambda K < 1$. An upper bound on K in terms of system and

cost parameters is

$$\bar{K} := \max_i \frac{d^2 P_i(x_{max})}{dx_i^2} + \frac{2(M_{eff}-1)\bar{\gamma}_{max}x_{max}}{(\bar{\gamma}_{min}+1)x_{min}^3} + \frac{2\sigma^2\bar{\gamma}_{max}}{x_{min}^3}. \tag{5.9}$$

Imposing the condition $\rho < 1$, it readily follows that for arbitrary $\mathbf{x} \in X$, $T^n(\mathbf{x}) \to \mathbf{x}^*$ as $n \to \infty$, since $\|T^n(\mathbf{x}) - \mathbf{x}^*\| \leq \rho^n \|\mathbf{x} - \mathbf{x}^*\|$. Furthermore, the condition $\rho < 1$ is satisfied if

$$\sum_{j \neq i} \frac{\bar{\gamma}_i^2 x_{jl}^2 + 2\bar{\gamma}_i x_i x_{jl}}{x_i^2(x_i + \bar{\gamma}_i x_{jl})^2} - \frac{\bar{\gamma}_i}{(x_i + \bar{\gamma}_i x_{jl})^2} > 0 \ \forall i.$$

Let $x_{max} = \alpha x_{min}$ for some $\alpha > 0$. Then, a sufficient condition for $\rho < 1$ is

$$\alpha < 1 + \sqrt{1 + \bar{\gamma}_{min}},$$

which follows from a straightforward algebraic derivation. Thus, under $\lambda \bar{K} < 1$ and $\alpha < 1 + \sqrt{1 + \bar{\gamma}_{min}}$, the synchronous power update scheme given in (5.8) converges to the NE solution, $\mathbf{x}^*$. This result is summarized in the following theorem:

Theorem 5.2 *Let $x_{max} = \alpha x_{min}$ for some $\alpha > 0$ and $X := \{\mathbf{x} \in \mathbb{R}^{Mx} : x_{min} \leq x_{il} \leq x_{max} \ \forall i, \ l\}$. The synchronous power update algorithm*

$$p_i(n+1) = p_i(n) - \lambda_i \frac{\partial J_i}{\partial p_i} \ \ \forall i \in \mathcal{M}$$

converges to the unique NE point of the power control game, $p^* := [x_1^*/h_1, \ldots, x_M^*/h_M]$, on the set X if

$$\lambda \left[\max_i \frac{d^2 P_i(x_{max})}{dx_i^2} + \frac{2(M_{eff}-1)\bar{\gamma}_{max}x_{max}}{(\bar{\gamma}_{min}+1)x_{min}^3} + \frac{2\sigma^2\bar{\gamma}_{max}}{x_{min}^3} \right] < 1,$$

and

$$\alpha < 1 + \sqrt{1 + \bar{\gamma}_{min}}.$$

Remark 5.2 *Given x_{min}, x_{max}, α, and system parameters M_{eff} and σ^2, the conditions of Theorem 5.2 can be satisfied by choosing λ and $\max_i d^2 P_i(x_{max})/dx_i^2$ sufficiently small while keeping $\bar{\gamma}_{min}$ sufficiently large. We refer to Section 5.5 for specific numerical examples that illustrate this.*

A natural generalization of the synchronous update is the asynchronous update scheme where only a random subset of mobiles update their power levels at a given time instance. This is in fact more realistic since it is difficult for the mobiles to synchronize their exact power update instances in a practical implementation. In this particular case, however, the convergence analysis above

also applies to the asynchronous update algorithm. Define a sequence of nonempty, convex, and compact sets

$$X(k) := [x_1^* - \delta(k), x_1^* + \delta(k)] \times [x_2^* - \delta(k), x_2^* + \delta(k)] \times \dots [x_M^* - \delta(k), x_M^* + \delta(k)],$$

where $\delta(k) := \|\mathbf{x}(k) - \mathbf{x}^*\|$. Since by Theorem 5.2, $\delta(k+1) < \delta(k)$, we have

$$\dots \subset X(k+1) \subset X(k) \subset \dots X.$$

We next give the definitions of two well known conditions which together are sufficient for asynchronous convergence of a nonlinear iterative mapping $\mathbf{x}(n+1) = T(\mathbf{x})$ [102, p. 431].

Definition 5.1 (Synchronous Convergence Condition) *For a sequence of nonempty sets $\{X(k)\}$ with $\dots \subset X(k+1) \subset X(k) \subset \dots X$, we have $T(\mathbf{x}) \in X(k+1), \ \forall k$, and $\mathbf{x} \in X(k)$. Furthermore, if $\{y^k\}$ is a sequence such that $y^k \in X(k)$ for every k, then every limit point of $\{y^k\}$ is a fixed point of T.*

Definition 5.2 (Box Condition) *Given a closed and bounded set Y in $\mathbb{R}$, for every k, there exist sets $X_i(k) \subset Y$ such that*

$$X(k) := X_1(k) \times X_2(k) \times \dots \times X_M(k).$$

In our case Y is defined as the interval $[x_{min}, x_{max}]$, and $X_i := [x_i^* - \delta(k), x_i^* + \delta(k)]$. Hence, the box condition is satisfied by the definition of $X(k)$. Since $\delta(k)$ is monotonically decreasing in k by Theorem 5.2 the synchronous convergence condition also holds. Therefore, the next convergence result for the asynchronous counterpart of the power update algorithm in (5.8) immediately follows from asynchronous convergence theorem [102, p. 431].

Theorem 5.3 *Let $x_{max} = \alpha x_{min}$ for some $\alpha > 0$ and $X := \{\mathbf{x} \in \mathbb{R}^{Mx} : x_{min} \leq x_{il} \leq x_{max} \ \forall i, \ l\}$. The asynchronous power update algorithm*

$$p_i(n+1) = \begin{cases} p_i(n) - \lambda_i \frac{\partial J_i}{\partial p_i}, & \text{if } i \in \mathcal{U}(k) \\ p_i(n), & \text{if } i \in \mathcal{M} \backslash \mathcal{U}(k), \end{cases}$$

where $\mathcal{U}(k) \subset \mathcal{M}$ denotes the random subset of mobiles updating their power levels at time k, converges to the unique NE point of the power control game, $p^* := [x_1^*/h_1, \dots, x_M^*/h_M]$, on the set X if $\lambda \bar{K} < 1$ and $\alpha < 1 + \sqrt{1 + \bar{\gamma}_{min}}$, where $\bar{K}$ is defined in (5.9).

5.4.2 A stochastic update scheme

In a real-life implementation of the power control scheme, communication constraints, approximations, estimation, and quantization errors, may not be negligible and, hence, may have to be taken into account in the convergence analysis. Hence, a mobile does not have access to the exact values of the system parameters such as its own channel gain or the feedback terms provided by the BS. These uncertainties can be captured by a stochastic update algorithm, as introduced below. For each $i \in \mathcal{M}$, let $\mathbf{x}_{-\mathbf{i}i}(n)$ $n = 1, 2, \ldots$ be a sequence of independent identically distributed (i.i.d.) random variables defined on the common support set $[1-\varepsilon, 1+\varepsilon]$, where $0 < \varepsilon < 1$. We further assume that the sequences $\{\mathbf{x}_{-\mathbf{i}i}\}$ are independent across $i \in \mathcal{M}$. Using these random sequences, we model the aggregate uncertainty in the term $\partial J_i/\partial p_i$ of (5.8) due to quantization, estimation, and multiplicatively approximation errors. Thus, the stochastic counterpart of the synchronous update algorithm is given by

$$p_i(n+1) = p_i(n) - \lambda_i \mathbf{x}_{-\mathbf{i}i}(n) \frac{\partial J_i}{\partial p_i} \quad \forall i \in \mathcal{M}, \tag{5.10}$$

which can also be described in terms of received power levels at the base station as

$$x_i(n+1) = x_i(n) - \lambda \mathbf{x}_{-\mathbf{i}i}(n) \frac{\partial J_i}{\partial x_i} =: T_i(\mathbf{x}(n);\, \mathbf{x}_{-\mathbf{i}i}(n)) \;\; \forall i \in \mathcal{M}. \tag{5.11}$$

We next follow steps similar to those in the previous subsection for the convergence analysis. We have, for an arbitrary $\mathbf{x} \in X$:

$$E\left(|T_i(\mathbf{x}; \mathbf{x}_{-\mathbf{i}i}) - x_i^*|\right) \leq E\Bigg(\left|1 - \lambda \mathbf{x}_{-\mathbf{i}i} \frac{\partial \phi_i}{\partial x_i}\right| |x_i - x_i^*| + \sum_{j \in \mathcal{M}_{l,eff},\, j \neq i} \lambda \mathbf{x}_{-\mathbf{i}i} \frac{\partial \phi_i}{\partial x_{jl}} \left|x_{jl} - x_{jl}^*\right| \Bigg),$$

where $E(x)$ denotes the expected (mean) value of x. Assume $\lambda(1+\varepsilon)K_i < 1$, where K_i, as defined earlier, provides an upper bound on $\partial\phi_i/\partial x_i$. Then, from the independence of $\mathbf{x}_{-\mathbf{i}i}$ and x_i for all i, we obtain (by dropping the dependence on n):

$$E\left(|T_i(\mathbf{x}; \mathbf{x}_{-\mathbf{i}i}) - x_i^*)|\right) \leq (1 - \lambda E(\mathbf{x}_{-\mathbf{i}i}) K_i') E\left(|x_i - x_i^*|\right) + \lambda E(\mathbf{x}_{-\mathbf{i}i}) \bar{K}_i \sum_{j \neq i} E\left(\left|x_{jl} - x_{jl}^*\right|\right),$$

where K_i' is a lower bound on $\partial\phi_i/\partial x_i$, and $\bar{K}_i$ is an upper bound on $\partial\phi_i/\partial x_j$ for all $j \neq i$. Let us redefine the maximum norm as $\|\mathbf{x}\| = \max_i E(|x_i|)$. Then, $E\left(|T_i(\mathbf{x}; \mathbf{x}_{-\mathbf{i}i}) - x_i^*)|\right) \leq \bar{\rho}_i \|\mathbf{x} - \mathbf{x}^*\| \;\; \forall i$, where $\bar{\rho}_i := 1 - \lambda E(\mathbf{x}_{-\mathbf{i}i})(K_i' - (M_{eff} - 1)\bar{K}_i)$. Defining $\bar{\rho} := \max_i \rho_i$, we obtain

$$\|T(\mathbf{x}; \mathbf{x}_{-\mathbf{i}}) - \mathbf{x}^*\| \leq \bar{\rho} \|\mathbf{x} - \mathbf{x}^*\|,$$

if $\lambda(1+\varepsilon)\bar{K} < 1$, where $\mathbf{x}_{-\mathbf{i}} := [\mathbf{x}_{-\mathbf{i}1}, \mathbf{x}_{-\mathbf{i}2}, \ldots, \mathbf{x}_{-\mathbf{i}M}]$. Now, imposing the condition $\bar{\rho} < 1$, it readily follows that for arbitrary $x \in X$ and $\mathbf{x}_{-\mathbf{i}_i}(n) \in [1-\varepsilon, 1+\varepsilon]\ \forall i,\ n$, we have $T^n(\mathbf{x}; \mathbf{x}_{-\mathbf{i}}) \rightarrow \mathbf{x}^*$ as $n \rightarrow \infty$, since $\|T^n(\mathbf{x}; \mathbf{x}_{-\mathbf{i}}) - \mathbf{x}^*\| \leq \bar{\rho}^n \|\mathbf{x} - \mathbf{x}^*\|$. We note that the condition $K_i' > (M_{eff} - 1)\bar{K}_i\ \forall i$ is equivalent to the one $\bar{\rho} < 1$. Hence, a derivation similar to the one in the deterministic case yields a sufficient condition for $\bar{\rho} < 1$ to hold, namely

$$\alpha < \frac{1}{2}\sqrt{\bar{\gamma}_{min}} + \frac{1}{4},$$

where α is defined as before with x_{max} and x_{min} being upper and lower bounds on the random variables x_i for all i.

We next show that the stochastic update scheme (5.11) converges almost surely (a.s.) [103] to the unique NE solution $\mathbf{x}^*$, under the given conditions, by an analysis similar to the one in [52]. From the Markov inequality and using the definition of the maximum norm, we obtain

$$\sum_{n=1}^{\infty} Pr(|x_i(n)| > \epsilon) \leq \sum_{n=1}^{\infty} \frac{E(|x_i(n)|)}{\epsilon} \leq \frac{1}{\epsilon}\sum_{n=1}^{\infty} \|\mathbf{x}(n)\| \leq \frac{1}{\epsilon}\sum_{n=1}^{\infty} \bar{\rho}^n \|\mathbf{x}(0)\| \leq \frac{\|\mathbf{x}(0)\|}{\epsilon(1-\bar{\rho})},$$

where $\epsilon > 0$ and $\|\mathbf{x}(0)\|$ are constants, $Pr(A)$ denotes the probability of the event A, and the last inequality follows from the contraction property of the normed random sequence. Hence, the increasing sequence of partial sums $\sum_{n=1}^{N} Pr(|x_i(n)| > \epsilon)$ is bounded above, and converges for every $\epsilon > 0$. Finally, from the Borel-Cantelli lemma [104, 105], it follows that

$$Pr(\limsup\{\omega : |x_i(\omega)| > \epsilon\}) = 0\ \forall i,$$

where ω is the probabilistic variable. Thus, the stochastic update scheme (5.11) converges a.s. to the unique NE point of the power control game under the conditions $\bar{\rho} < 1$ and $\lambda(1+\varepsilon)K < 1$.

Theorem 5.4 *Let $\mathbf{x}_i(n)$ $(\mathbf{x}_{-\mathbf{i}_i}(n))$ be random (random i.i.d.) sequences for all i, where $\mathbf{x}_{-\mathbf{i}_i}$ is also independent across i and has the support set $[1-\varepsilon, 1+\varepsilon]$, $0 < \varepsilon < 1$. The random vector $\mathbf{x}$ takes values in the set $X := \{\mathbf{x} \in \mathbb{R}^{Mx} : x_{min} \leq x_{il} \leq x_{max}\ \forall i,\ l\}$. Furthermore, let $\alpha > 0$ be defined as $\alpha := x_{max}/x_{min}$. The stochastic power update algorithm*

$$p_i(n+1) = p_i(n) - \lambda \mathbf{x}_{-\mathbf{i}_i}(n)\frac{\partial J_i}{\partial p_i}\ \ \forall i \in \mathcal{M},$$

converges almost surely to the unique NE point of the power control game, p^*, if $\alpha < \frac{1}{2}\sqrt{\bar{\gamma}_{min}} + \frac{1}{4}$ and $\lambda(1+\varepsilon)\bar{K} < 1$ where $\bar{K}$ is defined in (5.9).

5.5 Simulations

The power control game based on outage probabilities is simulated in MATLAB for a wireless network consisting of 6 arbitrarily placed base stations and 20 mobiles. The channel gain of the i^{th} mobile is determined by the Rayleigh fast-fading and log-normal shadowing path loss model, given by $g_i = (0.1/d_i)^{2.5} \cdot Y_\sigma^{-1} \cdot f_i$, where d_i denotes the distance to the BS, $\log(Y_\sigma)$ is a zero-mean Gaussian random variable with a standard deviation of $\sigma = 0.1$, and f_i is a random variable with Rayleigh distribution, modeling the fast-fading channel. We generate the random variable f_i at each time step and Y_σ every 20 time steps according to their respective distributions. The distance-based loss exponent is chosen as 2.5, which corresponds to a low density urban environment [85]. Each mobile connects to a single BS, which happens to be in the closest geographical location. Hence, the cells in the network are irregularly shaped polygons. The system parameters are chosen as $L = 128$ and $\sigma_l^2 = 0.1\ \forall l$.

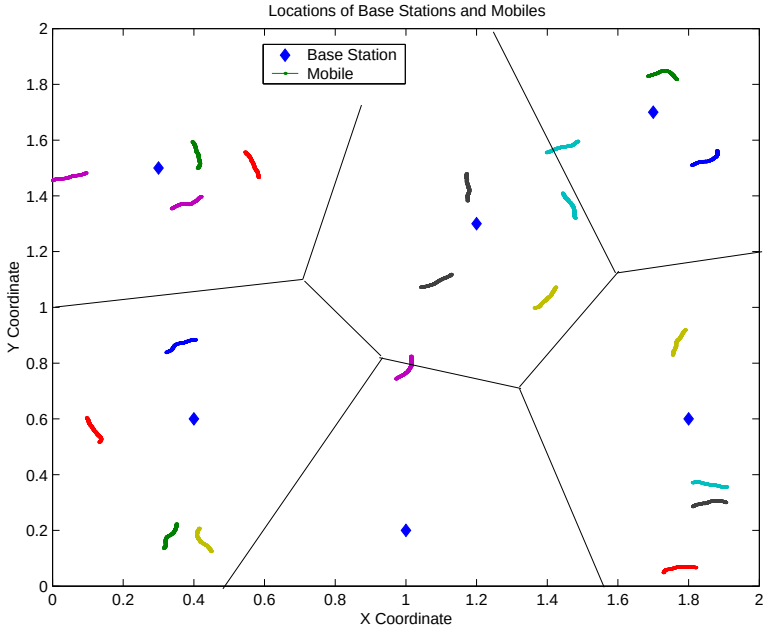

Figure 5.1: Locations of base stations and the paths of mobiles.

The mobiles are initially distributed randomly over the network, and their movement is modeled after a two-dimensional random walk with a speed of 0.0001 units per update. In order to relate the values of the simulation to real physical quantities, we assume an update frequency of 1 kHz and geographical unit size of 100 m. Thus, mobiles move with a speed of 10 m/s or 36 km/h. We note, however, that these are arbitrarily fixed values, for illustration purposes only. Figure 5.1 depicts the locations of the BSs and the paths of all mobiles.

The class of user pricing functions which satisfy the earlier convexity assumptions is fairly

large. The relationship between the pricing function and the performance of the system at the NE point is in fact a very complex one, and therefore the question of finding the "optimum" pricing function, though interesting, does not seem to be within reach. Consequently, we adopt a specific one without any optimality consideration; namely we choose a quadratic function parametrized by v_i for the i^{th} user as a representative pricing function in our numerical studies. Thus, the cost function for the i^{th} user (mobile) is

$$J_i(\mathbf{x}) = \frac{1}{2} v_i x_i^2 - u_i \log(Pr_i(\gamma_i(\mathbf{x}) \geq \bar{\gamma}_i)),$$

where pricing and utility parameters are $u_i = 10$, $v_i = 1$, and $\bar{\gamma}_i = 10$ (20 dB), which are chosen to be the same for all users for comparison purposes.

We first simulate a discrete update scheme with "perfect" information where we ignore the communication constraints between the BS and the mobiles. In order to estimate the slow varying $x_i\,(= h_i p_i)$ value of the i^{th} mobile, the BS implements a maximum likelihood estimator (MLE) using the last 20 independent identically exponentially distributed samples of the received power level $[g_i^{(1)} p_i, g_i^{(2)} p_i, \ldots, g_i^{(20)} p_i]$. Here, we consider a sufficiently high sampling frequency so that we can assume p_i to be constant within an interval of 20 samples. A straightforward derivation of this unbiased MLE yields

$$h_i p_i = \sqrt{\frac{\pi}{4 \cdot 20} \sum_{k=1}^{20} \left(g_i^{(k)} p_i \right)^2}.$$

The output of this estimator is then filtered with a simple infinite impulse response (IIR) low pass filter (LPF) to cancel out the effect of high frequency estimation errors and other disturbances. Figure 5.2 depicts the instantenous and filtered estimation channel gains from mobile 1 to its BS. Thus, given the feedback information from the BS, the mobiles update their power levels according to

$$p_i(n+1) = p_i(n) + \lambda u_i \frac{\sigma_l^2 \bar{\gamma}_i}{h_{il}^2 p_i^2(n)} + \frac{\lambda u_i}{h_{il} p_i(n)} \sum_{j \neq i} \frac{1}{1 + \dfrac{h_{il} p_i(n)}{h_{jl} p_j(n) \bar{\gamma}_i}} - \lambda v_i h_i p_i(n), \qquad (5.12)$$

where $\lambda = 0.1$ and n denotes the time, and mobile i is connected to the l^{th} BS.

The power levels and SIR values of a randomly selected subset of mobiles for the duration of the simulation are shown in Figures 5.3 and 5.4, respectively. The average SIR values in Figure 5.4 are obtained by using the filtered channel gains of mobiles instead of instantenous ones. They are provided in order to visualize the trends in SIR values. The minimum and maximum received power levels of the mobiles at their respective BSs are $x_{min} = 2.5$ and $x_{max} = 90$. Hence, we obtain $\alpha = x_{max}/x_{min} = 36$. Figure 5.5 depicts the evolution of the received power levels of se-

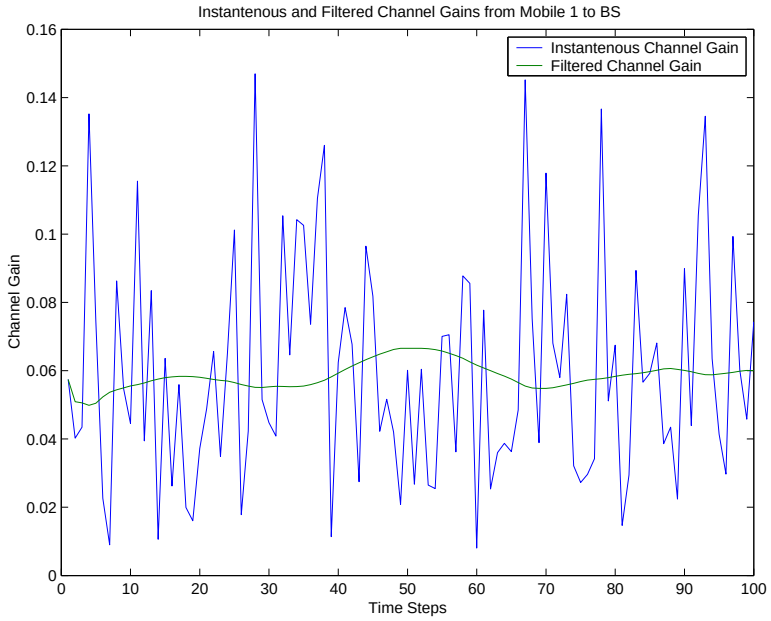

Figure 5.2: Instantenous and filtered channel gain from mobile one to its respective BS.

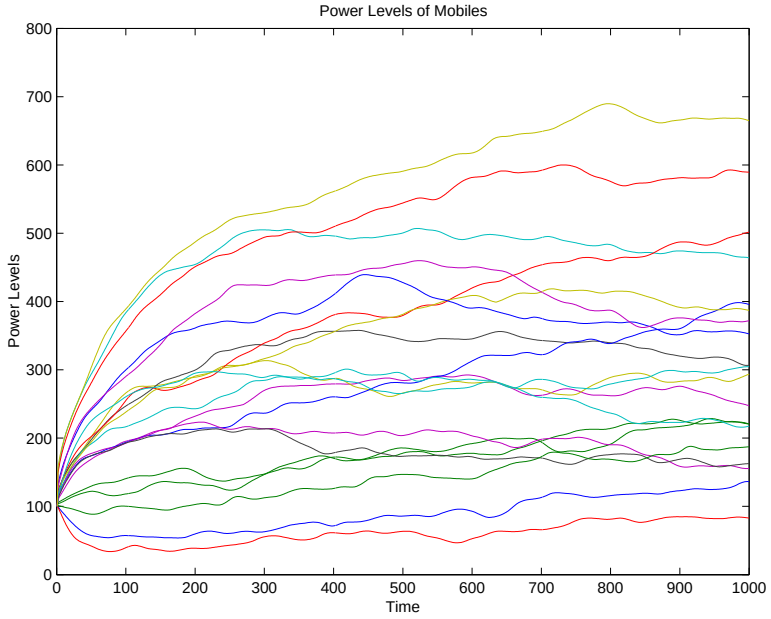

Figure 5.3: Power levels of selected mobiles with respect to time.

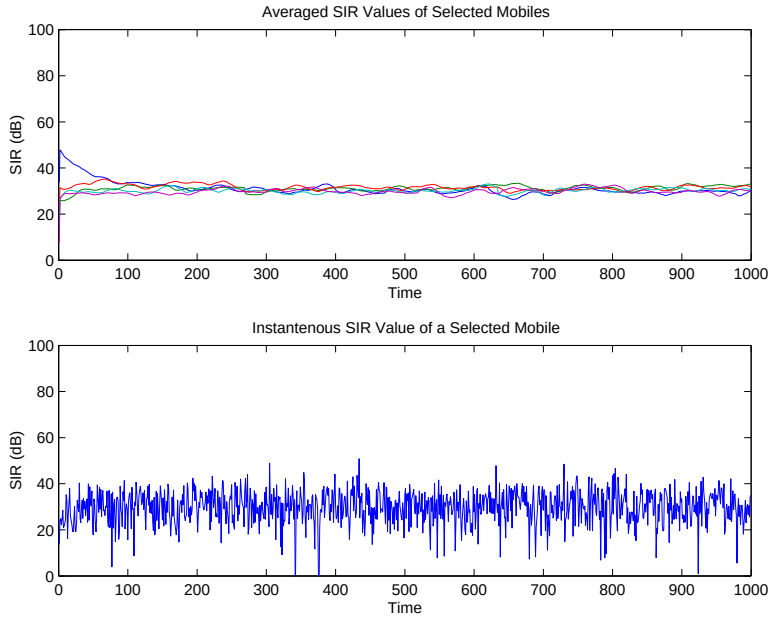

Figure 5.4: SIR and averaged SIR values of selected mobiles (in dB) with respect to time.

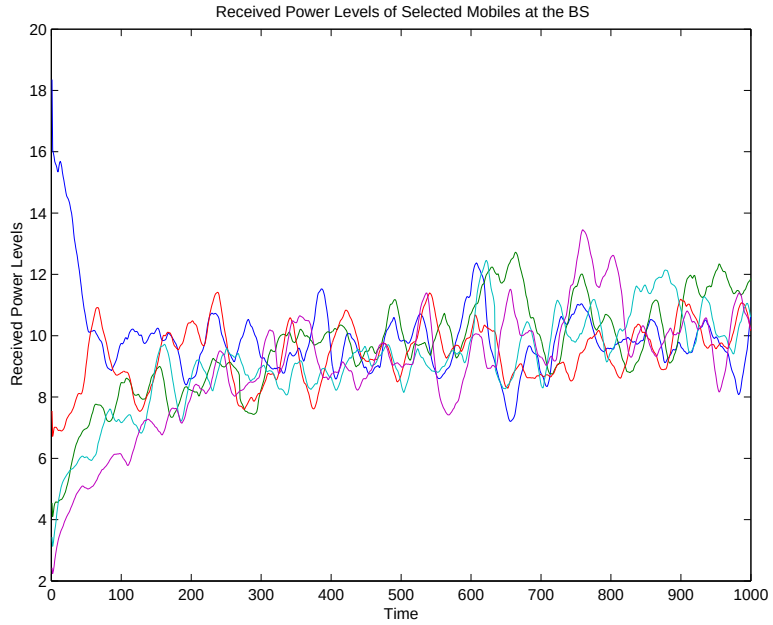

Figure 5.5: The received power levels of selected mobiles at their respective BSs.

lected mobiles at their respective BSs. While these parameters satisfy Assumption 5.2, they violate Assumption 5.4 as well as conditions of Theorem 5.2. Since the derived analytical conditions in previous sections were only sufficient, and not necessary, it is not surprising that the power levels still converge to the equilibrium points which slowly shift due to the movements of the mobiles.

In the next simulation, we change the SIR threshold value of mobiles to $\bar{\gamma}_i = 1000\,(60\,\mathrm{dB})$ and let $\lambda = 0.01$. Furthermore, we have $x_{min} = 3$ and $x_{max} = 48$, and hence, $\alpha = 16$. It is easy to see that these parameters satisfy Assumptions 5.2 and 5.4, and the conditions of Theorem 5.2. The results in Figures 5.6 and 5.7 show convergence as expected. However, we observe that the convergence speed in this case is slower due to the smaller step size. We conclude that although the sufficient conditions derived analytically provide a guideline for the convergence of the algorithm, they are by no means necessary and may be too stringent in some cases.

We next consider a more realistic information feedback scheme, where we take into account the distortion in feedback information due to quantization and other effects. Multiplying the parameter $\lambda = 0.1$ in the update algorithm (5.12) with $\mathbf{x_{-i}}$, which is a random variable uniformly distributed on $[0.7,\ 1.3]$, we rerun the previous simulation with this imperfect feedback algorithm. Figures 5.8 and 5.9 depict, respectively, the power levels and SIR values of selected mobiles. In accordance with Theorems 5.2 and 5.4, the convergence characteristics of the system are not significantly affected.

We finally study the effect of the pricing parameter v on the overall performance of the system. We calculate the sum of the utility values of static arbitrarily located mobiles for $u = 5$. Figure 5.10 displays the sum of the utility values of mobiles averaged over the fast fading process at the NE solution. After repeating this analysis several times for various distributions of mobiles, we conclude that there is a complex and nonlinear relationship between the NE point and the pricing parameter v, which can be interpreted as the cost on the battery usage of the user.

5.6 Conclusions

In this chapter, we have considered a power control game similar to the one in Chapter 4, with a utility function defined as the logarithm of the probability that the SIR level of the mobile is greater than a predefined individual threshold level. Hence, we have established a relationship between the preferences of the mobiles and outage probabilities. We have proven that the noncooperative power control game admits a unique Nash equilibrium for uniformly strictly convex pricing functions and under some technical assumptions on the SIR threshold levels. Furthermore, we have established the global convergence of continuous-time as well as discrete-time synchronous and asynchronous iterative power update algorithms to the unique NE of the game under some con-

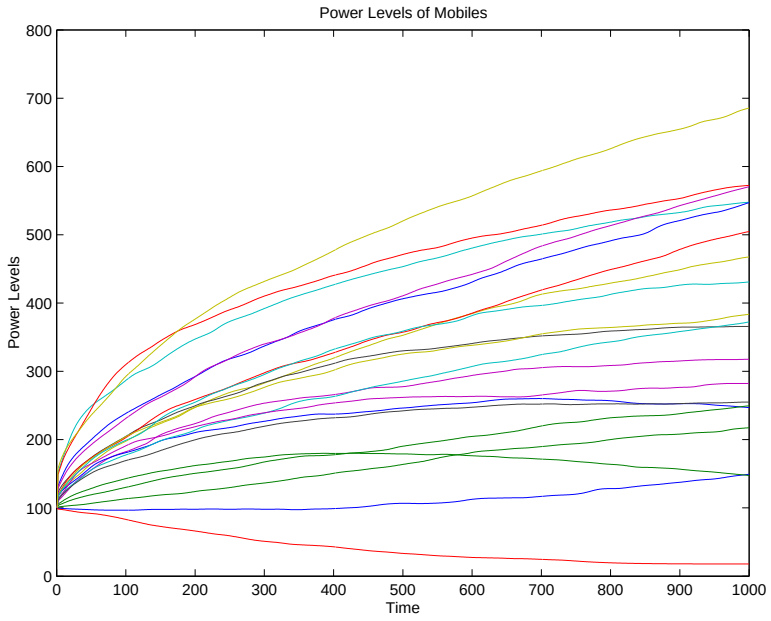

Figure 5.6: Power levels of selected mobiles with respect to time.

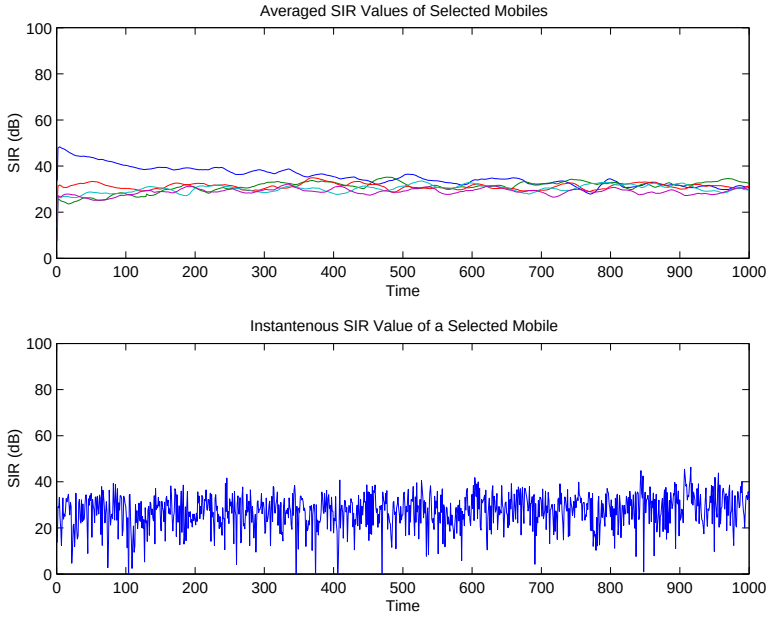

Figure 5.7: SIR and averaged SIR values of selected mobiles (in dB) with respect to time.

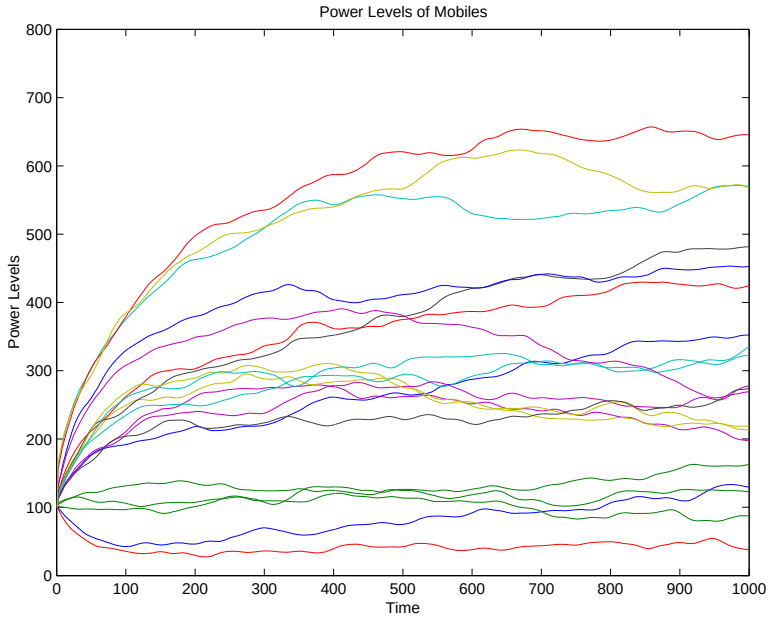

Figure 5.8: Power levels of selected mobiles with respect to time under imperfect feedback information.

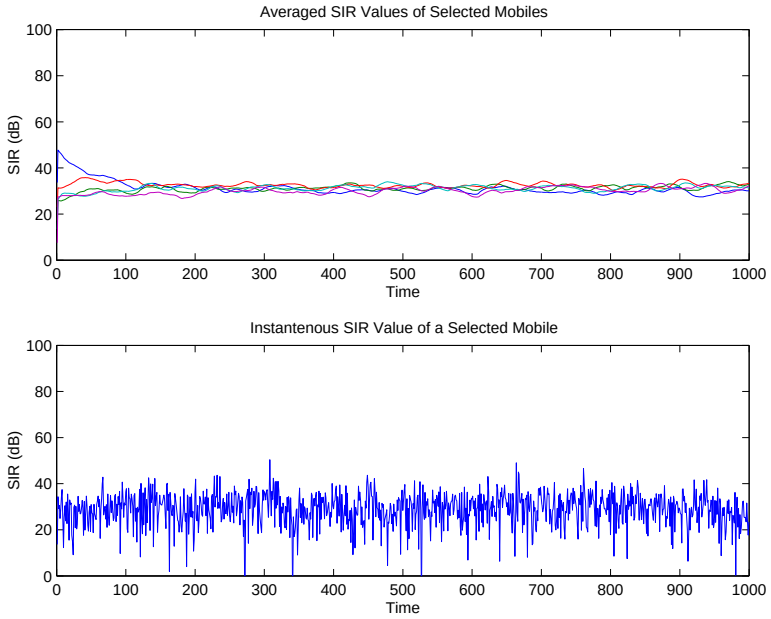

Figure 5.9: SIR and averaged SIR values of selected mobiles (in dB) with respect to time under imperfect feedback information.

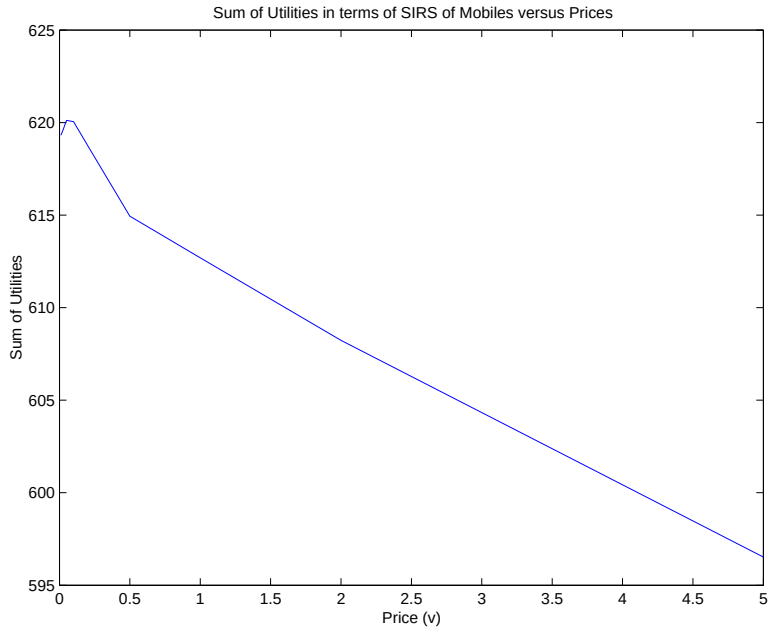

Figure 5.10: Sum of the utility values of mobiles for different v values.

ditions. Likewise, a stochastic version of the discrete-time synchronous update scheme, which accounts for the uncertainty due to quantization and estimation errors, has been shown to converge to the unique NE point almost surely. Finally, through extensive simulation studies we have demonstrated the convergence and robustness properties of power update schemes developed.

CHAPTER 6

A POWER CONTROL-JOINT BASE STATION ASSIGNMENT GAME AND POWER CONTROL AS A TEAM OPTIMIZATION PROBLEM

In this chapter we study an extension to the power control game of Chapters 4 and 5 and a formulation of the power control as a team optimization problem. In the first half of the chapter, we investigate the hybrid noncooperative game motivated by the practical problem of joint power control and base station (BS) assignment in code division multiple access (CDMA) wireless data networks. Specifically, we model the integrated power control and BS assignment problem in such a way that each mobile's action space not only includes the transmission power level but also the choice of the BS. The outcomes of the user actions are reflected in a specific cost structure, and each user is associated with a cost function that is parametrized by user-specific prices. We investigate the existence and uniqueness of pure Nash equilibrium (NE) solutions of the hybrid game, which constitute the operating points for the underlying wireless network, numerically using grid methods and randomized algorithms. In Section 6.3 we discuss the NE solution. Subsection 6.3.1 describes randomized algorithms for numerical analysis. We present our simulation results in Section 6.4 where we investigate the existence and uniqueness properties of NE solutions in Subsection 6.4.1, and analyze a power update and BS assignment scheme in Subsection 6.4.2.

In the second half of the chapter, we study power control in multicell CDMA wireless networks as a team optimization problem where each mobile attains at the minimum its individual fixed target signal to interference level and beyond that optimizes its transmission power level according to its individual preferences. We derive conditions under which the power control problem admits a unique feasible solution. Using a Lagrangian relaxation approach similar to [12] we obtain two decentralized dynamic power control algorithms: primal and dual power update, and establish their global stability utilizing both classical Lyapunov theory and the passivity framework [57]. The remainder of this chapter is organized as follows. We define in Section 6.5 the system problem and its decomposition to user and network problems. In Section 6.6, we investigate a relaxation of the system problem as well as primal and dual algorithms. In addition, system dynamics and a passivity approach for stability and robustness are studied. Section 6.7 discusses some of the basic principles of call admission control from the perspective of the model adopted in this paper. Lastly, we illustrate the power control schemes introduced through MATLAB simulations in Section 6.8. The chapter concludes with a recap of the results in Section 6.9.

6.1 A Joint Power Control-Base Station Assignment Game

For the joint power control and base station assignment game, the multicell CDMA wireless network model we consider is similar to the ones described in Chapters 4 and 5. The system consists of a set $\mathcal{B} := \{1, \ldots, N\}$ of base stations and a set $\mathcal{M} := \{1, \ldots, M\}$ of users. The number of users on the network is limited through an admission control scheme. The i^{th} mobile transmits with a nonnegative uplink power level of $p_i \leq p_{max}$, where p_{max} is an upper bound imposed by physical limitations of the mobiles. Here, we investigate the case where mobiles are given the freedom of choosing the BS connection in addition to determining their transmission power levels. Hence, each mobile connects to a BS which it chooses from the set of BSs on the network, $\mathcal{B}$. We define $h_{il}p_i$ as the instantaneous received power level from user i at the l^{th} BS. We assume that a mobile connects to one BS only at any given time. The quantity h_{il} $(0 < h_{il} < 1)$ represents the channel gain between the i^{th} mobile and the l^{th} BS [85]. Ignoring fast-time scale fading (such as Rayleigh fading) and shadowing effects in order to simplify the analysis, we model h_{il} in such a way that it depends only on the location of the mobiles with respect to the base stations. Hence, the channel gain h_{il} is given by

$$h_{il} := \left(\frac{0.1}{d_{il}}\right)^2, \tag{6.1}$$

where d_{il} denotes the (Euclidean) distance of the mobile to the BS, and the loss exponent is chosen as 2, which corresponds to a free space environment [85]. In addition, we assume that the location of a mobile, which is the main factor affecting the channel gain, h, does not change significantly over the time scale of this analysis. This assumption is justified by the fact that the power control algorithm operates with a high frequency.

The level of service a mobile receives is described in terms of SIR. In accordance with the interference model considered, the SIR obtained by mobile i at the base station l is given by

$$\gamma_{il} := \frac{Lh_{il}p_i}{\sum_{j \neq i} h_{jl}p_j + \sigma_l^2}. \tag{6.2}$$

6.2 The Hybrid Power Control Game

We consider a power control game where each user (mobile) is associated with a specific cost function. Since a user can choose both its power level, which is a continuous variable, and the BS it connects, which is discrete in nature, we call this a *hybrid power control game*. The action space, S_i of the i^{th} user is then defined as

$$S_i = \{(b, p) : b \in \mathcal{B} = \{0, 1, \ldots, N\} \text{ , and } \ p \in [0, p_{max}]\}, \tag{6.3}$$

and the actions are denoted by $s_i := (b_i, p_i)$. The cost function, J_i, of user i is defined as the difference between the utility function of the user and its pricing function, $J_i = P_i - U_i$. The utility function, $U_i(\phi, b_i)$, is chosen as a logarithmic function of the i^{th} user's SIR, which we denote by $\gamma_i(\phi, b_i)$. It quantifies approximately the demand or *willingness to pay* of the user for a certain level of service. The pricing function, $P_i(p_i)$, on the other hand, is imposed by the system to limit the interference created by the mobile, and hence to improve the system performance [49]. At the same time, it can also be interpreted as a cost on the battery usage of the user. It is a linear function of p_i, the power level of the user. Accordingly, the cost function of the i^{th} user is defined as

$$J_i(\phi, b_i) = \lambda_i p_i - \log(\gamma_i(\phi, b_i)), \tag{6.4}$$

where λ_i is a user-specific pricing constant and $\gamma_i(\phi, b_i)$ is the i^{th} mobile's SIR level under the given vector of power levels, ϕ, of all mobiles and its BS choice, b_i.

In the hybrid power control game defined, the i^{th} user's optimization problem is to minimize its cost (6.4), given the sum of power levels of all other users as received at the base stations. Thus, the reaction function of user i is

$$p_i(b_i, \phi) = \arg \min_{\mathrm{s_i}=(\mathrm{b_i},\mathrm{p_i})} \mathrm{J_i}(\mathrm{b_i}, \phi). \tag{6.5}$$

Furthermore, if the mobile is connected to the l^{th} BS, i.e. $b_i = l,\ l \in \mathcal{B}$, then the optimal power level is given by

$$p_i(b_i = l,\ \phi) = \begin{cases} \dfrac{1}{\lambda_i} - \dfrac{1}{Lh_{il}} \left(\sum_{j \neq i} h_{jl} p_j + \sigma_l^2 \right), & \text{if } \sum_{j \neq i} h_{jl} p_j < \dfrac{\lambda_i}{Lh_{il}} - \sigma_l^2 \\ 0, & \text{else} \end{cases} \tag{6.6}$$

We note that, given a specific BS, the user's optimization problem admits a unique solution (power level), although it may be a boundary solution. The nonnegativity of the power vector ($p_i \geq 0\ \ , \forall i$) is an inherent physical constraint of the model. We refer to [52] for details on the boundary analysis and conditions for an inner solution.

The reaction function (6.5) is the optimal response of the user to the varying parameters in the model. It depends not only on the user-specific parameters like b_i, λ_i, and h_i but also on the network parameter, L, and total power level received at the BS $l\,(= b_i)$ to which the mobile is connected, $\sum_{j=1}^{M} h_{jl} p_j$. Each BS provides the user total received power level using the downlink. We refer to [52] as well as Chapter 4 for communication constraints and effects.

6.3 Study of the Nash Equilibrium

The NE in the context of the hybrid power control game is defined as a set of actions s^* consisting of the BS choice b^*, power levels p^*, and corresponding set of costs J^* of users with the property that no user in the system can benefit by modifying its action while the other players keep theirs fixed. Mathematically speaking, the vector of user actions, $\mathbf{s}^* := (\beta^*, \phi^*)$, is in NE when s_i^* of any i^{th} user is the solution to the following optimization problem given the equilibrium actions of other mobiles, $\mathbf{s}_{-i}^*$:

$$\min_{s_i} J_i(s_i, \mathbf{s}_{-i}^*). \tag{6.7}$$

We have shown in [52] that once mobiles make the decision on BS connections, the power control game admits a unique NE under certain conditions. In the hybrid power control game defined, however, it is not possible to establish the existence or uniqueness of NE solution analytically. Therefore, we resort to numerical methods and *randomized algorithms* [94, 95] stand out as a useful tool for numerical analysis [38].

6.3.1 Randomized algorithms and Monte Carlo methods

We utilize randomized algorithms in order to obtain an estimate on the probabilities of existence and uniqueness of NE solutions in the hybrid power control game. Following the approach in 3, these probability estimates are obtained both through *random sampling* or *gridding* techniques on the parameter space. In this case, the parameter space consists of the locations of the mobiles, user-specific parameters such as λ, and system parameters such as L and σ^2. For illustrative purposes, let us call the specific parameter (vector) we are interested in α, while we keep all other parameters fixed.

In the case of the random sampling method, the parameter vector α is chosen to be random with given probability density function f_α, having support sets $\mathcal{S}_\alpha$. We can take, for example, $\mathcal{S}_\alpha$ to be the hyper-rectangular set

$$\mathcal{S}_\alpha = \{\alpha : \alpha_i \in [\alpha_i^-, \alpha_i^+],\ i = 1, 2, \ldots, M\}, \tag{6.8}$$

and the density function f_α to be uniform on these sets. That is, for $i = 1, 2, \ldots, M$,

$$f_{\alpha_i} = \begin{cases} \dfrac{1}{\alpha_i^+ - \alpha_i^-} & \text{if } \alpha_i \in [\alpha_i^-, \alpha_i^+] \\ 0 & \text{otherwise} \end{cases} \tag{6.9}$$

Then, we generate N_α independent identically distributed (i.i.d.) vector samples from the set $\mathcal{S}_\alpha$

according to the density function f_α: $\alpha^1, \alpha^2, \ldots, \alpha^{N_\alpha}$.

Another method for generating the sample points of the parameter is to utilize a gridding technique on the support set $\mathcal{S}_\alpha$. In this case, the samples are generated such that they are evenly spaced on the support set. Since this technique provides a nicely distributed sample set, one might think that random sampling is not necessary. However, gridding techniques suffer from a significant drawback called *curse of dimensionality*. That is, as the dimension of the parameter space increases, the number of samples required to cover the set $\mathcal{B}$ with a uniform grid grows exponentially. Therefore, we resort to random sampling methods when the dimension of the parameter space gets large.

Once the sample points are generated using either random sampling or gridding techniques, we investigate the existence of NE solutions for each sample point or set of parameters. Towards this end, we construct the indicator function

$$\mathcal{I}(\alpha^i) := \begin{cases} 1 & \text{if the game admits a NE} \\ 0 & \text{otherwise.} \end{cases}$$

The estimated probability of existence of a NE is readily given by

$$\widehat{p}_{N_\alpha} = \frac{1}{N_\alpha} \sum_{i=1}^{N_\alpha} \mathcal{I}(\alpha^i), \tag{6.10}$$

which is equivalent to

$$\widehat{p}_{N_\alpha} = \frac{N_{NE}}{N_\alpha},$$

where N_{NE} is the number of vector samples such that the hybrid game admits a NE. A separate indicator function can be defined in a similar manner to compute the probability of having multiple NE solutions.

In order to obtain a "reliable" probabilistic estimate it is important to know how many samples N_α are needed. Let us denote the real probability of existence of a NE by p_α. The Chernoff bound [94] states that for any $\epsilon \in (0,\, 1)$ and $\delta \in (0,\, 1)$ if

$$N_\alpha \geq \frac{1}{2\epsilon^2} \ln\left(\frac{2}{\delta}\right),$$

then, with probability greater than $1 - \delta$, we have $|\widehat{p}_{N_\alpha} - p_\alpha| < \epsilon$. Note that, this is a problem independent explicit bound which can be computed *a priori*. We refer to [94,95,106] for a detailed discussion on this issue.

6.4 Numerical Analysis

We first investigate the existence and uniqueness of Nash equilibrium solutions of the hybrid power control game defined in Section 6.2 numerically on the wireless network described in Section 2.2.1. Then, we simulate a dynamic power update and BS assignment scheme for mobiles.

6.4.1 Existence and uniqueness of NE

In order to be able to visualize (some of) the results we start with a one-dimensional (1-D) network model where both mobiles and BSs are located along a line. Although we consider this model only for illustrative purposes it can also be interpreted in such a way that mobiles staying on a road connect to BSs located at the road side. In the first simulation, we analyze two mobiles on a 1-D network of two BSs. The system and user parameters are chosen as $L = 128$, $\sigma_1^2 = \sigma_2^2 = 0.1$, and $\lambda_1 = \lambda_2 = 0.1$. The mobiles are located using a gridding method such that each sample point is evenly spaced with a distance of 0.125. The locations of the two BSs are chosen to be 0.5 and 1.5, respectively. Figure 6.1(a) depicts the projected locations of the mobiles and BSs where the game admits a unique or multiple NE. We observe that the game admits a unique NE in all cases except from a single location where both BSs are "equidistant" in terms of SIR levels.

We repeat the analysis above with three mobiles instead of two on the same network. While the game admits a NE in all of the 4913 sample points, there are 39 points with multiple NE corresponding to a percentage of 0.79%. Multiple NE solutions occur again at specific (symmetric) locations as shown in Figure 6.1(b).

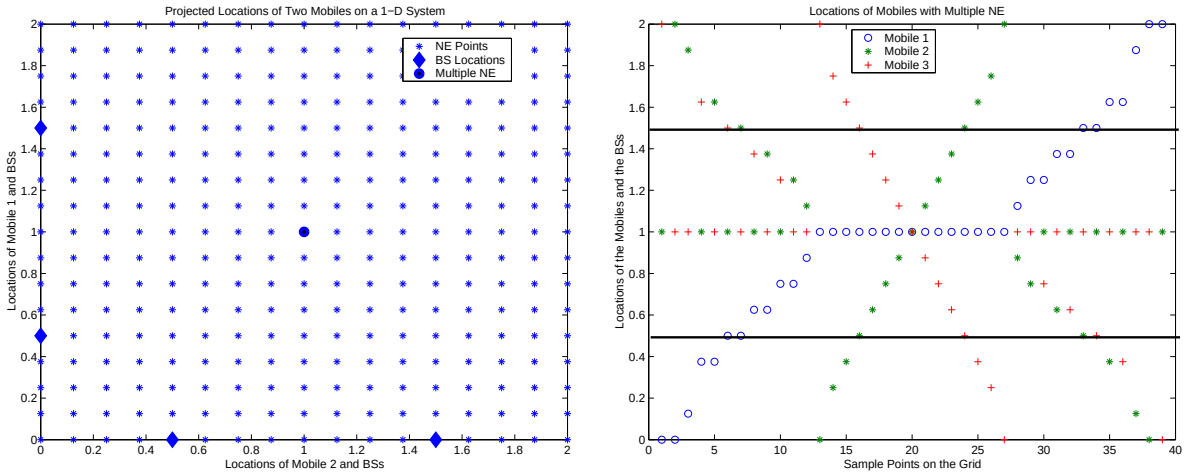

(a) (b)

Figure 6.1: (a) Projected locations of two mobiles on a 2BS 1-D network where the game admits a NE. (b) Locations of 3 mobiles on a 2BS 1-D network where the game admits multiple NE.

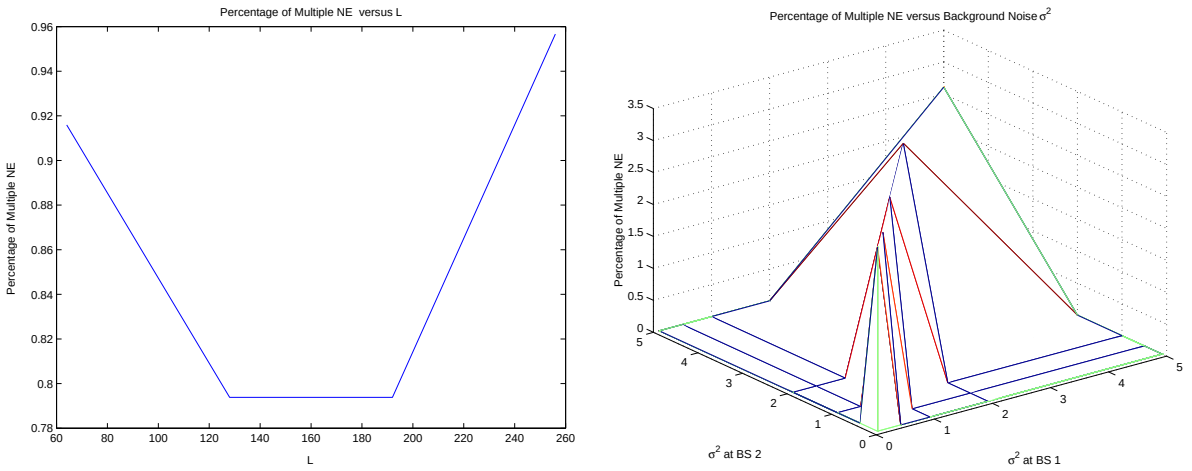

(a) (b)

Figure 6.2: (a) Percentage of mobile locations with multiple NE solutions for different values of L. (b) Percentage of mobile locations with multiple NE solutions for different values of σ_1^2 and σ_2^2.

We now investigate the effect of system and user parameters on the NE solutions of the hybrid power control game. We first vary L by choosing its values from the set $\{64,\ 128,\ 192,\ 256\}$. For each value of L, 4913 location points are generated on a grid with sample distance of 0.25. It is observed that the game admits a NE in all instances. The percentage of samples with multiple NE, on the other hand, are shown in Figure 6.2(a). Next, we set $L = 128$ and vary the background noise at the BSs such that $\sigma_1^2,\ \sigma_2^2 \in \{0.1,\ 0.5,\ 1,\ 2\}$. Figure 6.2(b) depicts the percentage of multiple NE whereas there is again at least one NE solution in all cases. We finally investigate the effect of pricing parameters $\lambda_1,\ \lambda_2$ while setting $\sigma_1^2 = \sigma_2^2 = 0.1$ and $\lambda_3 = 0.1$. The results are shown in Figure 6.3(a). Analyzing the individual cases of the game admitting multiple NE, we conclude that a high percentage of multiple solutions is partly a result of one or more mobiles transmitting with zero NE power due to high prices. In other words, although these cases technically constitute multiple NE solutions, they do not play a significant role in practice. We refer to [52] for a discussion on the relationship between prices and (soft) admission control.

We observe that the simulations conducted using gridding techniques yield somewhat distorted results in terms of multiple NE solutions due to the inherent lattice structure which exhibits specific symmetry properties. Therefore, we repeat the analysis above with samples generated using random sampling methods. The locations of the mobiles are chosen randomly with uniform distribution on the support set defined by the boundaries of the network. We repeat the first three simulations with 1000 randomly generated location points. In accordance with the discussion in Section 6.3.1, 1000 sample points guarantee that our estimates on the percentage of the existence and uniqueness of NE solutions are accurate within $\epsilon = 6\%$ with a probability of at least

$1-\delta = 0.998$. In other words, $Probability\left(|\widehat{p}_N - p| < 0.06\right) \geq 0.998$, where $\widehat{p}_N$ and p denote the estimated and real probabilities of the analyzed property, respectively. In all of these three simulations we observe that the game admits a unique NE with 100% estimated probability. Hence, the probability of having a unique NE solution in 94% of the possible configurations is at least 0.998. This clearly indicates that multiple NE solutions are obtained only at very specific symmetric configurations, which coincide with the lattice structure of the gridding techniques. Figure 6.3(b), on the other hand, shows the effect of varying pricing parameters $\lambda_1,\ \lambda_2$ where $\lambda_3 = 0.1$. We note an overall decrease in the number of instances of the problem with multiple NE solutions due to the random nature of samples.

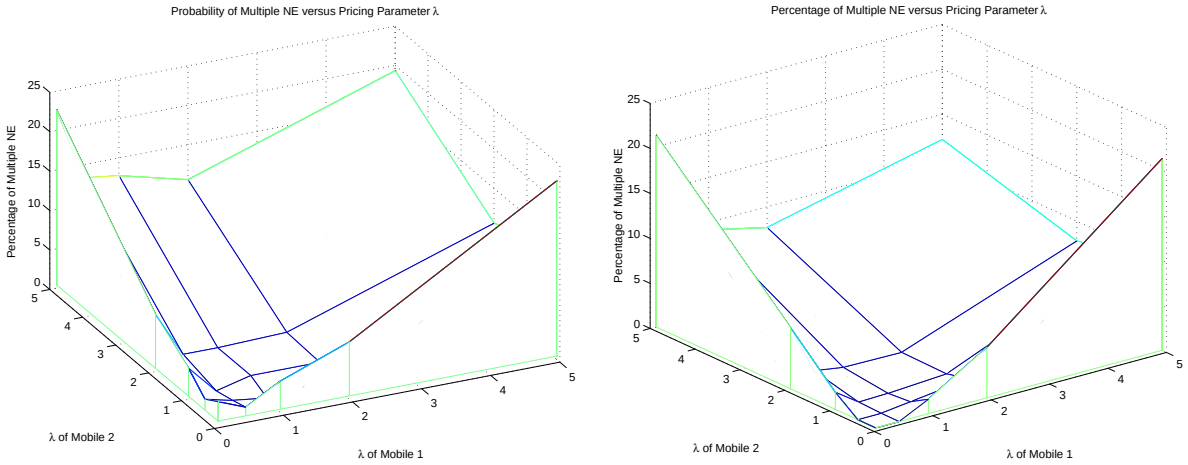

(a) (b)

Figure 6.3: (a) Percentage of mobile locations with multiple NE solutions for different values of λ_1 and λ_2. (b) Percentage of mobile locations with multiple NE solutions for different values of λ_1 and λ_2.

Next, we consider a more realistic two-dimensional (2-D) wireless network model. The previous simulations are repeated on the 2-D network again using random sampling. We observe that almost all of the results are comparable with the ones on the 1-D network. Figure 6.4 depicts the effect of pricing varying pricing parameters $\lambda_1,\ \lambda_2$ with $\lambda_3 = 0.1$. Finally, we investigate the existence and uniqueness of NE on a network of three BSs with four mobiles. The hybrid game admits a unique NE solution in all instances considered corresponding to a probability estimate of 100%. A subset of 1000 randomly generated location points of two of the mobiles and locations of the BSs are depicted in Figure 6.5(a).

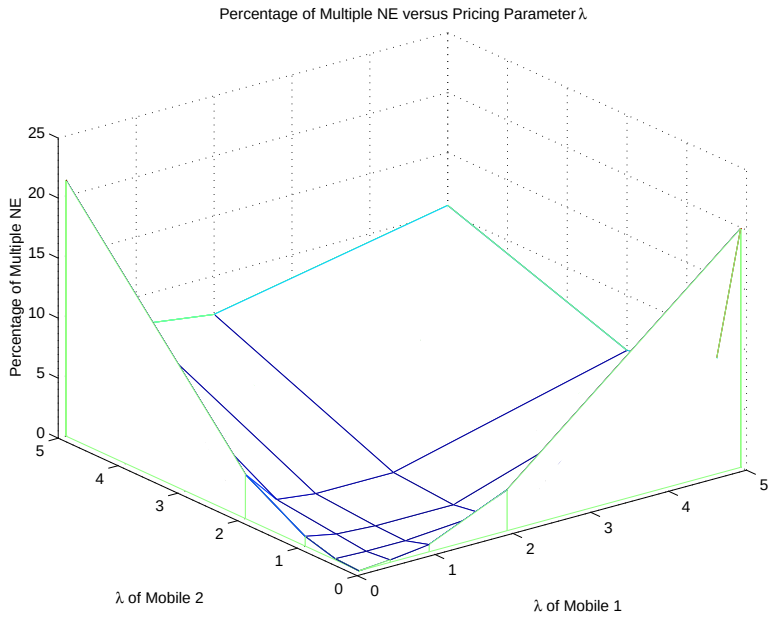

Figure 6.4: Percentage of mobile locations with multiple NE solutions for different values of λ_1 and λ_2 on a 2-D wireless network.

6.4.2 System dynamics and convergence

We simulate a joint power update and BS assignment scheme for a 2-D wireless network consisting of four BSs and arbitrarily placed 20 mobiles. The system parameters are chosen as $L = 128$ and $\sigma_l^2 = 0.1\ \forall l$. Locations of BSs and mobiles are shown in Figure 6.5(b).

In order to minimize its cost function (6.7), the i^{th} mobile chooses the BS that maximizes its SIR level and updates its transmission power level using the algorithm (6.6) such that

$$p_i^{(n+1)} = \frac{1}{\lambda_i} - \frac{1}{L\, h_{il}} \left(\sum_{j \neq i} h_{jl} p_j^{(n)} + \sigma_l^2) \right),$$

where n denotes the time, and BS choice of mobile i is $b_i = l$. In addition, through a projection operation it is ensured that $p_i^{(n)} > 0\ \forall\, i,\ n$. Figures 6.6(a) and (b) depict the evolution of the power and SIR levels of the mobiles. We repeat the same simulation where the mobiles connect only to the nearest BS and update their power levels. The sums of the SIR levels achieved by the users in both cases are compared in Figure 6.7. Clearly, the additional freedom of BS choice, and hence, the hybrid power control game provides an improvement over "classical" noncooperative power control.

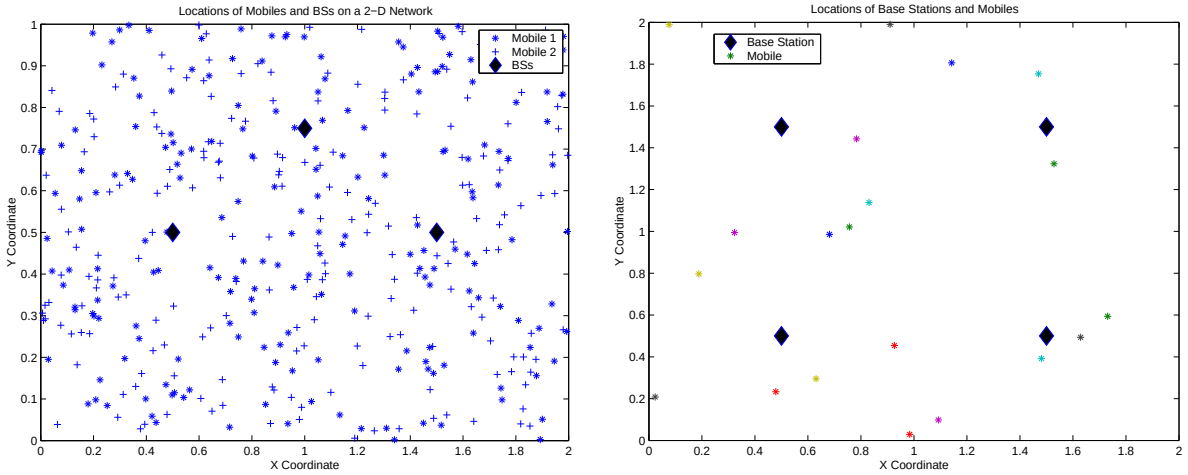

(a) (b)

Figure 6.5: (a) Randomly generated locations of two mobiles on a 2-D wireless network with 3 BSs. (b) Locations of base stations and mobiles for dynamic simulations.

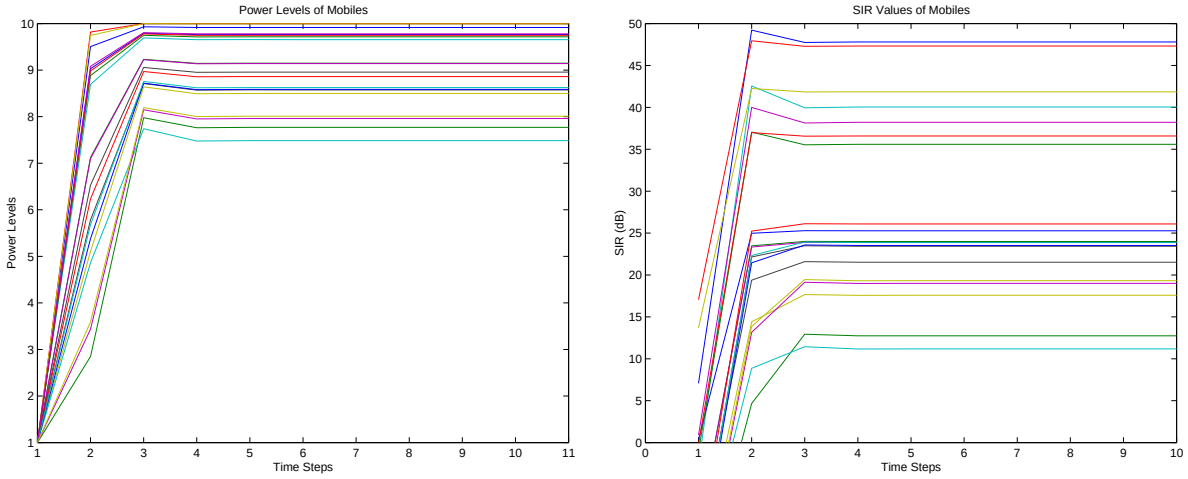

(a) (b)

Figure 6.6: (a) Power levels of mobiles with respect to time. (b) SIR values of mobiles (in dB) with respect to time.

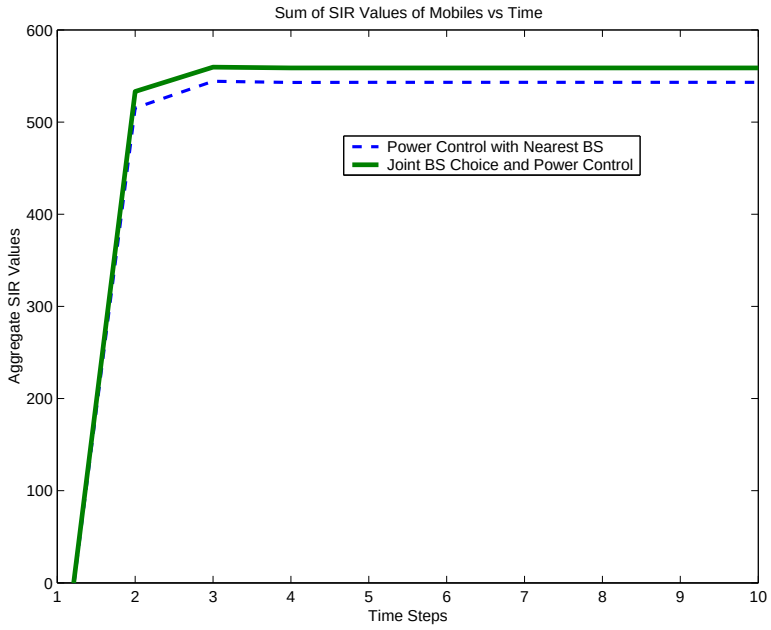

Figure 6.7: Sums of the SIR values of mobiles (in dB) with respect to time for power control with nearest BS choice and hybrid power control scheme.

6.5 A Team Optimization Approach to Power Control for Multicell CDMA Wireless Networks

In this section, we consider a multicell CDMA wireless network model similar to the one described in 6.1, where the wireless network consists of a set $\mathcal{L} := \{1, \ldots, K\}$ of cells, with the set of users in cell l being $\mathcal{M}_l := \{1, \ldots, M_l\},\ l \in \mathcal{L}$, and the set of all users is defined as $\mathcal{M} := \bigcup_l \mathcal{M}_l$ with cardinality M. Unlike in Section 6.1 and similar to the models in Chapters 4 and 5, however, we assume that users connect to the BS with the least channel attenuation within the network, where the BS with least channel attenuation corresponds to the nearest BS of a mobile.

We formulate the power control problem as one of team optimization where each mobile i attains its individual fixed target SIR level, $\bar{\gamma}_i$, while optimizing its transmission power level and respecting quality of service (QoS) constraints of other users. This formulation, which we refer to as the *centralized problem*, addresses two main issues while ensuring that mobiles achieve QoS targets. First, it reduces the overall interference to neighboring cells, which is of particular importance for frequency reuse in a multicell network. Second, it reduces the battery usage of mobiles according to their individual preferences. Define $\phi = [p_1, p_2, \ldots, p_M]$ as the vector of mobile power levels. In addition, we define $\phi_l = [p_1, \ldots, p_{M_l}]$ as the vector of mobile power levels in cell $l \in \mathcal{L}$ and $\mathbf{x}_l = [x_{1l}, x_{2l}, \ldots, x_{M_l}]$ as the vector of received power levels at the l^{th} BS. We establish in this section that the centralized problem, $\gamma_i(\phi) = \bar{\gamma}_i\ \forall i \in M$, admits a unique

solution, ϕ^*.

One of the main objectives of this paper is to study decentralized power control schemes. Therefore, we relax the centralized problem to a constrained team optimization problem, which will be referred to as the *system problem* in the remainder of the paper. Let $C_i(p_i)$ be the i^{th} mobile's individual cost function which we assume to be strictly convex and continuously differentiable. This cost function can be defined, for example, as the difference between a convex increasing cost on mobile's transmission power (battery usage) and a strictly concave utility-like function representing its willingness to increase transmission power with the aim of attaining better QoS. Then, the system problem is

$$\min_{\phi} \sum_{i=1}^{M} C_i(p_i) \text{ such that } \gamma_i \geq \bar{\gamma}_i,\ 0 \leq p_i \leq p_{max}\ \forall i \in \mathcal{M}, \tag{6.11}$$

where $\bar{\gamma}_i$ is i^{th} mobile's target SIR and p_{max} is defined as a finite but sufficiently large upper bound on $p_i\ \forall i$, so that the solution to (6.11) does not hit $p_i = p_{max}$ for any i. We note that this system problem is more general than the one in [61], which studies the special case of $C_i(p_i)$ being strictly increasing in p_i for all i.

It is convenient to rewrite the set of conditions $\gamma_i \geq \bar{\gamma}_i$, $i = 1, 2, \ldots, M$, in terms of received power levels at each BS and in matrix form. Define the $M_l \times M$ matrix

$$\mathcal{A}_l := \begin{pmatrix} h_{1l} & -h_{2l}\frac{\bar{\gamma}_1}{L} & \cdots & \frac{-h_{M_l l}\bar{\gamma}_1}{L} \\ \frac{-h_{1l}\bar{\gamma}_2}{L} & h_{2l} & \cdots & \frac{-h_{M_l l}\bar{\gamma}_2}{L} \\ \vdots & & \ddots & \vdots \\ \frac{-h_{1l}\bar{\gamma}_{M_l}}{L} & \frac{-h_{2l}\bar{\gamma}_{M_l}}{L} & \cdots & h_{M_l l} \end{pmatrix}_{M_l \times M} \tag{6.12}$$

and the matrix $\mathcal{A}$ as the vertical concatenation of the $\mathcal{A}_l,\ l = 1, 2, \ldots, K$, matrices, $\mathcal{A} := \left[\mathcal{A}_1^T \cdots \mathcal{A}_K^T\right]^T$, where $[X]^T$ denotes the transpose of the matrix X. Define also the vector

$$\beta_l := \left[\bar{\gamma}_1\sigma_l^2/L, \ldots, \bar{\gamma}_{M_l}\sigma_l^2/L\right]^T,$$

and the vector $\beta := [\beta_1, \beta_2, \ldots, \beta_K]^T$. Thus, the system problem is formulated by

$$\begin{aligned} &\min_{\phi} \sum_{i=1}^{M} C_i(p_i), \quad \text{such that} \\ &\phi \in \Omega := \{\phi \in \mathbb{R}^M : \mathcal{A}\phi \geq \beta, \text{ and} \\ &\qquad 0 \leq p_i \leq p_{max}\ \forall i \in \mathcal{M}\}. \end{aligned} \tag{6.13}$$

Lemma 6.1 *Let Ω be nonempty. Then, the system problem (6.13) is a strictly convex optimization problem with a convex, compact constraint set, and hence admits a unique global minimum.*

Proof. The objective function $\sum_{i=1}^{M} C_i(p_i)$ is clearly strictly convex in its arguments due to strict convexity of C_i with respect to p_i for all $i \in \mathcal{M}$. We now establish the convexity and compactness of the constraint set Ω. Let $\mathrm{row_i(X)}$ denote the i^{th} row of the matrix X. First, note that Ω is bounded by definition due to $0 \leq \phi \leq p_{max}$. In addition, it is closed since it consists of intersection of half-spaces, $\mathrm{row_i}(\mathcal{A}_\mathrm{l})\,\phi \geq \mathrm{b_{il}}\ \forall \mathrm{i} = 1, 2, \ldots, \mathrm{M_l},\ \forall \mathrm{l} \in \mathcal{L}$, which include their respective separating hyperplanes, and the closed set $0 \leq \phi \leq p_{max}$. Thus, the constraint set of the problem, Ω, is compact. Finally, following a similar argument it is easy to see that it is also convex, being the intersection of convex sets. □

We next derive a set of necessary and sufficient conditions under which Ω is nonempty and thus there exists a feasible solution to the system problem (6.13).

Lemma 6.2 *Let*

$$\eta_l := \sum_{j \in \mathcal{M}_l} \frac{\bar{\gamma}_j}{L + \bar{\gamma}_j}. \tag{6.14}$$

If $\eta_l < 1\ \forall l \in \mathcal{L}$, then with p_{max} picked sufficiently large, Ω is nonempty. In particular, every p_l satisfying $A_l p_l \geq b_l$ also satisfies $p_l \geq 0$. If $\eta_l \geq 1$ for some $l \in \mathcal{L}$, then Ω is empty.

Proof. We first rewrite $A_l p_l \geq b_l$ as $\tilde{A}_l x_l \geq b_l$, where $x_{il} := h_{il} p_{il}$, and

$$\tilde{A}_l = \begin{bmatrix} 1 & -\frac{\bar{\gamma}_1}{L} & \cdots & -\frac{\bar{\gamma}_1}{L} \\ -\frac{\bar{\gamma}_2}{L} & 1 & \cdots & -\frac{\bar{\gamma}_2}{L} \\ \vdots & & \ddots & \vdots \\ -\frac{\bar{\gamma}_l}{L} & -\frac{\bar{\gamma}_l}{L} & \cdots & 1 \end{bmatrix} = \begin{bmatrix} 1+\frac{\bar{\gamma}_1}{L} & 0 & \cdots & 0 \\ 0 & 1+\frac{\bar{\gamma}_2}{L} & \ddots & \vdots \\ \vdots & \ddots & \ddots & 0 \\ 0 & \cdots & 0 & 1+\frac{\bar{\gamma}_l}{L} \end{bmatrix} - \begin{bmatrix} \frac{\bar{\gamma}_1}{L} & \frac{\bar{\gamma}_1}{L} & \cdots & \frac{\bar{\gamma}_1}{L} \\ \frac{\bar{\gamma}_2}{L} & \frac{\bar{\gamma}_2}{L} & \cdots & \frac{\bar{\gamma}_2}{L} \\ \vdots & & \ddots & \vdots \\ \frac{\bar{\gamma}_l}{L} & \frac{\bar{\gamma}_l}{L} & \cdots & \frac{\bar{\gamma}_l}{L} \end{bmatrix}.$$

Next, dividing the ith row of this matrix by $1 + \frac{\bar{\gamma}_i}{L}$ for each $i = 1, \cdots, l$, we note that $\tilde{A}_l x_l \geq b_l$ is equivalent to

$$\hat{A}_l x_l \geq \hat{b}_l \tag{6.15}$$

where $\hat{b}_{il} := b_{il}/(1 + \frac{\bar{\gamma}_i}{L})$ and

$$\hat{A}_l := I - \underbrace{\begin{bmatrix} \frac{\bar{\gamma}_1}{L+\bar{\gamma}_1} & \frac{\bar{\gamma}_1}{L+\bar{\gamma}_1} & \cdots & \frac{\bar{\gamma}_1}{L+\bar{\gamma}_1} \\ \frac{\bar{\gamma}_2}{L+\bar{\gamma}_2} & \frac{\bar{\gamma}_2}{L+\bar{\gamma}_2} & \cdots & \frac{\bar{\gamma}_2}{L+\bar{\gamma}_2} \\ \vdots & & \ddots & \vdots \\ \frac{\bar{\gamma}_l}{L+\bar{\gamma}_l} & \frac{\bar{\gamma}_l}{L+\bar{\gamma}_l} & \cdots & \frac{\bar{\gamma}_l}{L+\bar{\gamma}_l} \end{bmatrix}}_{=: T_l}. \tag{6.16}$$

To show that Ω is nonempty when $\eta_l < 1$, we note that the nonnegative matrix T_l defined above has eigenvalues $\{0, \cdots, 0, \eta_l\}$, and thus, spectral radius η_l. This means that, if $\eta_l < 1$, then $\hat{A}_l = I - T_l$ is a nonsingular *M-Matrix* as defined in [107, Chapter 6]. It follows from characterization (N_{39}) in [107, Chapter 6] of nonsingular M-matrices that $\hat{A}_l x_l \geq \hat{b}_l \geq 0$ implies $x_l \geq 0$. This proves that every p_l satisfying $A_l p_l \geq b_l$ also satisfies $p_l \geq 0$, and thus, Ω is nonempty.

To prove that if $\eta_l \geq 1$ then Ω is empty, we proceed with a contradiction argument. Suppose, to the contrary, that Ω is nonempty; that is, there exists $x_l \geq 0$ such that $\hat{A}_l x_l \geq \hat{b}_l$. Because each entry of $\hat{b}_l$ is strictly positive ($\hat{b}_l \gg 0$ in the notation of [107]) this means that $x_l > 0$ and $\hat{A}_l x_l \gg 0$. From characterization (I_{28}) in [107, Chapter 6], this leads to the conclusion that $\hat{A}_l$ is a nonsingular M-matrix, which contradicts $\eta_l \geq 1$. □

We now combine the results of Lemmas 6.1 and 6.2 in the following theorem.

Theorem 6.1 *Let*

$$\sum_{j \in \mathcal{M}_l} \frac{\bar{\gamma}_j}{L + \bar{\gamma}_j} < 1 \; \forall l \in \mathcal{L}. \tag{6.17}$$

Then, with p_{max} picked sufficiently large, Ω is nonempty, and there exists a unique positive solution, ϕ^*, to the system problem (6.13), which has the property that $p_i^* < p_{max}$ $\forall i$.

The condition in Theorem 6.1 provides an upper bound on the achievable target SIR levels as well as for the number of mobiles in a given cell, and hence, provides a soft capacity constraint for the underlying CDMA system. Consequently, we will utilize condition (6.17) as a guideline for the admission control scheme based on soft constraints in Section 6.7.

6.5.1 User and network problems

We have already established that there exists an optimal solution ϕ^* to (6.13) under the conditions (6.17), the cost functions are strictly convex, and the constraints are linear. Then, it readily

follows [81, p. 310] that there exist Lagrange multiplier vectors λ, ν, and $\mathbf{x_{-i}}$, such that ϕ^* minimizes the following Lagrangian function over $\mathbb{R}^M$:

$$L(\phi, \lambda, \nu, \mathbf{x_{-i}}) = \sum_{i \in M} C_i(p_i) - \lambda^T(\mathcal{A}\phi - \beta) + \nu^T\phi + \mathbf{x_{-i}}^T(\phi - p_{max}), \tag{6.18}$$

and since L is differentiable,

$$\nabla_\phi L(\phi^*, \lambda, \nu, \mathbf{x_{-i}}) = 0. \tag{6.19}$$

Furthermore, since p_{max} was taken to be sufficiently large, and any feasible solution is positive under (6.17), both ν and $\mathbf{x_{-i}}$ are zero. Moreover, the Lagrange multiplier λ is unique, since the matrix $\mathcal{A}$ is full rank (and in fact invertible).

Let us introduce the vector $\mathbf{q} := \mathcal{A}^T\lambda$. Since $\lambda^T\mathcal{A}\phi = \phi^T\mathcal{A}^T\lambda = \phi^T\mathbf{q}$, the Lagrangian in (6.18) can be rewritten as $L(\phi, \lambda, \nu, \mathbf{x_{-i}}) = \sum_{i \in M}[C_i(p_i) - q_i p_i] + \lambda^T\beta$. Then, (6.19) is equivalent to

$$\frac{\partial L(\phi^*, \lambda)}{\partial p_i} = \frac{dC_i(p_i)}{dp_i} - q_i = 0, \ i = 1, 2, \ldots, M.$$

A noteworthy fact is that the set of constraints $\mathcal{A}\phi \geq \beta$ ensure positivity of ϕ^*, which follows directly from Theorem 6.1.

Remark 6.1 *We note that if the function $C_i(p_i)$ is chosen to be strictly increasing for all i, then the solution of the system problem ϕ^* simultaneously solves the centralized problem, $\gamma_i(\phi^*) = \bar{\gamma}_i \ \forall i \in M$, under (6.17), and is given by*

$$p_i^* = \frac{\sigma_l^2 + \sum_{k \notin \mathcal{M}_l} h_{kl} p_k^*}{h_{il}\big(1 + L/\bar{\gamma}_i\big)\left[1 - \sum_{j \in M_l} \bar{\gamma}_j/(L + \bar{\gamma}_j)\right]} \ \ \forall i \in \mathcal{M},$$

where l denotes the BS to which i^{th} mobile is connected.

Having thus established the existence of a centralized solution to the system problem (6.13), our goal is now to find a decentralized power control algorithm that solves the system problem. As the first step in this direction, we decompose the system problem into a *User*$_i$ problem for the i^{th} user and a *Network* problem by defining $r_i := p_i q_i \ \forall i$, where $q_i = \mathrm{row_i}(\mathcal{A}^{\mathrm{T}})\lambda$ and λ is the Lagrangian multiplier vector in (6.18). Following the approach in [12] in the context of congestion control, we define

$$\begin{aligned} &\text{User}_i : \min_{r_i} C_i(r_i/q_i) - r_i, \ r_i \geq 0, \quad \text{and} \\ &\text{Network} : \ \min_{\phi} \textstyle\sum_{i \in \mathcal{M}} -r_i \log(p_i), \ \phi \in \Omega. \end{aligned} \tag{6.20}$$

Mobile i solves its own convex *User*$_i$ problem to obtain $r_i^* = q_i\,(C_i')^{-1}(q_i)$. The Lagrangian for the network problem (which is another convex optimization problem on Ω) is given by $\tilde{L}(\phi, \mu) =$

$\sum_{i\in M} -r_i \log(p_i) + \mu^T(\mathcal{A}\phi - \beta)$. Using the same reasoning as in the system problem $\partial\tilde{L}(\phi^*, \mu)/\partial p_i = 0,\ \forall i$, which in turn leads to $q = \mathcal{A}^T\mu$. Using the full rank property of $\mathcal{A}$, it follows from the definition of $\mathbf{q}$ that $\mu = \lambda$. From [12] and Theorem 2 in [11] it is known that there always exist vectors ϕ, $\mathbf{r}$, and $\mathbf{q}$ satisfying $p_i = r_i/q_i\ \forall i$, such that r_i solves the User$_i$ and ϕ solves the Network problems. Thus, the vector ϕ is the unique solution of the original system problem.

6.6 A Relaxation of the System Problem and System Dynamics

Although the user and the network problems (6.20) are tractable, it would be difficult to implement a solution in any centralized manner [12]. Furthermore, there is the need to devise a decentralized power control scheme which will operate under various communication constraints limiting the flow of control information between the mobiles and the BSs. In order to circumvent these difficulties we consider a relaxation of the system problem (6.13) by defining appropriate penalty functions. Then, we study two distributed algorithms (primal and dual) and show that they converge to the unique solution of the relaxed system problem, which is arbitrarily close to the solution of the original problem.

Let us define the penalty or barrier function, ρ_i, corresponding to the constraint $\mathrm{row_i}(\mathcal{A})\phi \geq \beta_\mathrm{i}$ as

$$\rho_i(\mathbf{x_{-i}}) := f(\beta_i - \mathbf{x_{-i}}_i), \tag{6.21}$$

where the scalar function $f(\theta)$ is nondecreasing and continuous in its argument θ, and attains the value 0 if $\theta < 0$. We note that an alternative penalty function $\tilde{\rho}_i$ can be defined in terms of SIR levels $\tilde{\rho}_i(\phi) := f(\bar{\gamma}_i - \gamma_i(\phi))$. The objective function based on penalty functions $\rho_i\ \forall i \in \mathcal{M}$ is defined as

$$V(\phi) := \sum_{i\in\mathcal{M}} C_i(p_i) - \int_{b_i}^{\mathrm{row_i}(\mathcal{A})\phi} \rho_i(\mathbf{x_{-i}}) d\mathbf{x_{-i}}. \tag{6.22}$$

It is straightforward to show that $V(\phi)$ is strictly convex in p_i for all i. We next define the relaxed system problem

$$\min_{\phi>0} V(\phi). \tag{6.23}$$

By an appropriate choice of penalty functions, the unique solution of (6.23) approximates the solution of the system problem (6.13) arbitrarily close, which is strictly positive under the conditions of Theorem 6.1. For example, let the function $f(\theta)$ in (6.21) be defined as $f(\theta) := [\theta + \varepsilon]^+/\varepsilon^2$, where the function $[x]^+$ maps x to zero if $x < 0$. Then, as $\varepsilon \to 0$, the relaxed system problem

approximates the solution of the system problem arbitrarily close [12]. For details on a similar relaxation of the system problem in a different context we refer to [9].

6.6.1 The primal power update algorithm

We define the primal power update algorithm as

$$\begin{aligned} \dot{p}_i = \frac{dp_i}{dt} = \kappa_i \left(-\frac{\partial C_i(p_i)}{\partial p_i} + q_i \right), \; i = 1, 2, \ldots, M \;\; \text{and} \\ \mathbf{q}(\phi) = \mathcal{A}^T \rho(\mathcal{A}\phi), \end{aligned} \tag{6.24}$$

where ρ_i is defined in (6.21), $\kappa_i > 0$ is the user-specific step-size constant, and $\rho(\mathcal{A}\phi)$ is defined as $\rho(\mathcal{A}\phi) := [\rho_1(\mathrm{row}_1(\mathcal{A})\phi), \rho_2(\mathrm{row}_2(\mathcal{A})\phi), \ldots, \rho_{\mathrm{M}}(\mathrm{row}_{\mathrm{M}}(\mathcal{A})\phi)]$. The primal power update algorithm enables us to implement a distributed power update scheme. Here, mobiles vary their power levels as described by $\dot{p}$ in (6.24) while the BS calculates the vector $\mathbf{q}$ from the received power levels and mobile preferences and feeds this information back to the mobiles. Other distributed schemes and further analysis on the communication constraints can be found in [56]. We present here a stability result for the primal algorithm.

Theorem 6.2 *The primal power update algorithm (6.24) admits a unique equilibrium ϕ^* that solves the relaxed system problem (6.23). Furthermore, it is globally asymptotically stable.*

Proof. It is straightforward to see that the unique equilibrium point of the set of differential equations (6.24) corresponds to the unique minimum of the convex function (6.22):

$$\begin{aligned} &\frac{\partial V(\phi)}{\partial p_i} = \frac{\partial C_i(p_i)}{\partial p_i} - q_i(\phi) = 0 \\ &\Rightarrow p_i^* = (C_i')^{-1}(q_i(\phi^*)). \end{aligned}$$

Hence, the primal algorithm solves the relaxed system problem. Note by definition of ρ_i that

$$\lim_{p_i \to \infty} \sum_{i \in \mathcal{M}} \int_{b_i}^{\mathrm{row_i}(\mathcal{A})\phi} \rho_i(\mathbf{x_{-i}}) d\mathbf{x_{-i}} \to \infty, \; \forall i \in \mathcal{M},$$

and hence,

$$\lim_{p_i \to \infty} V(\phi) \to \infty, \; \forall i \in M.$$

Therefore, the function $V(\phi)$ is strictly convex by Lemma 3.2 in [9] and constitutes a Lyapunov function for system (6.24), which yields, for all $\phi \neq \phi^*$,

$$\dot{V}(\phi) = \frac{\partial V(\phi)}{\partial t} = \sum_{i=1}^{M} \frac{\partial V(\phi)}{\partial p_i} \cdot \dot{p}_i = -\sum_{i=1}^{M} \left(\frac{\partial C_i(p_i)}{\partial p_i} - q_i(\phi) \right)^2 < 0.$$

Thus, the primal power update algorithm (6.24) is globally asymptotically stable. For an analysis parallel to this, we refer to Theorem 3.4 in [9]. □

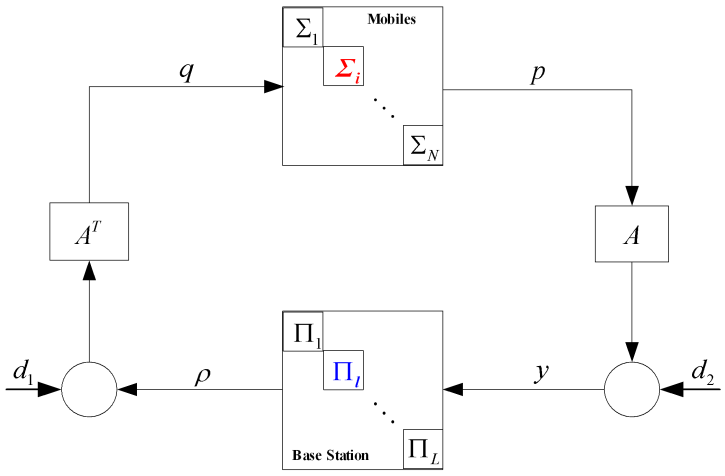

Figure 6.8: The primal update algorithm is represented in terms of a forward and a feedback blocks within the passivity framework.

6.6.2 A passivity approach to system stability and robustness

We next utilize a passivity approach to analyze stability and robustness of the primal power update algorithm. Let us study the system (6.24) by decomposing it into forward and feedback blocks as depicted in Figure 6.8, where $y := \mathcal{A}\,\phi$. In this representation, the forward block corresponds to the mobiles and the feedback path corresponds to the base station algorithm in (6.24). We then have the following result:

Theorem 6.3 *Consider the feedback system (6.24) represented as in Figure 6.8. The forward system from $(q - q^*)$ to $\dot{p}$, and the return system from $\dot{y}$ to $(q - q^*)$ are both passive. Thus, the system is globally asymptotically stable.*

Proof. For the forward system, we let

$$V_1(p-p^*) = \sum_i \left((C_i(p_i) - C_i(p_i^*)) - q_i^*(p_i - p_i^*) \right)$$

where $V_1(0) = 0$. The derivative of each component of V_1 with respect to p_i is

$$\frac{\partial V_1}{\partial p_i} = \frac{dC_i(p_i)}{dp_i} - q_i^*$$

which, when set to zero, has the unique solution at $p = p^*$. Because the second derivative is

$$\frac{\partial^2 V_1}{\partial p_i^2} = C_1''(p_1) > 0,$$

we conclude that V_1 is a positive definite function.

Next, we note that the derivative of V_1 is

$$\begin{aligned}
\dot{V}_1 &= \sum_i \left(\frac{dC_i(p_i)}{dp_i} - q_i^* \right) \dot{p}_i \\
&= \sum_i \left(\frac{dC_i(p_i)}{dp_i} - q_i \right) \dot{p}_i + (q_i - q_i^*)\dot{p}_i \\
&= \sum_i \left(\frac{dC_i(p_i)}{dp_i} - q_i \right) K \left(-\frac{dC_i(p_i)}{dp_i} + q_i \right)_{p_i}^{+} + (q_i - q_i^*)\dot{p}_i.
\end{aligned} \tag{6.25}$$

Because the first term is negative definite, as can be shown from the uniqueness of the equilibrium p^* and the discussion in Appendix C in [57], the forward system from $(q - q^*)$ to $\dot{p}$ is passive. Now consider the return system, and let

$$V_2(y - y^*) = \sum_i -\int_{y_i^*}^{y_i} \left(f(\mathbf{x}_{-\mathbf{i}_i}) - f(y_i^*) \right) d\mathbf{x}_{-\mathbf{i}_i} \tag{6.26}$$

where $V_2(0) = 0$, $\nabla V_2(0) = -\left(f(y) - f(y^*)\right)|_{y=y^*} = 0$, and $\nabla^2 V_2 = -f'(y) \geq 0$, so V_2 is a non-negative definite function. This return system from $\dot{y}$ to $(q - q^*)$ is passive since

$$\dot{V}_2 = -\left(f(y) - f(y^*)\right)\dot{y} = -(\rho - \rho^*)\dot{y}. \tag{6.27}$$

We can now use $V = V_1 + V_2$ as a Lyapunov function and obtain

$$\dot{V} \leq \sum_i \left(\frac{dC_i(p_i)}{dp_i} - q_i \right) K \left(-\frac{dC_i(p_i)}{dp_i} + q_i \right).$$

The right-hand side is negative definite, as can be shown from the uniqueness of equilibrium p^* and the discussion in Appendix C in [57]. We thus conclude that p^* is globally asymptotically

stable. □

The passivity framework enables robustness to be directly analyzed in the nonlinear system context. First, consider the disturbances d_1 and d_2 as shown in Figure 6.8. Using the storage functions from Theorems 1 and 2 in [108], the L_p stability (i.e., if d_1 and d_2 are L_p signals, $\left(\int_0^\infty |d_i|^p\, dt\right)^{1/p} < \infty$, then all internal signals within the loop are also L_p, $p \in [1, \infty]$) and robustness with respect to delays (A and A^T in Figure 6.8 replaced by delay operators) can be achieved in a similar way as in [108]. Also without losing passivity from $(q - q^*)$ to $\dot{p}$ in (6.25) and $\dot{y}$ to $(q - q^*)$ in (6.27), generalized primal algorithms can be designed and projection functions can be handled as in [57].

6.6.3 The dual power update algorithm

We now study the associated dual problem (6.18), given by

$$\max_{\mu \geq 0} \sum_{i \in \mathcal{M}} C_i \left((C_i')^{-1}(q_i(\mu)) \right) - q_i(\mu) \cdot (C_i')^{-1}(q_i(\mu)) + \mu^T \beta, \tag{6.28}$$

where q_i is defined as $q_i := \mathrm{row_i}(\mathcal{A}^{\mathrm{T}})\mu$. The dual power update algorithm is:

$$\begin{aligned} &\dot{\mu}_i = \kappa_i (b_i - \mathrm{row_i}(\mathcal{A})\phi(\mu)), \;\; \mathrm{q_i}(\mu) := \mathrm{row_i}(\mathcal{A}^{\mathrm{T}})\mu, \\ &p_i = (C_i')^{-1}(q_i(\mu)), \; i = 1, 2, \ldots, M \; . \end{aligned} \tag{6.29}$$

The dual algorithm presented here is similar to the one in [9, Chapter 3] and is a special case of the dual algorithm originally presented in [11, 12]. In addition, it can be interpreted as a gradient descent algorithm to solve the dual problem (6.29). The next theorem is the counterpart of Theorem 6.2 and states the corresponding results for the dual algorithm.

Theorem 6.4 *The dual power update algorithm (6.29) admits a unique equilibrium that solves the dual system problem. Furthermore, it is globally asymptotically stable.*

Proof. It is straightforward to see that the unique equilibrium of the dual algorithm (6.29) coincides with the one of (6.28). In addition, the matrix $\mathcal{A}$ is full rank under the condition (6.17), and hence, given $\mathbf{q}$ there exists a unique μ such that $\mu = (\mathcal{A}^T)^{-1}\mathbf{q}$. The rest of the proof follows directly from the one of Theorem 3.5 in [9]. For the analysis of stability and robustness of the algorithm within the passivity framework, we refer to [108]. □

The dual algorithm can also be implemented as a distributed power control scheme. As in the case of the primal algorithm, the BS to which the mobile i is connected provides the term q_i, and the mobile determines its power level in accordance with (6.29). Hence, the algorithm (6.29) can be rewritten as

$$\begin{aligned} &\text{BS}: \dot{\mu}_i = \kappa_i(b_i - \mathrm{row_i}(\mathcal{A})\phi(\mu)), \\ &\qquad q_i(\mu) := \mathrm{row_i}(\mathcal{A}^{\mathrm{T}})\mu,\ \mathrm{i} = 1, 2, \ldots, \mathrm{M}\,, \\ &\text{Mobile}: p_i = (C_i')^{-1}(q_i(\mu)),\ i = 1, 2, \ldots, M\ , \end{aligned} \tag{6.30}$$

It is possible to interpret the implementation of the dual algorithm in (6.30) from an economic perspective. As in [12], one can consider the terms q_i as *prices* to be paid by the mobiles for creating interference to other mobiles, and hence utilizing network resources. On the other hand, the dual network problem (6.28) can be interpreted as one of revenue maximization from the perspective of the network operator.

Remark 6.2 *In a multicell network, each BS provides feedback to (regulates) only the mobiles within its own cell and implements the relevant portion of the algorithm described in (6.30). Likewise, the mobiles determine their power levels by taking only the feedback from their own BSs into account. Nevertheless, our interference model takes extracell interference from all of the cells in the network into account in calculating the SIR levels of the mobiles. We will further investigate information flow between the BSs in Section 6.8 and present two schemes to implement the algorithms presented.*

6.7 Principles for Call Admission Control

The capacity of CDMA systems is interference limited. In a CDMA system, the performance for each mobile increases (decreases) as the number of mobiles decreases (increases) [85]. In addition, the requested SIR threshold levels of mobiles, and hence their equilibrium power levels, significantly affect the capacity of a system which utilizes the power control schemes described in this paper. Therefore, a call admission control (CAC) scheme should take into account both the number of mobiles and their target SIR levels. We briefly discuss here some of the main issues for developing CAC schemes in systems implementing primal and dual power update algorithms.

We consider a local CAC scheme where each BS (cell) makes its call admission decisions individually according to a local criterion. In our case, a natural criterion is the set of sufficient conditions (6.17) for the existence of a solution to the system problem. Let δ_l denote the spare capacity in cell l for the incoming (handoff) mobiles from neighboring cells. Since interrupting an ongoing transmission is much less desirable than not admitting a call in the first place, opti-

mization of this value is important. Define the minimum SIR level for transmission as γ_{min}. Then, from (6.17) and given δ_l the maximum number of incoming (handoff) mobiles from neighboring cells, which the BS l can handle, is $N_{handoff} = \lfloor \delta_l (1 + L/\gamma_{min}) \rfloor$, where $\lfloor \cdot \rfloor$ denotes the floor function. On the other hand, a new call requesting an SIR threshold of $\bar{\gamma}_{new}$ is admitted to cell l if the following feasibility condition is satisfied:

$$\bar{\gamma}_{new} < \frac{L}{1 - \delta_l - \sum_{j \in \mathcal{M}_l} \bar{\gamma}_j / (L + \bar{\gamma}_j)}. \tag{6.31}$$

We note that call-blocking probability for new calls (sessions) is inversely proportional to $1 - \delta_l - \sum_{j \in \mathcal{M}_l} \bar{\gamma}_j/(L+\bar{\gamma}_j)$ in cell l. Similarly, call interruption probability is inversely proportional to the values δ_l, $l = 1, 2, \ldots, K$. All of these parameters play a significant role in designing the CAC schemes which may be posed as an optimization problem. The allocation of network resources to mobiles starting a new session and determining pricing schemes for the allocation are additional optimization issues.

6.8 Simulations

We simulate the primal and dual power update schemes in MATLAB. The wireless network is similar to the one in [56] and consists of 4 base stations and 10 mobiles. We consider for clarity of presentation a simple channel fading model based on large-scale path loss. Hence, the channel gain of the i^{th} mobile is determined by $h_i = (0.1/d_i)^2$ where d_i denotes the distance to the BS, and the path loss exponent is chosen as 2 corresponding to open air path loss. The system parameters are chosen as $L = 64$ and $\sigma_l^2 = 0.1$ for all cells. The mobiles are distributed randomly over the network. Figure 6.9 depicts the locations of the BSs and the mobiles. In order to calculate the q vector for both the primal and the dual algorithms, each BS has to communicate with other BSs the value of the $\mathcal{A}$ matrix and μ or ρ vectors. Clearly, this "full information" case brings an additional communication overhead to the system. In order to circumvent this problem we propose a "low-overhead information" scheme where q is calculated at each BS using only the $\mathcal{A}_l$ matrix and the vector μ (or ρ) which contains only information on mobiles connected to that BS. Using this "approximate" information is justified due to the fact that the channel gain between the BS and other mobiles is much smaller. Hence, the remaining terms which require information exchange with neighboring BSs can be ignored in calculating the q values for mobiles in the BS. We note that better approximations can be achieved if a BS communicates with its immediate neighbors and ignores more distant ones.

We first simulate the *primal power update* algorithm (6.24) in the full information case. The

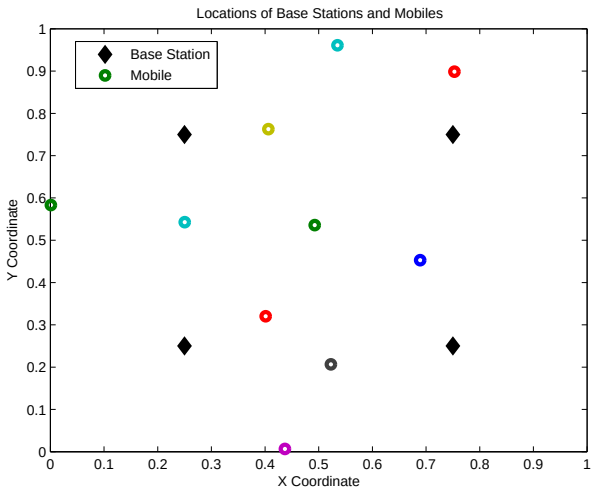

Figure 6.9: Locations of base stations and mobiles.

penalty function (6.21) for mobile i is chosen to be $\rho_i = 1000(b_i - (\mathcal{A}\phi)_i)^4$ if $b_i > (\mathcal{A}\phi)_i$ and zero otherwise.The fixed step-size of the update algorithm is $\kappa_i = 0.2$. The cost function of the i^{th} mobile is the difference between its cost on battery usage (which is quadratic and proportional to the channel gain of the mobile, since distant mobiles (to the BS) need higher transmission powers) and a logarithmic function of its transmission power level: $C_i(p_i) = 5 \cdot 10^{-3} h_i p_i^2 - 10^{-4} \log(p_i)$. We arbitrarily define the target SIR levels of half of the mobiles as 10 dB and of the other half as 7 dB. The power levels and SIR values of mobiles for the duration of the simulation are shown in Figures 6.10(a) and 6.10(b), respectively. We observe that the power levels converge to their respective equilibrium points and the SIR values are slightly higher than the target values. This is due to the logarithmic terms in the cost functions of the mobiles representing the willingness to achieve higher than target SIR levels by increasing the transmission power as long as all users reach their target SIR levels. Note that, if these additional terms are not part of the cost functions as it is the case in [61], then we observe that the final SIR values of mobiles are very close to their respective target levels.

Next, we simulate the *dual power update* algorithm (6.29) using both the full and low-overhead information schemes. Here, the cost function on the i^{th} mobile's battery usage is given by $C_i(p_i) = h_i p_i^2 - \log(p_i)$. Figures 6.11(a) and (b) depict the power and SIR values of mobiles for the full information case. We observe that the power levels here converge faster than the ones in the primal algorithm. The difference in the equilibrium power levels of dual and primal algorithms is due to the difference in the cost parameter. Finally, the dual algorithm is simulated using the low-overhead information scheme. From Figures 6.12(a) and 6.12(b) we conclude that the results are similar to those in the full information case.

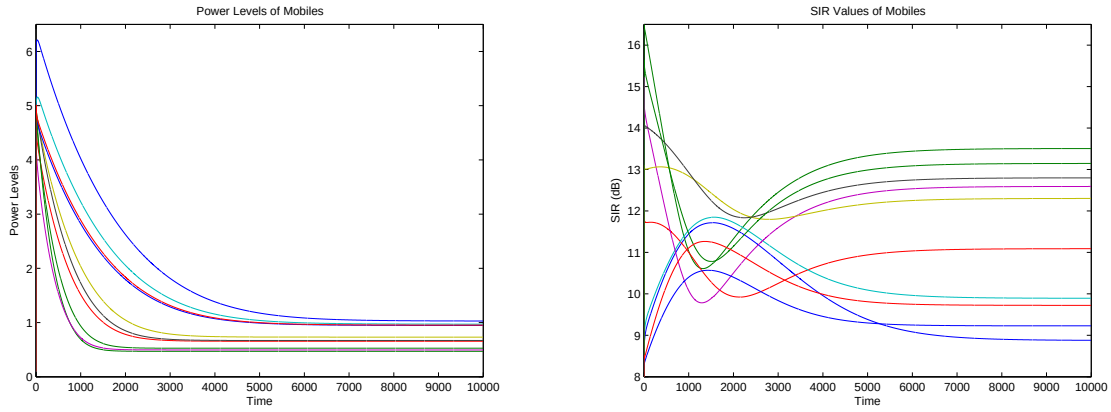

(a) (b)

Figure 6.10: (a) Power levels of mobiles with respect to time. (b) SIR values of mobiles (in dB) with respect to time.

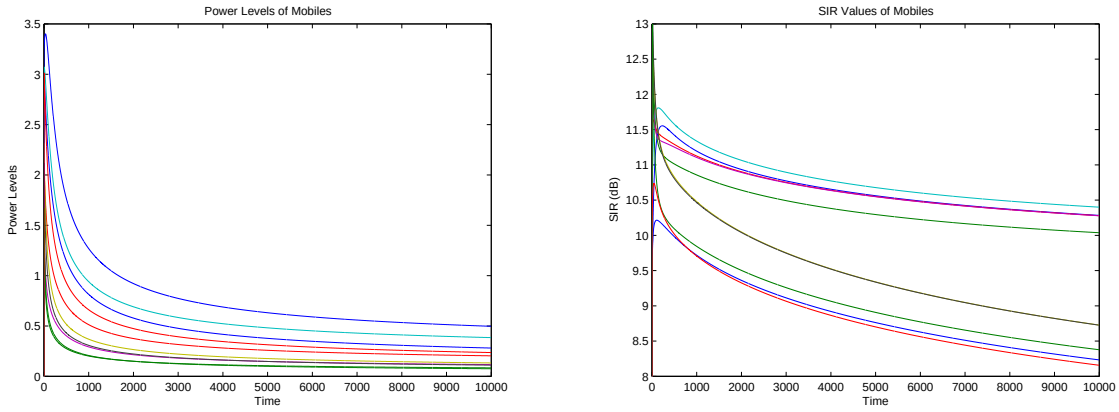

(a) (b)

Figure 6.11: (a) Power levels of mobiles with respect to time (full information). (b) SIR values of mobiles (in dB) with respect to time (full information).

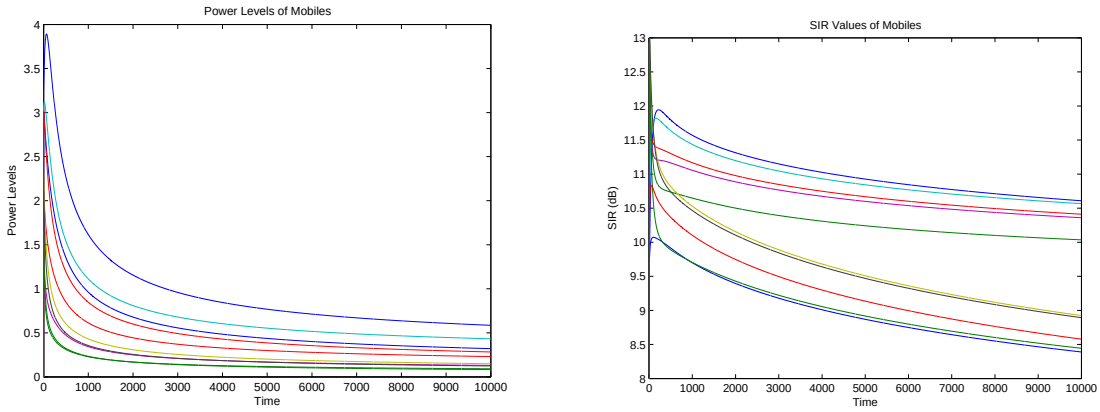

(a) (b)

Figure 6.12: (a) Power levels of mobiles with respect to time (approximate information). (b) SIR values of mobiles (in dB) with respect to time (approximate information).

6.9 Conclusions

In the first half of this chapter, we have studied a hybrid noncooperative game motivated by the practical problem of joint power control and BS assignment in CDMA wireless data networks, and have extended the noncooperative game theoretic approach presented in previous chapters. We have investigated the existence and uniqueness of pure NE solutions numerically using randomized algorithms, where we have utilized both gridding techniques and random sampling. We have also simulated a dynamic BS assignment and power update scheme. Simulation results show that the power levels and SIR values of the users converge to their respective equilibrium points. Furthermore, the hybrid power control game has a distinct advantage over "classical" noncooperative power control algorithms in terms aggregate SIR levels obtained by all users (for most parameter values and configurations). A possible extension of the results in this section would involve analytical and further numerical investigation of NE properties as well as convergence characteristics of the joint power update and BS assignment scheme.

In the second half of the chapter, we have defined power control in multicell CDMA wireless networks as a team optimization problem, which admits a unique optimum solution under certain conditions. Using a Lagrangian relaxation approach similar to [11, 12] we have obtained two decentralized dynamic power control algorithms: primal and dual power update, and have established their global stability utilizing both classical Lyapunov theory and the passivity framework [57]. Furthermore, we have discussed briefly some of the basic principles of call admission control from the perspective of this paper. Finally, the power control schemes proposed are implemented and studied numerically through MATLAB simulations.

CHAPTER 7

A GAME THEORETIC APPROACH TO DECISION AND ANALYSIS IN NETWORK INTRUSION DETECTION

In this chapter we investigate the basic decision and analysis processes involved in information security and intrusion detection, as well as possible usage of game theory for developing a formal decision and control framework. We develop a generic model for distributed IDSs by defining a network of sensors, and propose two simple, flexible, and easy-to-implement schemes utilizing both cooperative and noncooperative game theoretic concepts [1, 78]. In Section 7.1, common trade-offs in information security, attack detection techniques, and application of game theory to intrusion detection are investigated. We introduce a game theoretic framework for distributed IDSs and two schemes making use of game theoretic concepts in Section 7.2, which is followed by the concluding remarks of Section 7.5.

7.1 Decision and Analysis Process in an Intrusion Detection System

Intrusion detection includes monitoring, analysis, and response processes of intrusion events occurring in a networked system. Intrusions can be described as the compromise of the confidentiality, integrity, and availability of the system [67]. Detection and analysis of intrusions is followed by the response, which can vary from a simple alarm to alert the administrator to automatic reconfiguration of the system to prevent further damage. The analysis, detection, and response actions in an IDS can be investigated as a decision and control paradigm. Game theory provides a suitable framework and the much needed formal decision and control mechanisms for modeling and development of these processes. In addition, a related topic of interest is the organization and representation of IDS data (e.g. attack signatures, detection rules, preferences of the network owner, etc.), which plays a crucial role in the operation of an IDS.

7.1.1 Trade-offs in network security

There are several common trade-offs in designing a security system whether it is a simple mechanical door-lock protecting a house or a large-scale distributed IDS. A basic trade-off is the one between security risk and ease of access: The more a system is protected by security mechanisms the more difficult it becomes to access it, hence less convenient, and vice versa. A simple real-life example is keeping a frequently used door locked against intruders versus leaving it unlocked as a security hole. Similarly, in the context of computer networks, users want to access data easily and instantly while expecting the sensitive data to be protected from unauthorized access. Obviously, achieving the latter requires sacrificing some of the convenience of the former by deploying and maintaining authentication and security mechanisms between the user and the sensitive data. A related trade-off is the overhead caused by the IDS or by other security systems like firewalls to the networked system. Deploying intrusion-detection mechanisms like packet filters, log analyzers, etc. have a cost in terms of system resources (bandwidth, memory, CPU time). Figure 7.1 depicts these trade-offs in graphic form.

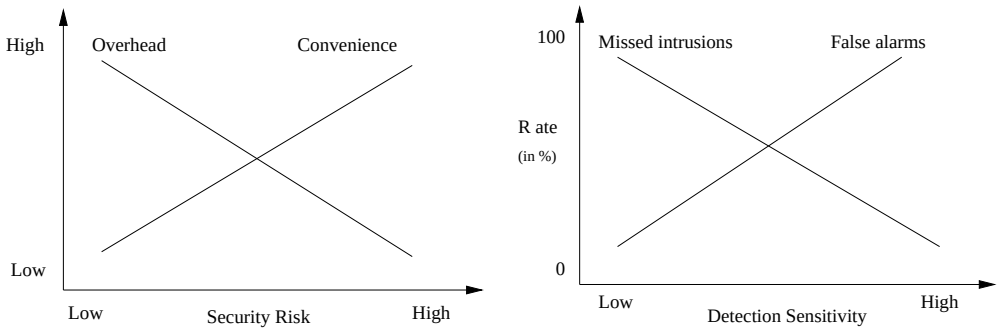

Figure 7.1: A visualization of basic trade-offs in network security.

A basic performance criterion for any intrusion detection system is the false alarm rate. There exists a trade-off between the reduction in the false alarm rate by decreasing the system sensitivity and the increase in the rate of undetected intrusions (see Figure 7.1). Clearly, on either extreme the IDS becomes totally ineffective. Therefore, the IDS should satisfy some upper and lower bounds on false alarm rate and undetected intrusions according to the specifications of the deployed network. Finally, in distributed IDSs with software agents there exists the question of how autonomous the agents should be. The robustness of a completely decentralized decision process has to be weighed against the communication overhead between the agents and the processing overhead of individual agent programs.

All these trade-offs, among others, have to be taken into account in the design and deployment of an IDS. Furthermore, the decision and analysis mechanisms of the IDS should be scalable and flexible enough to allow configuration for the specific network at hand.

7.1.2 Detection of security attacks

Several different approaches have been proposed for detecting intrusions. A currently widely used method is to check monitored events (packets in the network, log files, etc.) against a known list of security attack (exploit) signatures. This approach has the advantage of enjoying a relatively small false alarm rate and ease of implementation. The disadvantages are the need to maintain and update the attack signature database, and the restriction to detection of only the known attacks documented in the database. Recent studies [68, 109] have proposed attack trees and profiles as a means to characterize network security attacks in a structured and reusable form. These information structures are also useful in detecting more organized multistep attacks.

An alternative approach is the *anomaly detection*, where changes in the patterns of nominal usage or behavior of the system are detected [71]. Although this approach increases the probability of detecting undocumented new attacks it is difficult to implement, and has often a higher false alarm rate. Among various schemes proposed for anomaly detection are the ones mimicking immune-systems, which have recently been a topic of interest [110, 111].

In either approaches, IDS relies on an established information base to detect attacks or distinguish anomalies, which may be security breaches. Therefore, successful design, operation, and maintenance of a database containing attack signature data and nominal operating characteristics of the networked system is crucial for an efficient operation of the IDS.

7.1.3 Application of game theory to intrusion detection

Each of the basic network trade-offs mentioned in the Sections 7.1.1 can be posed as resource-allocation problems. It is difficult, however, to quantify and solve these problems using classical optimization methods. Another issue is the interpretation of the incoming data from various detection mechanisms in the network. A significant shortcoming of the current IDSs is the lack of a unifying mathematical framework to put the pieces into a perspective. Game theory can provide a basis for development of formal decision and control mechanisms for intrusion detection as depicted in Figure 7.2. Specifically, game theoretic models can be used to address issues like the following:

- Interpreting and efficiently using huge amounts of input data from various detection mechanisms containing a significant percentage of false alarms.
- Modeling and estimating the real intent and the target of an attacker in a large system by using additional information like context, history, etc.
- Reconfiguring the security system given the severity of attacks and making decisions on

trade-offs like increasing security versus increasing system overhead or decreasing efficiency.

- Deciding on where to allocate or reallocate limited resources in real time to detect significant threats to vital subsystems in a large networked system.
- Analyzing of and modeling the interaction between different types of detection schemes.
- Modeling, developing, and analyzing distributed decision and control schemes using autonomous software agents.

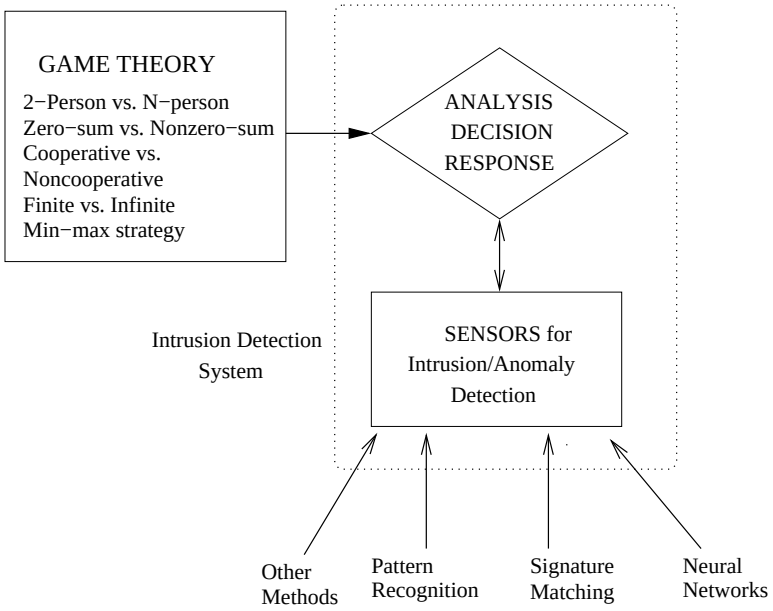

Figure 7.2: The role of game theory in intrusion detection.

Min-max optimization, dynamic noncooperative games, and cooperative games are applicable to resource allocation and risk management problems mentioned above. Furthermore, N-player (non)cooperative game theory can also be used to model, develop, and organize software agents as a scalable, distributed decision and control system for intrusion detection.

7.2 A Game Theoretic Framework

We construct two game theoretic schemes to address some of the issues in Section 7.1. While the foremost goal of the first scheme is simplicity and ease-of-implementation, the second scheme models and analyzes attacker and IDS behavior within a two-person, non-zero-sum, noncooperative game framework. We also note that both schemes are flexible and can be implemented regardless of the underlying architecture.

7.2.1 The model

We consider a distributed IDS with a network of sensors, $\mathcal{S} := \{s_1, s_2, \ldots, s_{max}\}$, which we call as a *virtual sensor network* in order to distinguish it from physical sensor networks.[1] A *virtual* sensor is defined as an autonomous software agent that monitors the system and collects data for detection purposes [112]. These sensors report possible intrusions or anomalies occurring in a subsystem of a large network using a specific technique like signature comparison, pattern detection, statistical analysis, etc. The system monitored by the IDS can be represented as a set of subsystems, $\mathcal{T} = \{t_1, t_2, \ldots, t_{max}\}$, which may be targeted by an attacker. We note that these subsystems could be actual computer programs or parts of the network, as well as abstract processes distributed over multiple hosts. Define $\mathcal{I} = \{I_1, I_2, \ldots, I_{max}\}$ as the set of documented threats and detectable anomalies, which may indicate a possible intrusion, as well as various types of possible attacks. Let us associate in this context the generic term "attack" with two specific attributes: target subsystem $t \in \mathcal{T}$ and threat or anomaly type $I \in \mathcal{I}$. We hence define the set of attacks $\mathcal{A} = \{a_1, a_2, \ldots, a_{t_{max} \times I_{max}}\}$ as the cross-product of the sets $\mathcal{I}$ and $\mathcal{T}$, $\mathcal{A} := \mathcal{T} \times \mathcal{I}$.

Next, let the linear mapping $\mathcal{D}_{\mathcal{A}} : \mathcal{S} \rightarrow \mathcal{A}$ describe the relationship between the sensors and attacks through the system matrix

$$D_{i,j} = \begin{cases} 1, & \text{if sensor } j \text{ is able to detect attack } i \\ 0, & \text{if sensor } j \text{ is not able to detect attack } i \end{cases}, \tag{7.1}$$

where $i \in \mathcal{A}$ and $j \in \mathcal{S}$. Finally, it is straightforward to associate real values with the output of sensors and construct a real-valued sensor output vector $\mathbf{d} := [d_1, d_2, \ldots, d_{max}]$. Thus, we obtain a quantitative threat value for each attack in $\mathcal{A}$: $\mathbf{a} = D \cdot \mathbf{d}$, where $\mathbf{a} := [a_1, a_2, \ldots, a_{t_{max} \times I_{max}}]$ is a real-valued attack vector. Notice that, due to the limitations of the sensor grid, the attack vector can reflect only an imperfect and partial profile of a real attack.

Finally, we define the system matrix A describing the relationship between the sensor output vector and subsystems as

$$A_{i,j} = \begin{cases} 1, & \text{if sensor j monitors subsystem i} \\ 0, & \text{if sensor j does not monitor subsystem i} \end{cases},$$

where $i \in \mathcal{T}$ and $j \in \mathcal{S}$.

[1] We will drop the adjective *virtual* in the rest of the study to simplify the terminology. For further information on "virtual" sensors we refer to [112].

7.2.2 The security warning system for distributed IDS

A large number of false-alarms is a considerable problem in the world of IDS deployment [68], which can be overwhelming for system administrators. It also increases the difficulty in managing an IDS significantly. There is no immediate solution to the false-alarm problem at the sensor level. Hence, a new approach is needed for interpreting sensor data. We devise an easy-to-implement yet flexible scheme using intrusion warning levels. The security warning system enables IDS to operate in different modes at each security level, and to switch automatically between the different levels. In addition, it provides the administrator an intuitive overview of the current security situation in the network.

We make use of the model introduced in Section 7.2.1. Define $f : \mathcal{I} \cup \{0\} \Rightarrow \mathbb{R}^+ \cup \{0\}$ as a one-to-one function assigning a positive real number to each element of $\mathcal{I}$ and $f(0) = 0$. Hence, each documented intrusion signature and anomaly is associated with a so-called "security risk value" quantified with a positive real number $f(I)$. The function f can also be defined in such a way that it assigns security risk values to function classes $\mathcal{F}$ instead of individual elements of $\mathcal{I}$. The security warning system is based on the concept of *security level*, $\mathcal{L}$. We define L security levels, $\{l_1, \ldots, l_L\}$, with $0 < m_1 < m_2 < \ldots < m_L$ being the corresponding threshold values. Given the sensor output vector $\mathbf{d}$, the security level, $\mathcal{L}$, of the IDS is equal to l if the sum of the security risk values of detected intrusions falls in the interval $[m_l, m_{l+1}]$:

$$\mathcal{L} = \begin{cases} l_1, & \text{if } \sum_{i=1}^{N} f(d_i) < m_1 \\ l_j, & \text{if } m_{j-1} \leq \sum_{i=1}^{N} f(d_i) < m_j \\ l_L, & \text{if } \sum_{i=1}^{N} f(d_i) \geq m_L. \end{cases}$$

Thresholds and security risk values can be assigned and fine tuned according to previous experience and specifications of the network. It is also possible to use learning-based techniques to obtain these values if there is a sufficient amount of prior data on the specific system.

Cooperative game theory provides a suitable framework for the design and analysis of the proposed security warning scheme. The sensor output $\mathbf{d}$ can be modeled as an *N-person game* with $\mathcal{N} := \{1, 2, \ldots, N\}$ being the set of *players*, and each subset $\mathcal{D} \subset N$, where $d_i \neq 0 \; \forall i \in \mathcal{D}$ is called a *coalition* [78, p. 213]. Thus, each such subset of $\mathcal{N}$ (*coalition*) represents an observed threat pattern. The aggregate value of the coalition is defined as the sum of the security risk values of the detected threats, $\sum_{j \in \mathcal{D}} f(d_j)$. The security level thresholds m determine whether the IDS security level $\mathcal{L}$ changes or not.

In order to analyze the relative importance of each sensor output, which indicates an intrusion threat, with respect to others and the effect of the threshold values on security levels,

we make use of a power index called *Shapley value* [78]. The Shapley value approach has been utilized in multiagent coalitions in earlier studies [113], albeit in different contexts. Let $f(C) := \sum_{i \in C} f(d_i),\ d_i \in \mathcal{I},\ C \subset \mathcal{N}$ be the value of the *coalition* C with cardinality c. Then, the Shapley value of the i^{th} element of the sensor output vector is defined by

$$\begin{aligned} \phi(i) &:= \sum_{C \subset \mathcal{N}} \frac{(c-1)!(N-1)!}{N!}[f(C) - f(C - \{i\})] \\ \Rightarrow \phi(i) &:= \sum_{C \subset \mathcal{N}} \frac{(c-1)!(N-1)!}{N!} f(i). \end{aligned} \tag{7.2}$$

In determining the effect of the i^{th} sensor output on the k^{th} warning level, however, the formula simplifies to

$$\phi(i) := \sum_{\tilde{C} \subset \mathcal{N}} \frac{(c-1)!(N-1)!}{N!}, \tag{7.3}$$

where $\tilde{C}$ denotes the "winning" coalitions with $\sum_{i \in \tilde{C}} f(d_i) > m_k$. In this case, the game is said to be *simple*. Notice that the computational complexity of Shapley value is of $o(2^N)$. Therefore, it becomes impractical to calculate the exact value for large N. Instead, we make use of multilinear extensions to approximate the Shapley value as N gets large [78, p. 296]. Since this approximation is based on the law of large numbers, it becomes more accurate as $N \to \infty$.

The Shapley value of the i^{th} sensor output indicates the relative security risk value for a given threshold (of a warning level). It hence plays an important role in the analysis and fine tuning of the warning system for the specific network to be deployed by providing a guideline for choosing security risk values, $f(.)$, and thresholds of the levels m. In the security warning system, each level can be associated with a different operation mode where agents and control mechanisms of IDS behave accordingly. The sensitivity of the agents and security measures in the network (e.g., firewall configurations, authentication mechanisms) are increased with the increasing security level. Therefore, the security-warning scheme addresses the problem of optimizing some of the network security trade-offs discussed in Section 7.1.1. A specific alert mechanism and a user interface can also be incorporated into this scheme to inform administrators. A simplified flow chart depicting principles of the security warning algorithm is given in Figure 7.3.

An illustrative example: Consider a three level security warning system consisting of *green*, *yellow*, and *red* levels with thresholds $m_{yellow} = 35$ and $m_{red} = 100$. The set of known intrusions (and anomalies) $\mathcal{I}$ is chosen to be small for illustrative purposes, and the corresponding risk values are $\{10, 20, 30, 40, 90\}$. Based on the sensor configuration, the sensor output vector is $\mathbf{d} = [10, 10, 10, 20, 20, 30, 30, 30, 40, 40, 90, 90]$. In order for the system to switch to yellow

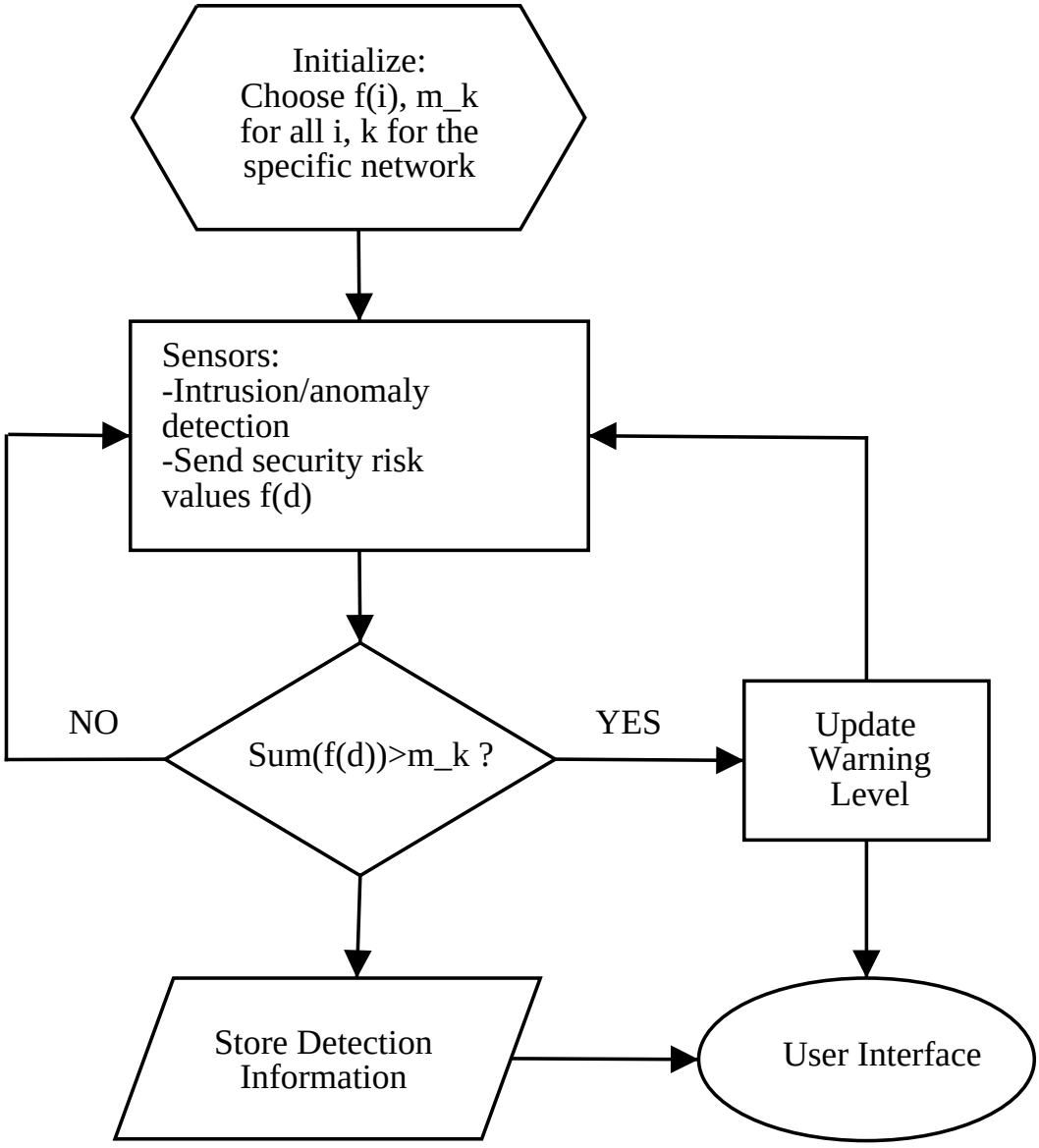

Figure 7.3: A simplified algorithm for the security warning system.

(respectively, red) , sum of the values of observed intrusions within a predefined time interval has to exceed the threshold 35 (respectively, 100). Since cardinality of $\mathbf{d}$ is small, the Shapley values can be calculated exactly using the formula in (7.3). As observed in Figure 7.4, the Shapley values of intrusions with high security risk values are larger for the red threshold than the ones for the yellow threshold. This indicates that intrusions with high values play a more significant role than others for switching to the red level.

We next increase the cardinality of $\mathbf{d}$ to 60, and thresholds for yellow and red levels to 40 and 1000, respectively. In this case, Shapley values are calculated approximately as exact calculation takes excessive amount of time. The results are similar to previous ones, and shown in Figure 7.5.

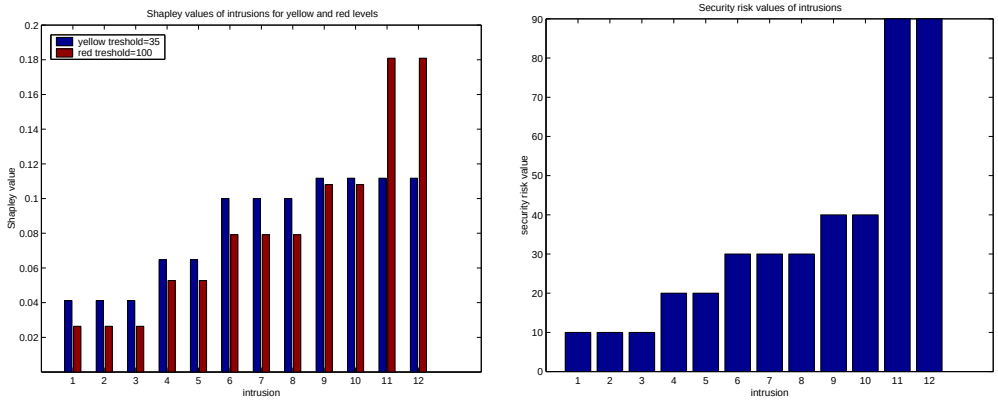

(a) (b)

Figure 7.4: (a) Shapley values for yellow and red levels, and (b) security risk values are shown for the sensor output vector $\mathbf{d}$ with 12 elements.

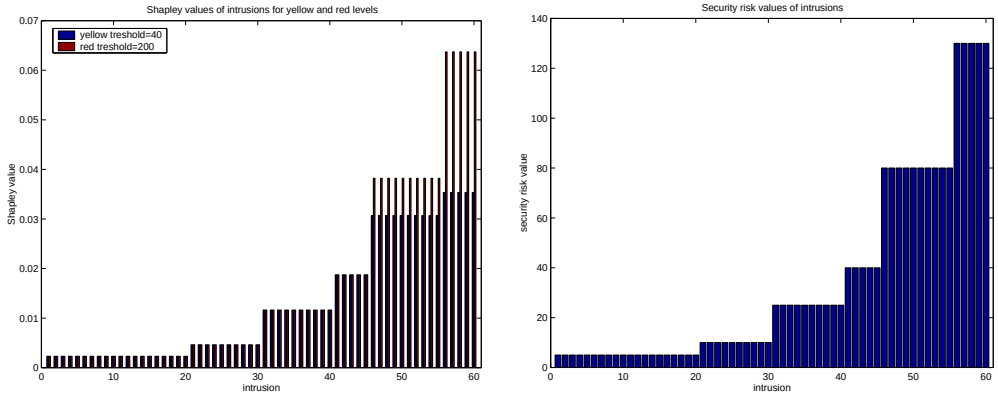

(a) (b)

Figure 7.5: (a) Shapley values for yellow and red levels, and (b) security risk values are shown for the sensor output vector $\mathbf{d}$ with 60 elements.

7.2.3 Game theoretic modeling of security attacks

Today's intrusion detection architecture is a passive information processing paradigm [68]. However, with the security attacks becoming more frequent and sophisticated, IDSs fail to distinguish the real intent and target of attackers. In order to accurately identify the target of an attack, IDS should be able to process the attack information within a context. Deploying a network of sensors in the system, and through game-theoretic analysis of the sensor output data, one can model an attacker's behavior, intent, and target. Furthermore, due to the flexibility of the model in Section 7.2.1 it is possible to capture not only attacks targeting specific portions of the network but also abstract targets such as processes distributed over multiple physical subsystems. In addition to modeling an attacker's behavior and intent, the game theoretic framework may also be used to analyze and model the IDS's response process by taking the basic security trade-offs in Section 7.1.1 into account. The IDS response actions vary from setting a simple alarm to a costly system reconfiguration, which may involve shutting down some relatively less important services in the system.

We model the interaction between the attacker and the IDS as a two-person, non-zero-sum, single act, finite game with dynamic information. Given the sensor output vector $\mathbf{d}$, we obtain for each subsystem $t \in \mathcal{T}$ a threat level, y_t, using the system matrix A. Hence, we define the threat level vector as

$$\mathbf{y} := A\,\mathbf{d}.$$

The elements of $\mathcal{T}$ (the set of subsystems) are then grouped into nonoverlapping information sets according to their respective threat levels in $\mathbf{y}$. To simplify the analysis, we assume that the attacker targets only a single subsystem. Hence, the actions available to the attacker in each information set is to attack a single subsystem in the set or do nothing, which indicates a false alarm in related sensors. We also limit the actions of the IDS to set an alarm for one target in the information set or do nothing. Since the IDS can distinguish between information sets but not actions within them, it is called a *dynamic information game*. Figure 7.6 depicts a sample security game, where $t1, t2$, and $t3$ denote the attacker's actions of targeting subsystems 1 to 3; $nt1$ and $nt2$ indicate false alarms (attacker doing nothing); $a1, a2$, and $a3$ represent the IDS's alarms for respective subsystems; and $na1$ and $na2$ denote the IDS choosing not to set an alarm.

We investigate the security game in Figure 7.6 recursively. Information set 1 is the simplest case, where the attacker either targets subsystem one ($t1$) or does nothing (nt) equivalent to a false alarm. The set of actions of the IDS are either to set the alarm for subsystem one ($a1$) or do nothing

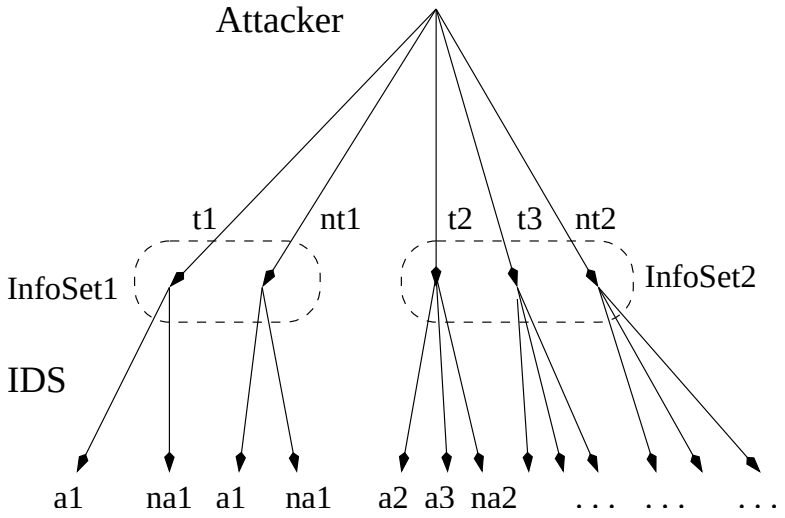

Figure 7.6: A simple security game with three subsystems and two information sets.

($na1$). This portion of the game can be represented by the following 2×2 bimatrix game

$$M_{att} := \begin{array}{|c|c|c|} \hline t1 & \beta_h & -\beta_s \\ \hline nt1 & 0 & 0 \\ \hline & a1 & na1 \\ \hline \end{array} \qquad M_{ids} := \begin{array}{|c|c|c|} \hline t1 & -\alpha_h & \alpha_m \\ \hline nt1 & \alpha_f & 0 \\ \hline & a1 & na1 \\ \hline \end{array} \tag{7.4}$$

where the entries of M_{ids} (M_{att}) represent the cost values, and columns (rows) correspond to the strategy spaces of the IDS and the attacker, respectively. The value $-\alpha_h$ is the gain of the IDS for detecting the target. On the other hand, α_f and α_m are the IDS's costs for false alarm and missing the attack, respectively. The cost β_h represents the detection penalty for the attacker whereas $-\beta_s$ represents the gain from an undetected intrusion. Notice that, although missing an attack is associated with a cost for the IDS, false alarms cost nothing to the attacker. The parameters α and β are always positive unless otherwise stated.

The *min-max* or *security strategy* of a player [1] guarantees a maximum cost, or so called *security level* regardless of the strategy of the opponent. Due to the detection cost of and attack, $\beta_h > 0$, the attacker's security strategy is not to attack at all (nt), which guarantees an upper bound on the cost of zero. The IDS's security strategy, however, depends on the relative values of α_f and α_m, false alarm and missing (an attack) costs. If $\alpha_f > \alpha_m$ then the IDS chooses not to alarm at all (na), and if $\alpha_f < \alpha_m$ then the IDS always sets on the alarm (a1). We note that the security strategies are extremely conservative in this setting, and give little insight into the dynamics of the game.

We next investigate the existence of an NE in the matrix game (7.4). Clearly, there is no NE in pure strategies. Therefore, we extend the analysis by considering mixed strategies of players

defined as probability distributions on the space of their pure strategies [1, p.23]. Let p_1 and $1-p_1$ be the probabilities for strategies $(t1)$ and (nt) of the attacker, respectively. Also let q_1 and $1-q_1$ be the probabilities for strategies $(a1)$ and (na) of the IDS. The pair (p^*, q^*) is said to constitute a noncooperative NE solution to the bimatrix game (M_{att}, M_{ids}) if the following inequalities are satisfied:

$$\begin{aligned} p_1^*(\beta_h q_1^* - \beta_s(1-q_1^*)) \leq p_1(\beta_h q_1^* - \beta_s(1-q_1^*)), \quad 0 \leq p_1 \leq 1 \\ p_1^*\alpha_m + q_1^*[\alpha_f - (\alpha_f + \alpha_h + \alpha_m)p^*] \leq \\ p_1^*\alpha_m + q_1[\alpha_f - (\alpha_f + \alpha_h + \alpha_m)p^*], \quad 0 \leq q_1 \leq 1, \end{aligned} \tag{7.5}$$

where $0 \leq p_1,\, q_1 \leq 1$. The only solution to the set of inequalities in (7.5) constitutes the unique NE of the game, and is given by

$$p_1^* = \frac{\alpha_f}{\alpha_f + \alpha_h + \alpha_m}, \text{ and } q_1^* = \frac{\beta_s}{\beta_h + \beta_s}. \tag{7.6}$$

Note in (7.6) an interesting, and rather counterintuitive, feature of NE solution in mixed strategies. While computing his mixed NE strategy, each player pays attention only to the average cost function of his coplayer, rather than optimizing his own average cost function. Hence, the nature of the optimization (i.e., minimization or maximization) becomes irrelevant in this case [1, p. 86]. The equilibrium costs of the attacker V_{att}^* and the IDS V_{ids}^* for this subgame are given by

$$V_{att}^* := [p_1^*\ (1-p_1^*)]M_{att}[q_1^*\ (1-q_1^*)]^T, \text{and } V_{ids}^* := [p_1^*\ (1-p_1^*)]M_{ids}[q_1^*\ (1-q_1^*)]^T.$$

In the context of intrusion detection, we interpret the NE (7.6) in the following way: The probability of attacker targeting subsystem one y_1^* at NE point decreases with decreasing α_f since the smaller the false alarm cost for the IDS, the more it is inclined to set an alarm and catch the attacker. One can argue that this can be achieved by setting the alarm very frequently as in the case with current IDSs. However, there are *hidden costs* with this approach like rendering the IDS practically useless under a flood of false alarms. Similarly, an increase in α_h and α_m play a deterrent role for the attacker. On the other hand, the probability of the IDS setting an alarm is affected by the gain of attacker from a successful intrusion, $-\beta_s$. If $\beta_s \gg \beta_h$, then the IDS is inclined to set the alarm more frequently. The penalty for the attacker of getting detected may vary significantly depending on the physical reachability of the attacker. If, for example, the attacker is employed by the same organization he or she tries to intrude, then β_h is much larger than the marginal detection cost of a script-based attack from the other side of the globe.

The parametric analysis is repeated for information set 2 in Figure 7.6. In order to simplify the analysis we associate the same costs with subsystems two and three. This game can also be

represented as a 3×3 bimatrix game given by

$$M_{att} := \begin{array}{|c|c|c|c|} \hline t2 & \beta_h & -\beta_d & -\beta_s \\ \hline t3 & -\beta_d & -\beta_h & -\beta_s \\ \hline nt2 & 0 & 0 & 0 \\ \hline & a2 & a3 & na2 \\ \hline \end{array}$$

$$M_{ids} := \begin{array}{|c|c|c|c|} \hline t2 & -\alpha_h & \alpha_d & \alpha_m \\ \hline t3 & \alpha_d & -\alpha_h & \alpha_m \\ \hline nt2 & \alpha_f & \alpha_f & 0 \\ \hline & a2 & a3 & na2 \\ \hline \end{array} \tag{7.7}$$

where α_d (β_d) is the cost (gain) of a deception for the IDS and the attacker, respectively. One can assume that $\alpha_d > \alpha_m$ and $\beta_d > \beta_s$ as alarming a wrong subsystem is more costly for the IDS than a missed attack, and by deceiving the IDS the attacker circumvents security mechanisms of the system more successfully. Let $\bar{p}_1$, $\bar{p}_2$, and $1 - \bar{p}_1 - \bar{p}_2$ be the probabilities for strategies ($t2$), ($t3$), and ($nt2$) of the attacker. Also let $\bar{q}_1$, $\bar{q}_2$, and $1 - \bar{q}_1 - \bar{q}_2$ be the respective probabilities for strategies ($a1$), ($a2$), and ($na2$) of the IDS. The security strategy of the IDS is determined by the relative values of α_d, α_f, and α_m as in the previous case. Furthermore, there is again no NE in pure strategies. The unique NE solution in mixed strategies is obtained by solving the counterpart of the set of inequalities (7.6), and is given by

$$\bar{p}_1^* = \bar{p}_2^* = \frac{\alpha_f}{2\alpha_f + 2\alpha_m + \alpha_h - \alpha_d}, \text{and} \quad \bar{q}_1^* = \bar{q}_2^* = \frac{\beta_s}{2\beta_s + \beta_h - \beta_d}, \tag{7.8}$$

if $\beta_d < \beta_h$ and $\alpha_d < 2\alpha_m + \alpha_h$. Notice that the attack and alarm probabilities for each subsystem is the same due to the same cost structure imposed on them. In fact, it is possible to adjust the cost parameters by taking into account various factors like relative importance of a subsystem for the organization, threat levels given the output of sensors, etc. The equilibrium probabilities of the attacker and the IDS strategies have a similar interpretation as the ones in the previous analysis. The increasing cost of deception for the IDS, however, has an encouraging effect on the attacker.

Given the equilibrium solutions and costs of each bimatrix game, the IDS and the attacker determine their overall strategies. The equilibrium strategy of the IDS, γ_{ids}^*, for example, is given

by

$$\gamma^*_{ids} = \begin{cases} a1 \text{ w.p. } q^*_1 \\ na1 \text{ w.p. } 1 - q^*_1 \end{cases}, \quad \text{if attacker chooses actions in InfoSet1}$$

$$\begin{cases} a2 \text{ w.p. } \bar{q}^*_1 \\ a3 \text{ w.p. } \bar{q}^*_2 \\ na1 \text{ w.p. } 1 - \bar{q}^*_1 - \bar{q}^*_1 \end{cases}, \quad \text{if Attacker chooses actions in InfoSet2}$$

On the other hand, the equilibrium strategy of the attacker depends on the equilibrium costs of the matrix games, V^*_{att} and $\bar{V}^*_{att}$.

The analytical investigation of the security game brings valuable insight to the attacker and the IDS behavior. In addition, the simplifying assumptions we have made in order to obtain analytical results can easily be extended to capture more realistic scenarios. Thus, the sample game of Figure 7.6 can be made arbitrarily large. Although increasing complexity prevents derivation of a closed form solution, one can easily solve such games numerically. Thus the developed framework can easily be applied to practical cases.

A numerical example: We solve a numerical example using the GAMBIT game theory analysis tool [114] to demonstrate the results in Section 7.2.3. Figure 7.7 shows the example security game in extensive form. For illustrative purposes, the action spaces of the players are again limited, and the cost parameters are chosen as shown in Table 7.1.

Table 7.1: Parameters of the numerical example.

$Parameter$	α_h	α_d	α_m	α_f	β_h	β_s	β_d
$Value$	7	10	8	9	6	4	5

In this game, there is no NE solution in pure strategies. In order to investigate NE in mixed and behavioral strategies, we associate the probability vector $\mathbf{p}$ with actions [$(t1)$ $(t2)$ $(t3)$ $(nt1)$ $(nt2)$] of the attacker and the vector $\mathbf{q}$ with actions [$(a1)$ $(a2)$ $(a3)$ $(na1)$ $(na2)$] of the IDS. We obtain two NE points in behavioral strategies, which are in accordance with Equations (7.6) and (7.8):

$$(\mathbf{p}^*_1, \mathbf{q}^*_1) = ([0\ 0.29\ 0.29\ 0\ 0.42], [0\ 0.44\ 0.44\ 0\ 0.11])$$
$$(\mathbf{p}^*_2, \mathbf{q}^*_2) = ([0.38\ 0\ 0\ 0.63\ 0], [0.40\ 0\ 0\ 0.60\ 0])$$

In both cases, the equilibrium cost for the attacker is zero, $V^*_{att} = 0$. Hence, choosing either of the equilibrium strategies is equivalent for the attacker.

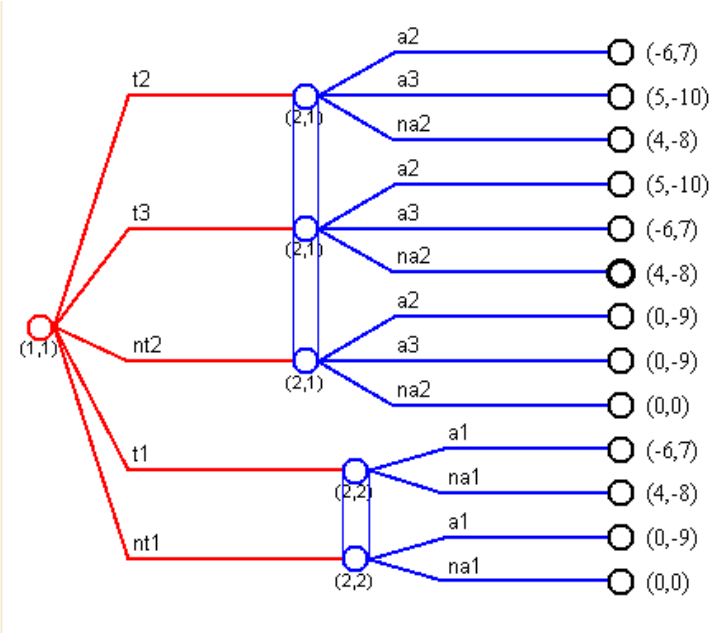

Figure 7.7: A security game example with negative costs and gains.

Finally, we investigate the NEs of the security game in mixed strategies by converting it to the normal form. Solving the resulting matrix game with GAMBIT, we obtain 18 different NE points in mixed strategies. Two of these coincide with the NE solutions in behavioral strategies as expected [1, p. 103]. Thus, the NE points in behavioral strategies characterize the behavior of the players more clearly, and provide more insight to the underlying system dynamics.

7.3 The Network Security Game

We investigate the interaction between the attacker(s) and the IDS within a noncooperative non-zero-sum game model which extends the one in Section 7.2.3. In addition to the attacker(s) and the IDS, we introduce the sensor network as a third "fictitious" player similar to the "nature" player in standard game theory [1, p. 57]. The strategy of this player consists of a fixed probability distribution given a specific attack, and it represents the output of the sensor network during that attack. This way, we capture the imperfect conveyance of the attack information to IDS by the sensors. We now consider, for illustrative and visualization purposes, a finite version of the security game, where players have a finite number of available choices of action. Next, we associate specific cost functions with the attacker and the IDS in order to quantify various security trade-offs and establish a formal cost-benefit framework.

7.3.1 The security game in extensive form

The finite version of the security game extends the ideas of the game in [76] and in Section 7.2.3 by modeling the general case of multiple attackers and/or complex attacks. Taking the false alarms into account, we define the strategy space of the attacker as $U^A := \mathcal{A} \cup \{NA\}$ with cardinality $t_{max} \times I_{max} + 1$, where NA corresponds to "no attack." Let us also define the set of responses available to the IDS as $\mathcal{R} := \{R_1, R_2, \ldots, R_{max}\}$. These responses may vary from a simple alert, which corresponds to a passive response, to reconfiguration of the sensors and limiting access of users to the system, which is an active one. Thus, the strategy space of the IDS is given by $U^I := \mathcal{R}$ with cardinality R_{max}. The action space of the sensor network is a simplex over the augmented attack set $\mathcal{A} \cup \{NA\}$ defined as $U^S = \{\phi \in \mathbb{R}^{t_{max} \times I_{max}+1} : \phi \geq 0,\ \sum_i p_i = 1\}$. The output vector of the sensor network may be interpreted as a probability distribution over the set $\mathcal{A} \cup \{NA\}$ or equivalently as a normalized indicator function given $u^A \in U^A$. Thus, it quantifies the likeliness of a specific set of attacks for the IDS. Finally, we associate as in [76] specific cost values with the attacker's and the IDS's actions, and hence, with each branch of the game tree.

We can explain and illustrate the finite security game through a specific example. For simplicity let us consider a network consisting of a single subsystem and a single detectable threat, i.e., $\mathcal{A} = \{a\}$. We also limit the possible actions of the IDS to "set an alert" or "do nothing." Thus, the strategy spaces of the attacker(s) and the IDS are $U^I = \{u_1^I, u_2^I\}$ and $U^A = \{u_1^A, u_2^A\}$, where u_2^A corresponds to "no attack." The strategy space of the sensor network is then $U^S = \{\phi_1, \phi_2\}$ given $u^A \in U^A$. Here, $\phi = [p_1, p_2] \in \mathbb{R}^2,\ \phi \geq 0,\ p_1 + p_2 = 1$, where p_1 and p_2 give the likeliness of an attack and of no attack at all, respectively. A representation of this game in extensive form is shown in Figure 7.8 using the GAMBIT software [114]. The payoff or benefit values for the IDS and the attacker are chosen for illustrative purposes and given by $[(R_1^A, R_1^I), \ldots, (R_8^A, R_8^I)]$.

The cost values are implicitly a function of the sensor network output vector ϕ in addition to the actions of the attacker and the IDS. They are chosen to reflect various network security trade-offs and risks [76]. Let us further explain the game in Figure 7.8 by describing a specific scenario step by step, which corresponds to following a path from left to right in accordance with the order of players' actions. The lower left branch in the figure labeled A indicates an attack by the attacker(s) to the system. The sensor network labeled here as "chance" is represented by the $Sensor\_A$ branch. Finally, given the information from the sensor network, the IDS decides in branch U to take a predefined response action. The outcome of this scenario is quantified by a benefit of -5 to the attacker and $+5$ to the IDS.

We next investigate the existence of an NE as in [76]. An NE for a two-player game is defined as a pair of strategies and the corresponding pair of costs, with the property that no player can benefit by modifying his or her own strategy while the other player keeps his or her strategy fixed.

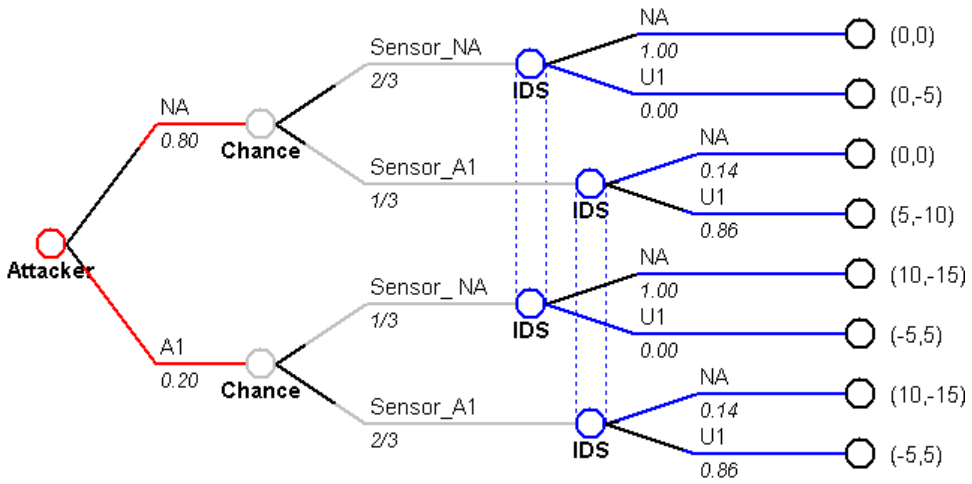

Figure 7.8: The finite version of the security game example shown in extensive form.

Hence, NE provides a suitable solution for the analysis of the security game. This particular game does not admit any NE solution in pure strategies, and hence, we extend the analysis by considering mixed strategies of the attacker and the IDS defined as probability distributions on the space of their pure strategies [1, p. 23]. Solving the game on this extended strategy space using GAMBIT, we obtain a unique NE in mixed strategies which also corresponds to the unique solution in behavioral strategies. Figure 7.8 depicts the game in extensive form and displays the probability values associated with the NE strategies of the players under the branches. Note that, unlike the other two players, the sensor network (chance player) is associated with a predefined probability distribution, which models the imperfect flow of information from the attacker to the IDS. In the NE, the attacker(s) target the system with a probability 0.20. A reason for this low probability is the discouraging effect of the sensor network's capability of correct detection with probability $2/3$. We note that there are two information sets for the IDS, one indicating an attack and one for no alarm. The NE strategy of the IDS given this information by the sensor network is "no response" (NR) with probability 1 if there is no alarm, and a response (U) with probability 0.86 if an alarm is set. We can argue that the IDS in this case has a high degree of trust on the information conveyed by the sensor network. However, it is important to note that the NE strategies of the players are very much dependent on the outcome payoffs of the game [76] as well as the detection probability distribution of the sensor network. Thus, it is crucial for correct analysis that the payoff values in the game reflect the trade-offs of the system at hand. A possible way of achieving this may be to utilize a supervised learning scheme to approximate the actual player payoffs and detection capabilities of the sensors.

Although the finite version of the security game provides a detailed visualization of the in-

teraction between the players, it has some limitations and disadvantages. One drawback is the scalability. The strategy spaces of the attacker and the IDS become too large for a more comprehensive analysis of a larger system. Another disadvantage is in the choice of the payoff values, which have to be determined separately for each branch of the game tree. This process may become tedious and inaccurate for a large system. In order to address these limitations, we next investigate a continuous-kernel version of the security game which is slightly different from the one above. In this game we adopt the convention that the players are minimizers (of costs) rather than being maximizers (of payoffs).

7.3.2 The cost functions of the security game

We address various security trade-offs and establish the continuous-kernel security game by associating specific cost functions with the IDS and the attacker. Given the set of attacks with cardinality A_{max}, the strategy space of the attacker is defined as $U^A := \{\mathbf{u}^A \subset \mathbb{R}^{A_{max}} : u_i^A \geq 0,\ i = 1, \ldots, A_{max}\}$. Similarly, the strategy space of the IDS is given by $U^I := \{\mathbf{u}^I \subset \mathbb{R}^{R_{max}} : u_i^I \geq 0,\ i = 1, \ldots, R_{max}\}$, where R_{max} is the cardinality of the set of responses available to the IDS. The actions of the sensor network, on the other hand, belong to the space $U^S := \{\mathbf{u}^S \subset \mathbb{R}^{A_{max} \times A_{max}} : 0 \leq u_i^S \leq 1\ \forall i\}$, and can be represented conveniently in matrix form by $\bar{P} := [\bar{p}_{ij}],\ \ \bar{P} \in U^S,\ i, j = 1, \ldots, A_{max}$. The matrix $\bar{P}$ represents how well the sensor network detects the attacks on the average, and maps the actions of the attacker to the sensor output. Furthermore, we define a simple metric for the detection of each attack, $a \in \mathcal{A}$, monitored by the sensor network

$$dq(i) := \frac{\bar{p}_{ii}}{\sum_{j=1}^{A_{max}} \bar{p}_{ij}},\ \ i = 1, \ldots, A_{max}.$$

For notational convenience, let us also define the matrix

$$P := [p_{ij}] = \begin{cases} p_{ij} = -\bar{p}_{ij} & \text{if } i = j \\ p_{ij} = \bar{p}_{ij} & \text{if } i \neq j \end{cases}. \tag{7.9}$$

We now introduce the cost parameters, which we take to be nonnegative. Let $\mathbf{c}^I := [c_1^I, \ldots, c_{A_{max}}^I]$ represent the cost of each attack for the IDS, whereas $\mathbf{c}^A := [c_1^A, \ldots, c_{max}^A]$ quantifies the gain of the attacker from the attack, if it is successful. The nonnegative matrix Q with diagonal entries greater than or equal to 1 models the vulnerability of a specific subsystem to attacks. On the other hand, the matrix $\bar{Q} := [\bar{Q}]_{A_{max} \times R_{max}}$ with entries of ones and zeros correlates IDS response actions with the attacks. The vectors $\alpha := [\alpha_1, \ldots, \alpha_{R_{max}}]$ and $\beta := [\beta_1, \ldots, \beta_{A_{max}}]$ are the cost of the response and the cost of the effort required to carry out an attack for the IDS and

the attacker, respectively. The cost of false-alarms and capture as well as the benefit of detection and deception for the IDS and the attacker are associated with the scalar value γ. Consequently, we define the cost function of the IDS, $J^I(\mathbf{u}^A, \mathbf{u}^I, P)$, and the one of the attacker(s), $J^A(\mathbf{u}^A, \mathbf{u}^I, P)$, as

$$J^I(\mathbf{u}^A, \mathbf{u}^I, P) := \gamma(\mathbf{u}^A)^T P \bar{Q} \mathbf{u}^I + (\mathbf{u}^I)^T \mathrm{diag}(\alpha)\mathbf{u}^{\mathrm{I}} + \mathbf{c}^{\mathrm{I}}(\mathrm{Q}\mathbf{u}^{\mathrm{A}} - \bar{\mathrm{Q}}\mathbf{u}^{\mathrm{I}}), \tag{7.10}$$

and

$$J^A(\mathbf{u}^A, \mathbf{u}^I, P) := -\gamma(\mathbf{u}^A)^T P \bar{Q} \mathbf{u}^I + (\mathbf{u}^A)^T \mathrm{diag}(\beta)\mathbf{u}^{\mathrm{A}} + \mathbf{c}^{\mathrm{A}}(\bar{\mathrm{Q}}\mathbf{u}^{\mathrm{I}} - \mathrm{Q}\mathbf{u}^{\mathrm{A}}), \tag{7.11}$$

where $(x)^T$ denotes the transpose of the vector or matrix, and $\mathrm{diag(x)}$ is a diagonal matrix with the diagonal entries given by the elements of the vector x.

With these specific structures of the cost functions J^I and J^A, we attempt to capture various aspects of the security game between the attacker and the IDS. The first terms of each cost function, $\gamma(\mathbf{u}^A)^T P \bar{Q} \mathbf{u}^I$ and $-\gamma(\mathbf{u}^A)^T P \bar{Q} \mathbf{u}^I$ represent the cost of false-alarms and benefit of detection for the IDS as well as the cost of capture and benefit of deception for the attacker, respectively. Notice that, this part of the cost is zero-sum. The second terms $(\mathbf{u}^I)^T \mathrm{diag}(\alpha)\mathbf{u}^{\mathrm{I}}$ and $(\mathbf{u}^A)^T \mathrm{diag}(\beta)\mathbf{u}^{\mathrm{A}}$ quantify the cost of specific responses and attacks. Depending on the response action, this reflects the cost of the use of resources, possible restrictions on system usage, or sensor reconfigurations for the IDS. On the other hand, it represents for the attacker the cost of resources required by the attack. The last terms $\mathbf{c}^I(Q\mathbf{u}^A - \bar{Q}\mathbf{u}^I)$ and $\mathbf{c}^A(Q\mathbf{u}^I - \bar{Q}\mathbf{u}^A)$ give the actual cost or benefit of a successful attack. False alarms and detection capabilities of the sensor network at a given time are incorporated into the values of the matrix P. In the ideal case of the sensor network functioning perfectly (i.e., no false alarms and 100% detection), the matrix $-P$ is equal to the identity matrix, $Id = \mathrm{diag}([1, \ldots, 1])$.

For notational convenience, define the vectors

$$\theta^I(\mathbf{c}^I, \bar{Q}, \alpha) := \left[(c^I \bar{Q})_1/(2\alpha_1), \ldots, (c^I \bar{Q})_{R_{max}}/(2\alpha_{R_{max}})\right]$$

and

$$\theta^A(\mathbf{c}^A, Q, \beta) := \left[(c^A Q)_1/(2\beta_1), \ldots, (c^A Q)_{A_{max}}/2\beta_{A_{max}}\right].$$

The reaction functions of the attacker and the IDS are obtained by minimizing the respective strictly convex cost functions (7.10) and (7.11). Hence, they are uniquely given by $\mathbf{u}^I(\mathbf{u}^A, P) = [u_1^I, \ldots, u_{R_{max}}^I]^T$ and $\mathbf{u}^A(\mathbf{u}^I, P) = [u_1^A, \ldots, u_{max}^A]^T$, respectively, where

$$\mathbf{u}^I(\mathbf{u}^A, P) = \left[\theta^I - \gamma[\mathrm{diag}(2\alpha)]^{-1}\bar{\mathrm{Q}}^{\mathrm{T}}\mathrm{P}^{\mathrm{T}}\mathbf{u}^{\mathrm{A}}\right]^+ \tag{7.12}$$

and

$$\mathbf{u}^A(\mathbf{u}^I, P) = \left[\theta^A + \gamma[\mathrm{diag}(2\beta)]^{-1}\mathrm{P}\bar{\mathrm{Q}}\mathbf{u}^{\mathrm{I}}\right]^+. \tag{7.13}$$

The function denoted by $[x]^+$ maps all negative values of x to zero. It is desirable for the IDS that the sensor grid is configured such that all possible threats are covered. It is also natural to assume a worst-case scenario where for each attack (type) targeting a subsystem there exists at least one attacker who finds it beneficial for him to attack. Hence, we expect in many practical cases $u_i^A > 0\ \forall i$ or $u_j^I > 0\ \forall j$.

The cost functions in (7.10)-(7.11) and the reaction functions in (7.12)-(7.13) provide an integrated model for the detection and the response process of the IDS as well as for the behavioral properties of the players and the sensors. A significant advantage of the cost based security game over the finite version one described in Section 7.3.1 is the ability to model the security trade-offs with a much smaller number of parameters.

7.3.3 Existence and uniqueness of a Nash equilibrium

The NE that has been widely utilized in noncooperative game theory is also a useful concept for the analysis of the continuous-kernel security game. Within the context of the security game defined in Section 7.3.2, a pair of strategies $(\mathbf{u}^{I*}, \mathbf{u}^{A*})$ of the IDS and the attacker is in NE if it satisfies $\mathbf{u}^{I*} = \arg\min_{\mathbf{u}^I} J^I(\mathbf{u}^{A*}, \mathbf{u}^I, P)$ and $\mathbf{u}^{A*} = \arg\min_{\mathbf{u}^A} J^A(\mathbf{u}^{I*}, \mathbf{u}^I, P)$. We state the existence of a unique NE solution in pure strategies for the security game in the next theorem. Furthermore, exploiting the special quadratic cost structure in (7.10)-(7.11), we provide a complete analytical characterization of the NE point.

Theorem 7.1 *There exists a unique NE in the security game defined in Section 7.3.2. Furthermore, if*

$$\gamma < \min\left(\frac{\min_i \theta^I}{\left[\max_i \left(\mathrm{diag}(2\alpha)\right)^{-1}\bar{\mathrm{Q}}^{\mathrm{T}}\mathrm{P}^{\mathrm{T}}\theta^{\mathrm{A}}\right]^+}, \frac{\min_i \theta^A}{\left[\max_i \left(\mathrm{diag}(2\beta)\right)^{-1}(-\mathrm{P})\bar{\mathrm{Q}}\theta^{\mathrm{I}}\right]^+}\right), \tag{7.14}$$

then the NE is an inner solution, $\mathbf{u}^{I*} > 0$ *and* $\mathbf{u}^{A*} > 0$*, and is given by*

$$\mathbf{u}^{A*} = (Id + Z)^{-1} \cdot \left[\theta^A + \gamma[\mathrm{diag}(2\beta)]^{-1}\mathrm{P}\bar{\mathrm{Q}}\theta^{\mathrm{I}}\right] \tag{7.15}$$

and

$$\mathbf{u}^{I*} = (Id + \bar{Z})^{-1} \cdot \left[\theta^I - \gamma[\mathrm{diag}(2\alpha)]^{-1}\bar{\mathrm{Q}}^{\mathrm{T}}\mathrm{P}^{\mathrm{T}}\theta^{\mathrm{A}}\right], \tag{7.16}$$

where

$$Z := \gamma^2[\mathrm{diag}(2\beta)]^{-1}\mathrm{P}\bar{\mathrm{Q}}[\mathrm{diag}(2\alpha)]^{-1}\bar{\mathrm{Q}}^{\mathrm{T}}\mathrm{P}^{\mathrm{T}},$$

$$\bar{Z} := \gamma^2[\mathrm{diag}(2\alpha)]^{-1}\bar{\mathrm{Q}}^{\mathrm{T}}\mathrm{P}^{\mathrm{T}}[\mathrm{diag}(2\beta)]^{-1}\mathrm{P}\bar{\mathrm{Q}},$$

and Id is the identity matrix.

Proof. The existence of a NE in the game follows from the facts that the objective functions are strictly convex, they grow unbounded as $|u| \to \infty$, and the constraint set is convex [1, p.174]. We next establish a unique strictly positive (equivalently inner) NE under the given sufficient condition. Let $\overline{\nabla}$ be the pseudo-gradient operator, defined through its application on the cost vector $J := [J^I \ J^A]$, as

$$\overline{\nabla} J := \left[\nabla^T_{u^I_1} J^I \cdots \nabla^T_{u^I_{R_{max}}} J^I \ \ \nabla^T_{u^A_1} J^A \cdots \nabla^T_{u^A_{A_{max}}} J^A\right]^T, \tag{7.17}$$

and define $g(\mathbf{u}) := \overline{\nabla} J$ where $\mathbf{u} := [\mathbf{u}^I \ \mathbf{u}^A]$. Let $G(\mathbf{u})$ be the Jacobian of $g(\mathbf{u})$ with respect to $\mathbf{u}$.

$$G(\mathbf{u}) := \begin{pmatrix} \alpha_1 & 0 & 0 & | & & & \\ 0 & \ddots & 0 & | & & \gamma[\mathbf{P}\bar{\mathbf{Q}}]^{\mathbf{T}} & \\ 0 & 0 & \alpha_{R_{max}} & | & & & \\ - & - & - & | & - & - & - \\ & & & | & \beta_1 & 0 & 0 \\ & -\gamma[\mathbf{P}\bar{\mathbf{Q}}] & & | & 0 & \ddots & 0 \\ & & & | & 0 & 0 & \beta_{A_{max}} \end{pmatrix}_{(A_{max}+R_{max})\times(A_{max}+R_{max})} \tag{7.18}$$

where the matrix $[\mathbf{P}\bar{\mathbf{Q}}]$ is of size $A_{max} \times R_{max}$. Define the symmetric matrix $\mathcal{G}(\mathbf{u}) := \frac{1}{2}(G(\mathbf{u}) + G(\mathbf{u})^T)$. It immediately follows that $\mathcal{G}(\mathbf{u}) = \mathrm{diag}([\alpha \ \beta])$, which is positive definite. Thus, due to the positive definiteness of the Hessian-like matrix $\mathcal{G}(\mathbf{u})$, the game admits a unique NE solution [79]. Note that this result does not use the condition (7.14) on γ, which however comes into picture if we further look for an inner solution as discussed below.

We now obtain an analytical description of the inner NE solution. Let us substitute for $\mathbf{u}^I$ in (7.13) the expression in (7.12). Hence, we obtain a fixed-point equation $\mathbf{u}^{A*} = \mathbf{u}^A(\mathbf{u}^I(\mathbf{u}^{A*}, P), P)$, given by

$$\mathbf{u}^{A*} = \theta^A + [\mathrm{diag}(\frac{2\beta}{\gamma})]^{-1}\mathrm{P}\bar{\mathrm{Q}}\theta^{\mathrm{I}} - \mathrm{diag}(\frac{\gamma}{2\beta})\mathrm{P}\bar{\mathrm{Q}}[\mathrm{diag}(\frac{2\alpha}{\gamma})]^{-1}\bar{\mathrm{Q}}^{\mathrm{T}}\mathrm{P}^{\mathrm{T}}\mathbf{u}^{\mathrm{A}*}. \tag{7.19}$$

Solving for $\mathbf{u}^{A*}$ yields (7.15) where the inverse exists because Z is nonnegative definite. The equilibrium solution $\mathbf{u}^{I*}$ in (7.16), on the other hand, can be derived by simply substituting for $\mathbf{u}^{A*}$ from (7.15) into (7.12). It is then straightforward to show that if (7.14) holds then $\mathbf{u}^{I*} > 0$,

and hence the NE is strictly positive. Moreover, there cannot be a boundary solution in this case due to the uniqueness of the NE. As a result, the game admits a unique inner NE under (7.14). □

7.3.4 The system dynamics and repeated games

The security games defined in Sections 7.3.1 and 7.3.2 are static one-shot games, which provide valuable insights into the behavior of the players (attacker and IDS) at a given time instance. However, given the dynamic nature of the system, the model in Section 7.3 has to be extended to take into account the interactions between players over a time period. Hence, we consider a discrete-time system model in order to capture dynamic nature of the system and take into account the interactions between players over a time period. Dynamics such as varying detection capability and (re)configuration of the sensor network given the strategies of the attacker and the IDS are quantified through the entries of the $\bar{P}$ matrix.

Let us define n as the time variable, and κ, δ, and ε as (small) scalar positive parameters. We define the random matrix $W := [w_{ij}], \quad i = 1, \ldots, A_{max}, \ j = 1, \ldots, R_{max}$ where w_{ij}'s are independent uniformly distributed on the interval $[-1, 1]$. Hence, W models the transients and imperfect nature of the sensor grid. Similarly, define ω as a scalar random variable uniformly distributed on the interval $[-1, 1]$, and independent of w_{ij}'s. Let us also define an upper bound, $dt_{max} < 1$, and a lower bound $dt_{min} > 0$ on the elements of $\bar{P}$. In doing so we can model the cases where sensors have a limited detection capability. A possible dynamic equation for $\bar{P}$ is then given by

$$\bar{P}(n+1) = \left[\bar{P}(n) + 2\delta\,(\omega+\kappa)\big(\mathrm{diag}(\mathrm{diag}(\mathbf{u}^{\mathrm{A}})\bar{\mathrm{Q}}\mathbf{u}^{\mathrm{I}}) - \delta\,\mathrm{col}(\mathrm{diag}(\mathbf{u}^{\mathrm{A}})\bar{\mathrm{Q}}\mathbf{u}^{\mathrm{I}})\big) + \varepsilon\mathrm{W(n)}\right]^{\mathrm{N}}, \quad (7.20)$$

where $col(x)$ is an $A_{max} \times A_{max}$ matrix with repeating x vectors constituting the columns, and the normalization function $[x]^N$ maps entries of x onto the interval $[dt_{min}, dt_{max}]$. With $\bar{P}$ generated by (7.20), $P(n)$ can then be obtained directly from (7.9). The dynamics in (7.20) represent a somewhat optimistic point of view, as it models a situation where a past attack and follow-up response result in better detection capabilities for the sensor network. A justification for this is the efficient reconfiguration of the sensors or direct intervention by the system administrator.

Taking (7.20) as the state equation, it is possible to define a finite or infinite horizon dynamic noncooperative game between the attacker and the IDS. Another alternative is to formulate the game as a receding-horizon one. Although the former approach seems ideal at first glance, two major problems prevent it from being practically useful. The first is the difficulty of finding a clear and concise analytical solution, if it exists at all. The second is the nonstationary nature of the

underlying dynamics. Although we have modeled the attacker(s) as a single player, in real life multiple attackers may choose to deploy multiple attacks intermittently, which makes optimization over a time horizon meaningless for the IDS as well as for the attacker. Therefore, we focus, instead, on repeated games as a simple and suitable dynamic model. In this case, the attacker and the IDS make instantaneous myopic optimizations given the state of the system (performance of the sensor network). Consequently, the set of equations characterizing the dynamic game under (7.9) and the reaction functions of the players (7.12)-(7.13) is

$$\mathbf{u}^I(n+1) = \left[\frac{\mathbf{c}^I\bar{Q}}{2\alpha} - [\mathrm{diag}(\frac{2\alpha}{\gamma})]^{-1}(\mathrm{P(n)})^{\mathrm{T}}\mathbf{u}^{\mathrm{A}}(\mathrm{n})\right]^+$$

$$\mathbf{u}^A(n+1) = \left[\frac{\mathbf{c}^AQ}{2\beta} + [\mathrm{diag}(\frac{2\beta}{\gamma})]^{-1}\mathrm{P(n)}\mathbf{u}^{\mathrm{I}}(\mathrm{n})\right]^+,$$

$$\bar{P}(n+1) = \left[\bar{P}(n) + 2\delta\,\mathrm{diag}(\mathrm{diag}(\mathbf{u}^{\mathrm{A}}(\mathrm{n}))\bar{\mathrm{Q}}\mathbf{u}^{\mathrm{I}}(\mathrm{n})) - \delta\,\mathrm{col}(\mathrm{diag}(\mathbf{u}^{\mathrm{A}})\bar{\mathrm{Q}}\mathbf{u}^{\mathrm{I}}) + \varepsilon\mathrm{W(n)}\right]^{\mathrm{N}}, \tag{7.21}$$

where P is related to $\bar{P}$ through (7.9). Existence of a unique NE for a fixed P ($\bar{P}$) has already been established in Theorem 7.1. Consequently, we investigate the convergence and stability properties of the system (7.21). Let us define

$$Idl := [idl_{ij}] = \begin{cases} idl_{ij} = dt_{max} & \text{if } i = j \\ idl_{ij} = dt_{min} & \text{if } i \neq j \end{cases},$$

which sets a limit on the best-case scenario in terms of detection capabilities of the sensor network. It immediately follows from (7.20) that

$$\begin{aligned} |\bar{p}_{ij}(n+1) - Idl_{ij}| < & \ |\bar{p}_{ij}(n) - Idl_{ij}| + \varepsilon\,|w_{ij}(n)| + \delta\,\mathbf{x_{-i}}\,|\omega(n)| \\ < & \ |\bar{p}_{ij}(n) - Idl_{ij}| + \varepsilon + \delta\,\mathbf{x_{-i}}, \end{aligned}$$

where

$$\mathbf{x_{-i}} := \max_{i,j,n}\left|\left[2\mathrm{diag}(\mathrm{diag}(\mathbf{u}^{\mathrm{A}}(\mathrm{n}))\bar{\mathrm{Q}}\mathbf{u}^{\mathrm{I}}(\mathrm{n})) - \mathrm{col}(\mathrm{diag}(\mathbf{u}^{\mathrm{A}})\bar{\mathrm{Q}}\mathbf{u}^{\mathrm{I}})\right]_{\mathrm{i,j}}\right|.$$

Hence, if $\varepsilon = 0$ and $\omega(n) = 0\ \forall n$ then as $n \to \infty$ $\bar{P}(n)$ clearly converges to the Idl matrix. Furthermore, for small fixed δ, $\varepsilon > 0$, and starting from any feasible initial point, $\bar{P}(0) \in U^S$, $E[\bar{P}(n)]$ converges asymptotically to the region $Reg(\varepsilon) := \{[\bar{p}_{ij}] \in U^S : dt_{max} - (\varepsilon + \delta\,\mathbf{x_{-i}}) \leq \bar{p}_{ii} \leq dt_{max}$ and $0 < dt_{min} \leq \bar{p}_{ij} \leq dt_{min} + \varepsilon + \delta\,\mathbf{x_{-i}}\ \forall i \neq j\}$.

7.3.5 Dynamic strategies and numerical analysis

We analyze some simple strategies available to the attacker and the IDS within the dynamic model (7.21) in order to gain further insight into IDS and attacker behaviors. Let us first consider strategies with fixed actions over a finite time period. Assume that the attacker starts an attack at a given time with action $\mathbf{u}^A(n)$ and sustains it over a fixed time period N such that $\mathbf{u}^A(n) = \mathbf{u}^A(n+1) = \ldots = \mathbf{u}^A(n+N)$. Then, given $\mathbf{u}^A(t), \quad t = n, n+1, \ldots, n+N$, the response of the IDS will be according to (7.12), as the IDS cannot know the fact that the attacker has chosen a fixed strategy. From (7.21) we immediately conclude that $J^A(n)$ will increase with n and $J^I(n)$ will decrease with n. In other words, it is suboptimal for the attacker to have a fixed action strategy. Similarly, deploying a fixed response strategy is suboptimal for the IDS as it gives the attacker an opportunity to exploit the weaknesses of the sensor network [115]. Another problem with choosing a fixed action strategy for both players is determining what this strategy should be. As we will soon demonstrate, any deviation from NE response results in higher costs for the player. Therefore, it is beneficial for both the IDS and the attacker to frequently update their strategies as part of a multistep optimization process.

The conclusions of the discussion above can be illustrated through numerical analysis. We choose a simple scenario with three specific attacks monitored by the sensor network. For comparison purposes cost parameters are chosen to be the same for both the attacker and the IDS: $\mathbf{c}^I = \mathbf{c}^A = [50,\ 50,\ 50]$, $\alpha = \beta = [10,\ 10,\ 10]$, $\gamma = 10$, $\varepsilon = 0.01$, $\kappa = 0.1$, and $\delta = 0.001$. The responses of the IDS are also limited to three, and $\bar{Q} = Q = Id$ for simplicity. In addition, $\bar{p}_{ij} \in [0.3, 0.7]$. We first simulate the system described in (7.21). The costs and actions of the attacker and the IDS as well as detection quality of sensors are shown in Figure 7.9.

In the next simulation, we fix the IDS response as $u^I = [5,\ 5,\ 5]$, which is roughly equal to the NE solution for the static game. From Figure 7.10, we observe that the attacker can exploit this by limiting his or her attack to a short time period. Furthermore, temporary degradations in sensor detection quality are utilized by the attacker to decrease his own cost, while they drive the IDS cost higher. Figures 7.11 and Figures 7.12, on the other hand, depict the cases when IDS response is chosen as $u^I = [8,\ 8,\ 8]$ and $u^I = [2,\ 2,\ 2]$, respectively. We observe in the former scenario that the IDS can increase the cost of the attacker if it accepts a significant cost for itself also. On the other hand, the latter case where the IDS does not take sufficient precautions proves to be very costly for it. Clearly, both of these suboptimal fixed actions result in higher costs for the IDS while benefiting the attacker.

In addition, we analyze the case where the attacker deploys a fixed strategy $u^A = [5,\ 5,\ 5]$ while the IDS adjusts its actions according to (7.21). For clarity of presentation we choose $\kappa = 0.3$. Figure 7.13 demonstrates that the cost of the attacker increases as the quality of sensor detection

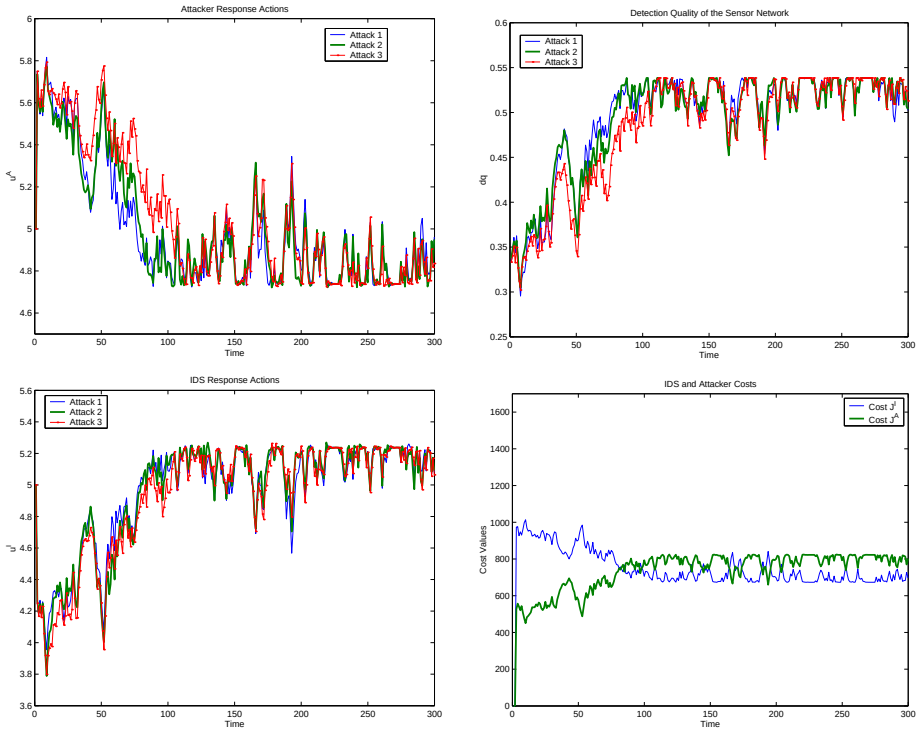

Figure 7.9: Dynamics of the system (7.21).

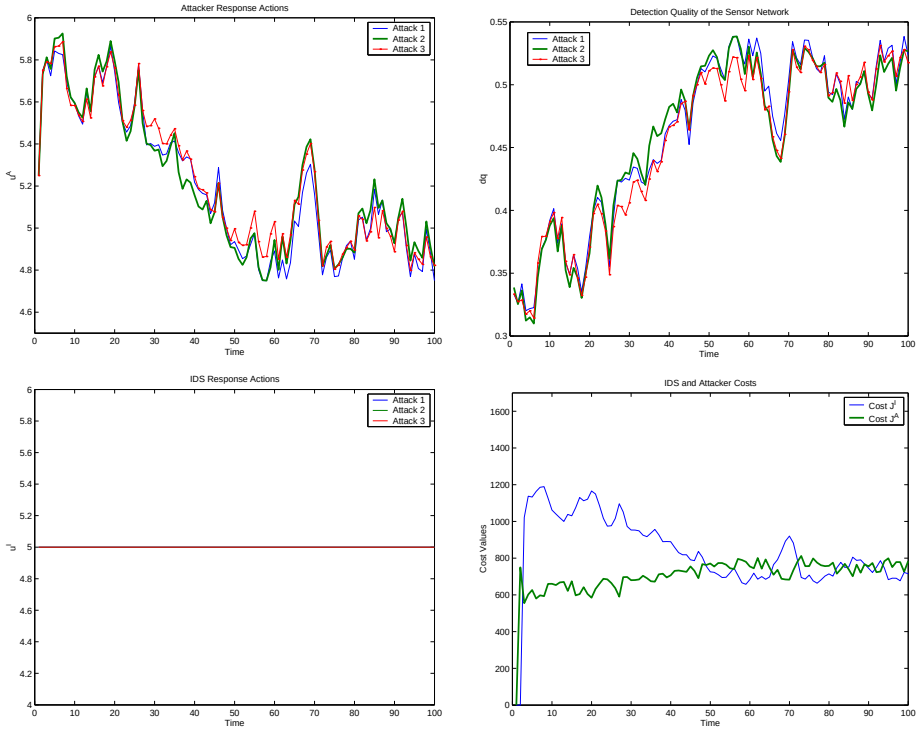

Figure 7.10: Simulation of the system (7.21) with the IDS's actions fixed as $u^I = [5,\ 5,\ 5]$.

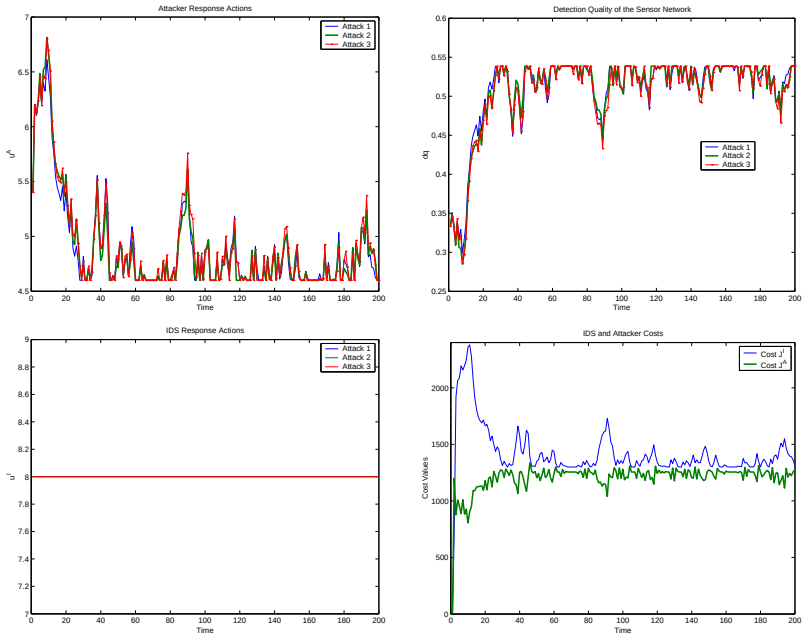

Figure 7.11: Simulation of the system (7.21) with the IDS's actions are fixed as $u^I = [8,\ 8,\ 8]$.

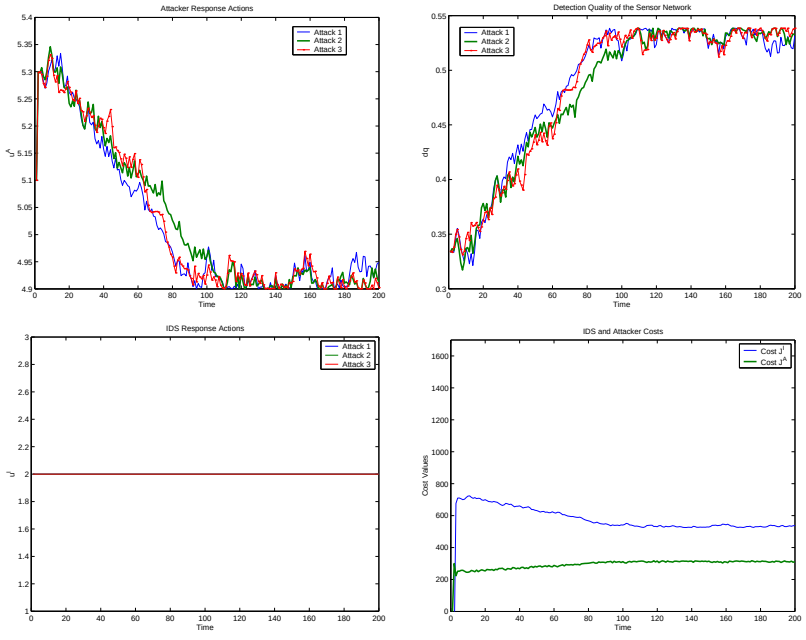

Figure 7.12: Simulation of the system (7.21) with the IDS's actions are fixed as $u^I = [2,\ 2,\ 2]$.

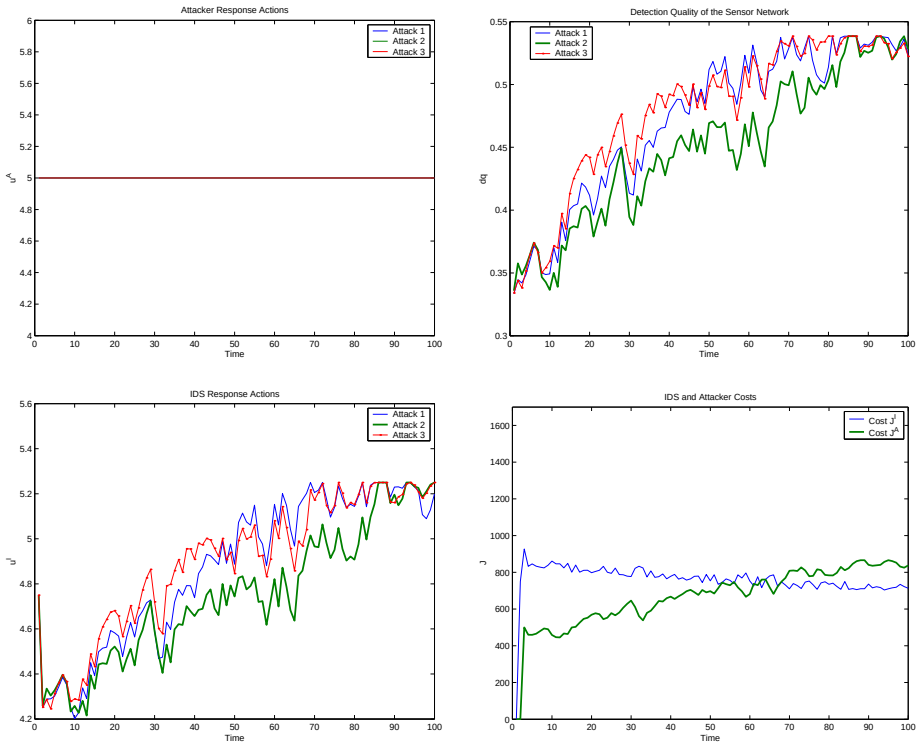

Figure 7.13: Simulation of the system (7.21) with the attacker's actions are fixed as $u^A = [5,\ 5,\ 5]$.

improves over time. Thus, it is a better strategy for the attacker to deploy short high intensity attacks intermittently over a time period.

Next, we investigate what happens if the attacker discovers an inherent vulnerability in the system monitored by the IDS. In order to capture this scenario within our model we increase Q to $\mathrm{diag}([2,\ 1,\ 1])$ after a fixed time point. As shown in Figure 7.14, the cost of the IDS increases significantly after the discovery of the vulnerability by the attacker. On the other hand, increased attack intensity on the first subsystem results in a stronger IDS response. We note the increased variation in the detection quality of the specific attack, which is due to the random imperfections in sensor reconfiguration mechanism.

Finally, the inherent assumption that both the attacker and the IDS have perfect knowledge on the performance of the sensor network is relaxed. Figure 7.15(a) depicts the NE costs of both players and the difference between the two costs under the assumption that IDS estimates (from left to right) a perfectly functioning sensor network ($\bar{P} = Id$) to the worst-case ($\bar{P} = Ones - Id$), where $Ones$ is the matrix of ones. The counterpart of this for the attacker is also depicted in Figure 7.15(b). Clearly, a correct estimation of $\bar{P}$ decreases the difference between the costs, which is beneficial to the player. We also observe that assuming a perfect detection the IDS can increase both its and the attacker's cost, and thereby, discouraging an attack at the IDS's own

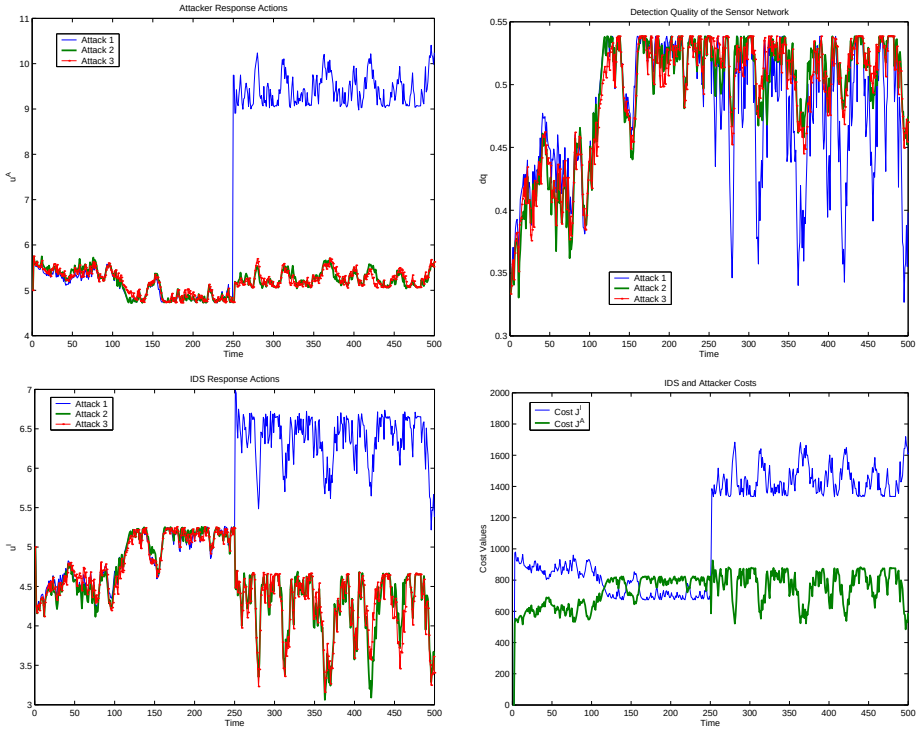

Figure 7.14: Simulation of the system (7.21) when Q is modified as $Q = \mathrm{diag}([2,\ 1,\ 1])$ after a time point.

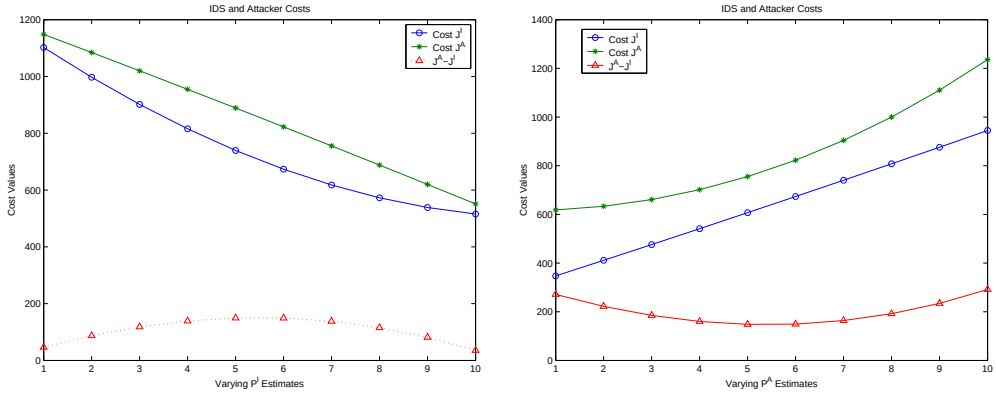

(a) (b)

Figure 7.15: The NE costs of both players under the assumption that (a) the IDS and (b) the attacker estimate $\bar{P}$, respectively. The estimates vary (left to right) from a perfectly functioning sensor network $(\bar{P} = Id)$ to the worst-case $(\bar{P} = Ones - Id)$.

expense. Likewise, Figure 7.15(b) shows that incentive to attack varies inversely proportionally to how the attacker perceives the success rate of the sensor network. As expected, IDS having a good sensor network discourages the attacker.

7.4 An Intrusion Detection Framework for Access Control

In this section we investigate a game theoretic approach for intrusion detection in access control systems by demonstrating the concepts introduced in previous sections under various scenarios through simulations in MATLAB, where we implement an IDS prototype for access control utilizing "virtual" sensors based on Kohonen self-organizing maps for anomaly detection. The goals of this demonstration are to illustrate the theoretical analysis and concepts, investigate problems associated with practical implementation, and provide a guideline for actual product (software) development. In light of these goals, MATLAB is chosen as the simulation environment for its extensive numerical calculation support and visualization capabilities. We next describe the data generation process and sensor design in the simulation. Subsequently, we consider a simple scenario for investigating effectiveness of the sensors.

7.4.1 System access data generation

The simulations in this study are based on mock-up data generated artificially as we do not have access to real world data from a deployed role based access control system. Since measuring performance is not one of our current goals, working with data generated is more advantageous because it provides us with the level of abstraction required to explore a variety of cases and scenarios. Furthermore, one should note that even with real world data it is not trivial to arrive at any definitive conclusions on the performance of an IDS.

Define a fixed set of users $Users := \{user_1, \ldots, user_N\}$, firms

$$Firms := \{firm_1, \ldots, firm_{max}\},$$

and roles $Roles := \{role_1, \ldots, role_{max}\}$. Each user $i \in Users$ in the system is associated with a firm $j \in Firms$ and a role $k \in Roles$ (within the firm). The IDS monitors a set of fixed resources $Res := \{res_1, \ldots, res_M\}$, where each resource may represent a class of data or services, e.g. databases, documents, web pages or services. Each user i is authorized to access only a subset of resources $Acc_i \subset Res$. Any unauthorized access attempt to the set $Res \setminus Acc_i$ by user i is accordingly denied and logged by access control system. Resource usage characteristics of users are modeled by associating each user with a probability distribution on resources. In the

simulations, time is discretized into fixed slots. Then, user access to the system at a given time step is modeled as a Poisson random process [103] with its mean defined as a function of the time of day.

We assume that the access control system provides the IDS at time t a log file with the following information and structure:

$$log\_file(t) = [time\_slot,\ user_{nbr},\ firm_{nbr},\ role_{nbr},\ resource_{nbr},\ access\_flag],$$

where the binary $access\_flag$ indicates whether the particular user is authorized and allowed to access that resource. This access log file constitutes the main source of information for IDS sensors, and hence, decision processes.

The system in our particular implementation consists of $N = 20$ users, two firms $Firms = \{$Firm A, Firm B$\}$, three roles $Roles = \{$engineer, accountant, manager$\}$, and $M = 10$ resources. Without any loss of generality the day is divided into 96 time slots of 15 min. The i^{th} user attempts to access the subsets of resources Acc_i and $Res \setminus Acc_i$ randomly with uniform probability within each set. However, the probability of attempting to access an authorized resource is chosen to be 10 times higher than the unauthorized one. By assigning a low but nonzero probability for unauthorized access attempts, regular users' unintentional mistakes are taken into account. The mean value of the Poisson process for system access is shown in Table 7.2. We note that, other than correlating the system usage with business hours, the values in the table are inconsequential for the purposes of this simulation.

Table 7.2: The mean value of the Poisson process for system access at a given hour of the day.

Hour (1-24)	1-4	5	6	7	8	9-18	19	20	21-24
Mean	.02	.04	.16	.4	.6	.8	.2	.12	.02

For simplicity and clarity of the presentation, we have made here a number of implicit assumptions. These assumptions should be noted and addressed in future and real world implementations of the IDS.

- The Poisson model for system access is only a mathematical approximation, and does not take correlated events such as sessions, meetings, etc. into account.
- We ignore factors like time zones, weekends, holidays etc. in characterizing system access rate, which is described by the mean value of the Poisson process.
- All users share the same usage characteristics. Individual and role/firm based variations are ignored for the time being.

7.4.2 Sensor design and implementation

Among the two main approaches for intrusion detection and designing sensors, rule-based detection depends more on the specific properties of the particular implementation. In addition, although it is easier to implement rule-based sensors they require maintenance and have limited capabilities. Anomaly-based sensors, on the other hand, are more flexible and have the ability to detect previously unknown attacks. Hence, the main focus in our simulations will be on anomaly-based detection.

We consider two classes of sensors: one for detecting usage anomalies and the other for detecting "misuse" anomalies, i.e., anomalies in unauthorized system access attempts. Note that some unauthorized system access attempts should be expected even under normal operation due to unintentional mistakes by regular users. For each class, we implement two sensors: one for aggregate system access and one for per resource access by all users. Hence, the simulated IDS has only four sensors. Although this number is very low for efficient operation of a real world IDS implementation, it is useful for clarity of presentation and visualization.

We design the anomaly detection sensors based on Kohonen self-organizing maps (SOM) [116] using a methodology similar to the one described in [117]. The SOMs are implemented in MATLAB Neural Network Toolbox, and trained using a standard *Kohonen learning rule*. In the case of system access and misuse attempt sensors the neurons of the SOM have weight vectors $\mathbf{w}$ with two dimensions: time and number of access (attempts). Neurons of the resource access (attempt) sensors have, on the other hand, three-dimensional weight vectors with the resource number being the third attribute. The neurons of the SOMs are initially located on a rectangular grid, and the standard Euclidean distance is used as the link distance function. The Kohonen learning rule for updating the neuron weights $\mathbf{w}$ basically consists of the following steps: Given the input vector $\mathbf{y}$ at step n determine first the neuron i with the nearest weight vector $\mathbf{w}_i$ to $\mathbf{y}$. Second, find the neighboring neurons $j \in N_i(d)$ having weight vectors within the maximum distance d from $\mathbf{w}_i$, i.e., $N_i(d) = \{j : \|w_i - w_j\| \leq d\}$. Finally, for all $k \in N_i(d)$ update the neuron weights by

$$\mathbf{w}_k(n+1) = \mathbf{w}_k(n) + \kappa(\mathbf{y}(n) - \mathbf{w}_k(n)) \; \forall k \in N_i(d),$$

where $\kappa > 0$ is a fixed step size. For further details on SOM implementation and training we refer to [118].

The SOM of each sensor is trained using a training data set obtained from system log files. For efficient anomaly detection the training data set should contain only data points of regular usage and exclude data points of attackers. After the training process we calculate for each SOM the average distance of samples to the nearest neuron, d_{avg}, and the standard deviation of these

distances, σ_d. Then, utilizing a positive sensitivity parameter ϕ the sensor determines whether a new data point $\mathbf{y}$ is an anomaly or not according to the following criterion:

Definition 7.1 *Assume the neuron weights, $\mathbf{w}$, of a SOM (of a sensor) are trained using a data set representing "normal" behavior. Let d_{avg} be the average distance of training points to the nearest neuron and σ_d be the standard deviation of these distances. Then, a data point $\mathbf{y}$ is defined as an **anomaly** if*

$$\min_i \|\mathbf{y} - \mathbf{w}_i\| - d_{avg} \geq \phi\, \sigma_d,$$

where $\phi > 0$ is a positive sensitivity parameter.

Notice that, if ϕ is chosen small enough, then even some of the data points in the training set may be classified as anomalies by the sensor. On the other hand, choosing a small ϕ enhances the detection capability of the sensor. Hence, the sensitivity parameter ϕ in effect quantifies the trade-off between false alarms and sensor sensitivity.

7.4.3 Attack scenarios and case studies

We investigate the effectiveness of the sensors described in Section 7.4.2 with a simple attack scenario, where a malicious attacker obtains access to a user's account without the knowledge of the user. The attacker accesses a high number of system resources randomly with a probability 0.05 at a given time slot. Using such a random and bursty access pattern the attacker aims to exploit the system as much as possible without leaving a large trace in terms of session lengths.

The IDS sensitivity parameter ϕ is chosen as 4 for all sensors. An early prototype of the IDS system administrator interface is illustrated in Figure 7.16.

Let us assume that activating both classes of sensors at the same time brings an unacceptably large overhead to the system. Hence, we deploy the usage and misuse sensors randomly with equal probability. The SOMs of sensors are trained using a training data set which is not tainted with attacks, and gathered over two days. Figure 7.17 depicts the weight vectors of the SOM neurons trained (in blue color) of both the system and resource usage sensors. In addition, a data point indicating an anomaly caused by the attacker is shown (in red). On the other hand, the neurons of the misuse sensor's SOMs are shown in Figure 7.18. Another anomaly is detected only by the system misuse sensor in this case. Finally, Figure 7.19 displays an overview of the daily IDS log with both detected anomalies and regular data points marked (in green).

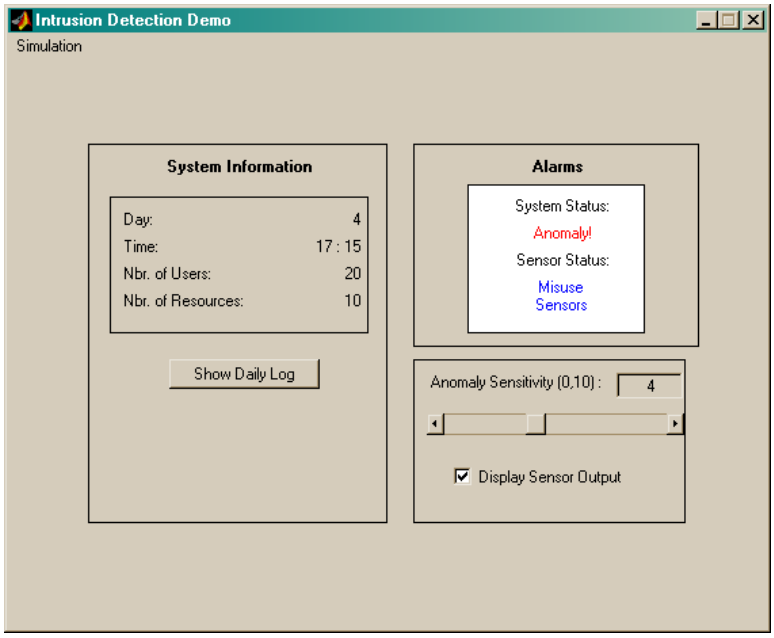

Figure 7.16: A prototype of the IDS system administrator interface.

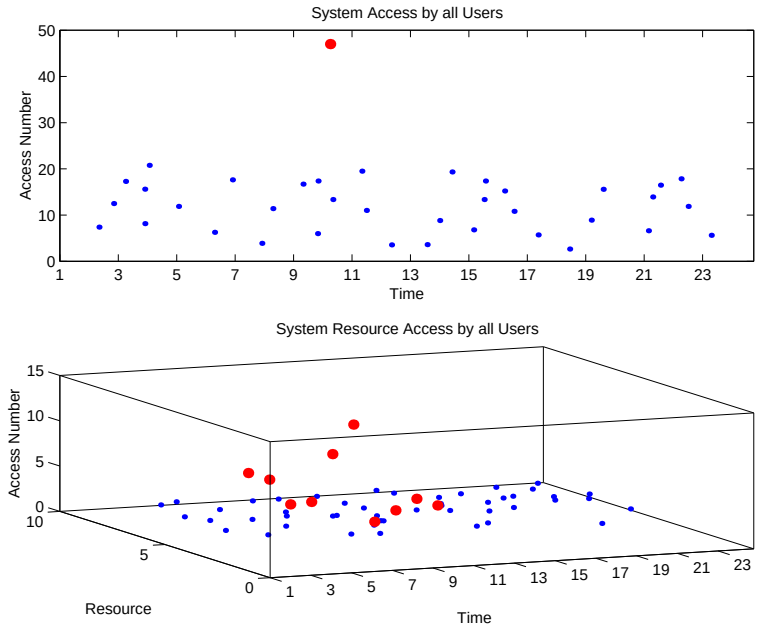

Figure 7.17: The neurons (blue) of system (top graph) and resource usage sensors (bottom graph), and a data point (red), which is identified as an anomaly by both of the sensors, is shown.

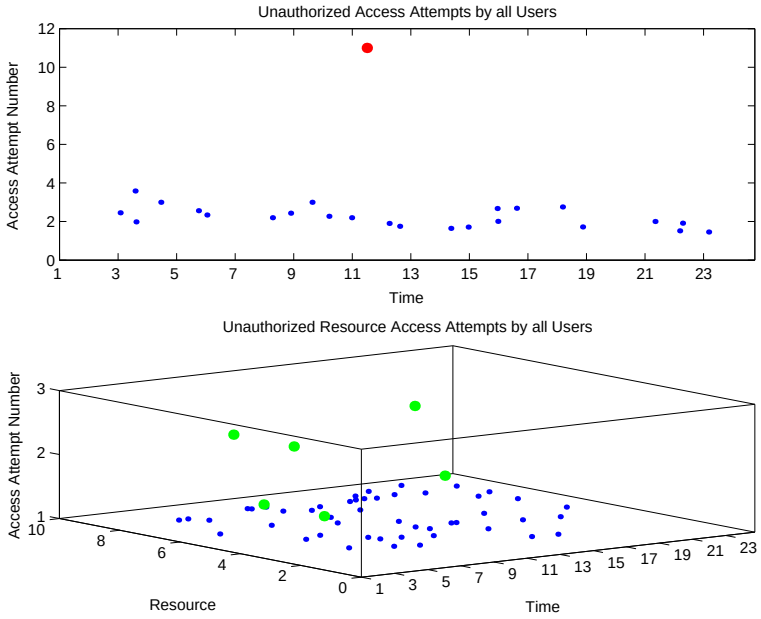

Figure 7.18: The neurons (blue) of system (top graph) and resource (bottom graph) misuse sensors, and a data point (red), which is identified by the system misuse sensor as an anomaly, are shown.

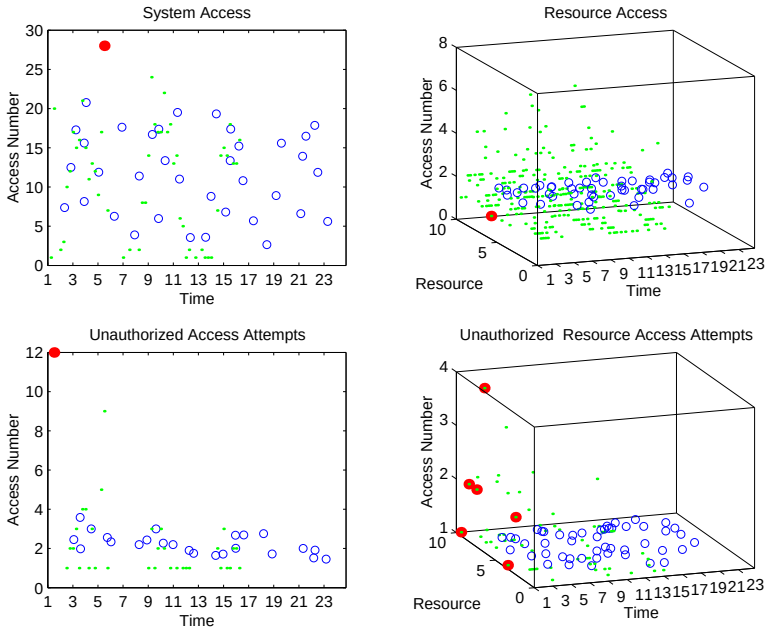

Figure 7.19: The IDS daily log file gives an overview of the sensor outputs up to the current time slot.

7.5 Conclusions

We have investigated the basic decision and analysis processes involved in information security and intrusion detection, as well as possible usage of game theory for developing a formal decision and control framework. A generic model has been developed for a distributed IDS with a network of sensors. Furthermore, two flexible, platform independent schemes based on game theoretic techniques have been proposed.

The security warning system provides system administrators an intuitive overview of the security situation in the network, and enables the IDS to operate in different modes specific to each warning level. In this simple and easy-to-implement scheme cooperative game theory, specifically Shapley values, are used for analysis and configuration. The second scheme, on the other hand, models the interaction between the attacker and the IDS as a two-person noncooperative game with dynamic information. Nash equilibrium solutions are derived analytically and analyzed for the finite security game defined in two special cases. Furthermore, the imperfect flow of information from the attacker to the IDS through a virtual sensor network is captured within both finite and continuous-kernel noncooperative network security games. Hence, we have established a quantitative mathematical framework which provides insight into and addresses a wide range of resource allocation problems in intrusion detection. Existence of a unique NE and best-response strategies for players under specific cost functions are investigated. In addition, the interaction between the players over a time period is analyzed using repeated games and a specific dynamic model for the sensor network. Consequently, some basic strategies for the IDS and the attacker are discussed through several numerical studies.

In both schemes, using game theoretic concepts we have addressed some of the basic network security trade-offs, and have given illustrative numerical examples. Thus, we have demonstrated the suitability of game theory for development of various decision, analysis, and control algorithms in intrusion detection.

Finally, we have implemented an IDS prototype for access control utilizing usage and misuse anomaly detection sensors based on self-organizing maps, and demonstrated its operation under a simple scenario. Despite the simplifying assumptions we make in the simulations we observe that the initial results are promising.

CHAPTER 8

SUMMARY AND CONCLUSIONS

We have presented in the previous chapters the results of our dissertation research on the network control problems of congestion control, CDMA power control, and network intrusion detection. We next provide an overview of the thesis and a brief summary of each topic separately, which include future research directions and concluding remarks.

8.1 Summary

Our goal in this research has been to design noncooperative games to address network control problems of congestion control, CDMA power control, and network intrusion detection and response. In the cases of CDMA power control and congestion control, we have developed and analyzed fairly general, distributed, market-based, resource allocation frameworks. The applicability of the underlying noncooperative network game's principles to both network control problems indicates the generality and usefulness of our approach. Based on this general framework we have also investigated various algorithms customized according to the specific nature of the network at hand. Making use of a variety of control theoretic tools, we have rigorously studied stability and robustness properties of these algorithms. Robustness with respect to feedback delays is of particular importance and therefore has been of major interest to this research. In the case of network intrusion detection, we have made use of dynamic noncooperative games to model the decision and analysis processes in an IDS. Again, both generic and system specific schemes and models are considered.

In addition to the theoretical analysis of the network control problems addressed, we have also focused on the implementation of the schemes and algorithms. For each algorithm, we have demonstrated theoretical results obtained either via high-level MATLAB simulations or using the NS-2 packet level network simulator. Through extensive simulations, we have gained insights to the problems associated with practical implementation of our algorithms, and have verified the applicability and underlying assumptions of the theoretical models.

8.2 Congestion Control

The multifaceted problem of network congestion control has been one of the main focal points of this dissertation. By developing and studying a fairly general congestion control framework based on noncooperative game theory, we have obtained results that can be utilized in designing decentralized congestion control algorithms for various types of networks. Making use of pricing and utility concepts we have defined a noncooperative network game, which admits under some mild convexity assumptions a unique NE solution concurrently being the unique operating point of the network. Furthermore, we have investigate system dynamics, its stability and robustness properties with respect to communication delays, and variations in network parameters. We have proposed a specific congestion control algorithm based on variations in queueing delay for Internet-style networks. Again, we have analyzed its stability and robustness properties by taking into account queue dynamics, the effect of boundaries, and communication delays. In addition, we have utilized randomized algorithms in this context, and have presented numerical results regarding stability of the system first for a single bottleneck node and subsequently under general network topologies. The algorithms and results obtained have been demonstrated and verified through numerical studies in Matlab as well as in Network Simulator 2 (NS-2) [77] over Internet Protocol (IP) for various network topologies. The congestion control schemes and the underlying framework have been discussed in detail in Chapters 2 and 3 and a detailed outline of these chapters has been given in Section 1.4.

In a more recent study, we have proposed a discrete-event system approach to the modeling of the congestion control problem [39], where the interaction between a communication link and multiple users are studied in packet level. However, issues such as prohibitively high number of states in the model and extensive information requirements of the supervisory control algorithm limit the usefulness of this approach, and confirm that fluid models provide the appropriate abstraction level for the congestion control problem in complex networks.

A future research direction would be to investigate hybrid system models similar to those we have proposed in Chapter 4 to address underlying issues of congestion control like capacity usage, avoiding jitter and packet losses, and resource allocation, under the constraints of limited/delayed feedback information, decentralized control, and compatibility with the existing schemes. Another interesting direction would be to study the chaotic nature of the congestion control schemes and development of a “control of chaotic systems” approach to the problem.

8.3 Power Control

By making use of hybrid system and noncooperative game theories we have modeled the multicell wireless data network, developed a market-based distributed power control scheme, and extended the single cell power control scheme of [52] to multiple cells and to a broader class of cost functions. Specifically, we have modeled the multicell wireless data network as a switched hybrid system where handoffs of mobiles between the individual cells (base stations) correspond to discrete switching events between different subsystems. Under a set of sufficient conditions, we have shown the existence and global stability of a unique NE for each subsystem, and established the global exponential convergence of the dynamics of the multicell power control game to a minimum convex set of Nash equilibria for any switching (handoff) scheme. Furthermore, we have investigated robustness of these results to various communication constraints such as feedback delays and quantization.

We have next considered a variation of the power control game, which captures the preferences of mobiles using a utility function defined as the logarithm of the probability that the frame success rate of the data user is greater than a predefined individual threshold level. We have analyzed this power control game as well as the global convergence of continuous-time as well as discrete-time synchronous and asynchronous iterative power update algorithms to the unique NE of the game. Furthermore, we have shown that a stochastic version of the discrete-time update scheme, which models the uncertainty due to quantization and estimation errors, converges almost surely to the unique NE point.

We have also studied yet another extension to these power control games. Specifically, we have investigated a hybrid noncooperative game motivated by the practical problem of joint power control and base station (BS) assignment in CDMA wireless data networks, where we have modeled the integrated power control and BS assignment problem in such a way that each mobile's action space not only includes the transmission power level but also the choice of the BS. We have analyzed the existence and uniqueness of pure Nash equilibrium (NE) solutions of the hybrid game, which constitute the operating points for the underlying wireless network, numerically using grid methods and randomized algorithms.

Finally, we have considered a formulation of the power control as a team optimization problem, where each mobile attains at the minimum its individual fixed target signal to interference level and beyond that optimizes its transmission power level according to its individual preferences. Using a Lagrangian relaxation approach similar to [12], we have obtained two decentralized dynamic power control algorithms (primal and dual power update), and have established their global stability utilizing both classical Lyapunov theory and the passivity framework [57]. Our results on the subject have been discussed in detail in Chapters 4, 5, and 6, and an outline has been provided

in Section 1.4.

One of the future research opportunities in this area would involve analytical and further numerical investigation of NE properties and convergence characteristics of the joint power update and BS assignment scheme. Another possible extension includes formulation of the power control games Chapters 4 and 5 as team optimization problems within the frameworks introduced in Chapter 6.

8.4 Intrusion Detection

In this dissertation we have developed several game theoretic models for the study and analysis of a formal decision and control framework in network intrusion detection. We have developed quantitative models to analyze common trade-offs in information security and have proposed a generic model for distributed IDSs by defining a network of sensors. In addition to two flexible easy-to-implement schemes, we have analyzed the interaction between the attacker and the IDS within a two-person noncooperative game with dynamic information. Nash equilibrium solutions have been derived analytically and analyzed for the finite security game defined in two special cases. Furthermore, the imperfect flow of information from the attacker to the IDS through a virtual sensor network has been captured within both finite and continuous-kernel noncooperative network security games. As an application of the framework proposed, we have implemented an IDS prototype for access control utilizing usage and misuse anomaly detection sensors based on self-organizing maps, and demonstrated its operation under a simple scenario. A detailed outline of Chapter 7, which discusses our results, has been presented in Section 1.4.

A future direction of research would involve development and analysis of (software) agent-based robust monitoring and decision making schemes in order to ensure and maintain trustworthiness of a networked system. The software agents constituting such a distributed control framework could be modeled as independent players who interact with each other on the same networked system.

REFERENCES

[1] T. Başar and G. J. Olsder, *Dynamic Noncooperative Game Theory*, 2nd ed. Philadelphia, PA: SIAM, 1999.

[2] D. Liberzon, *Switching in Systems and Control*. Boston, MA: Birkhauser, 2003.

[3] G. Calafiore, F. Dabbene, and R. Tempo, "Randomized algorithms for probabilistic robustness with real and complex structured uncertainty," *IEEE Transactions on Automatic Control*, vol. 45, no. 12, pp. 2218–2235, December 2000.

[4] J. E. Gentle, *Statistics and Computing: Random Number Generation and Monte Carlo Methods*. Berlin, Germany: Springer-Verlag, 1996.

[5] H. Niederreiter, *Random Number Generation and Quasi-Monte Carlo Methods*. Philadelphia, PA: SIAM, 1992.

[6] V. Anantharam and J. Walrand, "A special issue on control methods for communication networks," *Automatica*, vol. 35, December 1999.

[7] L. Bushnell, "Special selection on networks and control," *Control Systems Magazine*, vol. 21, February 2001.

[8] W. Gong and T. Başar, "Special issue on systems and control methods for communication networks," *IEEE Transactions on Automatic Control*, vol. 47, June 2002.

[9] R. Srikant, *The Mathematics of Internet Congestion Control*. Boston, MA: Birkhauser, 2004.

[10] V. Jacobson, "Congestion avoidance and control," in *Proc. of the Symposium on Communications Architectures and Protocols (SIGCOMM)*, Stanford, CA, August 1988, pp. 314–329. [Online]. Available: citeseer.ist.psu.edu/jacobson88congestion.html

[11] F. P. Kelly, "Charging and rate control for elastic traffic," *European Transactions on Telecommunications*, vol. 8, pp. 33–37, January 1997.

[12] F. Kelly, A. Maulloo, and D. Tan, "Rate control in communication networks: Shadow prices, proportional fairness and stability," *Journal of the Operational Research Society*, vol. 49, pp. 237–252, 1998.

[13] J. Mo and J. Walrand, "Fair end-to-end window-based congestion control," *IEEE/ACM Transactions on Networking*, vol. 8, p. 556 567, October 2000.

[14] R. J. La and V. Anantharam, "Charge-sensitive TCP and rate control in the Internet," in *Proc. IEEE Infocom*, 2000, pp. 1166–1175.

[15] S. H. Low and D. E. Lapsley, "Optimization flow control-i: Basic algorithm and convergence," *IEEE/ACM Transactions on Networking*, vol. 7, no. 6, pp. 861–874, December 1999.

[16] S. Deb and R. Srikant, "Global stability of congestion controllers for the Internet," *IEEE Transactions on Automatic Control*, vol. 48, no. 6, pp. 1055–1060, June 2003.

[17] S. Kunniyur and R. Srikant, "A time-scale decomposition approach to adaptive explicit congestion notification (ECN) marking," *IEEE Transactions on Automatic Control*, vol. 47(6), pp. 882–894, June 2002.

[18] G. Vinnicombe, "On the stability of networks operating TCP-like congestion control," in *Proc 15th IFAC World Congress on Automatic Control*, Barcelona, Spain, July 2002.

[19] L. Massoulie, "Stability of distributed congestion control with heterogeneous feedback delays," *IEEE Transactions on Automatic Control*, vol. 47, no. 6, pp. 895–902, June 2002.

[20] R. Johari and D. Tan, "End-to-end congestion control for the Internet: Delays and stability," *IEEE/ACM Transactions on Networking*, vol. 9, no. 6, pp. 818–832, December 2001.

[21] A. Elwalid, "Analysis of adaptive rate-based congestion control for high-speed wide-area networks," in *Proc. of IEEE International Conference on Communications (ICC)*, vol. 3, Seattle, WA, June 1995, pp. 1948–1953.

[22] S. Liu, T. Başar, and R. Srikant, "Controlling the Internet: A survey and some new results," in *Proc. of the 42nd IEEE Conference on Decision and Control*, Maui, Hawaii, December 2003, pp. 3048–3057.

[23] J. Wen and M. Arcak, "A unifying passivity framework for network flow control," in *Proc. of the IEEE Infocom*, San Francisco, CA, April 2003.

[24] T. Alpcan and T. Başar, "A utility-based congestion control scheme for Internet-style networks with delay," in *Proc. IEEE Infocom*, vol. 3, San Francisco, CA, April 2003, pp. 2039–2048.

[25] S. Floyd and K. Fall, "Promoting the use of end-to-end congestion control in the internet," *IEEE/ACM Transactions on Networking*, vol. 7, no. 4, pp. 458 –472, August 1999.

[26] H. Yaiche, R. R. Mazumdar, and C. Rosenberg, "A game theoretic framework for bandwidth allocation and pricing in broadband networks," *IEEE/ACM Transactions on Networking*, vol. 8, pp. 667–678, October 2000.

[27] E. Altman, T. Başar, T. Jimenez, and N. Shimkin, "Competitive routing in networks with polynomial costs," *IEEE Transactions on Automatic Control*, vol. 47(1), pp. 92–96, January 2002.

[28] E. Altman and T. Başar, "Multi-user rate-based flow control," *IEEE Transactions on Communications*, vol. 46(7), pp. 940–949, July 1998.

[29] A. Orda, R. Rom, and N. Shimkin, "Competitive routing in multiuser communication networks," *IEEE/ACM Transactions on Networking*, vol. 1, pp. 510–521, October 1993.

[30] E. Altman, T. Başar, and R. Srikant, "Nash equilibria for combined flow control and routing in networks: Asymptotic behavior for a large number of users," *IEEE Transactions on Automatic Control*, vol. 47, no. 6, June 2002.

[31] T. Başar and R. Srikant, "Revenue-maximizing pricing and capacity expansion in a many-users regime," in *Proc. IEEE Infocom, New York, NY*, June 2002.

[32] S. Kunniyur and R. Srikant, "End-to-end congestion control schemes: Utility functions, random losses and ECN marks," in *Proc. of the IEEE Infocom*, 2000, pp. 1323–1332.

[33] L. S. Brakmo and L. L. Peterson, "TCP vegas: End to end congestion avoidance on a global internet," *IEEE Journal on Selected Areas in Communications*, vol. 13, no. 8, pp. 1465–1480, 1995.

[34] J. Mo, R. J. La, V. Anantharam, and J. C. Walrand, "Analysis and comparison of TCP Reno and Vegas," in *Proc. IEEE Infocom*, 1999, pp. 1556–1563.

[35] R. J. La and V. Anantharam, "Utility-based rate control in the Internet for elastic traffic," *IEEE/ACM Transactions on Networking*, vol. 10, no. 2, pp. 272–286, April 2002.

[36] T. Alpcan and T. Başar, "A game-theoretic framework for congestion control in general topology networks," in *Proc. of the 41st IEEE Conference on Decision and Control*, Las Vegas, NV, December 2002, pp. 1218–1224.

[37] T. Alpcan and T. Başar, "Global stability analysis of an end-to-end congestion control scheme for general topology networks with delay," in *Proc. of the 42nd IEEE Conference on Decision and Control*, Maui, HI, December 2003, pp. 1092 – 1097.

[38] T. Alpcan, T. Başar, and R. Tempo, "Randomized algorithms for stability and robustness analysis of high speed communication networks," in *Proc. of IEEE Conference on Control Applications (CCA)*, Istanbul, Turkey, June 2003, pp. 397–403.

[39] K. R. Rohloff, T. Alpcan, and T. Başar, "A discrete-event systems model for congestion control," in *Proc. 16th IFAC World Congress*, Prague, Czech Republic, July 2005.

[40] T. Alpcan, T. Başar, and R. Tempo, "Randomized algorithms for stability and robustness analysis of high-speed communication networks," *IEEE Transactions on Neural Networks*, vol. 16, no. 5, pp. 1229–1241, September 2005.

[41] T. Alpcan and T. Başar, "Global stability analysis of an end-to-end congestion control scheme for general topology networks with delay," *Elektrik, the Turkish Journal of Electrical Engineering and Computer Sciences, Tubitak*, vol. 12, no. 3, pp. 139–150, November 2004.

[42] T. Alpcan and T. Başar, "Distributed algorithms for nash equilibria of flow control games," in *Advances in Dynamic Games: Applications to Economics, Finance, Optimization, and Stochastic Control*, ser. Annals of Dynamic Games. Boston, MA: Birkhauser, 2005, vol. 7, pp. 473–498.

[43] T. Alpcan and T. Başar, "A utility-based congestion control scheme for Internet-style networks with delay," *IEEE Transactions on Networking*, vol. 13, no. 6, pp. 1261–1274, December 2005.

[44] D. Falomari, N. Mandayam, and D. Goodman, "A new framework for power control in wireless data networks: Games utility and pricing," in *Proc. Allerton Conference on Communication, Control, and Computing*, Monticello, Illinois, September 1998, pp. 546–555.

[45] C. U. Saraydar, N. Mandayam, and D. Goodman, "Pareto efficiency of pricing-based power control in wireless data networks," *WCNC*, 1999.

[46] H. Ji and C. Huang, "Non-cooperative uplink power control in cellular radio systems," *Wireless Networks*, vol. 4(3), pp. 233–240, April 1998.

[47] P. Marbach and R. Berry, "Downlink resource allocation and pricing for wireless networks," in *IEEE Infocom*, New York, NY, June 2002.

[48] V. A. Siris, "Resource control for elastic traffic in cdma networks," in *ACM MOBICOM*, Atlanta, GA, September 2002.

[49] C. U. Saraydar, N. Mandayam, and D. Goodman, "Pricing and power control in a multicell wireless data network," *IEEE Journal on Seleceted Areas in Communications*, pp. 1883–1892, October 2001.

[50] J. Blom and F. Gunnarsson, "Power control in cellular radio systems," Ph.D. dissertation, Linkoepings Universitet, Linkoeping, Sweden, 1998.

[51] C. W. Sung and W. S. Wong, "Power control for multirate multimedia CDMA systems," in *Proc. of IEEE Infocom*, vol. 2, 1999, pp. 957–964.

[52] T. Alpcan, T. Başar, R. Srikant, and E. Altman, "CDMA uplink power control as a noncooperative game," *Wireless Networks*, vol. 8, pp. 659–669, November 2002.

[53] R. D. Yates, "A framework for uplink power control in cellular radio systems," *IEEE Journal on Selected Areas in Communications*, vol. 13, pp. 1341–1347, September 1995.

[54] S. Ulukus and R. D. Yates, "Stochastic power control for cellular radio systems," *IEEE Transactions on Communications*, vol. 46, pp. 784–798, June 1998.

[55] J. Papandriopoulos, J. Evans, and S. Dey, "Optimal power control in CDMA networks with constraints on outage probability," in *Proc. WiOpt'03*, INRIA Sophia Antipolis, France, March 2003, pp. 279–284.

[56] T. Alpcan and T. Başar, "A hybrid systems model for power control in multicell wireless data networks," *Performance Evaluation*, vol. 57, no. 4, pp. 477–495, August 2004.

[57] J. T. Wen and M. Arcak, "A unifying passivity framework for network flow control," *IEEE Transactions on Automatic Control*, vol. 49, no. 2, pp. 162– 174, February 2004.

[58] T. Alpcan and T. Başar, "A hybrid systems model for power control in multicell wireless networks," in *Proc. of the WiOpt'03 Workshop: Modeling and Optimization in Mobile, Ad Hoc and Wireless Networks*, April 2003, pp. 65–72.

[59] T. Alpcan, T. Başar, and S. Dey, "A power control game based on outage probabilities for multicell wireless data networks," in *Proc. of American Control Conference (ACC) 2004*, Boston, MA, July 2004, pp. 1661–1666.

[60] T. Alpcan and T. Başar, "A hybrid noncooperative game model for wireless communications," in *Proc. of 11th International Symposium on Dynamic Games and Applications*, Tuscon, AZ, December 2004.

[61] T. Alpcan, X. Fan, T. Başar, M. Arcak, and J. T. Wen, "Power control for multicell CDMA wireless networks: A team optimization approach," in *Proc. of the WiOpt'05 Workshop: Modeling and Optimization in Mobile, Ad Hoc and Wireless Networks*, Riva del Garda, Trentino, Italy, April 2005, pp. 379–388.

[62] T. Alpcan and T. Başar, "A power control game based on outage probabilities for multicell wireless data networks," *IEEE Transactions on Wireless Communication*, to be published.

[63] T. Alpcan and T. Başar, "A hybrid noncooperative game model for wireless communications," in *Advances in Dynamic Games: Applications to Economics, Finance, Optimization, and Stochastic Control*, ser. Annals of Dynamic Games. Boston, MA: Birkhauser, (to be published).

[64] E. Rabinovitch, "The neverending saga of Internet security: Why? how? and what to do next?" *IEEE Communications Magazine*, pp. 56–58, May 2001.

[65] R. Ellison, D. Fisher, R. Linger, H. Lipson, T. Longstaff, and N. Mead, "Survivable network systems: An emerging discipline (cmu/sei-97-tr-013)," Software Engineering Institute, Carnegie Mellon University, Pittsburgh, PA, Tech. Rep., November 1997, citeseer.nj.nec.com/ellison97survivable.html.

[66] R. Ellison, R. Linger, H. Lipson, N. Mead, and A. Moore, "Foundations for survivable systems engineering," *The Journal of Defense Software Engineering*, pp. 10–15, July 2002.

[67] R. Bace and P. Mell, "Intrusion detection systems," NIST Special Publication on Intrusion Detection Systems, http://www.snort.org/docs/nist-ids.pdf.

[68] M. Y. Huang, R. J. Jasper, and T. M. Wicks, "A large scale distributed intrusion detection framework based on attack strategy analysis," in *Intl. Symp. on Recent Advances in Intrusion Detection (RAID)*, Louvain la Neuve, Belgium, 1998.

[69] J. Grant, P. Attfield, and K. Armstrong, "Distributed firewall technology," presented at EWA-Canada, March 2001.

[70] G. Helmer, J. Wong, V. Honavar, and L. Miller, "Intelligent agents for intrusion detection," in *Proc. of IEEE Information Technology Conference*, Syracuse, NY, September 1998, pp. 121–124, citeseer.nj.nec.com/helmer98intelligent.html.

[71] J. S. Balasubramaniyan, J. O. Garcia-Fernandez, E. Spafford, and D. Zamboni, "An architecture for intrusion detection using autonomous agents," in *In Proc. of 14th Annual Computer Security Applications Conference (ACSAC)*, Scottsdale, AZ, December 1998, pp. 13–24.

[72] R. L. Axtell, "Non-cooperative formation of multi-agent teams," in *Proc. of Intl. Conference on Autonomous Agents and Multi-Agent Systems (AAMAS)*, Bologna, Italy, July 2002.

[73] S. N. Hamilton, W. L. Miller, A. Ott, and O. S. Saydjari, "The role of game theory in information warfare," in *4th Information Survivability Workshop (ISW-2001/2002)*, Vancouver, BC, Canada, March 2002.

[74] S. N. Hamilton, W. L. Miller, A. Ott, and O. S. Saydjari, "Challenges in applying game theory to the domain of information warfare," in *4th Information Survivability Workshop (ISW-2001/2002)*, Vancouver, BC, Canada, March 2002.

[75] T. Alpcan and T. Başar, "A game theoretic analysis of intrusion detection in access control systems," in *Proc. of the 43rd IEEE Conference on Decision and Control*, Paradise Island, Bahamas, December 2004, pp. 1568–1573.

[76] T. Alpcan and T. Başar, "A game theoretic approach to decision and analysis in network intrusion detection," in *Proc. of the 42nd IEEE Conference on Decision and Control*, Maui, HI, December 2003, pp. 2595–2600.

[77] UCB, LBNL, and VINT, "Network simulator ns (version 2)," http://www.isi.edu/nsnam/ns/.

[78] G. Owen, *Game Theory*, 3rd ed. New York, NY: Academic Press, 2001.

[79] J. B. Rosen, "Existence and uniqueness of equilibrium points for concave n-person games," *Econometrica*, vol. 33, pp. 520–534, July 1965.

[80] H. L. Royden, *Real Analysis*, 3rd ed. Upper Saddle River, NJ: Prentice Hall, 1999.

[81] D. Bertsekas, *Nonlinear Programming*, 2nd ed. Belmont, MA: Athena Scientific, 1999.

[82] H. K. Khalil, *Nonlinear Systems*, 2nd ed. Upper Saddle River, NJ: Prentice Hall, 1996.

[83] J. K. Hale and S. M. V. Lunel, *Introduction to Functional Differential Equations*. New York, NY: Springer Verlag, 1993.

[84] J. A. Yorke, "Asymptotic stability for one dimensional differential-delay equations," *Journal of Differential Equations*, vol. 7, pp. 189–202, 1970.

[85] T. S. Rapaport, *Wireless Communications: Principles and Practice*. Upper Saddle River, NJ: Prentice Hall, 1996.

[86] C. V. Hollot, Y. Liu, V. Misra, and D. Towsley, "Unresponsive flows and AQM performance," in *Proc. of the IEEE Infocom*, San Francisco, CA, April 2003.

[87] L. Devroye, *Non-Uniform Random Variate Generation*. New York, NY: Springer-Verlag, 1996.

[88] G. Calafiore, F. Dabbene, and R. Tempo, "Uniform sample generation in l_p balls for probabilistic robustness analysis," in *Proc. of the IEEE Conference on Decision and Control (CDC)*, Tampa, FL, December 1998, pp. 3335–3340.

[89] L. F. Shampine and S. Thompson, "Solving delay differential equations with dde23," March 2000, http://www.radford.edu/ thompson/webddes.

[90] T. A. Burton, *Stability and Periodic Solutions of Ordinary and functional differential equations*. Orlando, FL: Academic Press, 1985.

[91] A. S. Tanenbaum, *Computer Networks*, 3rd ed. Upper Saddle River, NJ: Prentice Hall, 1996.

[92] S. Floyd, M. Handley, J. Padhye, and J. Widmer, "Equation-based congestion control for unicast applications," in *Proc. of ACM SIGCOMM Conf.*, August 2000, pp. 45–58.

[93] P. Hellekalek, "Good random number generators are (not so) easy to find," *Mathematics and Computers in Simulation*, vol. 46, pp. 485–505, 1998.

[94] R. Tempo, G. Calafiore, and F. Dabbene, *Randomized Algorithms for Analysis and Control of Uncertain Systems*. London, UK: Springer-Verlag, 2005.

[95] M. Vidyasagar, *A Theory of Learning and Generalization with Applications to Neural Networks and Control Systems*. Berlin, Germany: Springer-Verlag, 1996.

[96] D. E. Knuth, *The Art of Computer Programming, Seminumerical Algorithms*. Reading, MA: Addison-Wesley, 1996.

[97] M. S. Branicky, S. M. LaValle, K. Olson, and L. Yang, "Deterministic vs. probabilistic roadmaps," 2002, unpublished manuscript.

[98] J. P. Hespanha and A. S. Morse, "Stability of switched systems with average dwell-time," in *Proc. of the 38th IEEE Conference on Decision and Control*, Phoenix, AZ, December 1999, pp. 2655–2660.

[99] S. Dey and J. Evans, "Optimal power control in wireless data networks with outage-based utility guarantees," in *Proc. of the 42nd IEEE Conference on Decision and Control*, Maui, Hawaii, December 2003, pp. 279–284.

[100] Y. D. Yao and A. Sheikh, "Outage probability analysis for microcell mobile radio systems with cochannel interferers in rician/rayleigh fading environment," *IEE Electronics Letters*, vol. 26, pp. 864–866, June 1990.

[101] S. Kandukuri and S. Boyd, "Optimal power control in interference-Limited fading wireless channels with outage-Probability specifications," *IEEE Transactions on Wireless Communication*, vol. 1 (1), pp. 46–55, 2002.

[102] D. Bertsekas and J. N. Tsitsiklis, *Parallel and Distributed Compuation: Numerical Methods*. Upper Saddle River, NJ: Prentice Hall, 1989.

[103] H. Stark and J. W. Woods, *Probability, Random Processes, and Estimation Theory for Engineers*, 2nd ed. Upper Saddle River, NJ: Prentice Hall, 1994.

[104] J. Doob, *Stochastic Processes*. New York, NY: Wiley, 1953.

[105] P. Billingsley, *Probability and Measure*, 2nd ed. New York, NY: Wiley, 1986.

[106] H. Chernoff, "A measure of asymptotic efficiency for test of hypothesis based on the sum of observations," *Annals of Mathematical Statistics*, vol. 23, pp. 493–507, 1952.

[107] A. Berman and R. J. Plemmons, *Nonnegative Matrices in the Mathematical Sciences*. Philadelphia, PA: Society for Industrial and Applied Mathematics, 1994, originally published by Academic Press, New York, 1979.

[108] X. Fan, M. Arcak, and J. T. Wen, "Robustness of network flow control against disturbances and time-delays," *Systems and Control Letters*, vol. 53, no. 1, pp. 13–29, 2004.

[109] A. M. Robert, "Attack modeling for information security and survivability (cmu/sei-2001-tn-001)," Software Engineering Institute, Carnegie Mellon University, Pittsburgh, PA, Tech. Rep., March 2001, citeseer.nj.nec.com/452508.html.

[110] P. K. Harmer, P. D. Williams, G. H. Gunsch, and G. B. Lamont, "An artificial immune system architecture for computer security applications," *IEEE Transactions on Evolutionary Computation*, pp. 252–280, June 2002.

[111] D. Dasgupta and F. Gonzales, "An immunity-based technique to characterize intrusions in computer networks," *IEEE Transactions on Evolutionary Computation*, pp. 281–291, June 2002.

[112] D. Zamboni, "Using internal sensors for computer intrusion detection," Ph.D. dissertation, Purdue University, August 2001.

[113] J. Contreras, M. Klusch, O. Shehory, and F. Wu, "Coalition formation in a power transmission planning environment," in *In Proc. of 2nd Intl. Conference on Practical Applications of Multi-Agent Systems, PAAM*, London, U.K., April 1997, pp. 21–23.

[114] The-Gambit-Project, "Gambit game theory analysis software and tools," 2002, http://econweb.tamu.edu/gambit.

[115] K. M. Tan, K. S. Killourhy, and R. A. Maxion, "Undermining an anomaly-based intrusion detection system using common exploits," in *Proc. of the Fifth International Symposium on Recent Advances in Intrusion Detection (RAID-2002)*, A. Wespi, G. Vigna, and L. Deri, Eds., Zurich, Switzerland, October 2002, pp. 54–73.

[116] N. K. Bose and P. Liang, *Neural Network Fundamentals with Graphs, Algorithms, and Applications*. New York, NY: McGraw-Hill, 1996.

[117] B. C. Rhodes, J. A. Mahaffey, and J. D. Cannady, "Multiple self-organizing maps for intrusion detection," in *Proc. of the 23rd National Information Systems Security Conference*, Baltimore, MD, 2000.

[118] H. Demuth and M. Beale, *MATLAB Neural Network Toolbox User's Guide*, 4th ed., The MathWorks Inc., January 2003.

AUTHOR'S BIOGRAPHY

Tansu Alpcan was born in Istanbul, Turkey, on April 8, 1975. He was accepted to Bogazici University, one of the most prestigious universities in Turkey, as being in the first 30 among more than a million students in national university entrance examination. As a result of his success, he received Sabanci Foundation Scholarship from 1993 to 1998. He received his B.S. degree in electrical engineering as a high honor student from Bogazici University, Istanbul, Turkey in 1998. After graduation, he worked in the R&D department of Alcatel Telecom for one year on S12 public communication systems. During this time he visited branches of the company in Berlin, Germany and Antwerp, Belgium, where he received a certification after completing a two month training program.

Alpcan started his studies in University of Illinois as a Fulbright Scholar (2000 to 2001). He has received M.S. degree in electrical engineering from the University of Illinois in 2001, and continued his studies towards a PhD degree in the Department of Electrical and Computer Engineering. He has worked as a research assistant in the Decision and Control Laboratory, CSL, under the guidance of Professor Tamer Başar. His research interests include game theory, resource allocation, control and optimization of wired and wireless communication networks, control of computing systems, network security, intrusion detection, and cryptography. Specifically, he has been doing research on the topics flow and congestion control of computer networks, power control in CDMA wireless networks, network intrusion detection applying game theoretic techniques, and chaotic cryptography. He has also worked as a teaching assistant in the ECE department and was the instructor (with full responsibilities) of the courses ECE 410: Digital Signal Processing in summer 2005 and ECE 486: Control Systems in fall 2005.

Alpcan is the first author of 8 published/accepted journal articles and 13 conference papers, which he has presented in conferences like IEEE Conference on Decision and Control (CDC), IEEE Infocom, IEEE Conference on Control Applications (CCA), IEEE American Control Conference (ACC), WiOpt: Modeling and Optimization in Mobile, Ad Hoc and Wireless Networks. He has received the best student paper award in IEEE CCA-2003 with his work titled "Randomized Algorithms for Stability and Robustness Analysis of High Speed Communication Networks." Alpcan has developed a chaotic cryptosystem which is in the patent process jointly with Univer-

sity of Illinois. He has worked as a reviewer in a variety of conferences and journals and was an associate editor for IEEE Conference on Control Applications (CCA) in 2005. Recently, Alpcan has been selected as the recipient of 2006 Robert T. Chien award. He has been a student member of IEEE since 1998.